TECHNISCHE UNIVERSITÄT MÜNCHEN

TUM School of Life Sciences

Lehrstuhl für Lebensmittel- und Bio-Prozesstechnik

Functionalisation of Pea Protein: Extraction, Gelation, and Microparticulation

Caren Alexandra Tanger

Vollständiger Abdruck der von der TUM School of Life Sciences der Technischen Universität München zur Erlangung des akademischen Grades einer

Doktorin der Ingenieurwissenschaften

genehmigten Dissertation.

Vorsitzender: Prof. Dr. Michael Rychlik

Prüfer der Dissertation:
1. Prof. Dr.-Ing. Ulrich Kulozik
2. Prof. Dr. Corinna Dawid
3. Priv.-Doz. Dr.-Ing.habil. Mario Jekle

Die Dissertation wurde am 26.01.2022 bei der Technischen Universität München eingereicht und durch die TUM School of Life Sciences am 24.05.2022 angenommen.

The world is full of great and wonderful things for those who are ready for them

Moominpappa (Moominpappa at sea)

I. ACKNOWLEDGEMENT

The presented work was conducted during my time at the chair of Food and Bioprocess Engineering at the Technical University Munich in Freising. First of all, I want to thank Prof. Dr.-Ing Ulrich Kulozik for giving me the chance of working on the first pea protein project at the chair and supervising me during my doctorate. Special thanks for scientific discussion, financial support as well as professional support during the different stages of my doctorate. I valued the freedom given to me in my work very much.

Special thanks to Friederike Schöpflin, Sabine Becker and Sabine Grabbe for administrative and IT support.

I would like to thank Annette Brümmer-Rolf and Christine Haas for countless measurements of my Elementar samples and help during method development and laboratory work. Next to them, I want to thank Franz Kuhnert, Andreas Matyssek and Günther Unterbuchberger for support during extrusion cooking and spray-drying. Claudia Hengst, Hermine Rossgoderer, Martin Hilz are thanked for laboratory support.

Next to these, I also want to thank the 'Werkstatt' Christian Ederer, Franz Frauenhofer and Erich Schneider for help during work in the pilot plant.

Special thanks goes to the students Phillip Sochatzky, Eugen Feldmann, Veronika Bauer, Patrick Gref, Maike Limmer, Jennifer Darmali, Thuy Vi Co, Paola Quintana-Ramos, Florian Schmidt, Michaela Müller, Lukas Hans, Khaled Al-Kayid, and Johannes Mertens for their valuable input for this thesis during their seminar's, bachelor's, and master's thesis.

Next to these, I also want to thank my projects partners Florian Utz and Corinna Dawid from the Chair of Food Chemistry and Molecular Sensory for good collaboration.

I want to thank Priska Pröll, Julia Engel and Regina Haindl for the great work atmosphere and gummy bears in the office. Additionally, Maria Weinberger, Marius Reiter and David Andlinger are thanked for personal support and fruitful scientific discussions. I am thankful for all my colleagues, who created a good working environment and memorable events. Most of the time I started the day at the chair with a good feeling. Especially during lockdown socializing with my colleagues was very supportive.

Lastly, I want to thank my parents and my sister for their endless support during my journey and their trials to understand the content of this work even though they are from an economics background.

II. ABBREVIATIONS/SYMBOLS

Latin symbols		Unit
A	area	m^2
A	Pre-exponentional factor	
AE-IP	Alkali extraction and isoelectric precipiation	
ANOVA	Analysis of variance	
BSA	Bovine serum albumin	
c	concentration	
$C_{n,bond,Bi}$	Concentration of cleaved proteins	
$C_{n,sup,Bi}$	Concentration of dissolved nitrogen	
CaB	Calcium bridge	
d	Particle diameter	µm
$d_{10,3}$	10^{th}-percentile of the particle size distribution	µm
$d_{50,3}$	Volume based median of the particle size distribution	µm
$d_{90,3}$	90^{th}-percentile of the particle size distribution	µm
DD	Degree of denaturation	%
DoT	Dose over threshold	
mDSC/DSC	(modulated) Differential Scanning Calorimetry	
DTT	Dithiothreitol	
E_a	Activation energy	J mol^{-1}
EB	Electrostatic interactions	
F	Force	N
f	Frequency	
FD	Freeze-dried	
FFA	Free fatty acids	
G*	Shear modulus	Pa
G´	Storage modulus/ indicator for gel strength	Pa
G´´	Loss modulus	Pa
Glob	Globulin	
H	enthalpy	J

h	Distance between plates	m
Hy	Hydrophobic interactions	
IEP	Isoelectric point	
K	Reaction rate	s^{-1}
k_{agg}	Aggregation rate	
L	Loss	%
LVE	Linear viscoelastic region	
m	mass	kg
m_{gel}	Mass of the gel	kg
m_s	Initial mass	kg
MC	Micellar precipitation	
MD	Milk dessert	
MP	Microparticle	
n	Reaction order	
n	Screw speed	rpm
NaCl	Sodium Chloride	
NEM	N-Ethylmaleimide	
OAV	Odour activity value	
p	Minimum significance	
P	Pellet	
Pat	Patatin /Potato protein	
pf	Pea flour	
pp	Pea flour	
PPc	Commercial pea protein	
PPe	Laboratory extracted pea protein	
Q_3	Volume based cumulative particle size distribution	%
q_3	Volume based particle size distribution	%
R	Universal gas constant	$J\ K^{-1}\ mol^{-1}$
rpm	Revolutions per minute	
s	Deflection	m
S	Sedimentation coefficient	
SDS	Sodium dodecyl sulphate	

SDS-PAGE	Sodium Dodecyl Sulfate Polyacrylamid Gel Electro-phoresis	
SD	Spray-dried	
SE	Salt extracted and dialysed (according to Stone et al. (2015))	
SE-D	Salt extracted and dialysed (according to Sun and Arntfield (2010))	
SH	Thiol group	
SS	Disulphide bonds	
t	Time	s
T_d	Denaturation temperature	
T_{onset}	Temperature of begin of endothermic reaction	
T_{50}	Temperature at which 50 % of protein is denatured	
$T_{p,max}$	Maximum product temperature	°C
V	Volume	
vdW	Van-der-Waals interaction	
w/o	without	
WB	Hydrogen bond	
WPI	Whey protein isolate	
WPC	Whey protein concentrate	
Y	Yield	%
Y_l	Yield stress	

Greek symbols

α	Significance level	
α	Degree of unfolding	
α-la	α-lactalbumin	
β-lg	β-lactoglobulin	
$\dot{\gamma}$	Shear rate	s^{-1}
ϒ	Shear deformation	
τ	Shear stress	
τ_f	Flow point	
τ_y	Amplitude threshold	

tanδ	Loss factor	
ϑ	Temperature	°C
ϕ	Deflection angle	
ω	Frequency	s^{-1}

III. CONTENT

1 GENERAL INTRODUCTION

With increasing concern about diet-related illnesses such as obesity, diabetes, and cardiovascular diseases, development of ‘healthy’ food products is of interest. In this thesis this problem is addressed by developing a concept for replacing fat with functionalized protein, which is lower in calory density and higher in satiety (Simpson and Raubenheimer 2005). Another increasing concern with world population growth and climate change is ecological sustainability. One of the proposed options in this regard is to use plant-based protein source instead of animal-based. One such alternative protein source is pea.

The aim of this work was to develop a process to produce microparticles from pea protein. These can be used to replace fat in food without sacrificing texture and taste. The microparticulation process was already analysed extensively for whey protein. However, little is known about pea proteins in general and pea protein microparticulation in particular. Thus, before transferring the process, research is needed to gain more insight into pea proteins and their thermal behaviour. This thesis covers three main topics, which build on each other.

First, the influence of extraction methods was investigated with the aim to control pea protein extraction and find suitable extraction methods for obtaining pea proteins mostly unaffected in the degree of nativity and functionality by previous processing steps, which is not the case for commercially available pea proteins. Solubilisation and precipitation during the extraction were found to influence the degree of ‘nativity’ and the protein profile. These characteristics then influenced other functionalities. This investigation resulted in a portfolio of extraction methods. From this portfolio, the most suitable extraction methods for the following experiments could be chosen.

Second, the thermal aggregation behaviour without shear stress at high protein concentration was investigated. This resulted in a deeper insight into pea protein gelation and its building blocks, which differs significantly from the one known from whey protein. The results also gave an idea of how pea protein aggregation would occur under thermo-mechanical treatment.

Third, additional shear stress was added during thermal treatment and resulting particles were analysed. This was done on small scale using a rheometer and on a large scale using an extruder. For a better understanding of the underlying mechanisms of the process a comparison of resulting between particles produced from pea protein, whey protein, and potato protein was made. This gave a better understanding of the differences and similarities between the three protein systems using the same process and helped to classify pea protein.

In order to validate whether the overall aim of producing a pea protein-based fat replacement without sacrifices in texture and taste was achieved, the particles were incorporated in a fat-reduced milk dessert. These milk desserts were tested sensorically in cooperation with a partner institute at TUM.

In the following, the general state of knowledge and basics of the microparticulation process, extraction of pea proteins from pea flour, thermal denaturation and aggregation of proteins, methods to analyse protein gels and aggregates, and extrusion cooking are presented.

1.1 Pea

Pea (*Pisum sativum L.*) is a pulse crop, which belongs to the family of the *Leguminosae*. It is cultivated throughout Europe and is used for human food and animal feed. The composition of the pea is dependent on the cultivar, place, and climate. Table 1-1 shows an average nutritional value for peas.

Table 1-1: Average nutritional value for peas (Wang et al. 2010)

Compound	The average amount in pea (%)
Crude fiber	5.2
Starch	47.0
Protein	24.8
Fat	0.8
Ash	0.3
Phytic acid	0.8

Due to the high amount of starch, peas are currently used as a base to extract starch. In recent years, also the protein in peas became of increasing interest because they are a non-allergenic alternative to soy protein (Barac et al. 2010). In addition, the demand for vegan food and alternatives to animal-derived protein, pea proteins are of increasing interest for human food production (Fasolin et al. 2019).

1.1.1 Pea Proteins

Peas contain around 24.8% protein, which is highly dependent on the cultivar (Wang et al. 2010). The proteins can be divided into four fractions based on their solubility. Globulins are salt soluble and are with around 55 – 80% the dominant fraction. Albumins are water-soluble and make about 18 – 25%. Prolamins and glutenins are soluble in ethanol and caustic soda, respectively, and make a minor amount of less than 10%. (Osborne 1909) Because prolamins and glutenins are minor proteins, focus is laid on the globulins and albumins in the following.

1.1.1.1 Globulins

The three proteins legumin, vicilin and convicilin belong to the globulins and can be separated by their sedimentation coefficient (Derbyshire et al. 1976). Legumin (11S) is the main protein and occurs as a hexamer of 360 kDa hold together by hydrophobic interactions at pH 7-9 (Shand et al. 2007; Dziuba et al. 2014). The monomers of 60 kDa consist out of an acidic (40 kDa) with pI of 4.5 – 5.8 and an alkaline (20 kDa) subunit with pI of 6.2 – 8.8, which are connected by a disulphide bridge (Dziuba et al.

2014; Shand et al. 2007; Casey and Short 1981). The 3D structure of legumin is shown in Figure 1-1.

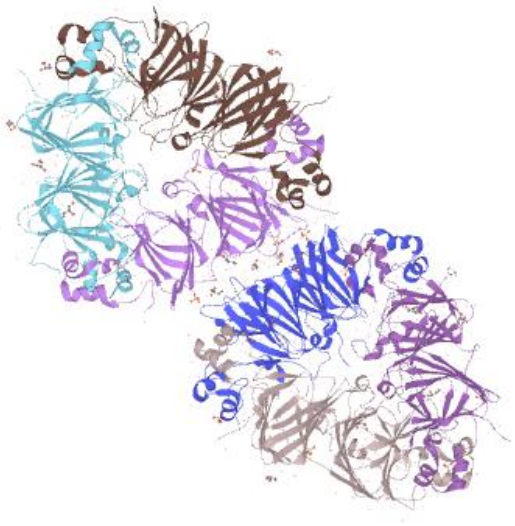

Figure 1-1: 3D structure of a legumin hexamer (source: https://www.uniprot.org/uniprot/P02857)

The structure of legumin is highly complex, much more than for example β-lactoglobulin. Dependent on cultivar, a legumin monomer contains approximately three or four methionine and between two and seven cysteine amino acids, thus six to nine potential amino acids that can form disulphide bonds (Chihi et al. 2016; O'Kane et al. 2004c; Casey and Short 1981).

Vicilin occurs as a trimer with monomers of each 50 kDa (Liang and Tang 2013), which fragments into 33 kDa (αβ), 30 kDa (βγ), 19 kDa (α), 13.5 kDa (β), and 16 or 12.5 kDa (γ) in an SDS-PAGE (O'Kane et al. 2004a). In contrast to legumin, vicilin is less hydrophobic and does not contain any disulphide bonds (O'Kane et al. 2004c). However, dependent on genotype, vicilin may contain one or two cysteine groups, which show a potential to form covalent bonds during aggregation (Chihi et al. 2016). In contrast to legumin, some vicilins are partly soluble at pH 4.8 (Casey 1982).

The third globulin protein is convicilin, which shows high homology to vicilin and occurs as a contaminant of vicilin purification (Gueguen et al.). It assembles as a tetramer of 290 kDa with monomers of 71 kDa (Derbyshire et al. 1976). It contains one cysteine group (Croy et al. 1980). O'Kane et al. (2004a) did not see convicilin as a third vicilin protein, but rather as the α-subunit of a vicilin fragment protein.

1.1.1.2 Albumins

Albumins (2S) are water-soluble. The main albumin proteins are PA1 and PA2. PA1 contains two polypeptides of 26 kDa. The low molecular PA2 contains two polypeptides of 6 kDa. The polypeptides are held together by non-covalent bonds (Gruen et al. 1987). Next to these two proteins the enzymes lipoxygenase, glycosidases, protease inhibitors, and lectins also belong to the albumins (Djoullah et al. 2015; Croy et al. 1984). The albumin proteins are rich in sulphur-containing amino acids. Therefore, they can form disulphide bridges between proteins (Gruen et al. 1987). Their isoelectric

point is at pH 6, which means they stay soluble during isoelectric precipitation at pH 4.5 and are often washed out during extraction (Swanson 1990; Arntfield and Maskus 2011).

1.2 Potato

Potato (*Solanum tuberosum*) is a plant of the family *Solanaceae* with a high amount of starch. The rough composition of the potato is shown in Table 1-2. Composition is dependent on the cultivar, climate, and place.

Table 1-2: Composition of raw potatoes (Singh and Kaur 2016)

Compound	The average amount in raw potato (%)
Dry matter	23
Carbohydrates	20
Protein	2
Fat	0.1

A side stream of the starch extraction of potatoes is the potato protein fruit juice, which is rich in functional protein (35% of dry matter) (Schmidt et al. 2017). From this potato protein containing `fruit juice´, potato protein can be extracted.

1.2.1 Potato proteins

There are three groups of potato protein in potato fruit juice: Patatin (40 %), protease inhibitors (50%) and other enzymes as polyphenol oxidase, lipoxygenase and enzymes associated with starch synthesis (10%) (Schmidt et al. 2019). In this study, only patatin is used, which is why it is explained in more detail below.

1.2.1.1 Patatin

Patatins are glycoproteins of 39 – 43 kDa, which occur as a dimer of 80 kDa. Their isoelectric point varies between 4.5 and 5.2 and they can differ in their glycosylation patterns (Schmidt et al. 2019). The patatins exhibit a lipid acylesterase activity (Pots et al. 1998a). The protein structure of patatins is not stabilized by a disulphide bridge, but it does contain one free thiol group, which lead to low heat stability (Creusot et al. 2011). High levels of exposed hydrophobicity of patatins lead to a very low protein concentration required for gelation (Creusot et al. 2011).

1.3 Whey

Sweet whey contains lactose (4.8%), protein (0.6%) and minerals (0.6%). By the usage of ultrafiltration and diafiltration, the sweet whey can be concentrated up to 80% protein concentration in dry matter. During the filtration lactose and minerals are washed out and their concentration decreases (Boland 2011). Liquid whey is then evaporated and spray-dried to result in a whey protein concentrate powder. By the addition of ion-exchange chromatography before drying the protein content can be increased to 90% protein in dry matter and higher with very low to no lactose and minerals content. This results in a whey protein isolate (Foegeding and Luck 2003).

1.3.1 Whey proteins

The major whey protein is β-lactoglobulin (β-lg) and minor proteins are α-lactalbumin (α-la) and bovine serum albumin (BSA). Next to these, also immunoglobulins, lactoferrin and lactoperoxidase belong to the whey protein (Foegeding and Luck 2003). Since β-lactoglobulin and α-lactalbumin are the two dominant whey proteins, they are discussed in more detail below.

1.3.1.1 β-Lactoglobulin

β-lactoglobulin is a globular protein and has a molecular weight of 18 kDa. It contains 162 amino acids and occurs as dimer at neutral pH, which is non-covalently bound (Boland 2011; Nicolai and Durand 2013). The transition of monomer and dimer is also known as tanford transition (Nicolai and Durand 2013). The protein contains two internal disulphide bridges that stabilize the protein structure and one ‘free’ cystein residue. The cystein residue is buried behind an α-helix and can only react after the α-helix is disrupted, which then can start a thiol-disulphide interchange reaction a key feature of protein functionality (Boland 2011).

1.3.1.2 α-Lactalbumin

α-lactalbumin is a smaller protein with a molecular weight of 14 kDa. Special about α-lactalbumin is the calcium-binding site. The form is called holo if calcium is bound, and apo if calcium is not bound. The form greatly determines the heat stability of the protein (Boye and Alli 2000). Calcium binding capacity is dependent on pH and ionic strength. The protein contains four intramolecular disulphide bonds and in contrast to β-lactoglobulin no free thiol group (Boye and Alli 2000).

1.4 Extraction of pea proteins from pea flour

Due to extensive processing and focus on starch separation commercial pea protein are, in contrast to commercial potato and whey protein, low in solubility, low in techno-functionality and low in the degree of nativity (Fuhrmeister and Meuser 2003; Sun and Arntfield 2010; Taherian et al. 2011). Therefore, most researchers extract pea protein from pea flour on a laboratory scale. There are several extraction methods established. Some contain centrifugation and pH or salt changes (Stone et al. 2015; Sun and Arntfield 2010; Kornet et al. 2020) and other also use membrane filtration (Taherian et al. 2011; Tian et al. 1999) or air classification (Reinkensmeier et al. 2015). In this work, pea proteins were extracted only using centrifugation, pH or salt shifts and dialysis. Therefore, these methods will be discussed in more detail. There are three commonly known methods for extraction of pea protein: Alkali extraction – isoelectric precipitation, micellar extraction, and salt extraction – dialysis (Stone et al. 2015). Micellar extraction and salt extraction – dialysis are also used in combination or in a modified version (Sun and Arntfield 2010).

For alkali extraction – isoelectric precipitation the pea flour is first dispersed in water at pH 8 - 9 (Kornet et al. 2020; Stone et al. 2015). Insoluble plant material is separated via centrifugation. The pea protein in the supernatant is precipitate at pH 4.5 and also separated via centrifugation. The pellet is collected and freeze-dried (Stone et al. 2015). Some researchers disperse the protein pellet in water and set the pH back to 7

before freeze-drying (Kornet et al. 2020). Due to the isoelectric precipitation and alkaline pH values, this extraction method can be detrimental for the pea proteins extracted (Stone et al. 2015).

For both salt and micellar extraction, the pea protein is dispersed in a salt solution with 0.3 M to 1 M NaCl or 6.4 % KCl (Stone et al. 2015; Sun and Arntfield 2010). Insoluble plant material is separated via centrifugation, similar to alkali extraction – isoelectric precipitation. For the salt extraction – dialysis described by Stone et al. (2015) the supernatant is dialysed and then freeze-dried. Due to the missing precipitation step also albumins end up in the dried protein product (Stone et al. 2015). The micellar precipitation described in this latter work and the salt extraction described by Sun and Arntfield (2010) follows a similar extraction process. In both extractions, the protein is precipitated by decreasing the salt content by diluting the supernatant 1:10 (Stone et al. 2015) or 1:2 (Sun and Arntfield 2010) with demineralised water. The globulins form micelles and get insoluble. They are separated from the soluble part by centrifugation. In the micellar extraction described by Stone et al. (2015) the protein pellet is freeze-dried after centrifugation and in the salt extraction described by Sun and Arntfield (2010), the protein pellet is dialysed before freeze-drying.

1.5 Thermal treatment of proteins

Thermal treatment of proteins can lead to a loss in native secondary, tertiary, and quarternary structure without a change in molecular weight. A different conformation of the amino acids can lead to different protein functionalities and protein-protein interactions.

1.5.1 Denaturation and aggregation of proteins

The denaturation of proteins can be divided into two steps: unfolding and aggregation. During heating monomer-dimer equilibrium shifts to the monomeric state (N) (Tanford and Taggart). Conformational changes expose buried reactive side chains normally hidden in the core of the native protein (R). Up until then, the reaction remains reversible. Further conformational changes lead to an irreversible reactive protein (S). The reaction is followed by aggregation via protein-protein interactions for example disulphide bonds and hydrophobic interactions (Loveday 2016). A generic reaction scheme is shown below:

$$N_2 \leftrightarrow N \leftrightarrow R \rightarrow S \rightarrow aggregates$$

Upon further aggregation, a gel is formed. A gel is a 3D network of protein, where the aggregates interact with each other. A schematic overview of the gelation of β-lactoglobulin at pH > 5.7 is shown in Figure 1-2.

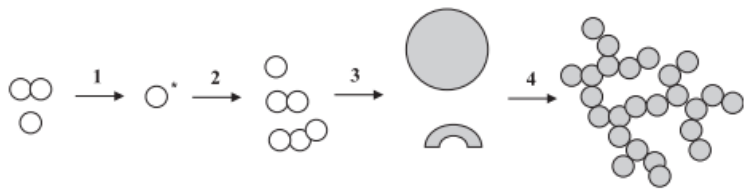

Figure 1-2: Schematic representation of the aggregation and gelation process of β-lactoglobulin (Nicolai et al. 2011b). Note: change in scale of the drawings after step 3 and step 4.

Step 1 shows the dissociation of dimers into monomers upon heating of β-lactoglobulin. These align to small oligomers in step 2. If the concentration is above a critical association concentration larger primary aggregates are formed with a size between 15 nm and 150 nm depending on pH and ionic strength (step 3). If the protein concentration is above the minimum gelation concentration the primary aggregates form large self-similar aggregates or form a gel (step 4) (Nicolai et al. 2011b).

1.5.2 Influencing factors on thermal-induced denaturation and resulting aggregate size

Influencing factors on the thermally induced denaturation are temperature, pH, ionic strength, type of salt, protein concentration and sugar content.

1.5.2.1 Temperature and heating time

Denaturation and aggregation are temperature-time effects. The higher the temperature the faster the reaction occurs. With increasing temperature the protein structure is destabilized by reduction of activation energy, increased protein diffusion and increased frequency of molecular collisions. In addition, hydrophobic interactions increase in intensity leading to protein-protein interaction and the formation of aggregates. Several studies have analysed the influence of temperature-time combinations on the denaturation of β-lactoglobulin and whey protein in general (Dannenberg and Kessler 1988; Tolkach and Kulozik 2007; Loveday 2016). The temperature effect can be described by the Arrhenius equation.

$$k = Ae^{\frac{-E_a}{RT}} \tag{1-1}$$

With k being the rate constant, A the pre-exponential factor, E_a the activation energy, R the universal gas constant, and T the absolute temperature in Kelvin. Plotting the reaction rate constant derived from the Arrhenius equation for β-lactoglobulin and whey protein, a bend temperature can be observed. This is schematically shown in Figure 1-3.

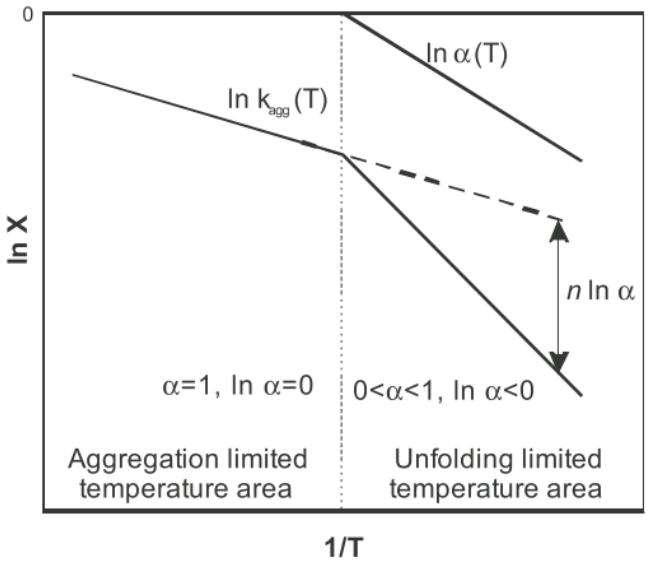

Figure 1-3: Schematic Arrhenius plot of β-lactoglobulin showing the bend between aggregation limited and unfolding limited temperature area (Tolkach and Kulozik 2007).

This bend temperature separates the unfolding limited temperature area and the aggregation limited temperature area from each other. The bend temperature was found to be 90°C for β-lactoglobulin and 80°C for α-lactalbumin (Dannenberg and Kessler 1988; Tolkach and Kulozik 2007). Such a separation of an aggregation limited, and an unfolding limited temperature area has also been found for patatin. There the bend temperature is lower with 50°C at pH 7 and dependent on pH value (Andlinger et al. 2021c).

Next to unfolding and aggregation kinetics, temperature-time also affects the inner aggregate structure. Without shear stress an increasing size of whey protein isolate aggregates analysing a temperature range of 90°C and 150°C was found (Kennel 1994). Similar findings were also reported by Elofsson et al. (1996) for a lower temperature range of 59°C to 63°C. In contrast to these findings, Delahaije et al. (2015) and Bon et al. (1999) found no significant effect on temperature on the aggregate size of β-lactoglobulin analysing temperature ranges of 65°C to 80°C and 55°C to 87.8°C, respectively. Patatin aggregates were found to increase in size with increasing temperature (Delahaije et al. 2015).

For proteins under shear stress, Spiegel (1999b) found that temperature had a significant effect on particle size, as shown in Figure 1-4. Increasing temperature to 80°C for low lactose content and 95°C for high lactose content, which is the bend temperature of the Arrhenius plot of these two whey protein concentrate, leads to smaller particles. At higher temperatures, an increasing temperature leads to bigger particles. The size of the particles can be explained by the serum binding capacity. The serum binding capacity decreases steadily with increasing temperature, leading to more compact aggregates with fewer pores.

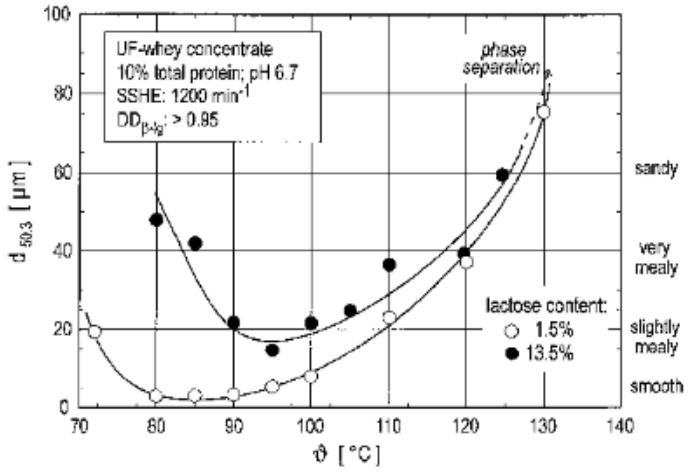

Figure 1-4: Particle size of thermo-mechanical treated whey protein concentrate (Spiegel 1999b).

Less compact aggregates can be deformed by the shear stress and shear stability is high. In the transition, range aggregates become much more compact and rigid leading to less shear-stable aggregates. These less shear-stable aggregates can be reduced in particle size by the shear stress leading to small aggregates. Above 100°C the un-

folding of whey proteins is very fast and each collision of two proteins results in aggregation. The aggregate structure is denser and solid than in the transition state providing high shear stability. This results in big aggregates. This model of whey protein aggregation under shear stress is schematically depicted in Figure 1-5.

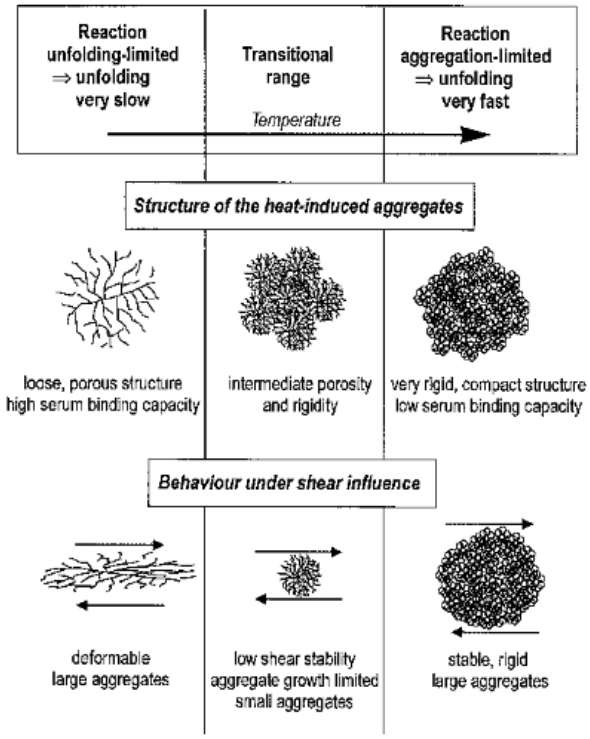

Figure 1-5: Schematic model of whey protein aggregation of whey protein concentrate under shear stress (Spiegel 1999b).

This is in line with the findings of Moakes et al. (2015), who reported that a higher heating rate will promote large aggregates formation. They explained their findings by the fast interactions and therefore an immediate resistance to shear.

1.5.2.2 Shear stress

Shear stress during thermal treatment can have three effects on protein aggregation. First, due to the shear stress and its mechanical forces, it can unfold proteins. However, for this extremely high shear stress is necessary. Second, the shear stress can break particles apart. This can occur due to pressure fluctuation in the fluid flow, by erosion of primary aggregates from the particle surface or by fragmentation of large aggregation in smaller aggregates by either or both mechanisms described above. Third, due to the higher collision probability of primary aggregates (0.25 – 1 µm), it can enhance aggregation (Wolz et al. 2016b; Taylor and Fryer 1994; Thomas and Geer 2011). By increasing the shear rate in a shear apparatus, the shear stress is linear increased (Mezger 2019).

Using a rheometer, Wolz et al. (2016b) found decreasing particle sizes with increasing shear rates for whey protein concentrate at protein concentration from 10% to 40%. At a lower protein concentration of 5 %, particle size increased with increasing shear rate up to a shear rate of 750 s^{-1}. At higher shear rates particle size decreased again with

increasing shear rate. The authors also found a rounder and denser aggregate structure with an increasing shear rate. Using an extruder Wolz et al. (2016a) also found decreasing particle sizes with increasing screw speed in the range of 100 rpm to 800 rpm. Quevedo et al. (2020b) found a decrease in aggregation onset temperature with increasing shear rate of mixed β-lactoglobulin and α-lactalbumin suspensions at high protein concentrations (60% and 70%) using a closed cavity rheometer. Moakes et al. (2015) found a decrease in particle size with increasing shear rate from 200 s^{-1} to 800 s^{-1} using a rheometer. Comparing particles formed at 200 s^{-1} and 800 s^{-1} show that low shear rates particles seem to interconnect trying to form a three-dimensional network, whereas particles at high shear rates seem to have not undergone secondary aggregation, thus forming small, separated particles.

1.5.2.3 Protein concentration

A higher protein concentration increases the collision probability of two unfolded proteins, which increases the aggregation. Increasing the protein concentration was shown to increase the reaction rate during denaturation (Wolz and Kulozik 2015). The increased protein concentration mainly affected the aggregation of the proteins. Since there is an equilibrium between unfolded protein and aggregated protein, a faster aggregation involves faster overall denaturation kinetics (Tolkach and Kulozik 2007). Under shear stress Wolz et al. (2016b) found that the aggregates formed get smaller, dense, rounder, and more compact with increasing protein concentration due to the increased shear stress acting on the particles.

The protein concentration during heating mainly is of relevance if a gel network or separate aggregates are formed. The critical gelation concentration is the minimum protein concentration needed to form a continuous gel network. This critical gelation concentration is dependent on pH, ionic strength and mainly on protein source (Creusot et al. 2011). For whey protein, this critical gelation concentration is around 15% at pH 7 in the absence of lactose (Nicolai et al. 2011b). Potato protein already starts gelling at concentrations of 3%, which is much lower than for whey proteins (Creusot et al. 2011; Schmidt et al. 2019). The low gelling concentration of potato protein can be explained by its high exposed hydrophobicity (Schmidt et al. 2019; Creusot et al. 2011). Salt-extracted pea protein was found to be from a gel network at a 5.5% protein concentration (Sun and Arntfield 2010). However, for pea protein, the minimum gelation concentration was dependent on the extraction method. Commercial pea protein and alkali extracted and isoelectric precipitated pea protein showed a much higher minimum gelation concentration of 14.5% and 16% at neutral pH, respectively (Sun and Arntfield 2010; O'Kane et al. 2005). For pea protein not only extraction method influences the minimum gelation concentration, but also the legumin to vicilin ratio and therefore the cultivar (O'Kane et al. 2005).

1.5.2.4 pH

The pH of the protein solution affects the reaction kinetics and denaturation temperature in whey, potato, and pea protein (Zúñiga et al. 2010; Andlinger et al. 2021c; Sun and Arntfield 2011). For β-lactoglobulin, a minimum reaction rate can be found in the unfolding limited temperature area. In the aggregation limited temperature area, the

reaction rate is highest for pH values around the isoelectric point between pH 4 and 5 (Tolkach and Kulozik 2005). A shift in pH does not only impact the reaction kinetic, but also aggregate morphology, size, and protein-protein interaction. This is schematically depicted in Figure 1-6 for β-lactoglobulin. Aggregates heated closer to the isoelectric point of the protein tend to be bigger than aggregates heated further away from the isoelectric point. Next to this, the reactivity of the thiol groups changes with the pH value. It increases with pH further away from the isoelectric point, whereas non-covalent bonds are more important in the formation of aggregates closer to the isoelectric point (Zúñiga et al. 2010; Andlinger et al. 2021c; Zhang et al. 2020a). This also affects the morphology of the aggregates at different pH values. Microscopic photographs of β-lactoglobulin aggregates formed at pH 2, pH 5.8, and pH 7 are shown in Figure 1-7.

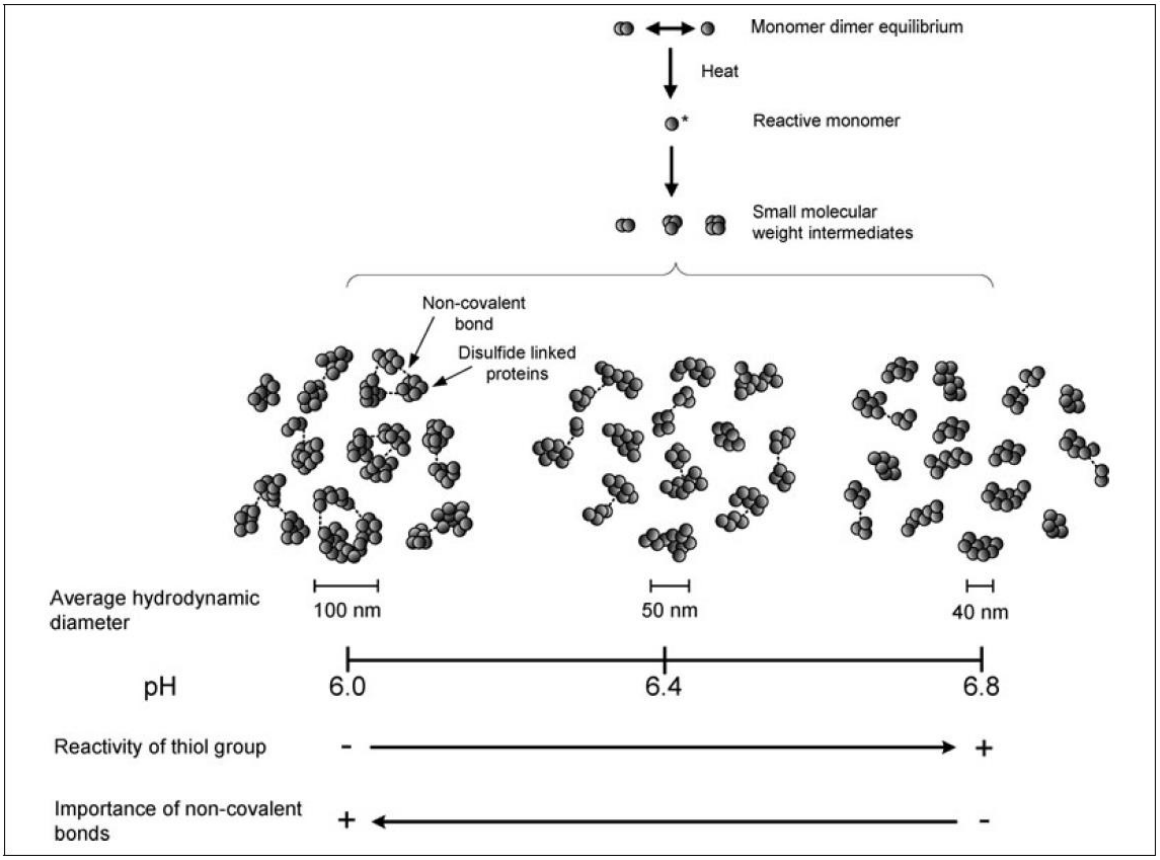

Figure 1-6: Schematic overview of β-lactoglobulin aggregation at different pH values (Zúñiga et al. 2010).

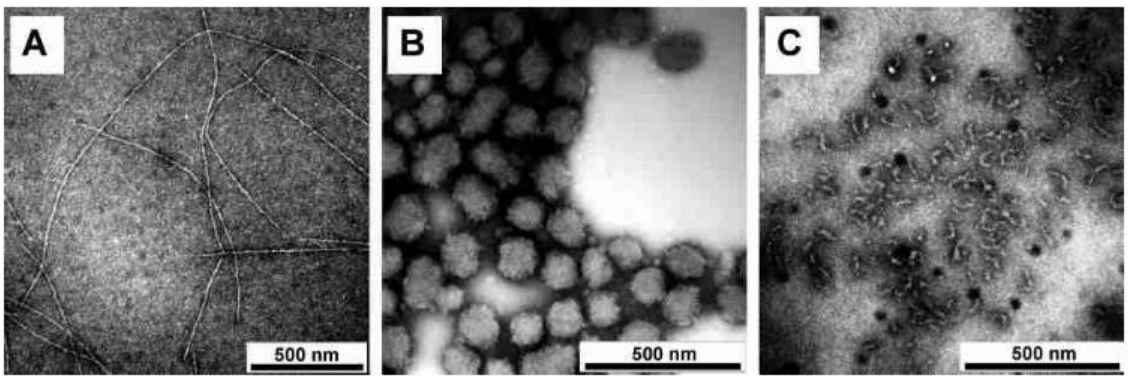

Figure 1-7: TEM micrographs of heating a 1 % β-lactoglobulin protein solution at pH 2.0 (A), pH 5.8 (B), and pH 7.0 (C) (Jung et al. 2008).

At pH 2 rod-like aggregates are obtained. They are also called fibrils. During heating at acidic pH, the protein hydrolysis and the peptides rearrange and interact with each other forming rod-like aggregates, which has also been found for pea protein (Munialo et al. 2014). At pH 5.8, which is the isoelectric point of β-lactoglobulin spherical aggregates are formed and at neutral pH worm-like primary aggregates are formed. These worm-like aggregates are also much smaller than the rod-like aggregates. At the isoelectric point of a protein, the net charge is zero and all repulsive forces are minimized. Thus, aggregation of the protein is favoured and bigger spherical aggregates can be formed (Jung et al. 2008; Nicolai et al. 2011b). Gels at pH values further away from the isoelectric point are transparent and gels at pH values close to the isoelectric point are turbid due to the aggregate structure of whey and potato protein (Schmidt et al. 2019)

1.5.2.5 Ionic strength

Ionic strength influences the aggregation of whey, potato and pea protein due to charge screening (Sun and Arntfield 2011; Nicolai and Durand 2013; Delahaije et al. 2015). Regarding reaction kinetics, the effect of ionic strength on the denaturation and aggregation of whey protein was bigger than that on potato protein (Delahaije et al. 2015). Overall reaction rate increases with increasing ionic strength (Pots et al. 1999; Delahaije et al. 2015). Regarding aggregates structure, a high ionic strength has a similar effect as a pH close to the isoelectric point, which is speculated to be due to micro phase separation (Nicolai and Durand 2013). A schematic representation of the influence of ionic strength on protein aggregation and gelation is shown in Figure 1-8.

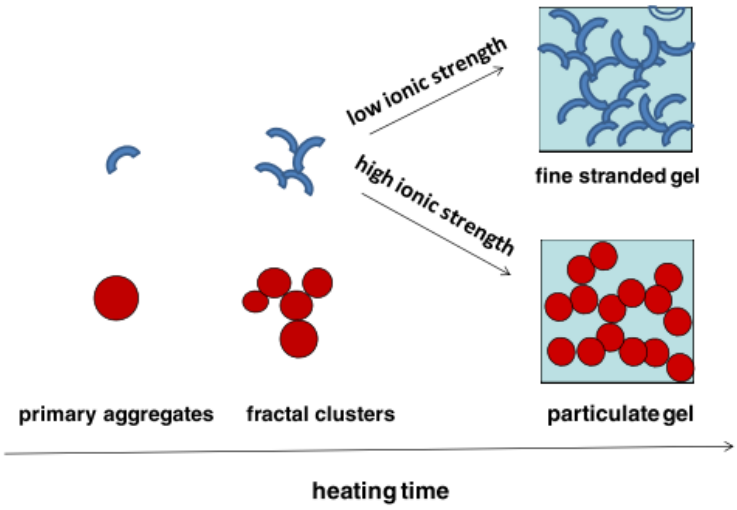

Figure 1-8: Schematic representation of the effect of ionic strength on the aggregate formation and gelation of proteins (Nicolai and Durand 2013).

Particulate gels and aggregates are formed at pH close to the isoelectric point or high ionic strength. There are two routes regarding how these particulate aggregates are formed. One route is simply to choose a pH close to the isoelectric point, where spherical aggregates are formed, which results in a particulate gel by secondary aggregation. The other route is establishing a high ionic strength at a pH far away from the isoelectric point, where first fine stranded aggregates are formed and then spherical

particles by secondary aggregation, which randomly associate to a particulate gel followed by micro-phase separation (Nicolai and Durand 2013; Ako et al. 2009). A state diagram about the influence of salt concentration and protein concentration is shown in Figure 1-9.

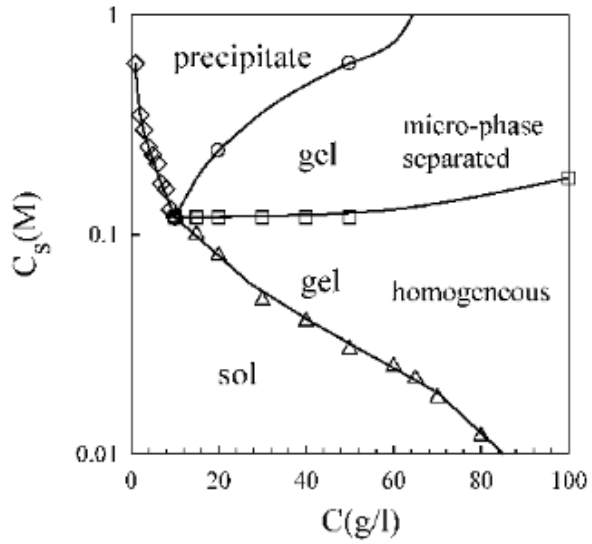

Figure 1-9: State diagram of influence of protein (C) and NaCl (C_S) concentration on β-lactoglobulin state at pH 7 (Ako et al. 2009).

From this state diagram, it becomes clear that not only the morphology of the gel and aggregates are dependent on the salt concentration, but also the gelling point. With a higher salt concentration, the gelling point decreases. Similar findings have been found for potato protein (Schmidt et al. 2019)

For pea protein, the opposite effect has been reported. With increasing NaCl concentration the gelling point increased for a protein concentration of 14.5% at natural pH of 5.65 (Sun and Arntfield 2011). A NaCl concentration range of 0 M to 2 M was tested. At 0 M NaCl, the gelation point was at 60.15°C and increased to 93.65°C at 1.5 M. For the 2 M NaCl sample, no gelation point was found by heating up to 95°C. Pea proteins, especially the globulins, are low in solubility at neutral pH without the addition of salt and become better soluble at higher salt concentrations (Tanger et al. 2020). At low salt concentrations, the globulins form micelles with their hydrophobic moieties pointed towards the centre and polar regions towards the outer aqueous solution. These micelles are thermodynamically more stable than single native globulins (Lam et al. 2018). The addition of salt adds to the thermal stability of the globulin by stabilization of its quaternary structure (Tanger et al. 2020; Sun and Arntfield 2011; Mession et al. 2013). The addition of salt has an effect on the protein and the dispersion medium. One way, how salt stabilizes the protein structure is by reduction of inter- and/or intramolecular chain repulsion by charge-shielding of the salt. The other is by weakening the hydrogen-bonded structure of the water, which affects the electrostatic and hydrophobic interaction of the water with the protein. This effect is dependent on the type of salt described in the lyotropic series (Damodaran 1988; Hippel and Schleich 1969;

Choi and Ma 2007). However, under shear stress particle size of pea protein aggregates was more dependent on pH than on ionic strength (Zhang et al. 2020a). Until 0.3 M NaCl pea protein gels became stronger and above that ionic strength, they became softer (Sun and Arntfield 2011).

1.5.2.6 Lactose

The effect of remaining sugars in pea and potato protein on the thermal reaction kinetics or aggregation behaviour has not been studied, yet. However, their effect could be similar to the better-analysed effect of lactose on the thermal reaction kinetics and aggregation behaviour of whey protein. A higher lactose content was shown to increase the bend temperature of whey protein (Spiegel 1999a). Lactose was found to have a heat stabilizing effect by preferential exclusion, which leads to better hydration of the protein. At high lactose content, the unfolding of the protein is slower, but aggregate growth is stronger. This leads to more loosely packed particles with a higher water holding capacity (Spiegel 1999b). Under shear stress, the aggregate size was reported to be higher with increasing lactose concentration (Spiegel 1999b).

1.5.2.7 Relevant types of molecular interactions during aggregation and gelation

Protein-protein interactions can be divided into two groups: covalent and non-covalent bonds. Covalent bonds are disulphide bonds. Non-covalent bonds are calcium bridges, electrostatic interactions, hydrogen bonds, van-der-Waals bonds and hydrophobic interactions. A schematic overview of the interactions is given in Figure 1-10.

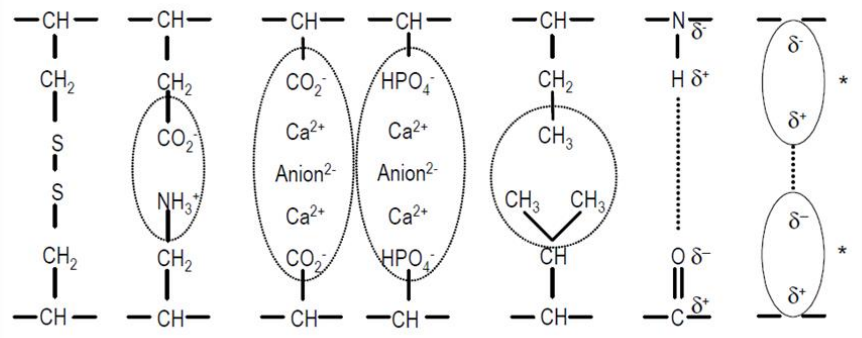

Figure 1-10: Schematic presentation of covalent (disulphide bonds (SS)) and non-covalent protein-protein interactions (electrostatic interactions (EB), calcium bridges (CaB), hydrophobic interactions (Hy), hydrogen bonds (WB) and van-der-Waals interactions (vdW)) based on (Nakai and Li-Chan 1988; Oakenfull and Fenwick 1977; Keim and Hinrichs 2004; Blond et al. 2005)

Disulphide bridges occur when two free thiol groups react with each other. For this, the proteins need the amino acids cysteine and/or methionine, because they are the only two amino acids containing a sulphur group. A protein can also contain an intra-molecular disulphide bridge within its native structure for example β-lactoglobulin, α-lactalbumin and legumin (Shand et al. 2007; Nicolai et al. 2011b). Upon heating, this disulphide bridge can react with a free thiol group and start a thiol-disulphide exchange, connecting several proteins via disulphide bridges. The reaction ends, when a free thiol

group reacts with a free thiol group. The reaction of two free thiol groups and the thiol-disulphide interchange reaction is schematically shown in Figure 1-11

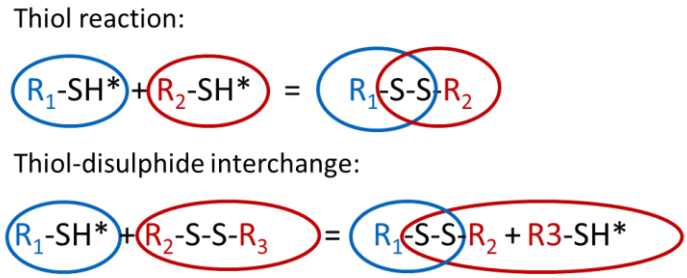

Figure 1-11: Schematic representation of the thiol reaction and the thiol-disulphide interchange.

This thiol-disulphide interchange is the main protein-protein interaction for whey proteins at neutral pH above denaturation temperature (Havea et al. 2004; Havea et al. 2009). Upon cooling down after heat treatment the intensity of disulphide bonds decreases (Bowland et al. 1995; Martin et al. 2014). Shear stress can enhance disulphide bond formation upon heating (Evans 2001).

Electrostatic interactions are interactions that are based on the attractive forces between two oppositely charged polar regions of proteins. This is similar to hydrogen bonds. In hydrogen bonds these two oppositely charged polar regions are a negatively charges oxygen molecule and a positively charged hydrogen molecule. For these interactions, the protein needs to have polar regions. The polarity of the protein is dependent on pH. Van-der-Waals interactions occur between nonpolar molecules. Due to electron shifting within the molecule gets temporally polar inducing an electron shift and temporally polar in surrounding molecules, which generates an attractive force between the temporarily oppositely charged polar regions of the molecules. Electrostatic interactions, hydrogen bonds and van-der-Waals interactions decrease in strength intensity upon heating at higher temperatures (Bowland et al. 1995).

Hydrophobic interactions are interactions between non-polar regions, which are low in water solubility. These interactions increase with increasing temperature (Bowland et al. 1995; van Dijk et al. 2015).

Calcium bridges connect two negatively charged polar regions via a negatively charged anion. This protein interaction is not of relevance for whey, potato and pea protein and therefore will not be discussed in more detail.

1.5.2.7.1 Protein interactions between pea proteins

Pea proteins, globulins and albumins, contain free thiol groups and disulphide bridges and therefore could theoretically start a thiol-disulphide interchange reaction (Chihi et al. 2016). However, it has been found that covalent bonds are only a minor part of protein-protein interactions and non-covalent bonds dominate in most cases (Chihi et al. 2016; Sun and Arntfield 2012; Mession et al. 2013). A proposed aggregate structure of pea protein globulin in comparison to β-lactoglobulin is shown in Figure 1-12.

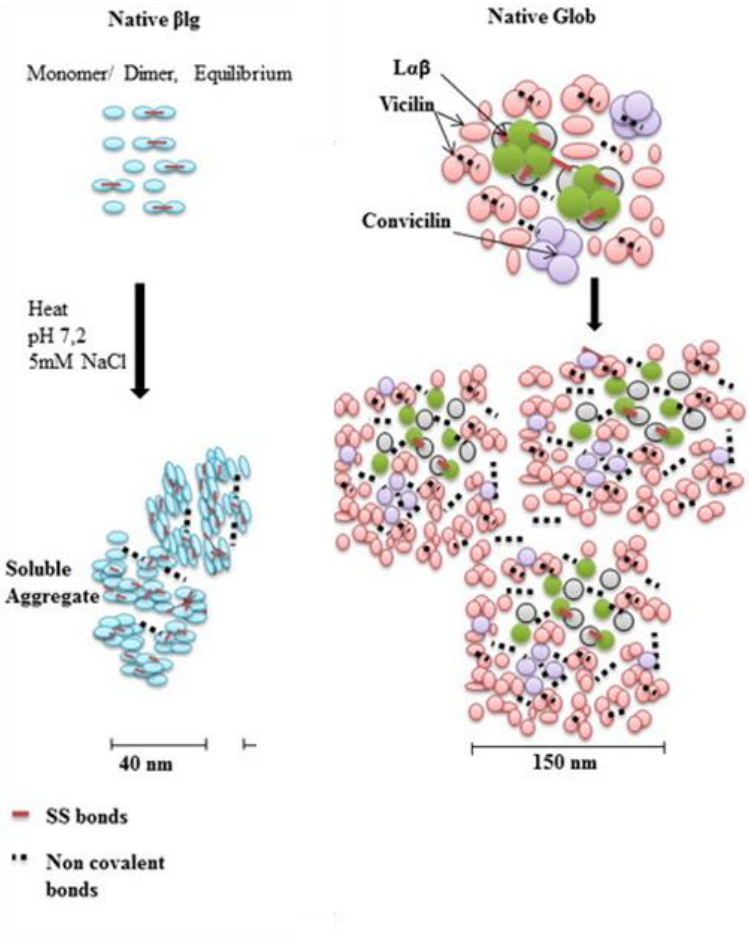

Figure 1-12: Schematic representation of pea protein globulin aggregates in comparison to β-lactoglobulin aggregation (adapted from (Chihi et al. 2016)).

Protein-protein interactions are dependent on pH. At higher pH, the impact of disulphide bonds increases, however, non-covalent interactions still dominate (Felix et al. 2017). When heating pea protein, Chihi et al. (2016) found an increase in free thiol groups and a decrease in disulphide bridges. This was the opposite to the behaviour of heating β-lactoglobulin. The authors explained their results with the disruption of pre-existing disulphide bonds and simultaneous random aggregation via non-covalent interactions. This results in a decreased accessibility of the free thiol-groups. Similar results were reported by Mession et al. (2013), who suggested that pea proteins aggregate fast via thermally exposed, previously buried hydrophobic groups. Yang et al. (2021) found that also the legumin to vicilin ratio has an impact on the gelation behaviour of pea protein and their pre-denaturation degree. Pre-denatured proteins can aggregate rapidly upon heating via already exposed reactive groups. However, the aggregation can hinder further denaturation due to steric hindrance, and therefore leading to a loose network (Yang et al. 2021).

Summarizing, disulphide bond formation when heating pea protein is possible, however, their role decreases during aggregation, because of more and more dominant hydrophobic interactions and rapid aggregation. Aggregation is also dependent on the pre-denaturation degree of the pea proteins.

1.5.2.7.2 Protein interactions between potato proteins

The main potato protein only contains one free thiol group and no intramolecular disulphide bonds, thus only two patatins can be connected via disulphide bonds and covalent bonds never form a continuous network (Creusot et al. 2011). The reactivity of the thiol group was found to be dependent on pH. The more alkaline the medium, the more disulphide bridges are formed (Andlinger et al. 2021c). However, since patatin has a high exposed hydrophobicity, patatin first aggregates via non-covalent bonds and disulphide bonds are formed at a later stage (Andlinger et al. 2021c; Pots et al. 1999). A schematic representation of the aggregation mechanism of patatin is shown in Figure 1-13.

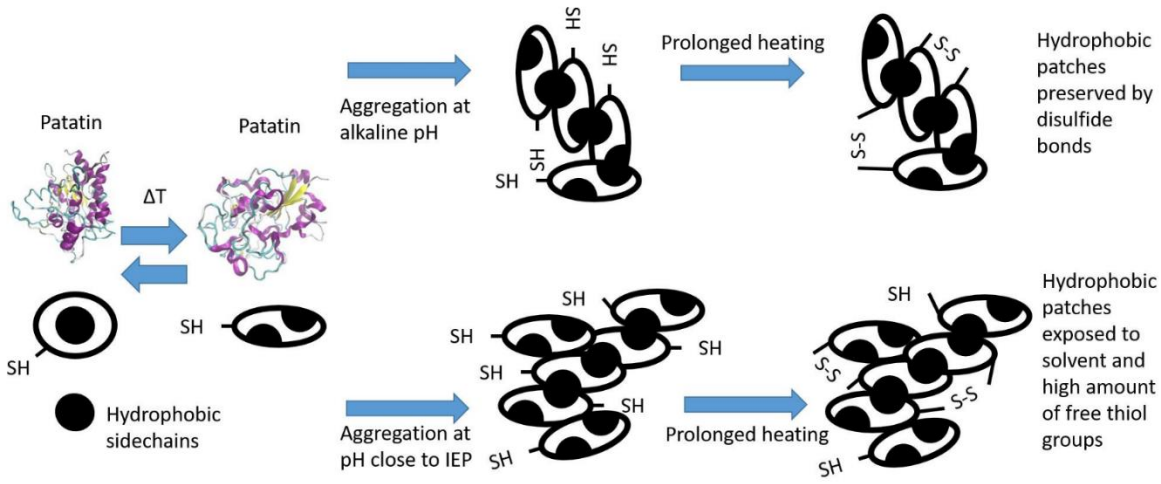

Figure 1-13: Proposed aggregation mechanism of patatin at alkaline pH and close to the isoelectric point (Andlinger et al. 2021c).

The main protein-protein interactions are hydrophobic interactions. The closer the pH is to the isoelectric point, also electrostatic protein-protein interactions play a role in aggregation (Pots et al. 1998b; Andlinger et al. 2021c).

1.5.2.7.3 Protein interactions between whey proteins

Both main whey proteins contain disulphide bonds. β-lactoglobulin also contains a free thiol group. Therefore, whey proteins can undergo a thiol-disulphide interchange reaction. Disulphide bonds are the dominant protein interaction in whey protein at neutral and alkaline pH (Monahan et al. 1995; Sava et al. 2005). As already explained above, the reactivity of the thiol-group increases with increasing pH (Zúñiga et al. 2010). A schematic aggregation mechanism for β-lactoglobulin is shown in Figure 1-6. In contrast to potato protein, aggregation is suggested to occur first via thiol-disulphide interchange and then the primary aggregates react further with each other via non-covalent bonds (Zúñiga et al. 2010). At pH close to the isoelectric point thiol-disulphide interchange is less important than electrostatic interactions and aggregates are mainly formed via electrostatic interactions, which is also shown in Figure 1-6 (Sava et al. 2005; Zúñiga et al. 2010).

1.5.2.8 Determination of protein interactions in gels and aggregates

There are several methods to determine interactions between proteins in gels and aggregates. These methods are of great importance for understanding gel and aggregate

structures. One option to determine the number of disulphide bonds and amount of three thiol groups is the spectrophotometric “Ellman’s assay”, reducing and non-reducing SDS-PAGE (sodium dodecyl sulphate polyacrylamide gel electrophoresis) or via RP-HPLC method for quantification of free and total thiol groups (Kurz et al. 2020; Hoffmann and van Mil 1997; Leeb et al. 2018). However, these methods are limited to the quantification of disulphide bonds.

Another method is to use protein-blocking agents. One example is N-Ethylmaleimide (NEM), which blocks the formation of disulphide bonds (Sun and Arntfield 2012). These blocking substances are added to the protein solution before heat treatment. Therefore, it can interact with the protein during heating and alter the aggregation and gelation process. NEM for example was shown to promote hydrophobic interactions in soy bean globulins (Hua et al. 2005) and β-lactoglobulin (Xiong et al. 1993). Thus, using blocking substances can give a falsified image of the protein interactions involved in the aggregation and gelation process.

A third method is to use a protein interaction assay (Tanger et al. 2021a). In this method, the nitrogen solubility of the gel in different buffers is determined. From this solubility, the amount of the different protein interactions can be calculated. The buffers contain protein interaction cleaving substances. Thus, these substances cleave the protein interaction and by doing so make the protein soluble. Buffer systems used in literature contained sodium dodecyl sulphate (SDS) (Keim and Hinrichs 2004; Shimada and Cheftel 1988; Martin et al. 2014), urea (Martin et al. 2014; Shimada and Cheftel 1988; Felix et al. 2017; Gómez-Guillén et al. 1997), β-mercaptoethanol (Martin et al. 2014; Shimada and Cheftel 1988; Gómez-Guillén et al. 1997), and dithiothreitol (DTT) (Keim and Hinrichs 2004; Shimada and Cheftel 1988). An overview of the type of protein interaction these cleaving agents cleave is given in Table 1-3. Within this approach, the gel is dissolved in the buffers and crushed. Then, the insoluble part is removed by centrifugation and the protein content of the supernatant is determined.

Table 1-3: Overview of reagents used for disruption of chemical bonds between proteins.

Reagent	Reported bonds to be disrupted	Source
Sodium dodecyl sulphate (SDS)	Hydrophobic interactions, ionic interactions	(Havea et al. 2009; Baldwin 2010)
Urea	Hydrophobic interactions, hydrogen bonds	(Cavallieri et al. 2007; Baldwin 2010)
β-mercaptoethanol	Disulphide bonds	(Cavallieri et al. 2007)
Dithiothreitol (DTT)	Disulphide bonds	(Havea et al. 2009; Baldwin 2010)

1.5.2.9 Rheological measurements for gel analysis

Protein gels are frequently analysed using oscillatory rheological measurements. During these measurements, G’ is the storage modulus, which described the elastic part, and G’’ is the loss modulus, which describes the viscous part. These two values are

calculated from the deformation of the samples. For these calculations, a two-plate model is used to describe several parameters as shown in Figure 1-14.

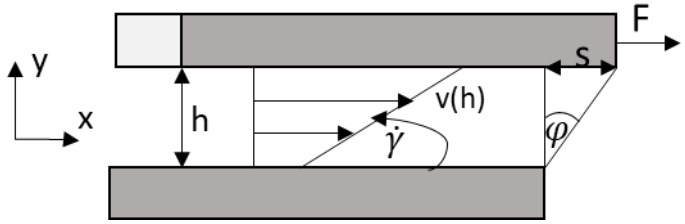

Figure 1-14: Two-plate model with labelled parameters.

Due to the impact of the applied force F on the sample, a deflection s by the deflection angle ϕ is caused. The ratio of the deflection s and the gap between the plates h gives the shear deformation γ:

$$\gamma\,[-] = \frac{s}{h} \tag{1-2}$$

$$\gamma\,[-] = tan\varphi \tag{1-3}$$

The shear rate $\dot{\gamma}$ is defined as the time derivative of the shear deformation, which also gives information about the relation of the velocity v(h) as a function of the distance between the two plates h:

$$\dot{\gamma}\,[\frac{1}{s}] = \frac{dv}{dh} \tag{1-4}$$

The shear stress τ gives the relation of applied force F and the certain area A of the upper plate:

$$\tau\,[Pa] = \frac{F}{A} \tag{1-5}$$

The viscosity η is defined as the flow resistance of the sample due to frictional forces between the moving plate and the sample:

$$\eta\,[Pa\;s] = \frac{\tau}{\dot{\gamma}} \tag{1-6}$$

Plotting the relation of shear stress τ and shear rate $\dot{\gamma}$ is also called flow curve and gives information about a fluid material. The flow point τ_f is the shear stress from which an original solid starts to flow and becomes liquid. γ(t) and τ(t) are in ideal case sinusoidal functions. Ideally, elastic materials show no phase shift between the two functions τ(t) and γ(t), according to the phase shift angle δ=0 ° whereas ideally, viscous materials show a phase shift by δ=90 °. For a viscoelastic behaviour, the phase shift angle δ is between those two extrema, 0 °< δ<90 °. Using Hooke's law, following equation is obtained:

$$\tau(t) = G * \gamma(t) \tag{1-7}$$

G* is called the shear modulus and is a material-specific constant and gives evidence about its stiffness. The relationship between G* and the storage modulus G' and loss modulus G'' is given in (1-8) to (1-9):

$$G^* \,[\mathrm{Pa}] = \frac{\tau(t)}{\gamma(t)} \tag{1-8}$$

$$G^* \,[\mathrm{Pa}] = \sqrt{G'^2 + G''^2} \tag{1-9}$$

The loss factor tanδ displays the relation between dissipated and stored deformation energy and gives the ratio of viscous and elastic behaviour as shown in equation (1-10):

$$tan\delta = \frac{G''}{G'} \tag{1-10}$$

A substance with a higher G' than G'' value is defined as a gel and a tan δ of bigger than 1 (Mezger 2019; Mitchell 1980). The gelling point is defined as G' = G'' and tanδ = 1 (Mezger 2019; Mitchell 1980).

In order to assess the viscoelastic characteristics of a gel, the measurement has to be performed in the linear-viscoelastic- (LVE) region. In this region, G'(Y) and G''(Y) are on a constant plateau and the sample is not destroyed or damaged during the measurement. To determine the LVE region an amplitude sweep is performed. In this test, the amplitude is increased, while frequency and temperature are constant. An example graph for a representative amplitude sweep is shown in Figure 1-15. The LVE region and the flow point, which will be introduced below, are labelled.

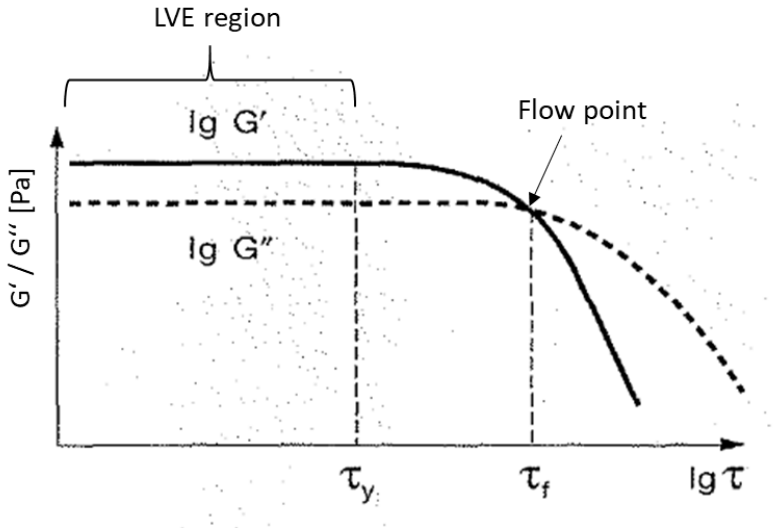

Figure 1-15: Representative amplitude sweep of a viscoelastic sample (Mezger 2019).

The amplitude threshold τ_{yi} is the amplitude, which marks the limit of the LVE region. For calculation of these normally the G' curve is taken. There are two ways to calculate this threshold value. One is to calculate the interception of the tangent of the downward curve and the extension line of the LVE plateau. The other is to take the point where

the G' deviates a before set tolerance limit (most of the time 5% or 10%) of the plateau (Mezger 2019). When leaving the LVE region, the sample is irreversibly changed in structure. Due to this, the LVE region of a new sample has to be determined before meaningful measurements can be started. The flow point τ_f is the point where G' and G'' crossover and gel structure is destroyed, such that it becomes fluid and begins to flow.

The gelation process during thermal treatment can be monitored. Interesting during these measurements is the course of the G' during cooling after thermal treatment. With decreasing temperature, hydrophobic interactions and disulphide bonds decrease in intensity (van Dijk et al. 2015) and electrostatic interactions and hydrogen bonds increase in intensity (Bowland et al. 1995). Thus, the ratio of the $G'_{cool\ gel}$ to $G'_{hot\ gel}$ can yield valuable information about the type of protein interactions within the gel. A high $G'_{cool\ gel}$ to $G'_{hot\ gel}$ value indicates a high amount of electrostatic interactions and hydrogen bonds and a low $G'_{cool\ gel}$ to $G'_{hot\ gel}$ value indicates a high amount of disulphide bonds and hydrophobic interactions. The method has first been used by Bowland et al. (1995). They analysed heat-induced whey protein isolate gels adding chaotropic and kosmotropic salts. The method has also been applied to analyse gels made from potato protein, egg white protein, whey protein, soy protein, pea protein, and lupine protein (Andlinger et al. 2021a; Andlinger et al. 2021b; Martin et al. 2014).

Another meaningful and used test in this study is the frequency sweep. In this test, the frequency ω is increased and amplitude and temperature stay constant. This test is also used to retain information about the time-dependent behaviour of the sample because the frequency is the inverse of the time. The G' is normally plotted against the frequency on a logarithmical scale, which in the ideal case leads to a linear curve. This curve can be described by using the following equation:

$$G' = n * \log(\omega) + K \tag{1-11}$$

From this, the slope n and y-intercept K can be calculated, which give information about the protein interaction in the gel. A slope closer to zero, thus a gel with lower frequency dependence gel is more formed by covalent interaction or elastic bonds. A higher frequency dependence and therefore a higher slope value is found for gels formed by non-covalent bonds, which is more a physical or viscous network (Creusot et al. 2011; Sun and Arntfield 2011). The strength of the molecular interactions expresses itself in the y-intercept (K) (Kim and Yoo 2009).

1.6 Microparticulation

1.6.1 Influencing factors during microparticulation on particle size

Microparticulation is a thermo-mechanical process, where heat and shear are controlled, to limit the aggregate size and inhibit gel formation. The effect of shear stress on aggregation of proteins is described in detail in 1.5.2.2. The resulting particles are called microparticles, or sometimes microgels. A schematic overview of the microparticulation process and the impact of the shear rate is given in Figure 1-16.

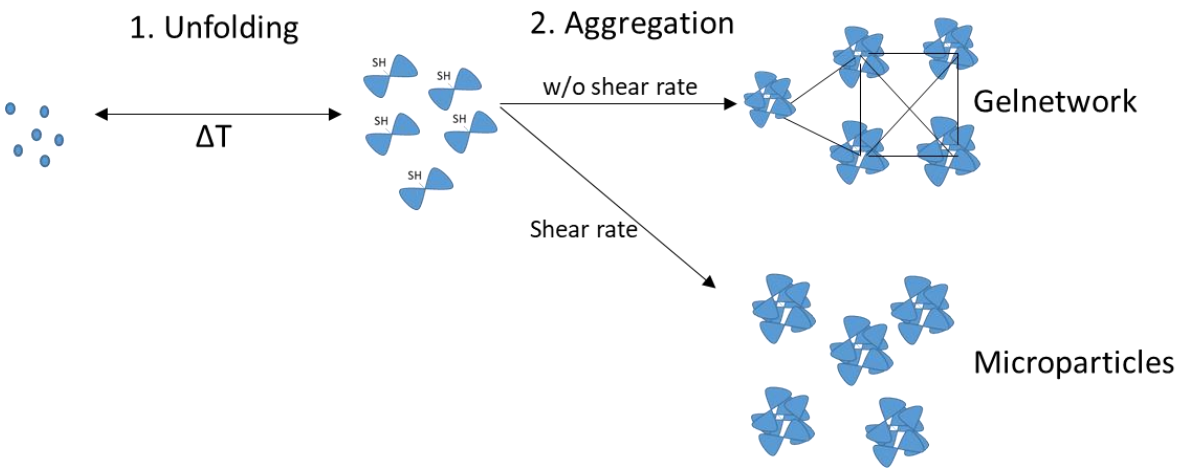

Figure 1-16: Schematic overview of the microparticulation process.

Heating and shearing can be applied simultaneously or sequentially. A simultaneous process would be in a scraped surface heat exchanger or extruder. Heating and shearing take place at the same time. In a sequential process, first, a gel or aggregates are produced by thermal treatment. After this, the particles are reduced in size by adding shear stress for example in a homogenizer or a dispersion unit. An overview of the methods is shown in Figure 1-17.

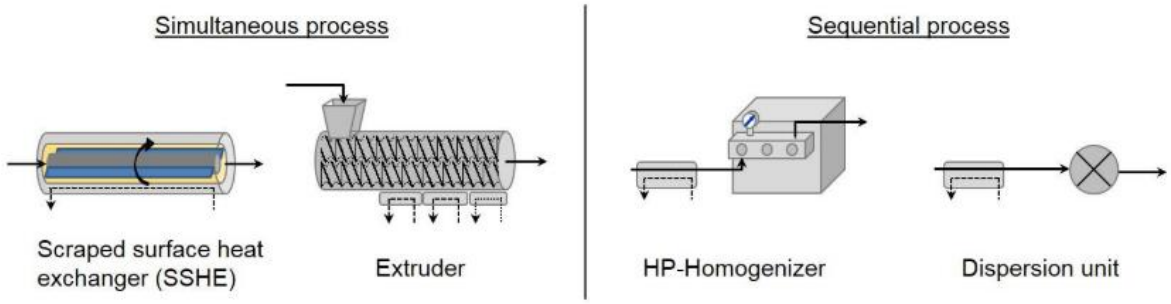

Figure 1-17: Overview of different microparticulation processes (Wolz 2018).

Singer et al. (1988) patented both the process and the use of microparticulated whey protein. They used a scraped surface heat exchanger and microparticulated WPC50 at acidic pH of 3.5 – 5.0 together with an emulsifier. The resulting particles were in a size range of 0.1 – 3 µm (Singer et al. 1988; Singer and Dunn 1990). NutraSweet (today CPKelco) launched a commercial fat replacer Simpless® based on this process. The patent is assigned to CPKelco today and microparticulated whey protein is still one of their products. Plock (1994) and Spiegel (1999a) analysed the microparticulation using a scraped surface heat exchanger. Particle size was found to increase with an increasing degree of denaturation and decreased with increasing shear rate and lactose concentration (Plock 1994). Spiegel (1999a) analysed microparticulation of whey protein at a higher degree of denaturation. He found that particle properties were dependent on the reaction kinetics and were dependent on temperature area, and unfolding limited or aggregation limited. Particulation was found to be dependent on lactose concentration and pH value (Spiegel 1999b; Spiegel and Huss 2002). The results

led to the creation of a commercial process with a specifically designed scraped surface heat exchanger (APV LeanCreme^{TM}, SPX Flow Technology). Also, Toro-Sierra (2016) used a scraped heat exchanger to generate whey protein microparticles.

Next to the scraped surface heat-exchanger also an extruder can be used to microparticulate proteins. The advantages of an extruder are the short residence times with a high degree of denaturation and the possibility to work with high viscosities, hence high protein concentration. This process has been used by Quéguiner et al. (1992) for whey protein isolate and Wolz (2018) for whey protein concentrate. Both used a twin-screw extruder. Quéguiner et al. (1992) analysed pH ranges of pH 3.5 - 4.5 and aimed for a semi-solid spread. This was achieved using an extruder barrel temperature of 90 - 100°C, 20% protein concentration and a screw speed of 100 -200 rpm. Due to the acidic pH protein aggregation occurred via electrostatic interaction in the absence of thiol-disulphide interchange reaction. Wolz (2018) analysed the microparticulation of WPC80 at neutral pH. She found that particle size decreased with increasing screw speed between 100 – 200 rpm. Extruder barrel temperature mainly affected the degree of denaturation. Particle size increased with increasing mass flow (Wolz et al. 2016a).

The sequential process comprises processes, where the protein solution is first heated and then sheared. This process has been used for several proteins. The heating step can occur in a tubular heat exchanger (Paquin et al. 1992), in a water bath (Zhang et al. 2020a), or a microwave discovery explorer (Amagliani et al. 2020). Following, shear treatment is performed by using a microfluidizer (Paquin et al. 1992) or a homogenizer (Zhang et al. 2020a; Amagliani et al. 2020). Since treatment methods and conditions were very different between the studies, a direct comparison is not meaningful. However, it has generally been agreed that the protein source has a big effect on the reduction in particle size by a homogenizer (Amagliani et al. 2020). Pea and soy protein microparticles resulted in higher particle sizes of 2 – 6 µm compared to potato and whey protein with 0.01 µm (Amagliani et al. 2020).

On a laboratory scale, shear apparatus such as closed cavity rheometer (Quevedo et al. 2020a) and rheometer (Moakes et al. 2015) are used to the analysed thermo-mechanical treatment.

1.6.2 Application

Microparticles can partially mimic the sensorical effect of fat, if they fulfil the necessary criteria, and are therefore proposed and applied as a fat replacer. Microparticles can generate a ball-bearing effect, which leads to the same creamy mouthfeel as fat. A schematic overview of the mechanism of the ball-bearing effect is seen in Fig. 1-18.

Fat droplets generate a creamy mouthfeel by lubricating the part between the tongue and palate. Microparticles roll between tongue and palate similar to ball-bearing. This also lubricates the mouth and leads to a creamy taste perception (Liu et al. 2016b; Cheftel and Dumay 1993). Particle properties, such as size and shape, are crucial to generate this ball-bearing effect. Too small particles are perceived as empty and too big particles are perceived as gritty and sandy (Kew et al. 2020; Singer and Dunn 1990).

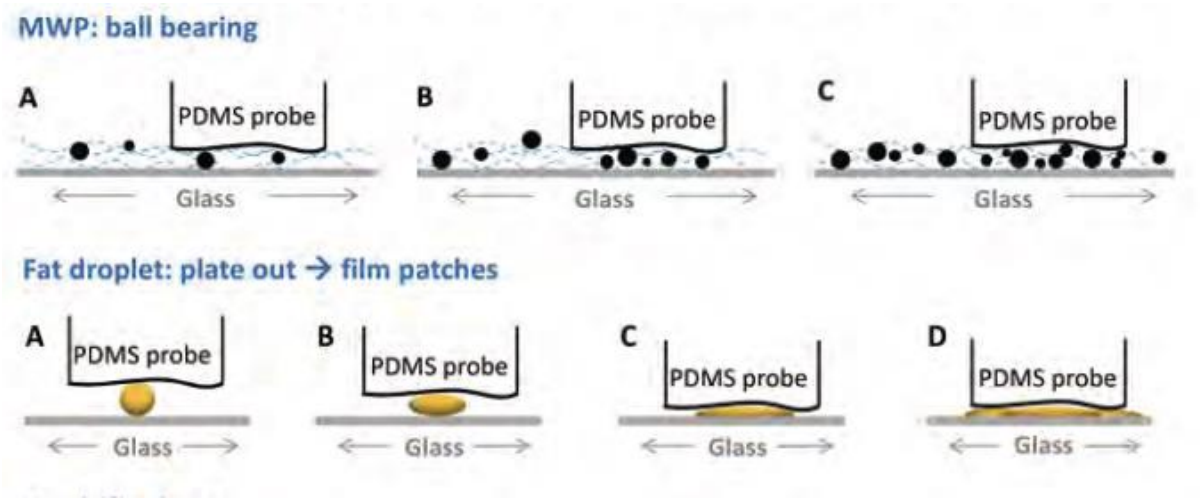

Figure 1-18: Schematic overview on the underlying lubrication behaviour of fat and microparticles (Liu 2016).

For whey protein microparticles a particle size of around 10 µm was found to be suitable (Kew et al. 2020; Spiegel 1999b; Wolz et al. 2016a; Yan et al. 2021). However, also shape and hardness of the particles were identified to influence the ball-bearing effect. For soft and spherical particles, the particle size threshold, from which particles were perceived as gritty, was higher than for hard and non-spherical particles (Engelen et al. 2005). Microparticles have been applied as fat reduces in several dairy foods such as cheese (El-Aidie et al. 2019; Urgu et al. 2019; Akin and Kirmaci 2015; Schädle et al. 2020; Steffl et al. 1999), yoghurt (Torres et al. 2011), kefir (Temiz and Kezer 2015), cookies (Aggarwal et al. 2016), and salad dressing (Liu et al. 2018a). In ice-cream, microparticles were also found to stabilize the structure and increased melt-down time (Koxholt et al. 1999). Next to this, microparticles can also be used to ensure gel strength and avoid syneresis in yoghurt (Ipsen 2017).

1.7 Extrusion

Extrusion is a process mainly used in the thermoplastic industry but is also used for the production of many food and feed products, such as expanded snacks, meat analogues, cereals and sweets (Cornet et al. 2021; Onwulata et al. 2001). During extrusion, products can be mixed, hydrated, sheared, compressed, conveyed, heated and shaped. Expansion of the product can occur during pressure drop upon existing the extruder (Cheftel et al. 1992; Cornet et al. 2021). The heating of the product occurs either directly via steam injection or double jackets and mechanical energy occurring by friction during shearing. Upon heating, proteins denature, starch gelatinizes, enzymes and microbes get inactivated, as well as toxic antinutrients to some extent (Cheftel 1986). Extrusion is divided in high moisture (< 30% water) and low moisture (10 – 30% water) extrusion (Cheftel et al. 1992). Within this work, it is focused on high moisture extrusion. Extruders vary in their design. They can contain one or more rotating screws. For food production, twin-screw extruders are of the highest relevance (Cornet et al. 2021). In this study, a co-rotating, intermeshing twin-screw extruder was used. Due to the constant interaction of the screws, the co-rotating, intermeshing twin-screw extruder shows a self-cleaning effect, a good heat transfer and conveying, a controlled narrow residence time distribution and a uniform, but flexible process (Cornet et al. 2021)

1.7.1 Extruder Set-up

The processing part of an extruder includes a liquid and a powder feeder, the rotating screws, which are inside the extruder barrel, and an end plate, where the die exists the extruder. A schematic overview of a twin-screw extruder is given in Figure 1-19.

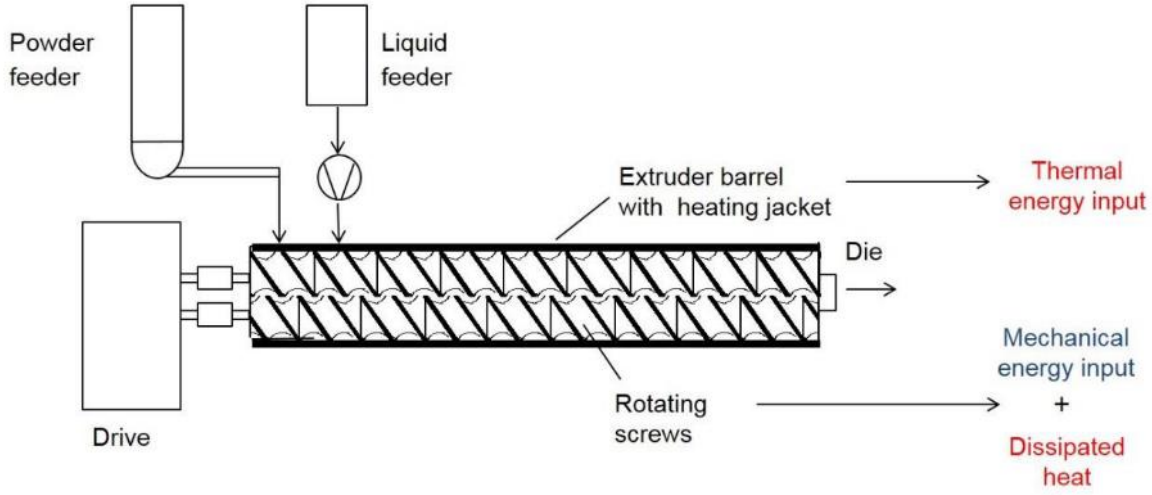

Figure 1-19: Schematic overview of a twin-screw extruder (Wolz 2018).

The electric drive generates the torque to convey and press the product through the die of the extruder. The feeding of the powdered raw material and the required amount of water happens by the mostly gravimetrically controlled powder feeder and with a pump for the liquid. The powder feeder is set at the beginning of the extruder barrel, whereas the liquid feeder can be at any place. The extruder barrel with the heating jacket heats the product. The extruder used in this study had nine heating segments, which are equipped with an independent temperature control except for the first segment. The segments are heated electrically and cooled with water. Depending on the choice of the end plate (i.e. the die), pressure can be build-up, which is done for an expanded snack, but not in this work (Cheftel et al. 1992). The screws are the most important part of the extruder, which influence the reaction occurring in the extruder. They rotate inside the extruder and convey, mix, and knead the product. The screws consist of a spine shaft, where the different screw elements are mounted on. The different screw elements can be removed from the spine shaft and the configuration of these can be changed. A set of the different elements with their different use is shown schematically in Figure 1-20.

The most often used elements are conveying elements. They convey the die through the extruder. They are usually only partially filled. Due to the low filling, they transfer only little energy and shear to the product (Harper 1986). Kneading and mixing elements increase the shear and mechanical input on the product. Reverse or left-handed elements increase the screw filling by conveying the die backwards. This also increases the residence time (Harper 1986; Cornet et al. 2021; Arêas 1992). Depending on the screw elements more or less shear stress can be generated (Onwulata et al. 2001). The production of meat analogues occurs in an extruder, where after the heating and kneading a cooling section follows, in which the fibrils are shaped (Cornet et

al. 2021; Osen et al. 2014; Cheftel et al. 1992). For microparticulation, the end plate is only a whole of 10 mm to prevent pressure build-up (Wolz et al. 2016a).

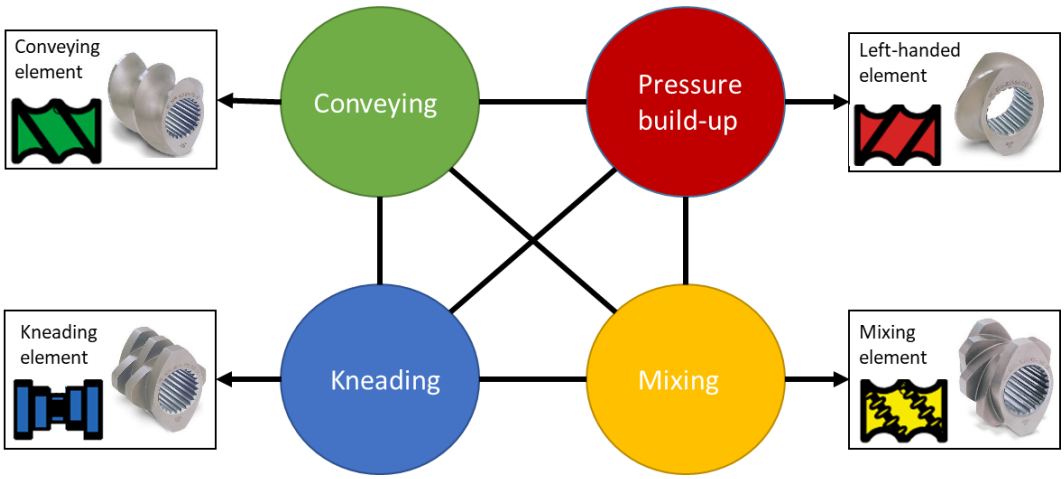

Figure 1-20: Schematic overview of different screw elements and their use.

Process parameters that can be changed during extrusion cooking are screw speed, screw configuration, mass flow, and extruder barrel temperature. The screw speed can affect particle size during microparticulation in an extruder by increasing or decreasing shear stress (Wolz and Kulozik 2017; Wolz et al. 2016a). It can also affect the protein-protein interactions within the particles because shear stress was found to promote thiol-disulphide interchange reaction (Choi and Ma 2005; Evans 2001). The mass flow affects the screw filling and therefore also the pressure and shear in the product (Yeh et al. 1992). The extruder barrel temperature affects the aggregation in the extruder, as already described in chapter 1.5.2.1.

1.8 Drying of microparticles

Drying describes the process of removing water from a fluid or semifluid by evaporation or vaporization. This increases the shelf-life of the product due to the decreased water activity. A short shelf-life was one of the major drawbacks of the successful implementation of whey protein microparticles in the first stage (Cheftel and Dumay 1993). In the following, the principles of spray-drying and freeze-drying are explained, because these are the two main drying methods used in this work.

1.8.1 Spray-drying

Spray-drying is usually used to dry fluids and is widely used in industry. It is time-efficient with high throughput and low energy consumption. A spray dryer consists of a chamber filled with hot air, typically inlet air ranges between 150°C and 220°C for food, where the liquid is dispersed (Kessler 2002). A schematic overview of a spray-dryer is given in Figure 1-21.

The liquid is dispersed via a nozzle or a dispersing plate into the hot air. This leads to a high surface of the liquid from which the water can evaporate by convective drying. The product temperature reaches 40°C to 50°C (Kessler 2002). The presence of air and elevated temperature can lead to oxidation reactions.

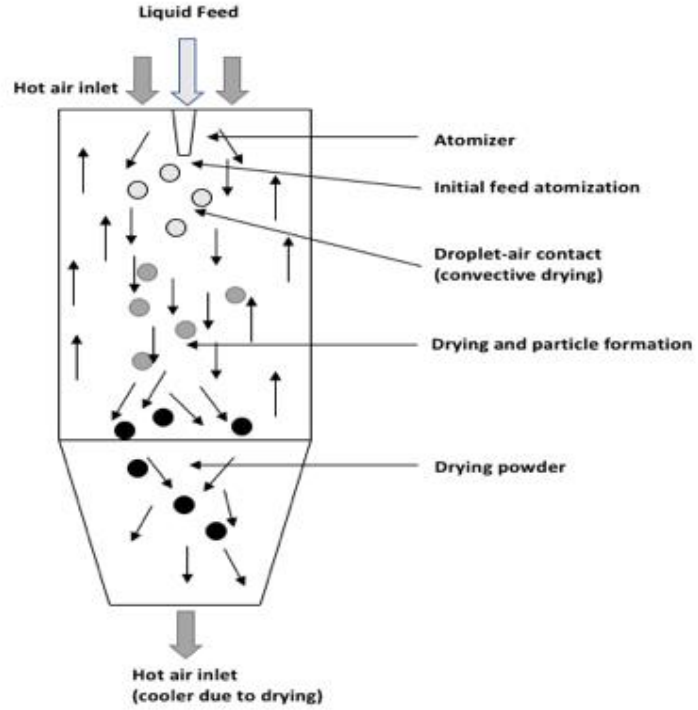

Figure 1-21: Schematic overview of a spray-dryer (Bhandari 2013).

Even though spray drying inlet and outlet temperatures are quite high and can be above the denaturation temperature of whey proteins (200/101°C – 160/89°C), these conditions do not significantly denature the whey protein during drying (Gaiani et al. 2010; Oldfield et al. 2005). Also, the size and morphology of spray-dried whey protein microparticles were not changed during spray-drying, which means that no interparticle bonds are created (Toro-Sierra et al. 2013; Toro-Sierra 2016).

In contrast to this, spray drying was found to affect protein-flavour binding (Cui et al. 2020). Co-spray drying of pea protein isolate with cyclodextrin was found to mitigate grassy, green, and beany off-flavour in pea protein, while preserving the same functional properties as a control pea protein isolate (Cui et al. 2020). In another study, solid dispersion-based spray-drying was found to even enhance the solubility of pea protein isolate and mitigate the off-flavour (Lan et al. 2019). The mitigation of off-flavour was explained by the unfolding of secondary structure by forming solid dispersions with gum arabic or maltodextrin during spray-drying (Lan et al. 2019).

1.8.2 Freeze-drying

Freeze-drying needs four times more energy than spray-drying, however, it is one of the mildest drying methods (Bhandari 2013). Freeze-drying is done in a vacuum and at low temperatures. For freeze-drying, the product has to be frozen before the drying step. In the drying chamber, the pressure is then decreased. A heating plate (radiation or microwave energy) conducts heat in the product so that ice crystals can sublimate. For that, the pressure and temperature have to be below the triplet point of 611.657 Pa and 273.16 K (Kessler 2002). This phase diagram for this process is shown in Figure 1-22.

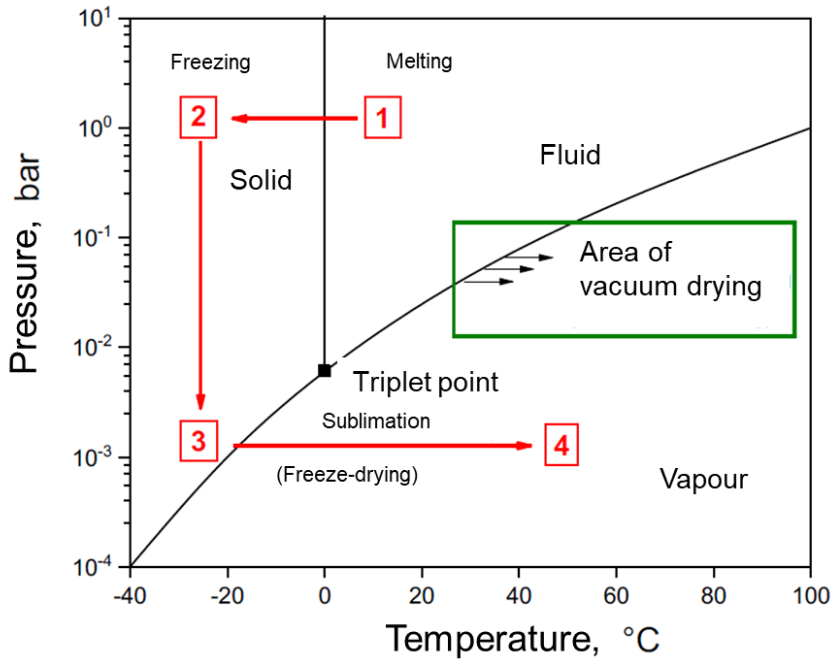

Figure 1-22: Phase diagram of water (modified based on (Kessler 2002))

The different steps during freeze-drying are labelled. During sublimation of the water, pores are created in the product. The porous structure emerges from the product surface to the core leaving holes in the places previously filled by ice crystals. The drying rate decreases with emerging drying (Kessler 2002). The drying constant is also dependent on the ice crystal size. The bigger the ice-crystals, the less dense the porous structure and the higher the drying rate (Wang and Chen 2005). After all ice-crystals are removed, water bound by sorption is removed (Kessler 2002).

The impact of freeze-drying on the particle size of microparticles has not been analysed, yet. Even though it is a very mild process, freeze-drying was found to affect the tertiary structure of proteins and polysaccharide complexes. Similar to spray-drying this can alter the flavour binding of proteins (Zhan et al. 2019). Freeze-drying is also one of the most popular methods during the extraction of pea proteins (Sun and Arntfield 2010; Stone et al. 2015; Kornet et al. 2021a; Rubio et al. 2014) because it is easy to control. However, freeze-dried pea protein isolate was found to be darker in colour and had a non-uniform size compared to spray-dried pea protein isolate (Tian et al. 1999).

1.9 Flavour

Food can be perceived visually, olfactory, gustatory, haptic, and auditory, thus with all our senses. All of these impressions determine, in brief, whether we like or dislike a food product. The term flavour describes all of these impressions. A-typical impressions are called off-flavour (Sondermann 1991). Therefore, flavour is defined as the sum of aroma and taste according to DIN 10950 (Sondermann 1991). Flavour molecules bind to our receptors in the mouth and nose, which then create a signal and a taste. An overview of how flavour molecules affect our food perception is given in Figure 1-23.

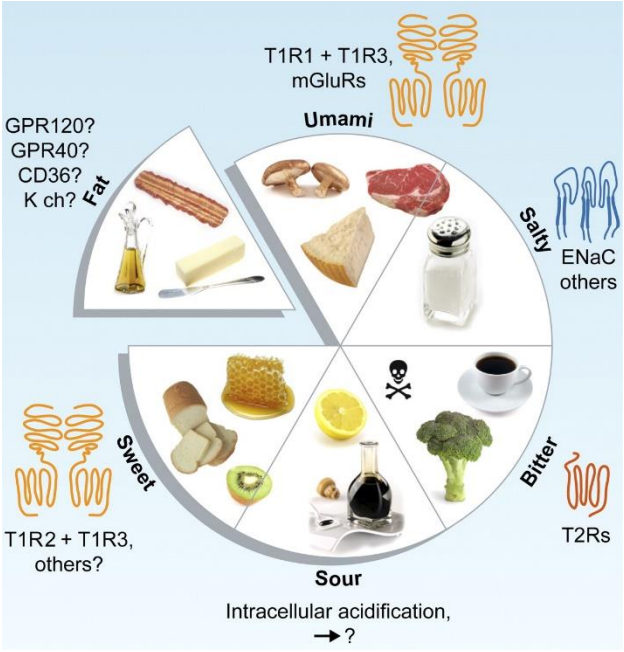

Figure 1-23: Overview of flavour perception in a food (Chaudhari and Roper 2010).

The flavour of food can be determined with sensory tests. Flavour molecules can be determined analytically via HPLC and GC methods.

1.9.1 The flavour of fat/creaminess

The most important attribute of fat is the perception of creaminess. The interaction of aroma, taste, and texture are responsible for the creamy perception (Mela 1988; Tournier et al. 2007). Since the textural effects have already been discussed in chapter 1.6.2, this chapter is focused on the aroma and taste part, which is only covered in brief, since this was mainly the part of the partnering research group. There are several volatiles, which were found to add to the creamy flavour of fat. These are for example octanoic acid, 3-methylbutanoic acid, and dimethyl sulfide (Hernández 2007). A positive and negative influence was also found for distinct concentrations of methanthiol (Hernández 2007). Schlutt et al. (2007) found that for milk fat semi-volatile long-chain δ-tetradecalactone, δ-hexadecalactone, and δ-octadecalactone are responsible for the creamy taste.

1.9.2 The flavour of pea protein

Pea protein isolates were found to have an off-flavour (Gläser et al. 2020). This means that the flavour was a-typical. The off-flavour was described to be grassy/beany and bitter/astringent, which is a challenge in the development of food containing pea protein isolate (Gläser et al. 2020). Gläser et al. (2020) found that octacosa- 6,9,19,22-tetraen was one of the key taste compounds responsible for the bitter taste in pea protein. The off-flavour mostly originates from the oxidation of polyunsaturated fatty acids. This can happen enzymatically by lipoxygenase and peroxidase or non-enzymatically by autoxidation and hydrolysis (Lv et al. 2011; Lan et al. 2019; Gläser et al. 2020). The flavour molecules bind via non-covalent interactions to the protein (Klotzbücher 2009; Schindler et al. 2012). However, the flavour of pea protein is also dependent on its processing history. Several processing steps were identified to improve the flavour of pea proteins and reduce the grassy/green/beany off-flavour. For example lactic acid fermentation was found to reduce off-flavours (Klotzbücher 2009; Schindler et al.

2012). Next to fermentation, also solid dispersion-based spray drying with maltodextrin, gum arabic or cyclodextrin was found to change the aroma profile and reduce off-flavours (Cui et al. 2020; Lan et al. 2019; Pang et al. 2015). Another method to decrease the off-flavour is by masking the flavour using cyclodextrins (Lan et al. 2019; Böttcher et al. 2015), where the flavour molecule is incorporated in the cyclodextrin ring. Next to these methods, thermal or non-thermal pre-treatments, which could inactivate lipoxygenase and peroxidase of the protein isolate were found to decrease the off-flavour. Such pre-treatments could be pressure treatments (Akyol et al. 2006; Quaglia et al. 1996; Wang et al. 2008), microwave heating (Jiang et al. 2016), and blanching and grinding (Lv et al. 2011). Additionally, also the extraction method of the pea protein from the pea flour was found to impact the off-flavour due to their protein conformation (Wang and Arntfield 2014)

2 OBJECTIVE AND OUTLINE

As already mentioned, controlled aggregation of whey protein leads to microparticles, which were found to be suitable as a fat replacement. Controlling the aggregation of whey protein is a key function to change their functionality. Next to a fat replacement, whey protein aggregates were also used to stabilize foams (Dombrowski et al. 2016), emulsions (Kurz et al. 2021), and can help in general to structure food. The aggregation process of interest in this thesis is the microparticulation process. As already said, the microparticulation process is a thermo-mechanical process, which, by adding a shear rate during thermal treatment, inhibits gel formation and results in particles in the size of micrometres, depending on the shear rate applied.

However, with the increasing world population and concerns about climate change, animal-based proteins cannot be the only protein source for humans anymore. Plant-based alternative proteins such as soy, pea, oat, and potato are of increasing interest for application in foods, due to their superior sustainability compared to animal-based protein for example whey protein. Currently, pea protein proteins are mostly used as meat alternatives and knowledge about pea protein is limited. Therefore, there is a continuous need for new insights into pea protein and altering its functionality by processing. In this thesis, the above named microparticulation process is used on the pea protein to increase their functionality and add a new concept of processing pea protein for food application.

Based on this, this thesis aimed to study the aggregation mechanism of pea protein with and without shear stress and on a small scale, rheometer, and a large scale, extrusion cooking. The main point of interest was to understand how to control pea protein aggregation to make it better suitable for food applications. For this, a bottom-up process, from native small protein to larger aggregates, and a top-down process, from large aggregates to smaller aggregates, were compared.

Since commercial pea protein, until today, is only available in denatured and aggregated form, as already observed long ago (Fuhrmeister and Meuser 2003). Therefore, “native” pea protein had to be extracted from pea flour first. Therefore, a comparison was made between different extraction methods described in the literature to determine the impact of the extraction method on the resulting pea protein product. The aim was to find the most suitable extraction method yielding best required protein nativity for further analysis and processing work.

Before analysis of aggregates, a reliable method for analysis of pea protein aggregates and gels had to be developed. The reason for this was that there was no suitable method for plant-based protein and whey protein for quantification of protein-protein interaction, which is essential for protein aggregation. This method could be used in the following studies to analyse the impact of process parameters on pea protein aggregation and be able to compare that with better-understood whey and potato protein aggregation.

In the third part, thermal aggregation of pea protein at varying pH and ionic strength was studied without shear stress in a gel system. A gel system has a high protein

concentration similar to the microparticulation processes used afterwards. This already resulted in valuable insights into pea protein aggregation, which could be used to hypothesize pea protein aggregation under shear stress.

After having gained insights into the aggregation of pea protein in a shear free system, shear stress during thermal aggregation was added on a small scale using a rheometer. The thermo-mechanical behaviour of pea protein was compared to whey protein and potato protein. Both the bottom-up process with extracted pea protein and the top-down process with commercial pea protein were analysed. With this as a starting point, the impact of extraction method of pea protein, pH and temperature on pea protein aggregation during thermo-mechanical treatment was analysed.

From the small-scale thermo-mechanical analysis, the aggregation process during a large-scale thermo-mechanical process using extrusion cooking was analysed. For this, only a top-down process was used, because of the large volumes of pea protein needed during extrusion cooking. The large volume could not be reached by laboratory extraction of pea protein. The impact of variation in extrusion process parameters on the aggregation of pea protein was analysed.

In the last part, the applicability of the pea protein in a model food was analysed. As already stated above, microparticles can be used as a fat replacer and structuring agent in food systems. Therefore, the effect of incorporation of pea protein microparticles in comparison to potato protein microparticles on texture and sensory properties during fat replacement in a model food was examined in cooperation with a project partner (Chair of Food Chemistry and Molecular Sensory Science).

The following chapters are organised along with the related published papers, discussing the topics mentioned above in the same order.

3 RESULTS

3.1 Influence of extraction conditions on the conformational alteration of pea protein extracted from pea flour

Summary and contribution of the doctoral candidate

Since commercially available pea protein was found to be already highly denatured and aggregated, different extraction methods for extracting pea protein from pea flour were compared and analysed. These extraction methods were alkali extraction – isoelectric precipitation, micellar precipitation and salt extraction. In alkali extraction – isoelectric precipitation the protein is solubilized at alkaline pH 9 and precipitated at its isoelectric point of pH 4.5 and then freeze-dried. This extraction was also tested in a modified version by changing the pH of 4.5 back to pH 7 before freeze-drying. In micellar precipitation, the protein is solubilized in 1 M NaCl and precipitated by reducing the salt content by diluting with demineralized water and subsequently freeze-dried. In salt extraction, the protein is solubilized in Na_3PO_4 and KCl and dialysed before freeze-drying. No precipitation step is included in salt extraction. The modified alkali extraction – isoelectric precipitation was found to have the highest yield. Micellar precipitation had the lowest yield. Due to the dialysis, the salt extraction was the extraction that took the longest. All extraction types including a precipitation step contained only globulins. Micellar precipitation showed the highest amount of legumin. Salt extraction was the only protein product, which also contained albumins. This made it the protein product with the highest solubility at all NaCl concentrations and all pH values with the lowest variation in particle size. The modified version of alkali extraction – isoelectric precipitation was better soluble than the unmodified version. Solubility of both alkali extraction – isoelectric precipitation protein products was lowest at their isoelectric point of pH 4.5, which went hand in hand with increased particle size. The solubility of micellar precipitated protein products was most dependent on salt concentration. Solubility was lowest at low salt concentrations and pH values of 5 to 6. This was due to the high amount of legumin in this protein product. Due to the strong alkaline pH during solubilisation, the salt extracted proteins were lowest in ‘nativity’. The method with the highest amount of ‘native’ protein was found to be micellar precipitation. With increasing salt concentration, the thermal stability of the pea proteins increased, due to charge shielding effects, which stabilized the quaternary protein structure against denaturation.

The major finding of this study was that the extraction type had a significant influence on the functionalities of the protein powders obtained. This research served as a base for choosing the right extraction type for the following analysis.

The doctoral candidate contributed substantially to the conceptualization and design of experiments based on the literature review. Major data analysis, interpretation of data set, and discussion of data set were carried out by the doctoral candidate, as well as writing and revision of the manuscript. Co-authors contributed to the experimental part or discussion of the results. They also provided input to the drafted publication before submission.

Adapted original manuscript[1]

Influence of extraction conditions on the conformational alteration of pea protein extracted from pea flour[2]

Caren Tanger*, Julia Engel, Ulrich Kulozik

Chair of Food and Bioprocess Engineering, Technical University of Munich, Weihenstephaner Berg 1, Freising-Weihenstephan, Germany

Graphical abstract

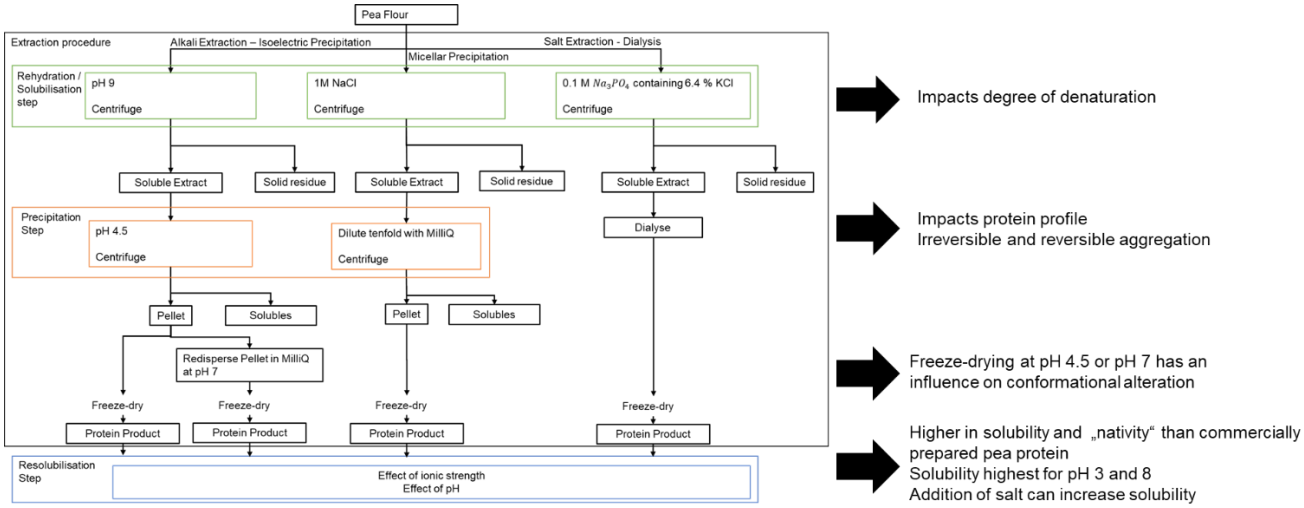

Highlights

- Extraction and precipitation step have an influence on the conformational alteration
- The main influence on the protein profile is determined by the precipitation step
- Denaturation and irreversible aggregation can occur during extraction and precipitation
- Freeze-drying at pH 7 versus pH 4.5 has an influence on conformational alteration

Abstract

Plant proteins are becoming of increasing interest since they are considered a more sustainable protein source than milk protein. One plant protein of interest would be pea protein. In contrast to milk proteins, there has been less research done on extracting native pea proteins. Currently, commercial pea proteins are only available highly de-

[1] Adaption refer to formatting issues: e.g., abbreviations, figure, table, equation and section numbering, citation style, notation of units, spelling, axis labelling. References of all chapters are merged at the end to avoid redundancies.

[2] Originally published in: Food Hydrocolloids (2020), Vol. 107, 105949 . Permission for reuse of this article was granted by Elsevier.

natured and aggregated. There are three commonly used extraction methods on laboratory scale: alkali extraction with isoelectric precipitation, salt extraction and micellar precipitation. Within this study, these three extraction methods next to one modified production process and a commercial pea protein isolate were compared with each other focusing on conformational alteration during the extraction process. Solubility and particle size in combination with charge at different pHs and ionic strengths, and denaturation temperature and enthalpy change at pH 7 in 0.1 M NaCl and 1 M NaCl have been taken as indicators of conformational alteration. Differences in structure between the obtained protein products were observed. Albumins were lost during precipitation in alkali extraction – isoelectric precipitation and micellar precipitation. Solubility was highest for pH 3 and pH 8. Micellar precipitated protein product formed micelles at low ionic strength and solubility of these could be increased by addition of salt. It has been found that both steps during the extraction process, solubilisation and precipitation, had an influence on the conformational alteration of the protein. Solubilisation had in impact on the denaturation of the protein. Precipitation had an impact on the protein profile and irreversible or reversible aggregation.

3.1.1 Introduction

With increasing awareness of climate change and growth of world population, food products are principally required to become more sustainable. An animal-based diet is considered an ecological burden. Therefore, there is a need to develop food products from alternative, more sustainable sources such as plant proteins. In order to develop high-quality food from plant proteins, the challenge of functionalising and making plant proteins tasty and nutritionally suitable needs to be overcome. One suitable plant protein is field pea (*Pisum sativum* L.). Peas are adapted to the climatic conditions in central Europe (Fuhrmeister and Meuser 2003). Currently, most of the pea protein is used for kettle feed (Mession et al. 2015). With rising awareness of healthy and sustainable nutrition, there is an increasing trend to also use pea protein in food products as an alternative to soy (Barac et al. 2010). Peas can be fractionated into starch and protein fractions. They contain 20-30% protein depending on the type and environment and factors in the growth phase (Koyoro and Powers 1987). Pea protein can be divided into globulins with around 55-80% of the total protein fraction and albumins with around 18-25% based on their solubility (Osborne 1909; Derbyshire et al. 1976). There are three known proteins, which belong to the globulin fraction. These can be separated based on their sedimentation coefficient: legumin, vicilin and convicilin (Derbyshire et al. 1976).

Legumin (11S) is a hexameric protein of 360 kDa, comprised of six subunits of 60 kDa. Each subunit contains an acidic (40 kDa) and an alkaline (20 kDa) subunit linked via a disulphide bridge (Dziuba et al. 2014; Shand et al. 2007). Vicilin (7S) is a trimeric protein of 150 kDa with three subunits of 50 kDa without any disulphide bond present (Liang and Tang 2013; Shand et al. 2007). It is less hydrophobic than legumin. Therefore, it is better soluble in water (Gueguen 1989). Convicilin is a tetrameric protein of 280 kDa with four subunits of 70 kDa. Similar to vicilin, there are no disulphide bonds

present in convicilin. (O'Kane et al. 2004a). Albumins have a higher content of tryptophan, lysine and threonine, while globulins tend to be higher in arginine, phenylalanine leucine and isoleucine (Swanson 1990; Koyoro and Powers 1987). Most research with pea proteins is done with extracted pea proteins at laboratory scale. Commercial pea protein has been shown to be already denatured and highly aggregated due to the processing conditions of separating the starch from the protein (Taherian et al. 2011; Fuhrmeister and Meuser 2003; Sun and Arntfield 2010). It was found that the solubility of the extracted protein decreases in case the extraction procedure alters the protein structure and forms aggregates (Chao and Aluko 2018; Shand et al. 2007). There are several extraction procedures used in industrial and scientific applications. It has been shown that these procedures lead to differences in the functionalities of extracted protein. As different extraction procedures may select different proteins, the final composition of the produced protein product may also differ (Stone et al. 2015; Taherian et al. 2011; Mession et al. 2012; Boye et al. 2010). There are three commonly used extraction methods: Alkaline extraction - isoelectric precipitation, salt extraction - dialysis and micellar precipitation (Stone et al. 2015).

Alkaline extraction - isoelectric precipitation is based on dissolving the protein in alkaline medium. Another method is to dissolve the protein at acidic conditions far away from the isoelectric point (Mession et al. 2012). Then, the proteins are precipitated at their isoelectric point at pH 4.5. Since the isoelectric point of globulins and albumins is different, mainly globulins are extracted with this method. In contrast, a mixture of globulins and albumins is extracted by salt (Stone et al. 2015). In micellar precipitation, the protein is extracted in a neutral salt solution. The soluble proteins are precipitated by reducing the salt content in the solution leading to micelle-type form. Hydrophobic interactions may play a major role in stabilization of the micelles. Both globulins and albumins are extracted with this procedure. They may be less denatured compared to proteins extracted by alkaline extraction - isoelectric precipitation (Paredes-López and Ordorica-Falomir 1986; Arntfield et al. 1985).

All extraction procedures have in common the first step of making the protein soluble. According to practical observation, none of the extracted protein is fully soluble after precipitation and drying. Both processing steps seem to have an effect on solubility. This supports the hypothesis that there are alterations in the structure of the protein during extraction, finally leading to aggregation (Shand et al. 2007; Chao and Aluko 2018). Stone et al. (2015) compared the surface, foaming and emulsion characteristics of pea proteins obtained by alkali extraction – isoelectric precipitation, micellar precipitation and salt extraction - dialysis also using different cultivars. The cultivars represented the three different market classes, comparing CDC Striker (green cotyledon, non-pigmented seed coat), CDC Meadow (yellow cotyledon, non-pigmented seed coat and CDC Dakota (yellow cotyledon, dun seed coat) with each other. The authors concluded that both the extraction procedure and the cultivar have an influence on the functionality of the resulting protein product. However, they neither compared the protein profile nor the alteration in structure. This means that no information on the degree of aggregation of the different extraction methods was provided. Shand et al. (2007)

compared commercial pea protein with pea protein product obtained from lab-scale preparation. They also considered the thermal properties and solubility as a function of pH. They claimed that their laboratory prepared pea protein product to be “native” using alkali extraction – isoelectric precipitation. Data for the two other extraction methods were not reported in this paper. Also, the influence of salt concentration on solubility was not investigated. Shand et al. (2007) further stated that the adjustment to pH 6.5 after the final centrifugation step and before freeze-drying minimized denaturation. An influence of pH during freeze-drying on nativity of the resulting protein product was not investigated in their study. Sun and Arntfield (2011) used salt extraction for thermal analysis. They claimed that this extraction procedure would lead to a low degree of denaturation. For extraction of another pulse flour from faba beans, it has been found that micellar precipitation is the mildest extraction method (Arntfield et al. 1985). This is in contrast to what has been generally claimed for pea proteins as described above. Thermal analysis of salt extracted pea protein has been examined over a wide range of pH and salt concentrations, but Sun and Arntfield (2011) did not consider solubility and particle size. Summarising, several authors state that their extraction procedure leads to “native” protein. However, they do not present the proof of their statement by taking neither protein profile, thermal analysis, solubility, particle size nor charge over a range of pH and salt concentration into account. In addition, micellar precipitation, which is stated to be the mildest extraction for faba beans, has not been investigated by thermal analysis so far. Considering the influence of the cultivar, as found by Stone et al. (2015), results from different studies are difficult to compare head-to-head. Therefore, this study aims at comparing all three extraction procedures, concerning their alteration in structure, using one cultivar and accounting for the effect of pH and salt concentration during resolubulisation. This should allow to make a statement, which extraction method leads to the lowest alteration in structure and can be claimed to lead to the most native pea protein product. In addition, particle size and charge should be used to depict the difference in protein structure of the differently extracted protein products. Besides comparing the three extraction methods, a particular extraction process modification of the alkali extraction – isoelectric precipitation is used to provide information about the effect of pH during freeze-drying. The hypothesis is that one should be able to choose the most suitable extraction method, depending on specific needs, and should also be able to modify each extraction method to maximize functionality and yield. This study focuses on the globulins because they are globular proteins and are studied in more detail than albumins. In addition, their functionality is mainly dependent on the protein conformation. Functionality can change upon denaturation.

3.1.2 Materials and methods

3.1.2.1 Materials

Pea flour was provided by Emsland Stärke (Emlichheim, Germany). Pea flour contained 18.27% protein on a dry basis. A commercial pea protein isolate (PPI) E86 with 70.8% protein on dry basis was also provided from Emsland Stärke (Emlichheim, Germany). The commercial PPI was used in some analyses for comparison of laboratory

extracted pea protein and commercially extracted pea protein. MilliQ water (Milli-Q Integral 3, Merck KGaA, Darmstadt, Germany) was used for all protein extractions and analysis experiments. All other materials and chemicals were purchased from regular supplies and were of analytical grade.

3.1.2.2 Extraction of proteins

Three extraction procedures were used: alkali extraction – isoelectric precipitation, salt extraction – dialysis and micellar precipitation. The extraction procedures are schematically displayed in Figure 3-1 and described in detail below. All procedures contain a rehydration/solubilisation step at first. Thereafter, soluble residues are separated via centrifugation. Only alkali extraction – isoelectric precipitation and micellar precipitation contain an additional precipitation step, in which the extracted proteins are made insoluble. Both steps are labelled in Figure 3-1.

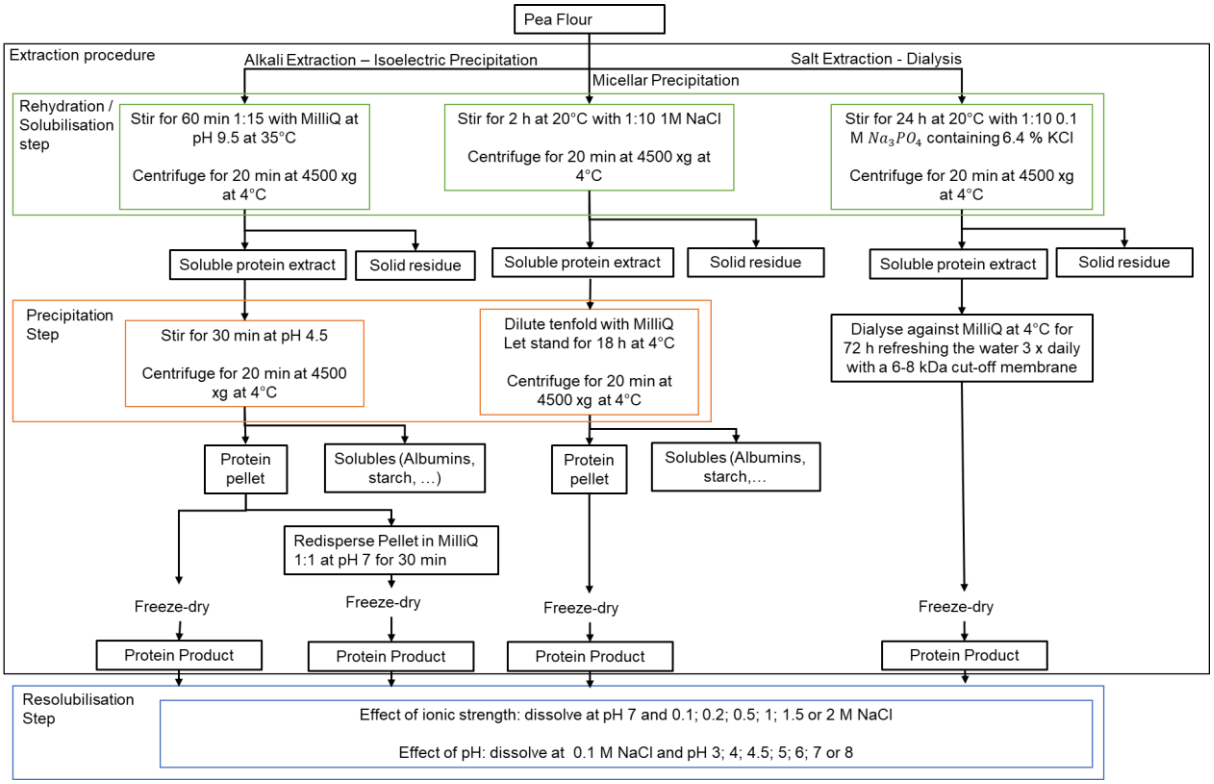

Figure 3-1: Schematic overview of the three different extraction procedures and the modified production process. Rehydration / solubilisation step, precipitation step and resolubilitzation step are labelled in the process

Following, the terms quaternary structure, micelle, aggregation and conformation are defined for clarification. Quaternary structure refers to the native hexameric conformation of legumin, the native trimeric conformation of vicilin and the native tetrameric conformation of convicilin. Micelles are the insoluble protein pellets obtained by micellar precipitation. A more detailed explanation about the conformation of the micelle is given in the effect of the ionic strength on solubility, particle size and zeta potential. The term aggregation is used for protein particles, which are bigger than the hexamer of legumin formed after denaturation and which are not micelles. Conformation is a general term used, for the protein structure at different circumstances.

3.1.2.2.1 Alkali extraction – isoelectric precipitation

The alkali extraction – isoelectric precipitation (AE-IP) method was developed based on the method used by Boye et al. (2010) with slight modifications (see Figure 3-1, left arm of extraction schema). In brief, 50 g pea flour was dispersed in 750 g water (1:15 w/w). The pH was adjusted to pH 9.5 with 1 M NaOH. After 1h stirring at 35°C, the mixture was centrifuged at 4500 x g for 20 min at 4°C. The pellet was discarded and the pH of the supernatant was adjusted to pH 4.5 with 1 M HCl and stirred for 30 min at room temperature (20-23°C). Next, the mixture was centrifuged at 4500 x g for 20 min at 4°C and the supernatant discarded. The pellet was collected, stored at -80°C and freeze-dried using a pilot-scale freeze dryer (Christ, Model: Alpha 1-4 LSC; Osterode, Germany). In order to improve the extraction procedure and study the influence of freeze-drying at different pH levels, the extraction was done twice, once as described above, the second time with the following modification in the production procedure: Before freeze-drying, the pellet was dissolved in water and adjusted to pH 7 with 1 M NaOH. This alkali extraction – isoelectric precipitation with freeze-drying at pH 7 will be named alkali extraction – isoelectric precipitation 2 (AE-IP 2).

3.1.2.2.2 Salt extraction – dialysis

The salt extraction – dialysis (SE) method was based on Liu et al. (2009) with slight modifications (see Figure 3-1, right arm of extraction schema). In short, 50 g pea flour was dispersed in 500 g 0.1 M sodium phosphate solution containing 6.4% KCl (1:10 w/w). The mixture was stirred for 24 h at 500 rpm at 20°C and then centrifuged for 20 min at 4500 x g at 4°C. The pellet was discarded, and the supernatant was dialysed against MilliQ water with a 6-8 kDa cut off membrane for three days. The water was refreshed 3 x daily. After dialysis, the extract was stored at -80°C until freeze-dried.

3.1.2.2.3 Micellar precipitation

Micellar precipitated (MC) (middle path in Figure 3-1) protein product was produced according to Lampart-Szczapa (1996) with slight modifications (see Figure 3-1, middle path of extraction schema). Summarizing, 50 g pea flour was dispersed in 500 g 1 M NaCl solution (1:10 w/w) and stirred for 2 h at 20°C at 500 rpm. Following, the mixture was centrifuged at 4500 x g for 20 min at 4°C. The pellet was discarded, and the supernatant was diluted tenfold with water and then left for 18 h at 4°C. The dispersion was centrifuged at 4500 x g for 20 min at 4°C. The pellet was collected, stored at -80°C and then freeze-dried.

3.1.2.3 Analysis of protein product

3.1.2.3.1 Protein content

Protein content of the extracted protein isolates was determined using the Dumas method with the Vario MAX cube (Elementar Analysensysteme GmbH, Langenselbold, Germany). A factor of 5.4 was used for conversion of nitrogen content into protein content as proposed by Mariotti et al. (2008) for pea proteins. Protein yield (Y) was calculated by using equation (3-1).

$$Y = \frac{x_{PP} * m_{PP}}{x_{Pf} * m_{Pf}} \quad (3\text{-}1)$$

With x_{PP} the percentage protein of the resulting protein product, m_{PP} the mass of the protein product, x_{Pf} the percentage protein of the pea flour and m_{Pf} the mass of the protein flour used.

In order to determine in which step most proteins get lost, the mass of the supernatant (m_{S1}) and pellet (m_{P1}) was determined after the centrifugation step following the extraction. The protein content of the supernatant (x_{S1}) and the pellet (x_{P1}) was measured. The protein of the pea flour can either be extracted and then ends up in the supernatant (S_1), or it stays in the plant cell and ends up in the pellet (P_1). If extraction is incomplete, parts of the proteins are found in the supernatant and the pellet (eq.(3-2)).

$$x_{Pf} * m_{Pf} = x_{S1} * m_{S1} + x_{P1} * m_{P1} \quad (3\text{-}2)$$

The pellet (P_1) is discarded in all extraction methods. Thus the protein in the pellet is lost and named loss (L) during the solubilisation step (L_1).

$$L_1 = x_{P1} * m_{P1} \quad (3\text{-}3)$$

The loss (L) in percentage relative to the amount of protein in the pea flour named (L_1) according to equation (3-4).

$$L_1 = \frac{x_{P1} * m_{P1}}{x_{Pf} * m_{Pf}} \quad (3\text{-}4)$$

After the precipitation step the protein of the supernatant (S_1) can either be precipitated and then forms a pellet (P_2) or it stays soluble and ends up in the supernatant (S_2). The supernatant of the precipitation step (S_2) is discarded and thus considered as lost. Since salt extraction – dialysis does not contain a precipitation step but a dialysis step, there is no supernatant. Therefore, the loss in the precipitation or dialysis step (L_2) was calculated by the difference in protein content in the supernatant of the solubilisation step (S_1) and the amount of protein extracted. This is calculated by equation (3-5).

$$L_2 = x_{S1} * m_{S1} - x_{PP} * m_{PP} \quad (3\text{-}5)$$

The loss in the precipitation or dialysis step (L_2) is also expressed as percentage of the amount of protein in the pea flour. This leads to equation (3-6).

$$L_2 = \frac{x_{S1} * m_{S1} - x_{PP} * m_{PP}}{x_{Pf} * m_{Pf}} \quad (3\text{-}6)$$

Both losses and yield, are expressed in percentage of the amount of protein in the pea flour used for the extraction. This means that it should all sum up to 100%.

3.1.2.3.2 Protein profile

For estimation of the protein polypeptide mass Sodium Dodecyl Sulphate – Polyacrylamide Gel Electrophoresis (SDS-PAGE) was carried out. Therefore, the protein solution

was diluted to 2 mg/l protein with a sample buffer containing 10% SDS, 0.5 M tris-HCl, 10% SDS and 0.5% bromophenol blue pH 6.8 for non-reducing condition and sample buffer containing 10 % SDS, 0.5 M tris-HCl, 10 % SDS, 0.5% bromophenol blue and 15 mg/ml dithiothreitol (DTT) pH 6.8 for reducing condition. Samples were heated at 100°C for 5 min. For analysis, a prepacked TGX gradient gel (4-20%) stain-free (Bio-Rad Lab., Hercules, CA, USA) was used. An amount of 10 µl was loaded in each well. A standard marker Precision Plus ProteinTM Standard (Bio-Rad Lab., Hercules, CA, USA) was loaded on a separate lane. Protein separation was run at 300 V, 50 mA/gel and 35 W for approximately 35 min. Protein bands were made visible at 300 nm and scanned using Molecular Imager Gel DocTM XR+ system (Bio-Rad Lab., Hercules, CA, USA) controlled with ImageLab (v 6.0) software.

3.1.2.4 Analysis of solubilized protein product

3.1.2.4.1 Protein solubility

Protein solubility was determined according to Stone et al. (2015) with some modifications. Summarizing, 0.2 g protein (based on weight protein content within the dried powder) was dispersed in 19 ml 0.1 M; 0.2 M; 0.5 M; 1 M; 1.5M or 2 M NaCl and the pH was adjusted to pH 7 using 0.1 M HCl or 0,1 M NaOH. Protein solubility was also measured as follows: the protein product was dispersed in 0.1 M NaCl adjusted to pH 3; 4; 4.5; 5; 6; 7 and 8 with 1 M, 0.1 M HCl or 0.1 M NaOH. The total solution weight was brought to 20 g with the solution of the same pH. The solution was mixed for 1 h at 20°C at 500 rpm. After that, the mixture was centrifuged at 6000 x g for 15 min at 20°C. The protein content in the supernatant was determined using Dumas and BCA assay. Bovine serum albumin (BSA) was used as standard. BCA working reagent was made by mixing 8 parts of bicinichoninic acid solution with 1 part 4% copper(II) sulphate pentahydrate. 25 µl sample were mixed with 200 µl BCA working reagent and incubated for 30 min at 37°C and 5 min at room temperature in a 96-well plate. Thereafter, the absorbance was measured at 562 nm in a Spark multimodal microplate reader (Tecan, Männedorf, Switzerland).

Dividing the total protein content in the supernatant by the protein content in the initial sample (x 100%) was used to calculate the percentage of the soluble protein relative to the total protein content.

3.1.2.4.2 Particle size measurement

Particle size distribution was measured with dynamic light scattering. A 0.2 µm filtered 1% protein solution prepared as described in protein solubility was measured. The measurement was performed with a ZetaSizer Nano ZS (Malvern Instruments Ltd, Malvern, Worcestershire, UK) at a fixed angle of 173° and a wavelength of 632.8 nm using a refractive index of 1.45. Before the start of the measurement, an equilibration time was set to 2 min. Each measurement consisted of 5 runs containing 1 to 15 sub runs.

3.1.2.4.3 Zeta potential

The zeta potential of each protein product dispersed in water was determined by measuring the electrophoretic mobility of the protein in the supernatant of a 1% solution prepared as described in the protein solubility section using a ZetaSizer Nano ZS (Malvern Instruments Ltd, Malvern, Worcestershire, UK). For each data point, 3 measurements were performed comprised of 1 to 100 runs. The electrophoretic mobility was

then converted to the zeta potential by the Zetasizer Software 7.13 (Malvern Instruments Ltd, Malvern, Worcestershire, UK)

3.1.2.4.4 Thermal analysis

Thermal analysis was performed using modulated differential scanning calorimeter (DSC Q1000, TA instruments). With DSC measurement the denaturation of the globular proteins was measured, which is referred to as thermal reactivity. The heating ramp was calibrated using Indium as reference material. An amount of 20 µl of a 10% aqueous solution was placed in an aluminium pan and hermetically sealed. An empty pan, closed with three lids to ensure the same pan mass, served as reference. The experiment was performed with the protein products dissolved in water adjusted to pH 7 with 0.1 M HCl and 0.1 M NaOH and dissolved in 1 M NaCl adjusted to pH 7 with 0.1 M HCl and 0.1 M NaOH. The pans were heated in modulated mode from a temperature of 25°C - 100°C at an underlying heating rate of 2°C/min and a modulation amplitude of ± 0.5°C every 60 s to determine the denaturation temperature (T_d), T_{onset} and enthalpy change (ΔH). Data obtained was analysed with TA Universal Analysis 2000 software.

3.1.2.5 Statistical analysis

Protein extraction was performed in duplicate and resulting protein products were pooled for each extraction method. Experiments were performed in at least duplicate from two different protein solutions prepared. Curves were plotted using OriginPro 2019 (originLAb Corporation, Northampton, USA). Mean values are shown in the graphs. Error bars represent standard deviation. A one-way analysis of variance (ANOVA) for significant difference for denaturation temperatures and onset temperatures were analysed. Minimum significance was set at the 5% level ($p < 0.05$) using Tukey's test by JMP Pro (SAS Institute Inc., Cary, USA/Version 13.1).

3.1.3 Results and discussion

3.1.3.1 Protein concentration and yield

Protein concentration results of the protein products and the yield results are recorded in Table 3-1

Table 3-1: Protein concentration, loss during extraction and yield of the four different extraction methods and resulting isolate (Alkali extraction – isoelectric precipitation (AE-IP), salt extraction (SE), micellar precipitation (MC) and alkali extraction – isoelectric precipitation freeze-dried at pH 7 (AE-IP2)).

Extraction method	Protein concentration (%)	Loss in the first step (% of protein in pea flour)	Loss in the second step (% of protein in pea flour)	Yield (% of protein in pea flour)
AE-IP	74.5 ± 0.3	31.3 ± 2.6	23.9 ± 1.3	46.0 ± 0.2
AE-IP 2	74.2 ± 0.7	31.3 ±2.6	23.9 ± 1.3	50.0 ± 0.4
MC	75.1 ± 2.1	39.6 ± 1.0	35.5 ± 0.5	25.0 ± 0.7
SE	73.2 ± 0.5	27.5 ± 1.6	33.8 ± 0.8	39.7 ± 0.3

*Means ± SD of duplicates

The protein content was above 70% in all protein products, which is in line with the findings by other works (Stone et al. 2015; Boye et al. 2010). However, protein yield was significantly lower from Stone et al. (2015) findings, while following a similar trend. The highest yield was found for both alkali extractions, followed by the salt extraction. Micellar precipitation was found to produce the lowest yield. A more efficient extraction with alkali extraction - isoelectric precipitation was also found for safflower (Paredes-López and Ordorica-Falomir 1986). The low protein yield with micellar precipitation on faba beans was explained by an inefficient solubilisation of the protein during the initial extraction (Arntfield et al. 1985). Compared to alkali extraction and salt extraction less protein was solubilized by the initial extraction (Table 3-1). However, the loss in the precipitation step was also highest for micellar precipitation. In general, the findings show that around 28-40% of proteins were lost in the initial rehydration/solubilisation step and around 23-36% in the second precipitation step. Both steps had an impact on the protein yield. In the initial solubilisation step, globulins and albumins were extracted from the pea flour. The precipitation step had an impact mainly on the protein profile of the protein products, depending on how proteins were precipitated in alkali extraction – isoelectric precipitation and micellar precipitation, while no precipitation step was applied in salt (Osborne 1909; Stone et al. 2015).

3.1.3.2 Protein profile

The protein profile of the soluble protein extracts after the rehydration/solubilisation step and of the freeze-dried protein products dissolved in water was analysed by SDS-PAGE. This was done with and without reduction of protein disulphide bonds (Figure 3-2).

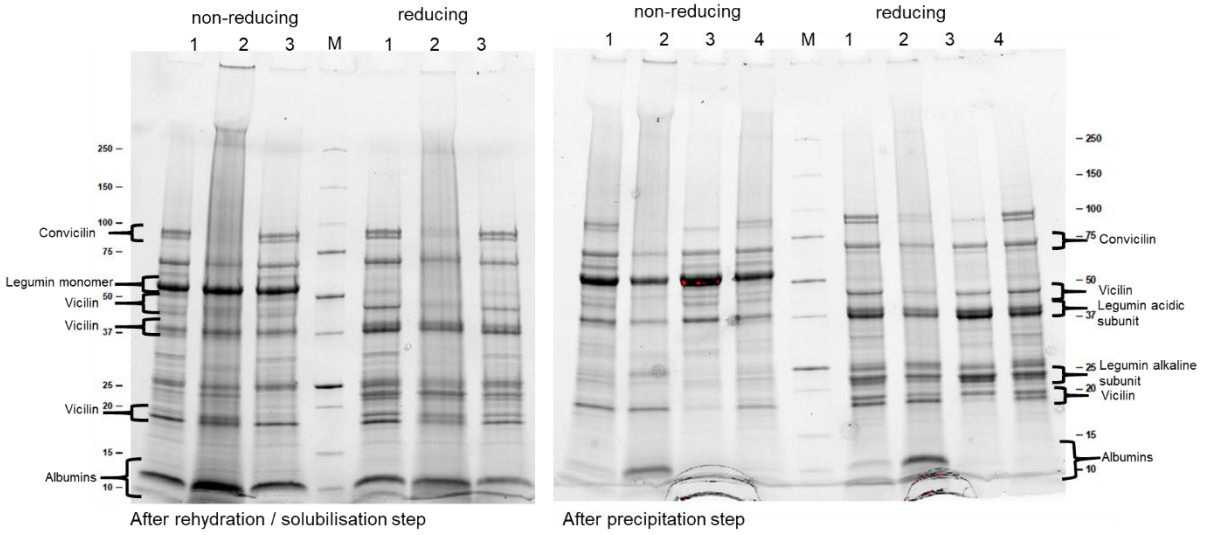

Figure 3-2 SDS-PAGE profile of pea proteins isolate under non-reducing and reducing conditions. The left SDS-PAGE depicts the protein profile after the solubilisation step and the right SDS-PAGE shows the protein profile of the dissolved protein product. Lane M indicates standard protein marker, lane 1: Alkali extraction – isoelectric precipitation, lane 2: Salt extraction - dialysis, lane 3: Micellar precipitation, lane 4: Alkali extraction – isoelectric precipitation 2. The main globulins (legumin, vicilin and convicilin) and albumins are labelled.

All protein products and soluble protein extracts show several bands depending on whether non-reducing and reducing conditions were applied. The band at 60 kDa was the most prominent band in all protein isolates under non-reducing conditions. How-

ever, this band was not present in all protein products and soluble extracts under reducing conditions; instead, the bands at 40 kDa and 20 kDa increased in proportion. These bands can be linked to legumin. The hexamer conformation of legumin of 360 kDa was reduced into monomers of 60 kDa by the SDS under non-reducing condition. Under reducing conditions, the disulphide bonds between the alkaline (20 kDa) and acidic (40 kDa) subunit of the monomer were split (Dziuba et al. 2014; Shand et al. 2007). This explains the disappearance of the 60 kDa band and the appearance of a 20 kDa and 40 kDa band under reducing condition. Legumin was present and most dominant in each soluble protein extract and protein product. Bands at 50 kDa, 35 kDa and 18 kDa can be linked to dissociated vicilin trimers and a band around 71-76 kDa, can be linked to convicilin.

Bands occurring below 15 kDa belong to the albumin fraction. Comparing the soluble protein extract with the protein product, it appears that there were many more protein bands visible in the soluble protein extract than in the final protein product. The albumin fraction was present in all soluble protein extracts, but they were only present in the salt extracted protein product. This means that during the precipitation step not all proteins were precipitated, but some stayed soluble. This would be the case for the alkali extracted – isoelectric precipitated and the micellar precipitated protein product. Both did not contain albumins. The protein profile of alkali extracted – isoelectric precipitated protein product was similar to the pea protein profile found by Shand et al. (2007). Alkali extracted – isoelectric precipitated protein product was precipitated at the isoelectric point for globulins. The isoelectric point for albumins is around pH 6, thus they stayed soluble during the precipitation step and was discarded (Swanson 1990). The same happened during micellar precipitation. In this extraction, the proteins were precipitated by lowering the ionic strength. Globulins are salt soluble and albumins are water soluble (Osborne 1909). As a result, globulins were precipitated and albumins stayed soluble (Arntfield et al. 1985). The salt extraction does not include a precipitation step. This means that all protein extracted ended up in the protein product. An exception were proteins below 8 kDa, which diffused through the pores of the dialysis membrane. This supports the hypothesis that the protein profile is mainly dependent on the precipitation step during the extraction procedure.

3.1.3.3 Effect of ionic strength on solubility, particle size and charge

The amount of soluble protein of the protein products and the commercial reference was measured at different ionic strengths. The expectation was that this could lead to an increased solubility, because globulins, the main protein fraction extracted, are per definition salt soluble (Osborne 1909; Lam et al. 2018). This is especially important for the micellar precipitated protein product. During micellar precipitation, ionic strength is lowered, which forces solubilized protein to adjust to the low ionic strength. Proteins with hydrophobic residues form thermodynamically stable spheres, called micelles. These micelles are arranged by minimizing the interfacial energy. Hydrophobic moieties are gathered towards the centre and polar moieties are exposed to the outer aqueous environment (Lam et al. 2018). Analysing the solubility over a wide range of ionic strength, the point at, which the micelles fall apart and the protein product becomes soluble again is shown. The results are shown in Figure 3-3.

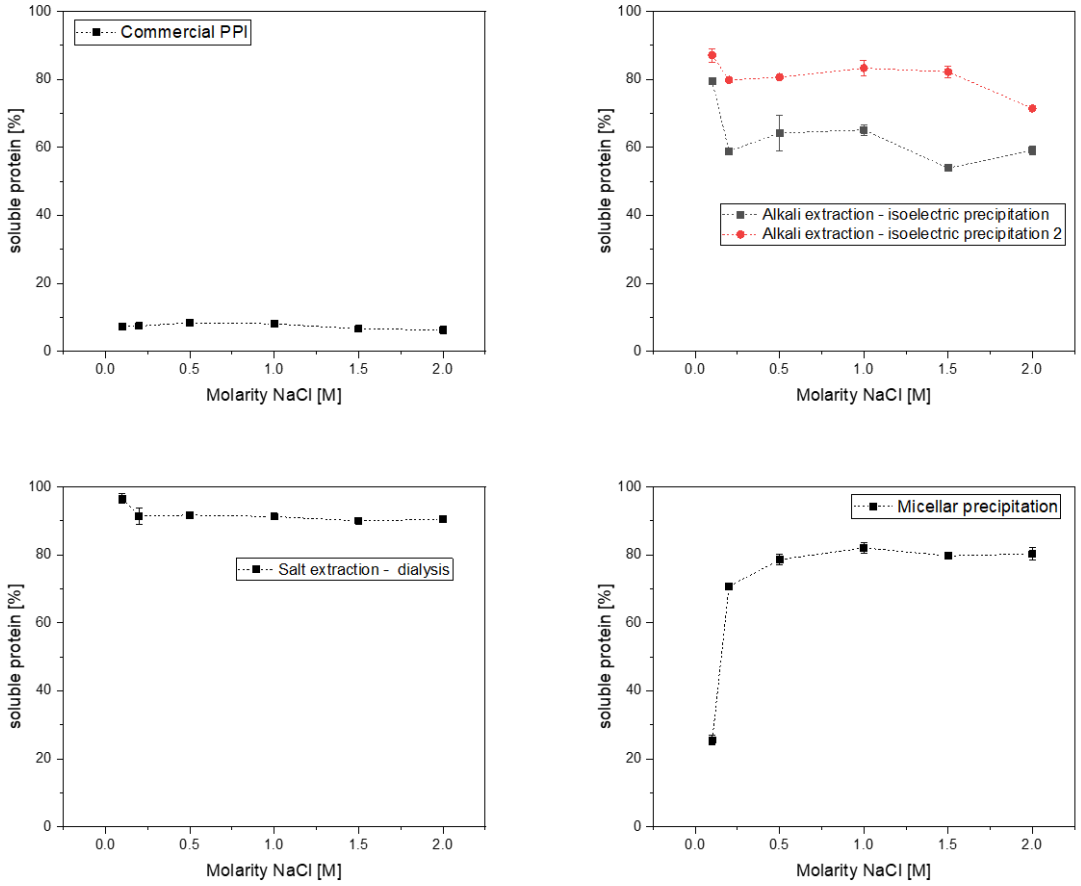

Figure 3-3 Solubility of the different protein products at pH 7 and 0.1 M NaCl -2 M NaCl.

At 0.1 M NaCl the salt extracted protein product shows the highest solubility of 96.6% soluble protein, followed by both alkali extracted protein products with 87.1% and 79.5% soluble protein. Micellar precipitated protein product showed the lowest solubility with 25.5% soluble protein at this ionic strength. These results are in line with findings by Stone et al. (2015) considering the differences between cultivars at pH 7 with 0.1 M NaCl. The commercial protein isolate showed the lowest protein solubility with 7.2% soluble protein. A low solubility of commercial pea protein compared to alkali extracted protein product at pH 7 has also been found in another study (Barac et al. 2010). The solubility of the alkali extracted protein product was different for both production processes. Freeze-drying at pH 7 led to a protein product with a higher solubility than freeze-drying at pH 4.5. This indicates that the conformation, in which the proteins were freeze-dried, had an influence on the solubility and the product obtained. In contrast to the other extractions, micellar precipitated protein product increased in solubility with increasing amount of salt. At 0.5 M NaCl, the micellar precipitated protein product showed a solubility similar to that of the alkali extracted protein product freeze-dried at pH 7 with 78.6% soluble protein. Fuhrmeister and Meuser (2003) defined that a higher solubility means that the proteins extracted are in a more native state. At 0.1 M NaCl, the micellar precipitated protein product shows the lowest solubility of all extracted protein products. According to Fuhrmeister and Meuser (2003), this would mean that micellar precipitated protein is the protein product with the lowest amount of native protein. This would be in contrast with the findings of Arntfield et al. (1985) and

Paredes-López and Ordorica-Falomir (1986), according to which the micellar precipitation is the mildest extraction for other pulses. However, with pea proteins, the proportion of the per definition salt soluble globulin fraction and water soluble albumin fraction have to be considered. The increasing solubility of the micellar precipitated protein product suggests that it contains a high amount of hydrophobic globulins. In addition, the increasing solubility with increasing salt concentration in micellar precipitated protein product indicates, that the micelles, were formed depending on the ionic strength and micelle formation is reversible. With decreasing salt concentration, the size of the micelles grows and they become insoluble. As mentioned above, the formation of micelles is depending on the ionic strength. Therefore, it is not accurate to take solubility in water as an appropriate measure of nativity for pea proteins. However, solubility in aqueous systems is important for food production. Therefore, it is measured in this study. Salt extracted protein product shows the highest solubility independent of ionic strength. However, it is the only protein product, which contains albumins as seen in the SDS-PAGE. In contrast to globulins, albumins are soluble at low ionic strength. This explains, why salt extracted protein product shows such a good solubility.

In order to explain the difference in solubility, the particle size and charge of the proteins has been measured. Note that for the size measurement aggregates bigger than 0.2 µm were cut off. This cut-off size has been chosen after several trials with other sizes. The aim of the measurement was to especially identify the non-aggregated proteins and which effect the salt had on those. A cut-off at 0.2 µm provided the best results for this assessment. The size distribution is shown in Figure 3-4.

All size distributions show one peak below 100 nm, around 10 nm to 30 nm, and a small peak above 100 nm. Some size distributions are multimodal. With increasing salt concentration, the size distribution shifted to smaller particles for the alkali extracted protein products and commercial pea protein isolate. The size of the micellar precipitated protein product and the salt extracted protein product did not change significantly with increasing salt concentration. For micellar precipitation, the particle size distribution is shown for 0.5 M NaCl instead of 0.1 M NaCl. This is due to the fact that the particles at 0.1 M NaCl blocked the filter. It indicates that a high amount of protein was larger in size than 0.2 µm and the measurement would not be reliable, because count rate was too low. This would be in line with the low solubility at low ionic strength.

However, it can be seen that the amount of small particles of the micellar precipitated protein product increased with increasing ionic strength similar to the commercial pea protein and both alkali extracted protein products. An explanation is the effect of salt on electrostatic and hydrophobic interactions. The salting-in effect increases electrostatic effects (Melander and Horváth 1977). Therefore, with increasing salt concentration, the repelling interactions between the proteins increases and proteins are hindered to aggregate. In case of the micellar precipitation, this would support Arntfield et al. (1985) statements, according to which the interaction between molecules within the micelle is non-covalent and possibly hydrophobic.

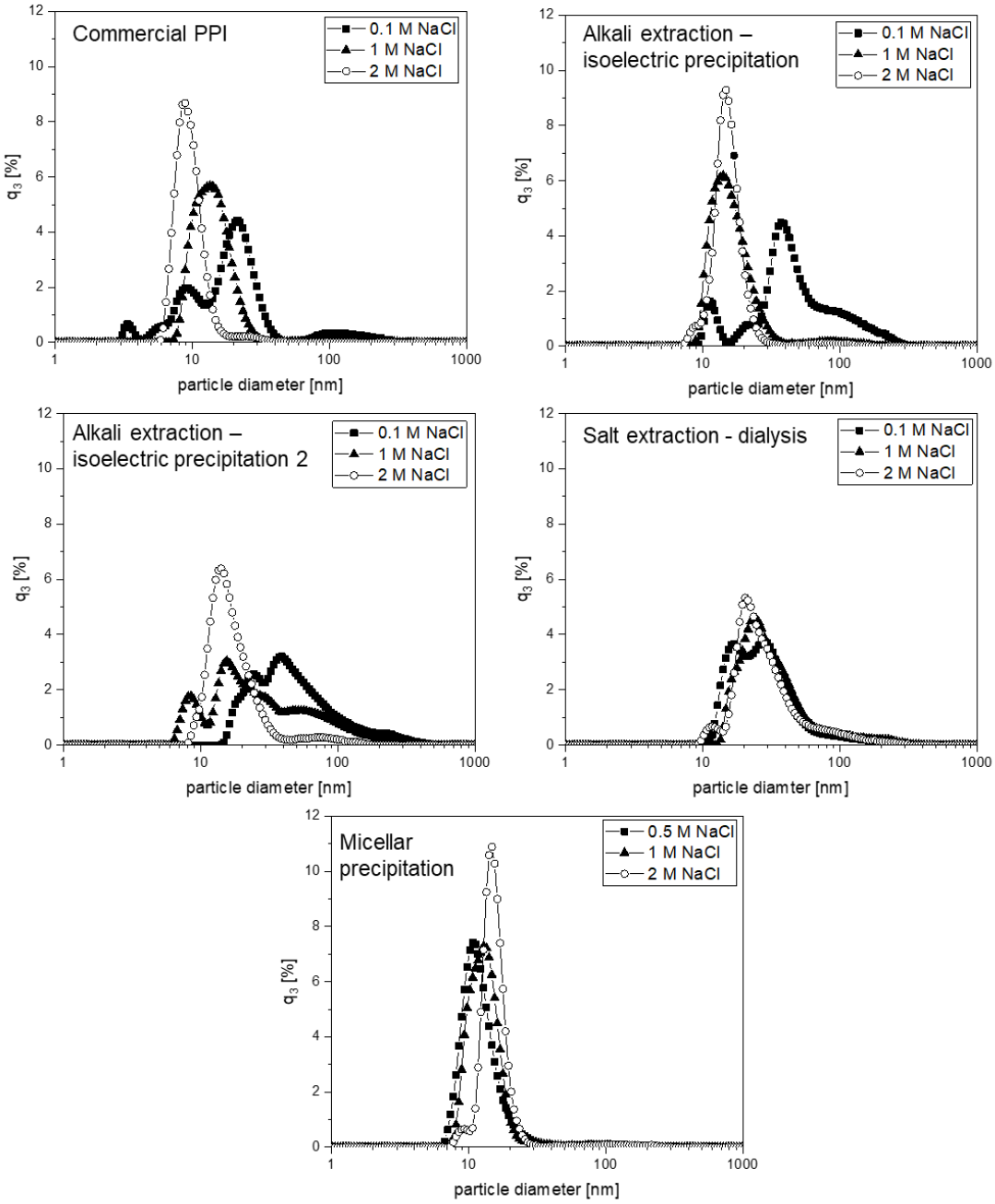

Figure 3-4 Particle size distribution (q_3) at 0.1 M NaCl, 1M NaCl and 2 M NaCl at pH 7 of the pea protein products measured by dynamic light scattering.

All proteins carried a net negative charge since they were above their isoelectric point (pI~4.50 for globulins and pI~6.00 for albumins) (Swanson 1990). Surface charge results can be found in Figure 3-5.

With increasing salt content, the charge of the proteins increased in all extraction methods until it plateaued around -6 mV.

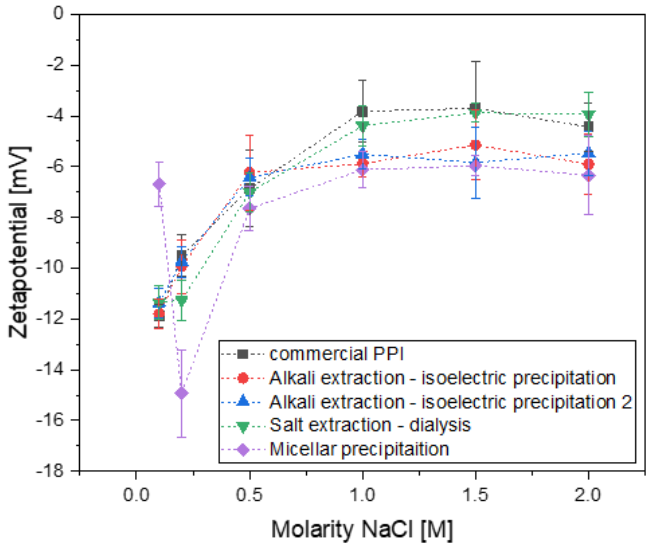

Figure 3-5 Zeta potential of the pea protein products dissolved at pH 7 at different salt concentration.

The values were slightly higher than those found for the three extractions at pH 7 and in 10 mM sodium phosphate (Stone et al. 2015). They were also higher than for alkali extracted and salt extracted pea protein at pH 7 in 10 mM sodium phosphate buffer (Karaca et al. 2011). Besides, the values found in this study were slightly higher than for salt extracted pea protein at pH 6.8 in the absence of salt (Liu et al. 2009). This can be due to the higher and varying salt content. The surface charges under these conditions were similar between the extraction methods. However, Stone et al. (2015) found a difference in hydrophobicity of the proteins obtained by the extraction methods. Based on this, they concluded that the extraction method has an influence on the conformation of the protein. The different particle size distributions could add to this, showing an influence on the conformation of the proteins by the extraction method.

3.1.3.4 Effect of pH on solubility, particle size and charge

The protein solubility was also measured at varying pH in 0.1 M NaCl. The expectation was that an optimum solubility exists if electrostatic repulsions would be maximized. The results are shown in Figure 3-6.

The commercial pea protein isolate shows a low solubility across the whole pH range. Jiang et al. (2017) measured low solubility values across the whole pH range for commercial pea protein from another supplier. Only when adding ultrasound or at highly alkaline pH, the solubility was increased. This low solubility over the whole range indicates, that the proteins were already denatured and/or aggregated. For all extraction methods, the solubility was lowest in the range of pH 4-6 and most soluble at pH 8. With alkali extracted – isoelectric precipitated pea and soy protein, Shand et al. (2007) found the lowest solubility at pH 4.5 and the highest at pH 8-10.

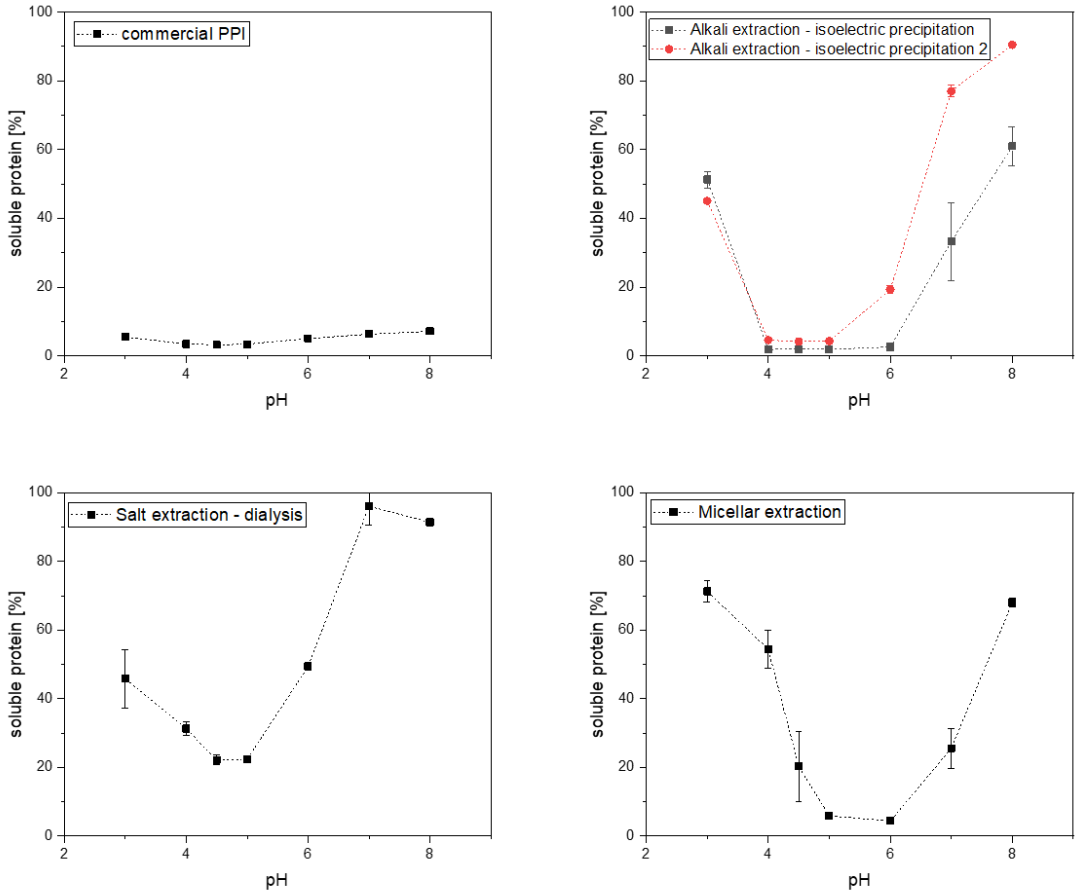

Figure 3-6 Solubility of the different protein products at 0.1 M NaCl and pH 3-8.

A possible explanation is that the IEP of globulins is at pH 4.5, which is the major protein fraction in each extracted isolate (Swanson 1990). The salt extracted protein product was the most soluble around pH 4-6. In contrast to the other extracted protein products, the salt extracted protein product also contained albumins, whose IEP is different to the one of globulins. Thus, the albumins stayed soluble at pH 4.5. The lowest solubility of micellar precipitated protein product was at pH 5-6. This was slightly higher compared to the other extracted protein products. The same difference between micellar precipitated protein product and alkali extracted protein product was also observed comparing different extraction methods of amaranth and mung beans. The shift in lowest solubility has been explained by the level of phytic acid. The level of phytic acid in extraction of proteins from mung beans has been reduced by micellar precipitation. (Rahma et al. 2000; Cordero-de-los-Santos et al. 2005). It has been found by Ali et al. (2010) that the phytic acid content has a major impact on the solubility of soy protein, which is comparable to pea protein. A low phytic acid content increases protein solubility in the pH range of 2 to 4.5 and results in a narrower protein solubility profile. This phenomenon can be seen, when comparing micellar precipitated protein product and alkali extracted protein product with each other. Therefore, the extraction procedure has an influence on the by-products extracted e.g. phytic acid, which then influences the solubility profile. These by-products also influence the conformational structure of the protein, as proposed by the model of Ali et al. (2010) and the digestibility

(Ali et al. 2010; Fredrikson et al. 2001). The alkali extracted protein product freeze-dried at pH 7 was more soluble across the whole pH range than the one freeze-dried at pH 4.5. This indicates that the conformation, in which the protein was freeze-dried, had a major influence on the solubility.

Particle size and charge were also measured as a function of pH. Particle size distributions are shown for pH 3, 7 and 8 in Figure 3-7.

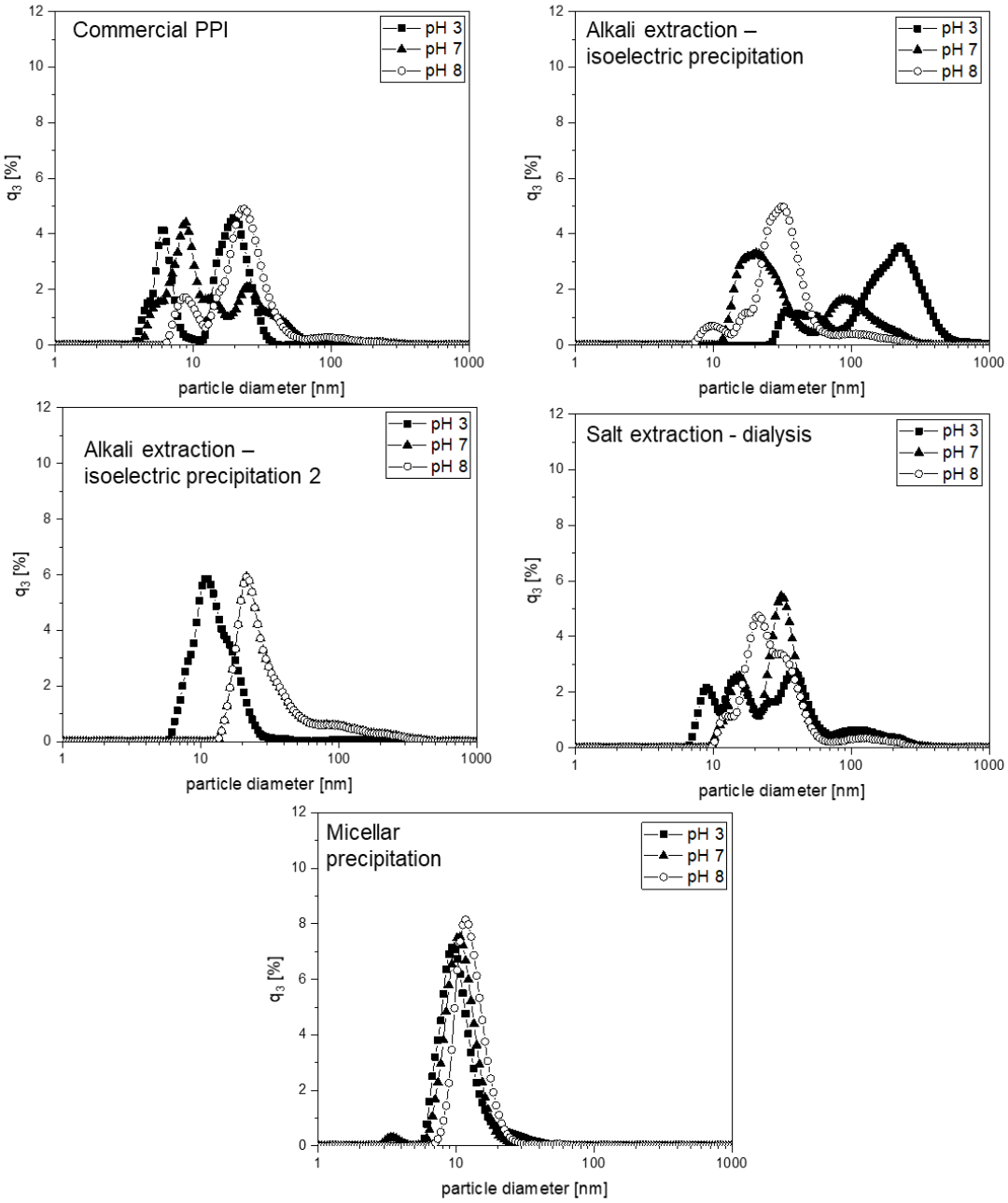

Figure 3-7 Particle size distribution (q_3) at pH 3; 7 and 8 with 0.1 M NaCl of the pea protein products measured by dynamic light scattering.

These pH levels were chosen because solubility was highest at these pH levels and particles still small enough to be measurable. At pH levels between 4 and 6 particle size was so high that the particles were already separated by centrifugation at 6000 x

g. Size distributions are monomodal, bimodal or multimodal. For commercial pea protein, the particles were smallest for pH 3 and highest for pH 8. Jiang et al. (2017) found the highest volume weights mean diameter for commercial pea protein dissolved at pH 4 using dynamic light scattering. Even with an ultrasound treatment, the particle size was highest at pH 4 than at pH 2, pH 10 or pH 12. There is a clear difference between the particle size distribution at those three pH values for both alkali extracted protein products. For the alkali extracted protein product freeze-dried at pH 4.5 particle sizes were highest at pH 3 and lowest at pH 7 and 8. In contrast, for the alkali extracted protein product freeze-dried at pH 7, particle size was lowest for pH 3 and highest for pH 7 and 8. There was no difference between pH 7 and 8 in particle size distribution. From this, it can be concluded that the pH of freeze-drying does not only have an influence on the solubility but also the particle size of the protein product. Salt extracted protein product shows a wide range of particle sizes at pH 3. At pH 7 and 8, it shows slightly higher particle sizes. The particle size distribution for micellar precipitated protein product was similar at all pH levels with a monomodal distribution with particles around 10 nm. An exception was pH 3, where small particles below 10 nm were measured. It can be seen that there are major differences between the particle size distributions of the different extraction procedures. Since there were also differences between the effect of pH on the particle size, one can conclude that the proteins extracted also have different conformations.

The results of the zeta potential of the proteins are shown in Figure 3-8.

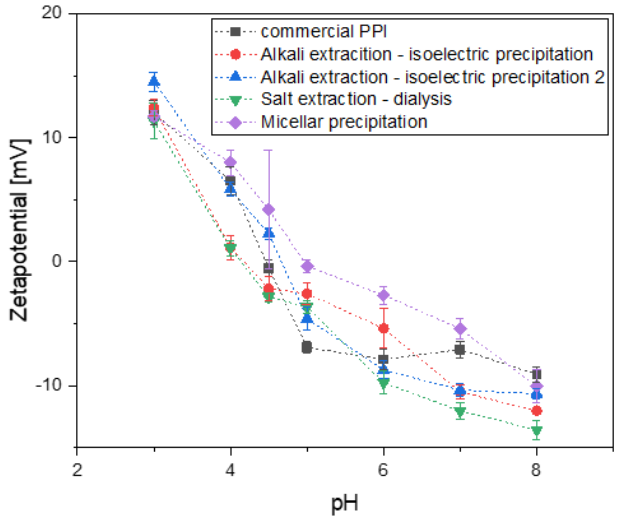

Figure 3-8 Zeta potential of the pea protein products dissolved at 0.1 M NaCl at pH 3-8.

The charge was zero around pH 4.5, the isoelectric point for globulins (Swanson 1990). At pH levels lower than 4 proteins were charged positively and at pH levels higher than 5 proteins were charged negatively. Only the micellar precipitated protein product was zero around pH 5. This can also be explained by the lower amount of phytic acid extracted as described above (Rahma et al. 2000; Cordero-de-los-Santos et al. 2005; Ali et al. 2010). The low charge around the isoelectric point also explains the increase in

size. Repelling electrostatic interactions decreased around that point leading to aggregation of the proteins. This made the proteins insoluble, which can be seen in the low solubility around pH 4 - 5. With increasing charge, the proteins became more soluble again at pH levels above pH 5 or below pH 4.

3.1.3.5 Thermal analysis

Denaturation temperature, enthalpy change and onset temperature of the event of unfolding of the differently produced protein products were measured in water and 1 M NaCl. T_d ranged from 75°C to 81°C. The results can be found in Table 3-2.

Table 3-2 Denaturation temperature (T_d) and T_{onset} for 10% solutions at pH 7 in 0 M NaCl and 1M NaCl for each extracted pea protein product measured by DSC.

	T_d (°C)		T_{onset}(°C)	
Extraction method	0M NaCl	1M NaCl	0M NaCl	1M NaCl
AE-IP	75.2 ± 0.2^{a}	77.8 ± 0.8^{a}	67.4 ± 0.2^{a}	70.7 ± 0.8^{ac}
AE-IP 2	75.1 ± 0.5^{a}	77.3 ± 0.6^{a}	67.3 ± 0.3^{a}	69.3 ± 0.3^{a}
SE	76.2 ± 1.6^{b}	77.6 ± 1.9^{a}	73.8 ± 2.0^{b}	73.8 ± 0.0^{b}
MC	79.2 ± 0.2^{ab}	81.3 ± 0.4^{b}	70.9 ± 1.4^{ab}	71.5 ± 0.4^{c}

$^{a-c}$ Column values followed by the same letter are not significantly different ($p > 0.05$)
*Means ± SD of triplicates

Thermograms show one endothermic peak except for the commercial pea protein sample, which showed no peak at all. This indicates that most of the protein is already denatured and/or aggregated supporting the statement of Taherian et al. (2011), Fuhrmeister and Meuser (2003) and Sun and Arntfield (2010). A high T_d suggests a high thermal stability (Choi and Ma 2007). The denaturation temperatures found are lower than found by Sun and Arntfield (2011) for salt extracted pea protein product using a 10 K/min heating rate, unmodulated. The difference can be explained by the differences in the method used. Since denaturation is a temperature-time effect, denaturation temperature is found lower with a lower heating ramp and modulation (Tang et al. 2007; Ricci et al. 2018; Mession et al. 2013). Using a 0.5 K/min heating rate a T_d of 74.5°C has been found for salt extracted and diafiltrated pea protein in 10 mM Na_2HPO_4 at pH 7.2 (Mession et al. 2015). In the same study a T_d of 76.6°C for legumin and a T_d of 68.5°C for vicilin was reported. The T_d of the differently produced protein products can be ranked as following: alkali extracted pea protein product < salt extracted pea protein product < micellar precipitated protein product. A higher T_d suggests a higher legumin to vicilin ratio, since vicilin trimers are lower in conformational compactness than legumin and thus easier to thermally unfold (Marcone et al. 1998; Mession et al. 2012). Additionally, legumin contains a disulphide bond between the two subunits, which adds to the thermal stability comparable for legumin in buckwheat (Choi and Ma 2005). Under this assumption it can be said that the micellar precipitated protein product had a higher legumin to vicilin ratio than both alkali extracted protein products and salt extracted protein product. This would be in line with the visivle inten-

sity difference of the legumin band in the SDS-PAGE. There was no significant difference between the two alkali extracted protein products and the salt extracted protein product. Therefore, the three protein products had a similar legumin to vicilin ratio. Other extrinsic factors also impact the compactness of the proteins. Denaturation temperatures for samples in 1 M NaCl have been found to be higher than samples dissolved in water. The stabilizing effect of the addition of NaCl has also been found in other studies. This has been explained by stabilization of the salt on proteins quaternary structure, which increases the energy required to unfold the protein (Sun and Arntfield 2011; Mession et al. 2013). The stabilizing effect can be attributed to nonspecific ion effects on electrostatic interactions between charged groups on the protein (Sun and Arntfield 2010). There are two ways in which this could work, working separately or cooperatively. One way is that inter- and/or intra-molecular chain repulsion are reduced by the charge-shielding effect of NaCl. The other is the impact of the salt on the water structure (Damodaran 1988; Sun and Arntfield 2010). The hydrogen-bonded structure is weakened by the salt. This affects the electrostatic and hydrophobic interaction of water with the protein. The effect is mainly dependent on the nature of the anions and cations, which is described in the lyotropic series (Hippel and Schleich 1969; Choi and Ma 2007). Additionally to T_d, also the enthalpy change ΔH was measured. The results are depicted in Figure 3-9.

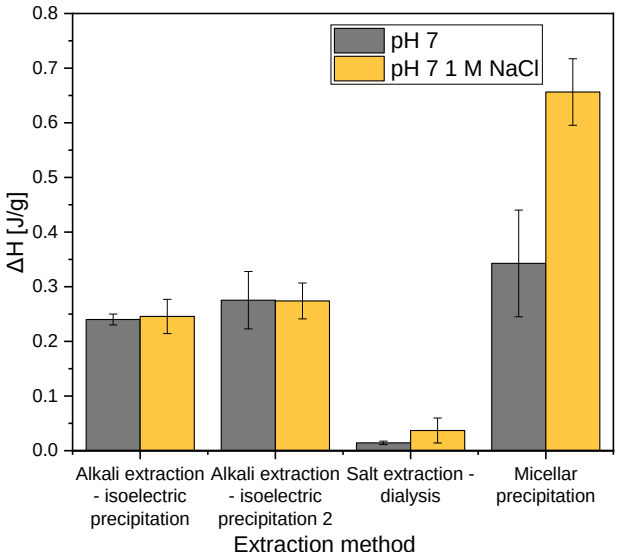

Figure 3-9 Enthalpy change (ΔH) for 10% solution at pH 7 in 0 M NaCl and 1 M NaCl for the extracted pea protein product measured by DSC.

Values found for ΔH were lower than those reported for buckwheat (Choi and Ma 2005). The values found for ΔH in this study were also lower than for salt extracted pea protein using a 10 K/min heating ramp (Sun and Arntfield 2011) and salt extracted diafiltrated pea protein using a 10 K/min and 5 K/min at pH 7.5 (Mession et al. 2013). Next to differences in heating ramp, there were also differences in sample mass and volume of the pan used in this study and the ones mentioned above. Comparable to the results of Shand et al. (2007) using alkali extracted pea protein ΔH was found higher in pea protein dissolved at higher ionic strengths than at lower ionic strengths. This can be explained by the same stabilizing effect of NaCl as for the increase in T_d (Sun and Arntfield 2010). A high heat flow and thus a high ΔH is an indication of a more

native sample. Comparing all extractions with each other, the micellar precipitated protein product shows the highest ΔH value. This leads to the conclusion that micellar precipitated protein product contains the highest amount of native protein. These findings would be in line with earlier findings for faba beans, stating that micellar precipitation is the mildest extraction (Arntfield et al. 1985). If only considering the solubility, the salt extracted protein seemed to be the most non aggregated. However, as already stated above, solubility is not the best criterion for nativity. This is especially the case when analysing globulins, which are per definition very low in solubility in water. Salt extracted pea protein product shows the lowest ΔH, leading to the conclusion that the salt extracted protein product is lowest in nativity, which is analysed in this study. The low ΔH measured by DSC can be explained by the strong alkaline pH (pH~11.60), at which the protein was extracted in the solubilisation step. This pH has been shown to partially unfold the protein, but in case of the pea protein, the protein is also best soluble at pH 12 (Jiang et al. 2017; Lam et al. 2018). Nativity of the salt extracted protein could be improved by adjusting the sodium phosphate solution to pH 8 as done by Stone et al. (2015) or use a more neutral salt as done by Sun and Arntfield (2010). With these adjustments, the salt extraction follows the same principle as the micellar precipitation. First pea protein is dissolved in a salt solution and then the salt concentration is reduced by either dilution as in the micellar precipitation or by desalting as by the salt extraction. Concluding from this, we can say that the solubilisation step has a major influence on the thermal reactivity of the protein product as seen with salt extracted protein product. Next to this, the precipitation step also has an influence on the thermal reactivity of the protein product. This can be seen by comparing alkali extraction protein product with micellar precipitated protein product with each other. The pH of freeze-drying had no influence on the thermal reactivity of the protein product.

3.1.4 Conclusions

As hypothesized, differences in protein quality in terms of yield, protein profile, solubility, zeta potential, particle size and nativity were found, depending on the conditions applied in the extraction procedures. Protein profile of the protein products and by-products e.g. phytic acid content were dependent on the extraction procedure used. Mainly the precipitation step had an influence on the protein profile of the protein product. Alkali extraction and isoelectric precipitation is the fastest extraction procedure. It led to a protein product, which mainly consisted of globulins. Albumins were removed during the precipitation step. Freeze-drying had an effect mainly on solubility and particle size. It did not influence the thermal reactivity. Since solubility is a desired functionality, freeze-drying at pH 7 leads to a higher yield of usable protein product, which also contains native proteins as measured by the DSC. However, protein solubility does not reach 100% and measured enthalpy change is lower than with micellar precipitated protein product. This means that precipitation at pH 4.5 was not fully reversible. Micellar precipitation on the other hand led to the highest enthalpy change in the DSC measurements. This leads to the conclusion that it is the mildest extraction method. It also had a reduced phytic acid content. This was observed by the solubility profile. However, it is only soluble at high salt concentrations and it shows the lowest yield. Salt extraction – dialysis led to the only protein product containing albumins and

was the most soluble protein product. However, salt extraction – dialysis is the extraction that takes the longest time, and it also shows a low enthalpy change during DSC measurement.

Comparing the three extraction methods with each other, no extraction methods can be claimed to be the best in all criterion. However, a protein product with high yield, high solubility and high nativity can be obtained by alkaline extraction – isoelectric precipitation with freeze-drying at pH 7. It can be concluded, that the rehydration/solubilisation step and the precipitation step have a major influence on conformation, solubility, protein profile and nativity. In order to extract native pea protein, the authors suggest to extract at a mild pH around pH 6-8 using a mild salt e.g. NaCl at high concentrations, because highly alkaline pH levels during the solubilisation step can lead to a denaturation of the protein. Furthermore, the precipitation method should be chosen wisely. This step can be used to remove albumins. It results in a purer protein product. Globulins can be precipitated either by isoelectric precipitation or by lowering the salt content. Isoelectric precipitation is not completely irreversible and lowering of the salt concentration leads to a protein product low in solubility in an aqueous solution. However, each extraction method led to a better solubility and lower degree of denaturation and aggregation than in commercial pea protein products. All pea proteins were freeze-dried in this study because it is the mildest drying. Further studies might also want to investigate the effect of drying on the conformation of extracted pea protein.

Acknowledgements

We would like to acknowledge the help of Annette Brümmer-Rolf and Christine Hass for measurements of the protein content with Dumas.

This project was executed as part of an Industrial Collective Research (IGF) project of the Forschungskreis der Ernährungsindustrie e.V., Bonn (FEI) supported by the German Ministry of Economics and Technology via AiF (AiF 20197N).

Compliance with ethical standards

This article does not contain any studies with human or animal subjects performed by any of the authors.

Conflict of interest

The authors declare that they have no conflict of interest.

3.1.5 Appendix

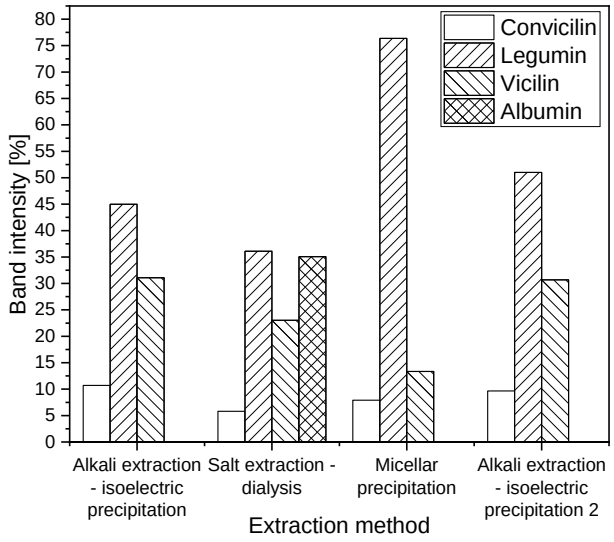

Figure A3-10: Band intensity of the SDS-PAGE bands that can be assigned to the proteins present in peas.

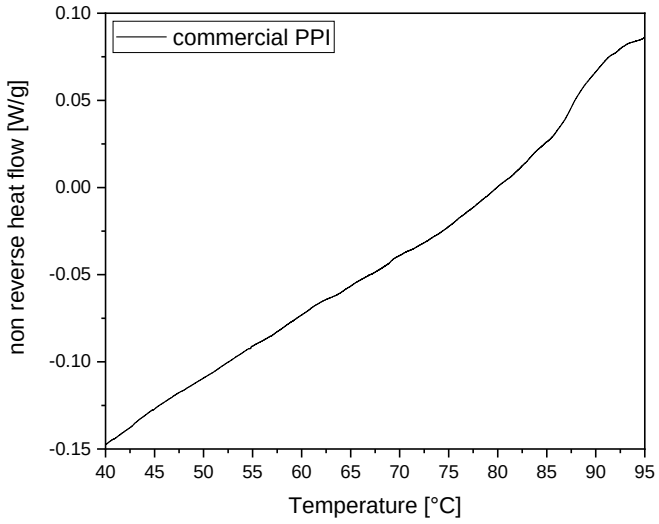

Figure A3-11: DSC thermogram of a 10% solution of a commercial PPI in water at pH 7.

3.2 Quantification of protein-protein interactions in highly denatured whey and potato protein gels

Summary and contribution of the doctoral candidate

An understanding of how proteins interact with each other is of high importance for analysing the aggregation and gelation of proteins. There are two methods to analyse protein interactions. One is to use protein interaction blocking agents. However, this method alters the aggregation and gelation mechanism and therefore the results.This is why the second method has been chosen as a base method. The second method is to dissolve the gel in different buffers, which cleave the interactions. From the solubility of the gels in the buffers, the number of different protein interactions can be quantified. The method presented in this study was one of the fundamental methods to analyse protein aggregates in the following chapters. As a reference method, the protein interaction assay of Keim and Hinrichs (2004) was used and improved. In the method used by Keim and Hinrichs (2004) the gels were dispersed in three different buffers, one phosphate buffer to cleave electrostatic interactions, one tris-acetate buffer containing SDS to cleave electrostatic and hydrophobic interactions, and one tris-acetate buffer containing SDS and DTT to cleave electrostatic and hydrophobic interactions and disulphide bonds. These buffers were found to be too weak for our protein gels and therefore the amount of SDS and DTT was increased. Since our gel systems did not interact with phosphate, all buffers were made on the base of a phosphate buffer to make the buffers more uniform. In the original method, the gels were crushed using an ultra-turrax. However, due to low reproducibility the ultra-turrax was substituted by a garlic press to ensure reproducible crushing of the gel. In the original method, a solubilisation time of 30 min was used. This was not found to be effective and solubilisation time was changed to at least 14 h. After solubilisation of the gel in the buffer, the dispersion was centrifuged in the original and our modified method. The protein content in the supernatant was determined via the Dumas method and soluble protein content was calculated. The amount of soluble protein content was then used for the calculation of protein interaction ratios. The developed protein interaction assay was tested with three different gels, one that is high in disulphide bonds (WPI pH 7), one that is high in hydrophobic interaction (PPI pH 7), and one that is high in electrostatic interactions (WPI pH 5). This was done to test if the method is suitable for a wide range of protein systems. The method was found to show expected results and be reproducible. The limitations of the method were that only the protein interactions between larger aggregates were identified. Protein interactions between small oligomers could not be detected and an additional SDS-PAGE would be needed.

This publication was a shared first authorship. Both first authors contributed equally to the work. The doctoral candidate was mostly involved in method improvement, statistical data analysis, and interpretation. The other first author was more involved in literature review and method development. Both contributed to writing the original draft and including feedback from revision. Co-authors contributed to experimental work and/or discussion.

Adapted original manuscript[3]

Quantification of protein-protein interactions in highly denatured whey and potato protein gels[4]

Caren Tanger*, David J. Andlinger*, Annette Brümmer-Rolf, Julia Engel, Ulrich Kulozik

Chair for Food and Bioprocess Engineering, Technical University of Munich, Weihenstephaner Berg 1, Freising-Weihenstephan, Germany

Graphical Abstract

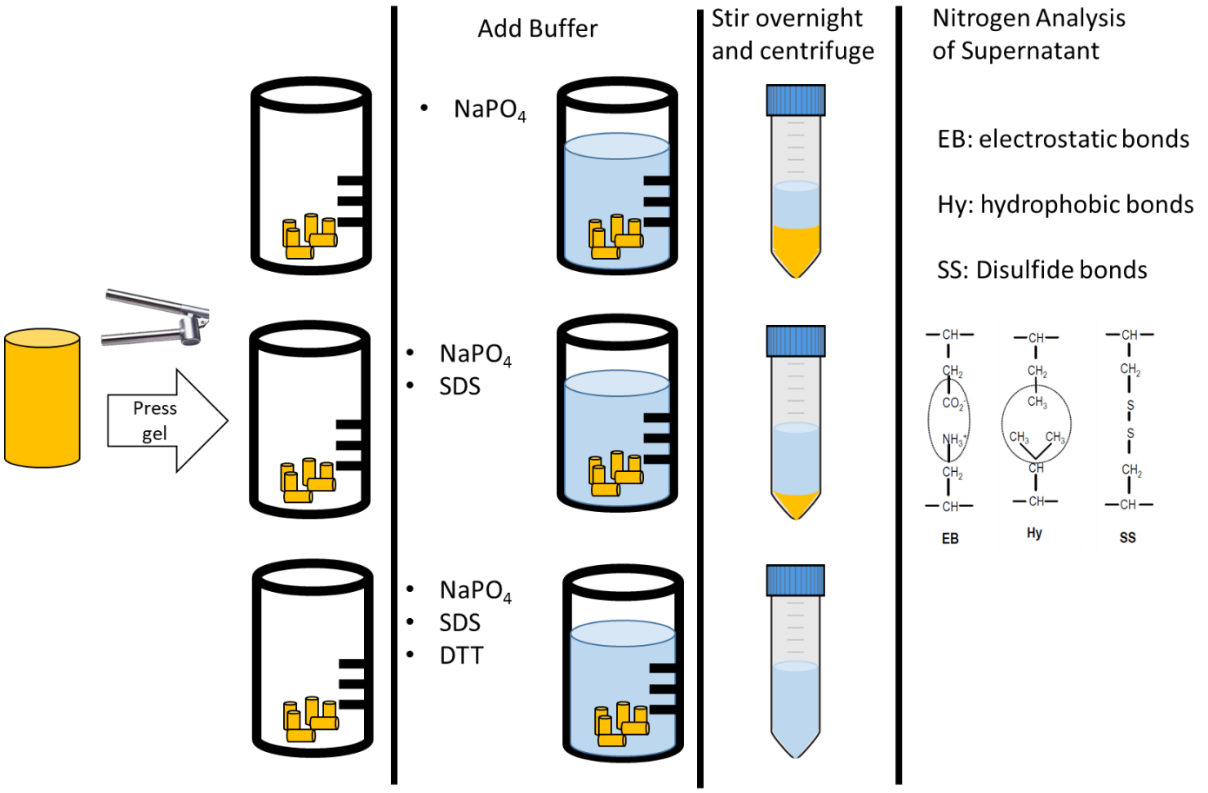

Abstract

Understanding the stabilizing protein interactions in protein gels is of high importance for food- and biotechnology. Protein interactions in protein gels can help to predict hardness, deformability and other gel parameters. Currently, there are two types methods used. One is to use protein interaction blocking agents and the other is to dissolve the gel in different buffer systems, which cleave the interactions. The first method alters the gelling mechanism, which is why the second method is the preferred one. However, currently published methods are often only suitable for specific gel systems as for example weakly bound protein gels. In this paper, a method is introduced, which is suitable for highly denatured whey and plant protein.

[3] Adaption refer to formatting issues: e.g., abbreviations, figure, table, equation and section numbering, citation style, notation of units, spelling, axis labelling. References of all chapters are merged at the end to avoid redundancies.

[4] Originally published in: MethodsX (2021), Vol. 8, 101243. Permission for reuse of this article was granted by Elsevier.

- Suitable for strongly cross-linked whey protein and plant protein gels
- Stronger buffer system to ensure cleavage of all protein interactions
- More reproducible and simplified crushing of the gel without the introduction of uncontrolled shear stress excessively affecting the analysis of chemical bonds

Specification table

Subject Area	Chemistry
More specific subject area	*Protein analysis*
Method name	*Protein interaction assay*
Name and reference of original method	Keim and Hinrichs (Keim and Hinrichs 2004) Influence of stabilizing bonds on the texture properties of high-pressure-induced whey protein gels. In: International Dairy Journal 14, S. 355-363
Resource availability	• Sodium phosphate • Sodium dodecyl sulfate • Dithiothreitol • Shaker or magnetic stirring plate • Garlic press • Centrifuge • Nitrogen analysis according to Dumas

3.2.1 Background information and applicability of the method

Elevated temperature, pressure, organic solvents and other conditions are known to denature proteins. Usually, this is accompanied by unfolding of the protein. During unfolding the hydrophobic core and buried reactive amino acid groups, as well as buried thiol groups, get exposed and proteins can react with each other. This leads to the formation of aggregates and gels. The interactions can be non-covalent (hydrophobic, electrostatic interactions) or covalent (disulphide bonds). The type of interaction determines the textural properties of a protein gel. By controlling the protein interaction by pH and other process parameters the structural properties gels from dairy and plant proteins can be manipulated (Nicolai et al. 2011a; Nicolai and Chassenieux 2019). This is of great importance in the food industry, where proteins are used as structuring agents, next to increasing the nutritional value. One can change the process parameters and analyze the outcome by texture and rheological measurements. However, this approach does not provide in-depth information about the types of bonds stabilizing the gel. This additional information is of increasing interest with the advance of plant proteins in the food industry. Animal protein are progressively substituted by plant proteins as structuring agents. However, animal and plant proteins differ greatly in their molecular structure. Examples are amount of free thiol groups, intramolecular disulfide bonds, molecular weight and surface hydrophobicity (Delahaije et al. 2015; Creusot et

al. 2011). Therefore, they also react differently on triggers inducing gelation and the resulting gels show large differences in textural properties (Martin et al. 2014). With this in mind, it is necessary to have a method available for analyzing the stabilizing bond interactions in animal protein gels and plant protein gels to tailor gel properties. This will allow more insights in the gelation behaviour and gelation mechanisms of animal and plant protein and provide the option to modify processing parameters to obtain desired gel structures in a targeted way.

In literature, there are two main methods to determine the stabilizing protein interactions in a gel: Blocking of protein interactions during gelation and analysing resulting textural properties (1) and measuring the protein/nitrogen solubility of the produced gel in different buffers cleaving specific stabilizing protein interactions (2).

The use of blocking substances can seriously alter the gelation mechanism. For example, N-Ethylmaleimide (NEM) is used to inhibit the reaction of thiol groups (Sun and Arntfield 2012; Mounsey and O'Kennedy 2007).

However, NEM was also shown to promote hydrophobic interactions in soy bean globulins (Hua et al. 2005) and β-lactoglobulin (Xiong et al. 1993). To determine stabilizing protein interactions in a gel, it is therefore preferred to determine the protein/nitrogen solubility in different buffer systems cleaving specific stabilizing protein interactions after gel formation has occurred. The salient buffer systems applied so far include cleaving agents such as sodium dodecyl sulfate (SDS) (Keim and Hinrichs 2004; Martin et al. 2014; Shimada and Cheftel 1988), urea (Felix et al. 2017; Gómez-Guillén et al. 1997; Martin et al. 2014; Shimada and Cheftel 1988), β-mercaptoethanol (Shimada and Cheftel 1988; Gómez-Guillén et al. 1997; Martin et al. 2014)and dithiothreitol (DTT) (Keim and Hinrichs 2004; Shimada and Cheftel 1988). These substances are known to disrupt hydrophobic (SDS and urea) and disulfide bonds (DTT and β-mercaptoethanol). This approach is reported in literature as suitable for different protein system such as egg protein gels (Martin et al. 2014), sardine muscle gels (Gómez-Guillén et al. 1997), pea protein gels (Felix et al. 2017), whey protein gels (Shimada and Cheftel 1988; Martin et al. 2014), lupine protein gels, soy protein gels and leaf protein (RuBisCO) gels (Martin et al. 2014). Different cleaving agents were used by the different authors. However, differences in the properties of the cleaving agents have to be considered. β-mercaptoethanol is toxic and its disulfide reduction potential is lower compared to DTT (Lukesh et al. 2012). Urea contains high amount of nitrogen, which can interfere in nitrogen content determination. Because of this, SDS and DTT are preferred as cleaving agents. The evaluation of the solubility can be either binary (Martin et al. 2014) (did the gel dissolve or not) or the amount of solubilized nitrogen can be used to provide semi-quantitative information on the contribution of each type of protein interaction (Gómez-Guillén et al. 1997; Felix et al. 2017; Keim and Hinrichs 2004; Shimada and Cheftel 1988). The semi-quantitative approach is preferred because it offers the possibility of setting the individual protein interactions in relation. For example, it could be shown that an increase in protein stabilized through disulfide bonds correlated with an increase in gel strength and other rheological parameters of pressure-induced whey protein gels (Keim and Hinrichs 2004). This was possible as the changes from

protein stabilized through disulfide bonds from 20% to 90% could be measured. With the binary approach, such fine differences could not have been detected.
Several methods are available for quantification of solubilized nitrogen/protein content as a base for determining the soluble protein content in the serum after cleavage of certain types of bonds. Three of these methods were recently used for quantification of stabilizing bonds, the Lowry method (Felix et al. 2017; Gómez-Guillén et al. 1997), absorbance at 280 nm (spectrophotometric) (Shimada and Cheftel 1988) and the Dumas method (Keim and Hinrichs 2004). It has to be considered that the cleaving agents chosen have an effect on the nitrogen/protein content determination and vice versa. The Lowry protein assay is a biochemical assay using colourimetric techniques. The biggest disadvantages of the Lowry method are the interferences of buffer and protein with the reactive agent. This can lead to inaccuracies (physico-chemical effects, sorption) (Shimada and Cheftel 1988). Physical interference refers to macroscopic particles. They interfere with the light scattering during photometrical absorption measurement. Physical interference also plays a role in spectrophotometric measurements. In case of DTT as the cleaving agent, the oxidized form of DTT has the same absorption maximum as the one of protein (Cleland 1964). This makes the method unnecessarily prone to experimental error. For two of these methods, Lowry and spectrophotometric measurement, a calibration curve is needed and this is highly labour intensive. The third method mentioned was the Dumas method. There, the nitrogen content in the buffer system is determined by controlled combustion of a sample. Therefore, there is no interference of a chemical reagent with the protein or buffer. An additional advantage is the reproducibility and the high throughput. This is the reason why the Dumas method is the method of choice of many laboratories to determine nitrogen/protein content. A disadvantage of the Dumas method, however, is that the total nitrogen content of the sample is determined. This means that nitrogen containing substances in the buffer are also measured as protein. This would be the case for urea and the common buffer substance 2-Amino-2-(hydroxymethyl)propane-1,3-diol (TRIS) leading to a high background noise. However, the method of Dumas can be considered advantageous. However, buffers with nitrogen containing substances should be avoided. The Dumas method was utilized by Keim and Hinrichs for the determination of pressure induced whey protein gels (Keim and Hinrichs 2004) and acid, rennet and pressure-induced milk protein gels (Keim et al. 2006) with some limitations or even restrictions regarding highly thermally denatured protein.
The aim of this work was to modify a protein interaction assay, which can be applied to both highly denatured animal-derived proteins (especially whey proteins) and plant proteins. The determination of protein interactions should be semi-quantitative. Furthermore, a high reproducibility and high throughput were aimed at.
Concluding from this, the method of Keim and Hinrichs (2004) was the most suitable for modification. It is a semi-quantitative method using the Dumas method for nitrogen quantification and the buffer system contains SDS and DTT as cleaving agents. The method was used for whey protein with a low degree of denaturation (Keim and Hinrichs 2004; Keim 2005), where protein interaction was weak. In order to extend the method and to make it suitable for highly denatured whey and plant protein with strong

protein interactions, adjustments to the buffer systems, dissolving method and dissolving parameters had to be made. The proposed and validated changes are discussed in detail below.

3.2.2 Explanation on changes made

The following buffer system was used by Keim and Hinrichs (2004). Buffer S1 was composed to cleave all hydrophobic and electrostatic interactions and contained a TRIS-Acetate buffer with SDS. Buffer S2 was composed to cleave all hydrophobic and electrostatic interactions and disulphide bonds and contained a TRIS-Acetate buffer, SDS and DTT. In theory, the gel should completely dissolve in buffer S2. Buffer S3 was composed to cleave all electrostatic interactions and contained a sodium phosphate buffer with NaCl. In later works, the authors added two new buffers, which were able to cleave calcium bridges (D) and non-specific bonds (H) (Keim et al. 2006). This addition made the method suitable for pressure-induced, heat-induced and rennet-induced milk protein gels. TRIS contains nitrogen, which leads to a high background noise during nitrogen measurement. The authors probably used a TRIS-Acetate buffer, because it does not interact with casein micelles. Casein micelles are present in milk protein gels. Phosphate buffers, on the other hand, are known to severely influence the casein equilibrium and alter micelle structure and composition (Udabage et al. 2000). However, caseins are not present in whey protein or plant protein. In order to reduce the background noise, the TRIS-Acetate buffer was substituted by a phosphate buffer. No differences were found between the usage of TRIS-Acetate and phosphate buffer for whey and plant protein gels. The buffers S1 and S2 were not able to cleave all hydrophobic interactions and disulfide bonds in highly denatured whey and plant proteins. Therefore, the concentration of SDS and DTT had to be increased. Additionally, the pH was increased to pH 7.5 to increase the reducing ability of DTT. Furthermore, stirring time was increased to a minimum of 16 h. These were found to be optimal condition for DTT and SDS to cleave all protein interactions. Stirring temperature was set to room temperature to avoid crystallization of SDS at low temperatures.

The cleaving agents can only work on the exposed surface of the gel. They cannot penetrate the inside of the gel. In order to increase the exposed surface of the gel Keim and Hinrichs (2004) as well as Gómez-Guillén et al. (1997), Felix et al. (2017) and Shimada and Cheftel (1988) used an ultra-turrax to crush the gel in the buffer. The ultra-turrax can shear the gel in small particles, which increases the exposed surface. However, it also induced an uncontrollable shear stress destroying bonds prior to the analysis in an uncontrolled or excessive way. This can lead to misconceptions regarding the types of bonds stabilizing a gel. Whey protein gels produced at pH 7 and 15% protein concentration heated for 30 min above denaturation temperature led to very hard gels. The gel either got partially stuck in the case of the ultra-turrax or was not comminuted at all, thus not allowing the buffer systems to enter the gel sample. This leads to a low reproducibility. The result of a six-fold measurement of such a gel using an ultra-turrax is shown in Figure 3-12.

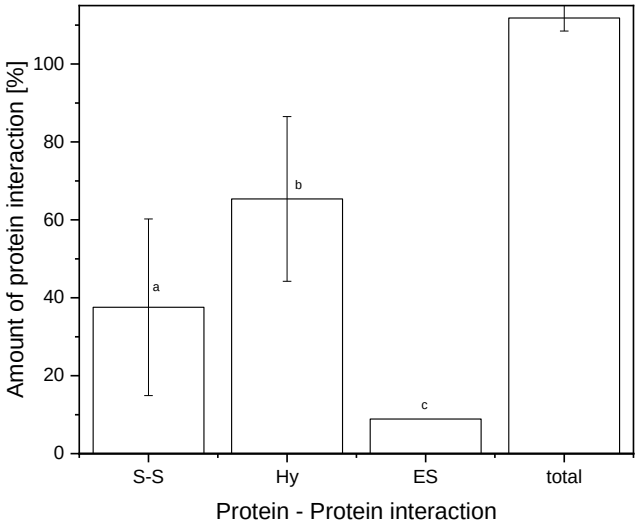

Figure 3-12: Protein interactions of a WPI gel prepared at pH 7 at 85°C crushed with an ultra-turrax, determined in six-fold. Error bars depict standard deviation. [a-c] different letters indicate significant differences between samples (P < 0.05).

The error bars depict the standard deviations, which are very high (>15%). Although the amount of disulphide bonds and hydrophobic interactions show a significant difference, the p-value was high with p=0.0239. There was also a significant difference between disulphide bonds and electrostatic interaction. Again the p-value was high with p=0.0210. Therefore, the method was not sufficiently reproducible. Because of this, it was chosen to replace the ultra-turrax as a device for mechanical sample pre-treatment. The requirements were that the crushing method was reproducible and it should not destruct the gel beyond the level required to allow the cleaving buffering systems to diffuse into the gel in an acceptable short period of time. The requirements were fulfilled by using a garlic press. Pressing the gel through the garlic press resulted in laces of 2 mm diameter. The laces were then chopped in smaller cylinders. The cleaving agents were thus able to reproducibly cleave all protein interactions.

3.2.3 Description of modified protein interaction assay

For the method development, heat-set protein gels at different pH values from patatin rich potato protein isolate and whey protein isolate were created. Commercial patatin rich potato protein isolate (PPI) powder (Solanic 200), was kindly provided by AVEBE (Veendam, The Netherlands). The protein powder had a protein content of 88.6% (w/w). Commercial WPI (BiPRO^{TM}) powder from Agropur Dairy Cooperative (Saint-Hubert, Longueuil, Canada) was obtained. The protein powder had a protein content of 90.9% (w/w). The protein content was determined using the method of Dumas with an accuracy of ± 0.1% (w/w) (Vario MAX CUBE, Elementar Analysensysteme GmbH, Hanau, Germany). The Dumas factor was 6.38 and 6.25 for WPI and PPI, respectively. However, the Dumas factors are not necessary to determine soluble nitrogen.

3.2.3.1 Preparation of buffer systems

Three buffers were prepared. The detailed composition of the three buffers can be found in Table 3-3. Buffer B1 dissolves proteins bound by electrostatic and non-specific

interactions. Buffer B2 additionally dissolves Proteins bound by hydrophobic interaction due to the addition of SDS. Buffer B3 additionally dissolves proteins bound by covalent disulfide bonds due to the addition of DTT.

Note: Higher concentrations of DTT and SDS, compared to Keim and Hinrichs (2004), were chosen to fully dissolve strongly bound globular proteins. Even higher concentrations of SDS were also tested (up to 10 g/L). However, this resulted in the formation of filaments of some covalent linked protein gels, which could not be separated through centrifugation.

Table 3-3: Composition of the three different buffers used in this study.

Buffer system	NaH_2PO_4 /Na_2HPO_4 [mol/L]	SDS [g/L]	DTT [g/L]	pH
B1	0.05	-	-	7.5
B2	0.05	2	-	7.5
B3	0.05	2	15	7.5

3.2.3.2 Dissolution of gel in buffer system

1. Press gel through a garlic press, for homogenization and size reduction
2. Weigh 0.5 g of crushed gel in each of three 50 ml glass beakers
3. Label the glass beakers B1, B2, B3
4. Pour 20 g buffer of the respective buffer into each beaker

Note: 0.5 g gel does refer to a gel with 10% - 15% protein content. Thus, the protein to buffer ratio is 0.01-0.015: 4. If the nitrogen content gets too high, the buffer is not able to cleave all protein-protein interactions in the gel.

3.2.3.3 Mixing

1. Stir overnight at room temperature with a magnetic stirrer

Note: Dissolving in centrifuge tubes and using a shaker instead of a beaker and a magnetic stirrer does also work and allows dissolving and centrifuging in the same tube increasing the reproducibility of the process.

3.2.3.4 Determination of soluble nitrogen content

1. Centrifuge stirred samples at 10 000 g at 20°C for 20 min
2. Separate supernatant from pellet. The pellet can be discarded.
3. Determine % nitrogen content in supernatant by the Dumas method
4. Determine also the % nitrogen content of the original gel by the Dumas method

Note: An SDS-PAGE of the supernatants of the gel dissolved in the three buffers can give an indication of which proteins are engaged in the different protein-protein interactions. Some pellets were very soft and the supernatant had to be removed with a pipette to avoid mixing between pellet and supernatant.

3.2.3.5 Quantification of protein interactions

First, the concentration of protein bonds that are cleaved by the different buffer systems ($C_{n,bond,Bx}$) has to be calculated. This is shown in equation (3-7):

$$C_{n,bond,Bx} = \frac{(m_S + m_{gel})}{m_{gel}} * C_{n,sup,Bx} \quad (3\text{-}7)$$

With m_S being the initial mass of the buffer (20 g), m_{gel} being the mass of the gel (0.5 g) and $C_{n,sup,Si}$ being dissolved nitrogen in the supernatant in [%], determined by the method of Dumas.

Buffer B1 cleaves electrostatic protein-protein interactions and hydrogen bonds [P(ES)]:

$$\frac{C_{n,bond,B1}}{C_{n,gel}} = P(ES) \quad (3\text{-}8)$$

With $C_{n,gel}$ being the nitrogen content in [%] of the analysed gel. P describing the relative amount of protein-bound by this protein interaction. ES is abbreviated for electrostatic bonds including hydrogen bonds

Buffer B2 cleaves all electrostatic [P(ES)] and hydrophobic protein-protein interactions [P(Hy)]. Therefore, it can be said that:

$$\frac{C_{n,bond,B2}}{C_{n,gel}} = P(ES) + P(Hy) \quad (3\text{-}9)$$

with Hy being short for hydrophobic interactions.

Buffer B3 cleaves all protein-protein interactions, including disulphide bonds [P(SS)]. Therefore, it can be said that:

$$\frac{C_{n,bond,B3}}{C_{n,gel}} = P(ES) + P(Hy) + P(SS) \quad (3\text{-}10)$$

With SS being short for disulphide bonds.

From Equation (3-7 - (3-10, we can deduce following equations to calculate the amount of protein-bound by the different protein interactions.

The quantity of electrostatic interactions including hydrogen bonds is given by the concentration of solubilized protein nitrogen in Buffer C divided by the protein nitrogen content of the analysed gel:

$$P(ES) = \frac{C_{n,bond,B1}}{c_{n,gel}} \quad (3\text{-}11)$$

The amount of protein nitrogen bound by hydrophobic interactions can be calculated by the difference of solubilized protein nitrogen in buffer B2 and B1:

$$P(Hy) = \frac{C_{n,bond,B2}}{c_{n,gel}} - \frac{C_{n,bond,B1}}{C_{n,gel}} \quad (3\text{-}12)$$

The amount of protein nitrogen bound by disulphide bonds can be calculated by the difference of concentration of solubilized protein nitrogen in buffer B3 and B2:

$$P(SS) = \frac{C_{n,bond,B3}}{C_{n,gel}} - \frac{C_{n,bond,B2}}{C_{n,gel}} \quad (3\text{-}13)$$

3.2.4 Method validation

3.2.4.1 Reproducibility of method

In order to validate the method and to test the buffer system, three different types of gels were tested six-fold. For each gel type samples for six-fold measurement were taken from the same gel. This was done to test the reproducibility of the method and not of the gel formation. Results were also analysed statistically using a one-way analysis of variance (ANOVA) and students t-test for significant difference between the amount of protein interactions (see Figure 3-14). Minimum significance was set at the 5% level ($p < 0.05$). The chosen test gels should be different in their dominant protein interactions. Therefore, two different whey protein gels and a potato protein gel were tested. One whey protein gel was made by heating a 15% whey protein solution for 30 min at 85°C at pH 7. The second whey protein gel was made by heating a 15% whey protein solution at pH 5 30 min at 70°C. The potato protein gel was made by heating a 10% potato protein solution at pH 7 for 30 min at 70°C. Differences in protein type, heating and milieu conditions will lead to different protein interactions being dominant within the gels. First, the reproducibility of the nitrogen solubilisation will be examined. Afterwards, the results of this will be discussed with literature findings.

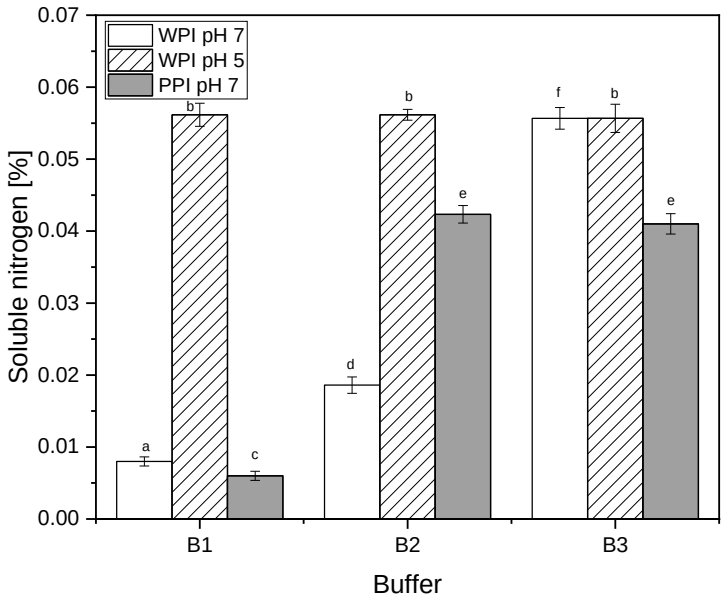

Figure 3-13: Soluble nitrogen content of the supernatant of the three gels dispersed in the three buffers (see Table 3-3 for composition) and centrifuged at 10000 g for 20 min. The three gels were: a WPI gel at pH 7 heated 85 °C, a WPI gel at pH 5 heated at 70 °C and a PPI gel at pH 7 heated at 70 °C. All gels where heated for 30 min. [a-f] different letters indicate significant differences between samples ($p < 0.05$).

The soluble nitrogen content in the different buffers with standard deviation are shown in Figure 3-13. The soluble nitrogen content already indicates; which protein interaction

is dominant in the gel. For PPI only a 10% (w/w) protein gel was used therefore less nitrogen can be solubilized. This explains the low soluble nitrogen content in buffer B3 of the PPI gel.

Most important in Figure 3-13 is the standard deviation. In contrast to Figure 3-12, the standard deviation is acceptably small. This implies that the changes made to the initial method of Keim and Hinrichs (2004) led to a reproducible method for highly denatured whey and plant proteins.

In the following the ability of the buffers to cleave all protein interactions is determined. First, the gels were dissolved in buffer and nitrogen content after solubilisation was determined. Afterwards, equations 1-7 were applied to the measured nitrogen solubility in each buffer. From this, the relative amount of each protein interaction within the gels were obtained. The results of the calculations are shown in Figure 3-14. It should be noted that the highest amount of nitrogen is dissolved in buffer B3 as this buffer cleaves all protein interactions. The total amount of protein interactions was found to be around 100% for each gel measured independent of dominant protein interaction found in the gel. Therefore, it can be said, that the buffer system and dissolving parameters were sufficient to cleave all protein interactions. Below, the results obtained with this method were compared to literature findings using other methods.

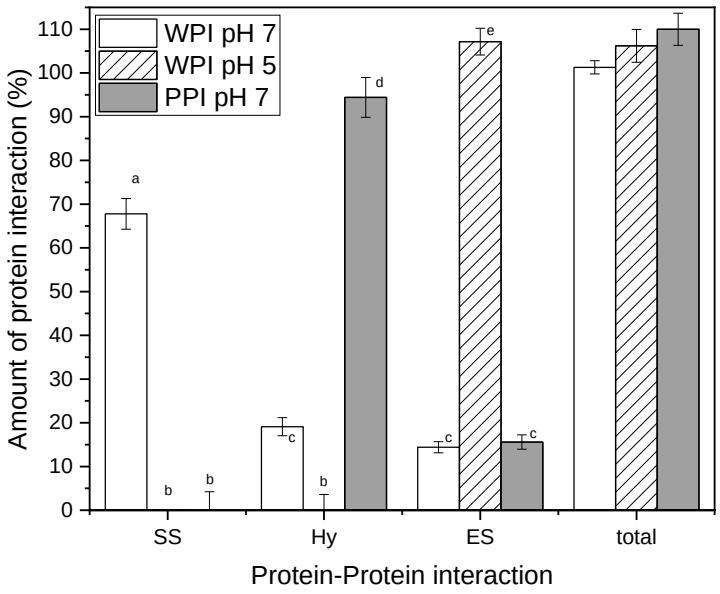

Figure 3-14: Protein interactions of a WPI gel at pH 7 heated at 85 °C, a WPI gel at pH 5 heated at 70 °C and a PPI gel at pH 7 heated at 70 °C. All gels where heated for 30 min. [a-e] different letters indicate significant differences between samples (P < 0.05)

As expected, the main protein interaction in whey protein gels, heated well above their temperature of denaturation and at pH 7, was by disulphide bonds (66%) followed by hydrophobic interactions (19%). Electrostatic interactions played a minor role. The formation of disulphide linked whey protein gels and the effect of pH and temperature on the gelation are described in detail elsewhere (Monahan et al. 1995; Sava et al. 2005).

Monahan et al. (1995) and Sava et al. (2005) also found that disulphide bonds were the dominant protein interaction in heated whey protein and β-lactoglobulin by measuring the sulfhydryl group content using Ellmann reagent.

In contrast, protein interactions in the whey protein gel heated at pH 5 below denaturation temperature were mainly found to be of electrostatic nature. For these types of gels, the low electrostatic repulsion of protein monomers led to electrostatic interactions without the formation of disulphide bonds. This is in line with the finding of Sava et al. (2005).

The potato protein gel was formed mainly by hydrophobic interactions. Patatin, the main potato protein, contains one free thiol group. Therefore, only two patatin monomers can be bound together by a disulphide bridge. In this case, no larger networks can be formed by disulphide bonds as compared to whey proteins which create multilateral networks by a thiol-disulphide exchange mechanism (Creusot et al. 2011; Pots et al. 1999). The lack of internal disulphide bonds in patatin leads to an extensive unfolding upon heating (Pots et al. 1998b). Upon unfolding, the hydrophobic core gets exposed and hydrophobic residues can react with each other. Several proteins can react with each other via hydrophobic interactions building a gel network. Gelation of potato protein is not dependent on the formation of disulphide bonds. This explains the dominant hydrophobic interactions in the potato protein gel.

Summarizing, the method was found to be reproducible and all protein interactions were cleaved by SDS and DTT. The dominant protein interactions of the three gels were in line with what was expected from the literature.

3.2.5 Limitation of the method

The method is based on the centrifugal separation. Cleaved particles became soluble and uncleaved gel particles remained insoluble. Disulphide linked dimers or small oligomers cannot be cleaved by buffer B2. However, these protein particles are small enough to stay soluble in buffer B2. They contribute to the calculated hydrophobic interactions even though they are cross-linked by disulphide bonds. To investigate those small oligomers, an SDS-PAGE with the supernatant of buffer B2 was performed. The SDS-PAGE of the three gels in buffer B2 can be seen in Figure 3-15.

Uncleaved oligomers can be found in the pocket of the SDS-PAGE. This is the case for whey protein gel prepared at pH 7 at 85°C for 30 min (Lane 1). Thus, there are aggregates bound via disulphide bonds, which are larger than 250 kDa, but small enough to stay soluble during centrifugation. The two other bands in lane 1 are monomeric β-Lg and α-La. No dimers were found. With this, it can be said that there are monomeric proteins, which are bound together by hydrophobic interactions. It can also be said that there are small oligomers cross-linked by disulphide bonds. These small oligomers are connected by hydrophobic interactions forming a gel network. No bands were found for proteins above 250 kDa in the whey protein gel prepared at pH 5, with heating below denaturation temperature. Thus, no disulphide bonds were formed. In the potato protein gel, no bands above 250 kDa could be found. The band at 95 kDa could be attributed to lipoxygenase and does not disappear in a reducing SDS-PAGE.

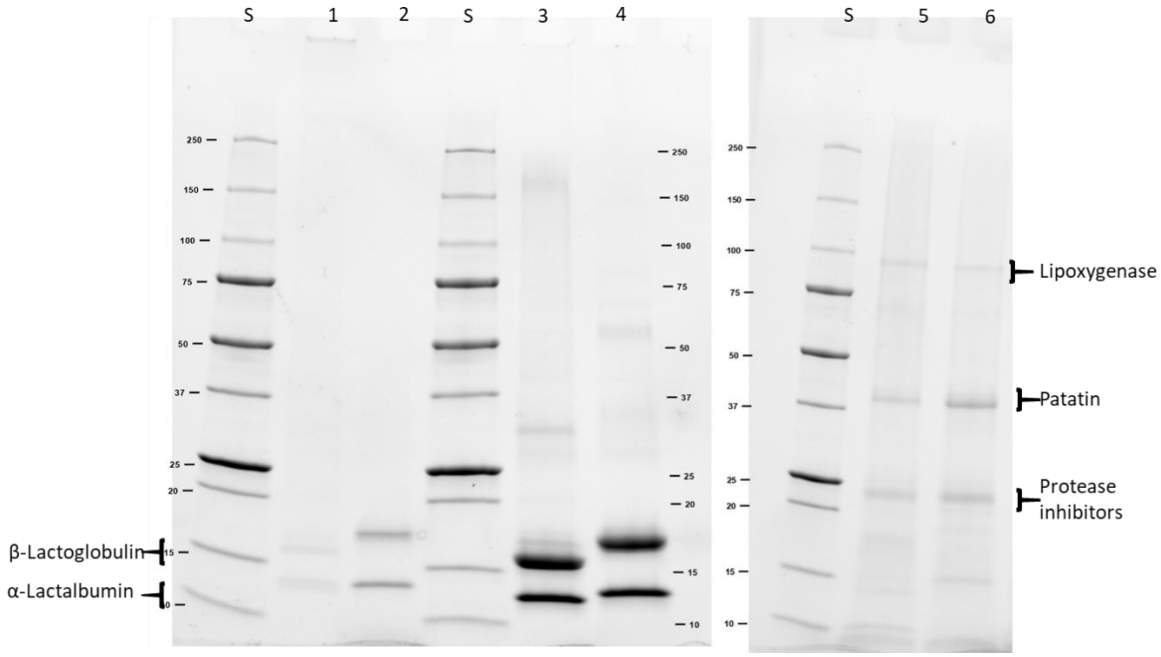

Figure 3-15: SDS-PAGE of supernatant of buffer B2 of the two WPI gels and the PPI gel. S marks the standard lane. Lane 1 and 2 are WPI gels at pH 7, non-reducing and reducing. Lane 3 and 4 are WPI pH 5, non-reducing and reducing. Lane 5 and 6 are PPI gels at pH 7, non-reducing and reducing.

Therefore, it can be said that this gel solely relies on hydrophobic interactions. The addition of performing an SDS-PAGE with the supernatant of the three buffers provides even more information to the protein interaction assay. It gives the opportunity to separate the protein interaction between big particles and between the proteins themselves. The SDS-PAGE gel also shows a limitation of the method presented in this paper. Separation of cleaved and uncleaved proteins and particles by the buffers is based on centrifugation. Therefore, smaller aggregates, such as dimers and trimers, bound together by disulphide bonds, stay soluble in buffer B2 and add to the calculated hydrophobic interactions. They can only be made visible by non-reducing SDS-PAGE.

Note: If not all protein is dissolved in buffer B3 an investigation into the pellet by SDS-PAGE could hint at the formation of isopeptide bonds, as described elsewhere (Rombouts et al. 2011). However, dissolution of the pellet in the SDS-PAGE buffer indicates that the buffer B3 is not strong enough to cleave all disulphide bonds. This was the case when WPI gels heated at pH 7 and 85 °C were investigated and the DTT concentration was below 15 g/L and the protein to buffer ratio was higher than described here.

3.2.6 Conclusion

In this paper, a method for the determination of stabilizing protein bonds in a protein gel is presented. The method was based on an existing method for weakly bound milk protein gels and adapted. Changes to the composition of the buffer system, the crushing method of gel and dissolution parameters had to be made. It could be shown that the presented method is reproducible and suitable for highly denatured whey and plant protein gels. A limitation is that stabilizing protein bonds of small aggregates such as dimers and small oligomers could not be determined. From this, it can be anticipated

that the presented method is of interest for further research in strongly bound protein gels from both animal and plant proteins. Especially for plant proteins, there is still a lot to be learned about the type of protein interactions forming aggregates and gels.

Acknowledgements

We would like to acknowledge the help of Christine Haas for Elementar measurement and Heidi Wohlschläger and Claudia Hengst for experimental idea generation. Maria Weinberger and Marius Reiter are thanked for valuable discussion. Prof. Dr. Jörg Hinrichs and Dr. Susanne Keim are thanked for giving insight into their methodology on which this work is based on. We would like to thank Marc Laus from AVEBE, Veendam, The Netherlands, for providing the potato protein isolate.

This work was funded by IGF Projects of the FEI (AiF 20197 N and 19712 N) and supported via AiF within the program for promoting the Industrial Collective Research (IGF) of the German Ministry of Economic Affairs and Energy (BMWi), based on a resolution of the German Parliament.

3.3 Influence of pH and ionic strength on the thermal gelation behaviour of pea protein

Summary and contribution of the doctoral candidate

Gelation is one of the functional properties of pea proteins. Analysing the gelation of pea proteins can give valuable information about the thermal aggregation behaviour of pea proteins. In contrast to whey and potato protein, there is still limited knowledge about the thermal behaviour of pea proteins and how the pea protein reacts with each other. Analysing the thermal gelation behaviour of pea protein is valuable information for manipulation aggregation of pea protein. In this study, the thermal gelation of pea proteins has been analysed at varying pH values (pH 3; pH 4.5, pH 7, pH 9) and ionic strength (0 to 1.5 M NaCl) using rheology and protein interactions assay. During rheological measurement, the elastic modulus $G'_{25°C}$, the ratio $G'_{25°C}$ to $G'_{95°C}$, and dependence on frequency and amplitude were analysed. For a better understanding of the thermal behaviour, the protein solubility and denaturation temperature of the starting solution were measured. The stiffest gels were observed at pH 4.5 at 0.6 M NaCl. These were also the milieu condition, where 50 % of the protein was soluble. High $G'_{25°C}$ and low tanδ indicated the incorporation of active fillers at pH 4.5, which was hypothesized to be unsoluble protein. A low $G'_{25°c}$ to $G'_{95°C}$ ratio indicated a high amount of hydrophobic and covalent interactions at all salt concentrations, which is supported by the findings in the protein interaction assay. At a more acidic pH of 3 proteins were acid denatured before gelation. However, the addition of salt could protect the protein from acid denaturation, which led to an increase in stiffness with increasing salt concentration and a decrease in $G'_{25°c}$ to $G'_{95°C}$ ratio. This indicated more hydrophobic and covalent interactions compared to the salt-free gel at pH 3. At pH 7 and pH 9 the denaturation temperature increased above 95°C and therefore not all proteins could denature during thermal treatment. This is seen back in an increase in electrostatic interactions, especially at pH 9. At pH 9 at a high salt concentration of 1 M NaCl and 1.5 M NaCl, a cross-over of G' and G'' with increasing frequency has been found. This indicated that these gels were rather an entangled solution than a gel. Even though non-covalent interactions were the most dominant interactions found in pea protein gels at all pH levels, small covalently bound oligomers have been found by SDS-PAGE at all pH and salt concentrations. Thus, covalent bonds occur during pea protein gelation, however, they do not form a continuous network. Overall, it was found that the pH had a more significant impact on the pea protein gelation than the ionic strength. This holds especially true for pH values around the isoelectric point of 4.5 of pea protein.

The doctoral candidate contributed to the conceptualization of the study and contributed to the development of the used methodology. Data analysis and interpretation were mainly carried out by the doctoral candidate. The doctoral candidate wrote the original draft and incorporated feedback from co-authors and reviewers. Co-authors contributed to the experimental part and/or discussion of the results. They also provided input on the drafted publication prior to submission.

Adapted original manuscript[5]

Influence of pH and ionic strength on the thermal gelation behaviour of pea protein[6]

Caren Tanger*, Michaela Müller, David Andlinger, Ulrich Kulozik

Chair of Food and Bioprocess Engineering, Technical University of Munich, Weihenstephaner Berg 1, Freising-Weihenstephan, Germany

Graphical Abstract

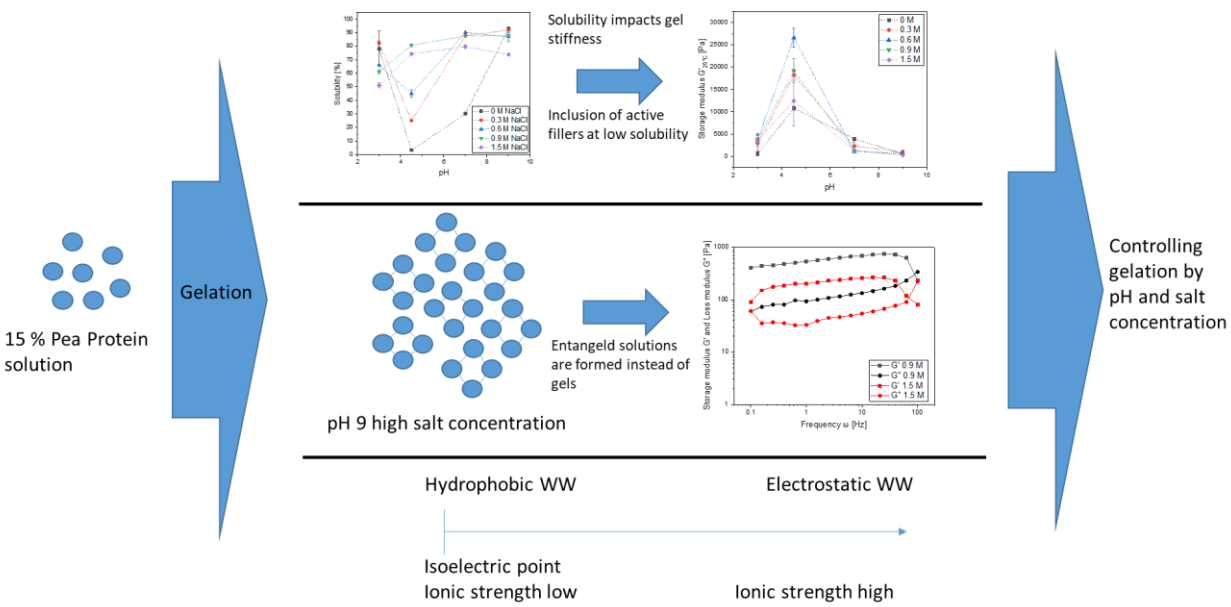

Highlights

- Ionic strength has a minor effect on gelation at neutral and alkaline pH and a major effect at acidic pH.
- Solubility impacts stiffness of pea protein gels
- Gels at pH 9 and high ionic strength resemble rather entangled solutions than a gel.
- Stabilizing protein interaction are non-covalent and dependent on pH and ionic strength

Abstract

Gelation is one of the functional properties of protein, which can be controlled by pH and ionic strength. However, knowledge related to gelation properties of emerging plant proteins is still limited. In this paper, the solubility, the thermal behaviour and

[5] Adaption refer to formatting issues: e.g., abbreviations, figure, table, equation and section numbering, citation style, notation of units, spelling, axis labelling. References of all chapters are merged at the end to avoid redundancies.

[6] Originally published in: Food Hydrocolloids (2022), Vol. 120 C, 106903 . Permission for reuse of this article was granted by Elsevier.

gelation behaviour of pea protein were analysed. Gels were analysed rheologically measuring the elastic modulus $G'_{25°C}$, the ratio of $G'_{25°C}$ to $G'_{95°C}$, and dependence on frequency and amplitude. In addition, the stabilising protein interactions within the gel were analysed. The stiffest gels were obtained at pH 4.5 at 0.6 M NaCl. The high $G'_{25°C}$ and low tan δ value indicate the inclusion of active fillers, which is proposed to be insoluble protein. Salt addition at acidic pH could protect the protein from acid denaturation leading to a low heat denaturation at 62°C to 68°C compared to heat denaturation at neutral pH. Addition of salt at pH 3 also led to a stiffer gel with a lower $G'_{25°C}$ /$G'_{95°C}$ ratio, which indicates more hydrophobic and covalent interactions. An increase in ionic strength at pH 7 and pH 9 led to an increase of denaturation temperature above gelation temperature and an increase of electrostatic interactions. At pH 9 at ionic strengths of 0.9 M NaCl and 1.5 M NaCl the frequency sweep showed that an entangled solution was formed, instead of a gel. It was observed that pea protein gelation were more influenced by the ionic strength at low pH values compared to neutral or alkaline pH.

3.3.1 Introduction

With increasing demand for proteins to feed the world population, animal proteins become an ecological burden. Therefore, food industry increases the use of plant proteins, which are low in cost and have a lower negative impact on the environment. Next to soy, pea is a widely used pulse protein in food of increasing interest (Barac et al. 2010). Depending on type and environment, peas contain a very high amount of protein between 20 – 30% (Koyoro and Powers 1987), which renders peas an interesting source for protein enrichment. Pea proteins can be divided into two main protein fractions: globulins and albumins. Globulins, which are salt soluble, contain legumin, vicilin and convicilin. Albumins are smaller proteins and are water soluble (Derbyshire et al. 1976).

Legumin (11 S) naturally occurs as a hexamer of 360 kDa. This hexamer comprises six monomers of 60 kDa, which are bound together by hydrophobic interaction. The monomers are built of an acidic sidechain (40 kDa) and an alkaline sidechain (20 kDa). They are bound together by a disulphide bond (Dziuba et al. 2014; Shand et al. 2007). Vicilin occurs as a trimer of 150 kDa. It is comprised of 3 subunits of 50 kDa without any disulphide bonds present (Liang and Tang 2013; Shand et al. 2007). Convicilin occurs as a tetramer of 280 kDa with four subunits of 70 kDa, which are bound non-covalently (O'Kane et al. 2004a).

Globular proteins are used in food as structure giving agents and to increase the nutritional value for example by the formation of a 3D protein network i.e. gelation. . One way to induce gel formation is by thermal treatment. Thereby, proteins denature and interact with each other by forming aggregates first or gels if the protein concentration is high enough. In addition, the formation and properties of protein networks are generally, and for some proteins specifically, known to depend on pH and ionic strength (Nicolai et al. 2011b; Nicolai and Durand 2013). Sun and Arntfield (2011) found that the pH and ionic strength has an influence on denaturation and heat set gelation of pea protein using differential scanning calorimetry (DSC) and rheological measurements. NaCl was found to have a stabilizing effect against denaturation. The stiffest gels were formed at 0.3 M NaCl and pH below 6 in the mentioned study. Due to the effect of pH and ionic strength on the molecular structure of pea proteins both pH and

ionic strength were found to have an effect on texture of pea protein gels (Munialo et al. 2015; Shand et al. 2007; Sun and Arntfield 2011). The effect of pH was found to be bigger than the effect of ionic strength (Shand et al. 2007). G' increased 16 x by a pH shift of pH 7 to pH 4.5 and G' only increased 12 x by an increase of 0.3 M NaCl compared to 0 M NaCl at pH 7 (Sun and Arntfield 2011). It was also found that temperature (Shand et al. 2007), cultivar (O'Kane et al. 2005) and extraction type (Bacon et al. 1990) had an effect on pea protein gelation. Protein concentration did not affect pea protein gelation (Munialo et al. 2015). In most of these studies, only small pH ranges of pH 4 to 8 with varying ionic strength of 0 M NaCl to 0.4 M NaCl are examined. A high ionic strength of up to 1.5 M NaCl at acidic pH and alkaline pH has not been analysed so far.

By using blocking agents stabilizing protein interactions are found to be mostly of non-covalent nature in pea protein gels at neutral pH (Arntfield et al. 1991; O'Kane et al. 2005; Sun and Arntfield 2012) and pea protein aggregates at neutral pH (Chihi et al. 2016). Disulphide bonds are not required to form a gel but add to the stiffness of the gel formed by pea protein according to Arntfield et al. (1991), O'Kane et al. (2005) and Sun and Arntfield (2012). However, blocking substances were shown to seriously alter the gelation behaviour (Hua et al. 2005; Xiong et al. 1993), which might lead to misconception of pea protein gelation. Felix et al. (2017) used a protein interaction assay to determine the stabilizing protein interaction in gels made of commercial pea protein and hydrolysed pea protein at pH 2; 6.5 and 8. Protein interactions were dependent on pH and degree of hydrolysis. Ionic interactions were found to be most important for commercial pea protein gels. However, at pH 6.5 and pH 8 disulphide bonds were nearly as important as ionic interactions. This finding for commercial pea protein gels using a protein interactions assay would be in contrast to what has been found for extracted pea protein gels using blocking agents.

This short review shows that a basic knowledge of pea protein gelation already exists. What is still lacking, though, is a wider range of conditions related to the impact of pH and ionic strengths and knowledge of how these factors interact. With this research, a deeper knowledge about pea protein gelation is aimed at in the wider pH range of 3 to 9 and ionic strength range of 0 M NaCl to 1.5 M NaCl and combinations thereof at all pH levels. First of all, in contrast to the presented studies, solubility of pea protein at all studied pH levels and ionic strength is taken into account. Solubility of a protein is known to have an influence on the gelation behaviour of pea protein (Britten and Giroux 2001; Klost et al. 2020) and this may explain some of the effects of pH and ionic strength seen. Insoluble aggregates might act as inactive filler and weaken the gel structure (Klost et al. 2020; Britten and Giroux 2001). Studying the impact of solubility on pea protein gelation is of great importance because pea protein is rather insoluble at the food relevant pH range between pH 4 and pH 7 (Tanger et al. 2020). This leads to the hypothesis of this study, that weaker gels are formed at pH and ionic strength levels, where the protein is more insoluble, and vice versa.

Second, this study takes another perspective on pea protein gelation. In well-studied proteins like whey proteins with high solubility and high nativity, gels are formed by a continuous, covalently crosslinked protein network. However, with pea proteins only weak gels are produced (O'Kane et al. 2004c; Sun and Arntfield 2010), which, how-

ever, could also be highly viscous aggregate solutions called entangled solutions. Entangled solutions are known from rheological analysis of polymer solutions. At low frequencies, such polymer solutions behave as a gel and at high frequency, it becomes a solution. This is because polymers interact via weak interactions with each other while stacking together at low frequencies The bonding forces are overruled at high frequencies (Brighenti et al. 2020). So the question would be: Do pea proteins form continuous protein networks or big aggregates, which lead to entangled solutions? This is of general interest and insights answering this question might explain, why only weak pea protein gels are formed as reported by Shand et al. (2007) and Sun and Arntfield (2011). The weak character of pea protein gels has not been further analyzed in literature. It is hypothesized that pH and ionic strength influence whether only an entangled solution is formed or a continuous protein network, i.e. a gel because pH and ionic strength influence solubility and charge of the proteins.

Third, stabilizing protein interactions of and between the pea protein gels over a wide range of pH and ionic strength will be analysed more in-depth. Non-covalent bonds are separated in hydrophobic interaction, electrostatic interactions and hydrogen bonds. The stabilizing bonds are analysed with two different methods in order to get a better idea of the stabilizing interactions. The first method is measuring the increase of the elastic modulus during cooling of the gel from 95°C to 25°C, expressing this as the ratio $G'_{25°C}/G'_{95°C}$. This ratio is used as an indicator of the ratio of covalent disulphide bonds and hydrophobic interactions to electrostatic interactions and hydrogen bonds, which form upon cooling. This method was first proposed by Bowland et al. (1995) for heat-induced whey protein isolate (WPI) gels in the presence of chaotropic and kosmotropic salts and later applied for gels made of potato protein, egg white protein, whey protein, soy protein, pea protein and lupine protein (Andlinger et al. 2021a; Martin et al. 2014). The second method is a protein interaction assay. A protein interaction assay is preferred over using blocking substances to identify different types of bonds in order to not interfere with the gelation process. It is hypothesized that the dominant protein interaction changes with pH and ionic strength, due to changes in molecular structure with varying pH value.

3.3.2 Materials and Methods

3.3.2.1 Materials

Pea flour was donated by Emsland Stärke (Emlichheim, Germany) and contained 18.27% protein on a dry basis. For protein extraction and all other analysis MilliQ water (Milli-Q Integral 3, Merck KGaA, Darmstadt, Germany) was used. All other materials and chemicals were of analytical grade and purchased from regular suppliers.

3.3.2.2 Methods

3.3.2.2.1 Extraction of pea protein

Pea proteins were extracted based on the salt extraction described by Sun and Arntfield (2010) and the micellar extraction described in Tanger et al. (2020) with some modifications. This extraction was chosen because it was shown to be the mildest treatment leading to the highest amount of native protein (Tanger et al. 2020). In short, 300 g pea flour was suspended in 1 L 1 M NaCl for 1.5 h with an overhead stirrer at

ambient temperature. The slurry was centrifuged at 4.500 g for 20 min at 4°C. The pellet containing insoluble plant material was discarded and the supernatant was diluted 1:2 with water and let stand at 4°C for 2 h. Globulins precipitated and were separated from soluble carbohydrates and albumins by centrifugation at 4.500 g for 20 min at 4°C. The supernatant was discarded and the pellet was redispersed in water 1:1. The resulting slurry was dialysed for 48 h against water using a membrane with a cut-off of 6-8 kDa for removal of salt. After dialysis, the protein slurry can be regarded as salt-free. Water was changed three times daily. Then the slurry was frozen at - 40°C and freeze-dried using a pilot-scale freeze dryer (Christ, Model: Alpha 1-4; Osterode). Legumin was the main protein in the protein product (63% as determined by SDS-PAGE) next to vicilin and convicilin. Albumins were not present in the protein product.

3.3.2.2.2 Solubility of pea protein at different pH values and ionic strength

The protein solubility of the extracted pea proteins was determined as described previously for different extraction methods (Tanger et al. 2020). In short, 0.2 g protein was dispersed in 19 g of 0.3; 0.6; 0.9 and 1.5 M NaCl. The pH was adjusted to pH 3; 4.5; 7 and 9 using 1 M HCl or 1 M NaOH. After that, the solution was filled up to 20 g. The dispersions were stirred for 1 h at room temperature and finally centrifuged at 6.000 g for 15 min at 20 °C. The amount of protein still soluble was measured using the Dumas method with the Vario MAX cube (Elementar Analysensysteme GmbH, Langenselbold, Germany). The soluble protein content was determined as protein content in the supernatant divided by the initial protein in the sample (x 100%).

3.3.2.2.3 Preparation of protein solution for modulated differential scanning calorimetry (mDSC) measurement and rheological measurements

A 15% protein solution was used in all following experiments. Protein was dissolved in 0 M NaCl; 0.3 M NaCl; 0.6 M NaCl; 0.9 M NaCl and 1.5 M NaCl. The pH was adjusted with 1 M HCl or 1 M NaOH to pH 3; 4.5; 7 and 9. All solutions were stored for at least 12 h at 4 °C for complete hydration of the powder.

3.3.2.2.4 mDSC measurement

Thermal properties, such as denaturation temperature (T_d), T_{onset} and enthalpy change (ΔH) were determined using modulated differential scanning calorimetry (DSC Q1000, TA instruments, New Castle, USA) as described in Tanger et al. (2020). 20 µl of a 15% protein solution was placed in a pre-weighed aluminium pan and hermetically sealed. An empty pan served as reference. The DSC cell had been calibrated using indium and sapphire. The pans were heated from 25°C - 120°C with a heating rate of 2 K/min and a modulation of ± 0.5°C every 60 s. Resulting thermograms were analysed using TRIOS software (Version: 5.1.1.46572; TA instruments, New Castle, USA).

3.3.2.2.5 Rheological measurement

Gelation of 15% protein solution and gel analysis was performed in a rotational rheometer MCR 302 (AntonPaar, Graz, Austria). A concentric cylinder CC10 with a sample volume of 1.02 ml was used (bob diameter: 10 mm; cup diameter: 10.8 mm; Anton-Paar, Graz, Austria). Samples were covered with 2 ml silicone oil 20cSt to avoid evaporation of water. Before measurement, the sample was equilibrated in the geometry for 10 min at 25°C with an input amplitude strain of 0.02 (Sun and Arntfield 2010). Then

the samples were heated from 25°C to 95°C at a controlled rate of 2 K / min, held at 95°C for 10 min and cooled down from 95°C to 25°C at a rate of 2 K / min and hold at 25°C for 10 min before further analysis. Data was collected every 10 s in oscillatory mode with an input amplitude strain of 0.02 (Sun and Arntfield 2010). A typical G' and G'' trend during gelation in the rheometer over time can be seen in Figure A3-25. After this, a frequency sweep was applied over a range of 0.1 to 100 rad /s at 25°C. The frequency sweep followed after a resting phase of 5 min by an amplitude sweep over a range of 0.01 to 100% at 25°C with a frequency of 10 Hz. Storage modulus (G') and loss modulus (G'') were determined for each sample.

3.3.2.2.6 Analysis of protein interaction

Gelation for protein interaction analysis was performed by heating 2 ml of a 15% protein solution in a stainless steel tube of 15 mm diameter in a water bath of 95°C for 30 min and afterwards cooled on ice for at least 15 min. The resulting gels were analysed using a protein interaction assay based on Keim and Hinrichs (2004) and Tanger et al. (2021a) with slight modifications. In short, gels were solubilized in three different buffer. 0.4 g of each gel was solubilized in 20 g of buffer B_1, B_2 and B_3. Buffer B_1 was a sodium phosphat buffer at pH 7.5 to cleave all electrostatic interactions. Buffer B_2 contained 2 g/l SDS to cleave all hydrophobic and electrostatic bonds and buffer B_3 contained 2 g/l SDS and 15 g/l DTT to cleave all bonds present. The gels were solubilized overnight and centrifuged at 10.000 g for 20 min at 20°C to remove insoluble material. The nitrogen content of the supernatant was determined using the Dumas method with the Vario MAX cube (Elementar Analysensysteme GmbH, Langenselbold, Germany). Nitrogen solubility in the various fractions was used to calculate the amount of stabilizing protein interactions. The following equations were used to determine electrostatic (ES), disulphide (SS) and hydrophobic (Hy) interactions:

$$C_{n,bond,Bi} = \frac{(m_S + m_{gel})}{m_{gel}} * C_{n,sup,Bi} \tag{3-14}$$

$$\frac{C_{n,bond,B1}}{C_{n,gel}} = P(ES) \tag{3-15}$$

$$\frac{C_{n,bond,B2}}{C_{n,gel}} = P(ES) + P(Hy) \tag{3-16}$$

$$\frac{C_{n,bond,B3}}{C_{n,gel}} = P(ES) + P(Hy) + P(SS) \tag{3-17}$$

$$P(ES) = \frac{C_{n,bond,B1}}{c_{n,gel}} \tag{3-18}$$

$$P(Hy) = \frac{C_{n,bond,B2}}{c_{n,gel}} - \frac{C_{n,bond,B1}}{C_{n,gel}} \tag{3-19}$$

$$P(SS) = \frac{C_{n,bond,B3}}{C_{n,gel}} - \frac{C_{n,bond,B2}}{C_{n,gel}} \tag{3-20}$$

With m_S being the initial mass (20 g), m_{gel} being the mass of the gel (0.4 g) and $C_{n,sup,Bi}$ being dissolved nitrogen in the supernatant in [%], $C_{n,gel}$ being the nitrogen

content of the microparticle in [%]. $C_{n,bond,Bx}$ is the concentration of cleaved protein bonds by the respective buffer.

3.3.2.2.7 SDS-PAGE

Sodium Dodecyl Sulphate – Polyacrylamide Gel Electrophoresis (SDS-PAGE) of the supernatant of buffer B_2 was performed to detect whether small oligomers, which stay soluble during the centrifugation step, are covalently linked. The experiment was performed as described in Tanger et al. (2020).

3.3.2.2.8 Statistical analysis

Measurements were performed in at least in duplicate from two different solutions. Mean values are shown. Error bars indicate the highest and the lowest value if not indicated otherwise. Graphs were plotted using OriginPro 2019 (originLAb Corporation, Northampton, USA).

3.3.3 Results and discussion

3.3.3.1 Effect of pH and ionic strength on solubility

Solubility of pea protein is highly dependent on pH, ionic strength (Shand et al. 2007) and the processing history, which is here the extraction method applied (Tanger et al. 2020). Solubility also has an effect on the gelation behaviour (Klost and Drusch 2019). Therefore, the solubility of the pea protein at different pH values and ionic strengths was measured to gain knowledge about the solubility of the extracted pea protein used in this study at the pH and ionic strength levels used for gelation in this study. The results are shown in Figure 3-16.

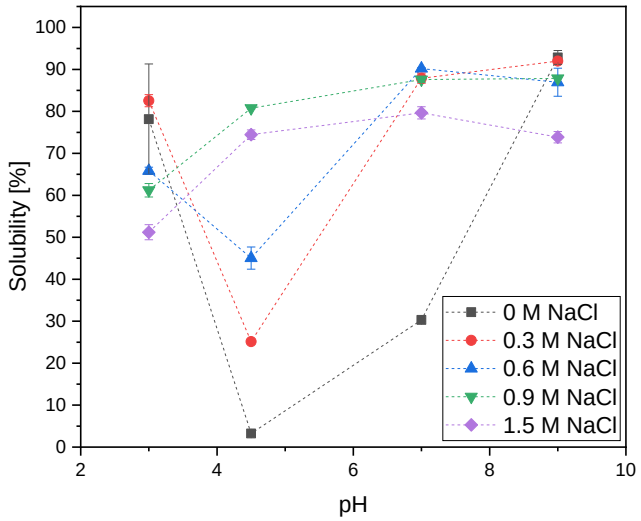

Figure 3-16: Solubility of the pea protein as function of pH and ionic strength.

As expected, the solubility increases at pH values further away from the isoelectric point of globulins at pH 4.5 (Swanson 1990) and is highest at pH 9. Shand et al. (2007) found a pH dependency for solubility of extracted and commercial pea and soy protein at 0 M NaCl. The solubility is lowest at pH 4.5, because of low electrostatic repulsion

around the isoelectric point (Shand et al. 2007; Tanger et al. 2020). The solubility increases with increasing ionic strength for pH 7 and pH 4.5. This increase in solubility at pH 7 has also been found for micellar extracted pea protein (Tanger et al. 2020). Globulins are found to form micelles, which are thermodynamical stable spheres. Hydrophobic moieties are gathered towards the centre of the micelle and polar regions are exposed to the aqueous outside. This reduces interfacial energy (Lam et al. 2018). This study shows that the impact of ionic strength on solubility of pea protein is biggest at pH 4.5, which increases from 3.25% at 0 M NaCl to 80.75% at 0.9 M by the salting-in effect. An increase in solubility with increasing ionic strength was expected, because globulins the major protein part, are as per definition salt soluble (Lam et al. 2018; Osborne 1909). Without the addition of salt, the protein solubility of pea proteins have been found to be low ranging between 42% and 91%, which is dependent on cultivar and extraction type (Stone et al. 2015). For pH 9 and pH 3 the contrary effect is seen in the increase of solubility with increasing ionic strength at pH 4.5. At acidic and alkaline pH the protein decreases in solubility with increasing salt concentration. A slight decrease of protein solubility is also seen for high ionic strength at pH 7. This suggests that there is an optimal ionic strength for high solubility and salting-out occurs at high ionic strength. This optimal ionic strength is dependent on the pH value. Therefore, the solubility can be controlled by pH and ionic strength. Controlling solubility can also mean controlling the gelation behaviour.

3.3.3.2 Effect of pH and ionic strength on denaturation of pea protein

Thermograms at 0 M NaCl showed one endothermic peak except for pH 3. A typical thermograph is can be found in Figure A3-26. At pH 3, no peak could be identified, thus the protein was already denatured by the acid. With increasing salt concentration, a small endothermic peak at pH 3 could be identified between 0.3 M NaCl and 1.5 M NaCl. Sun and Arntfield (2010) could not identify a peak at pH 3 and 0.3 M NaCl. The detection of a denaturation peak at pH 3 0.3 M NaCl can be explained by the usage of a modulated DSC, which is more sensitive than a conventional DSC, and a higher protein concentration of 15%. In other words, reactive protein can be found with increasing salt concentration, which can be connected with the stabilizing effect of salt on pea protein (Sun and Arntfield 2011; Tanger et al. 2020). For all other pH values and ionic strengths, the thermograms were analysed on their peak maximum, peak area and peak onset. The peak maximum represents the denaturation temperature (T_d). When two peaks were present, both were analysed separately on their peak maximum (T_{d1} and T_{d2}). The peak area obtained by integration is measure for the enthalpy change (ΔH) upon protein unfolding. When two peaks were present, the peak integration was performed over both peaks combined. This was done because the peaks often overlapped and the two peaks could not be properly separated. The peak integration area shows the reaction of the protein and therefore, it also represents the amount of reactive protein. Since the peak integration area shows the reaction of the protein, in addition to the denaturation temperature, the temperature at which 50% of the protein had reacted (T_{d50}), was analysed. The results can be found in Table 3-4, and the results of the T_{d50} are shown in Figure 3-17.

Table 3-4: Denaturation temperature and enthalpy change of pea protein at different pH-values and NaCl concentrations measured by mDSC.

NaCl concentration		T_{peak1} [°C]	T_{peak2} [°C]	T_{d50} [°C]	ΔH [J/g]
pH 3	0 M	-	-	-	-
	0.3 M	61.24 ± 0.87	-	62.35 ± 1.10	0.23 ± 0.09
	0.6 M	63.95 ± 0.09	-	64.69 ± 0.01	0.41 ± 0.01
	0.9 M	63.58 ± 0.47	-	75.09 ± 5.71	1.05 ± 0.35
	1.5 M	67.79 ± 3.03	-	70.42 ± 4.74	0.66 ± 0.11
pH 4.5	0 M	82.39 ± 0.16	-	80.82 ± 0.05	1.92 ± 0.32
	0.3 M	81.05 ± 0.30	-	82.44 ± 0.03	1.88 ± 0.34
	0.6 M	83.37 ± 0.62	-	85.74 ± 0.58	1.92 ± 0.01
	0.9 M	84.66 ± 0.17	-	87.73 ± 0.11	2.01 ± 0.10
	1.5 M	87.55 ± 0.46	100.93 ± 0.22	97.68 ± 0.13	2.01 ± 0.20
pH 7	0 M	79.18 ± 0.67	-	79.64 ± 1.23	2.45 ± 0.04
	0.3 M	82.58 ± 0.04	95.51 ± 0.18	85.79 ± 0.56	2.18 ± 0.01
	0.6 M	85.14 ± 0.28	98.23 ± 0.13	87.64 ± 0.05	2.22 ± 0.16
	0.9 M	88.16 ± 0.06	101.75 ± 0.05	90.49 ± 0.07	1.90 ± 0.25
	1.5 M	94.71 ± 0.06	110.08 ± 0.02	97.01 ± 0.10	2.46 ± 0.02
pH 9	0 M	75.64 ± 0.05	-	78.77 ± 2.07	2.16 ± 0.73
	0.3 M	79.42 ± 0.82	97.47 ± 4.28	83.54 ± 0.97	2.51 ± 0.68
	0.6 M	83.83 ± 0.05	97.41 ± 0.11	87.95 ± 0.26	2.17 ± 1.11
	0.9 M	87.98 ± 0.09	102.10 ± 0.30	91.34 ± 0.51	2.71 ± 0.41
	1.5 M	93.03 ± 0.09	108.33 ± 0.13	94.56 ± 0.29	2.13 ± 0.11

Two major endothermic peaks were found for the samples with pH 7 and pH 9 at 0.3 – 1.5 M NaCl and pH 4.5 1.5 M NaCl. The first peak maximum is around 80°C and the second is around 95°C. The peak maximum increases with increasing salt concentration. The first peak maximum is much higher than 65°C, which was found to be the starch gelatinization temperature in pea protein (Sosulski et al. 1985). Since it also was not found in all thermograms the first peak around 60°C for pH 3 samples and 80 – 90°C for all other samples can rather be attributed to protein denaturation than to starch gelatinization. It is reported that the 11 S legumin has a slightly different denaturation temperature than the 7 S vicilin (Marcone et al. 1998; Mession et al. 2012; Sosulski et al. 1985). Usually, the two peaks overlap (Shand et al. 2007). From this, the shape of the second peak can be explained by the diverging denaturation temperatures of legumin and vicilin. The diverging denaturation temperatures of legumin and

vicilin can be attributed to the difference in effect of NaCl concentration and pH on the two proteins.

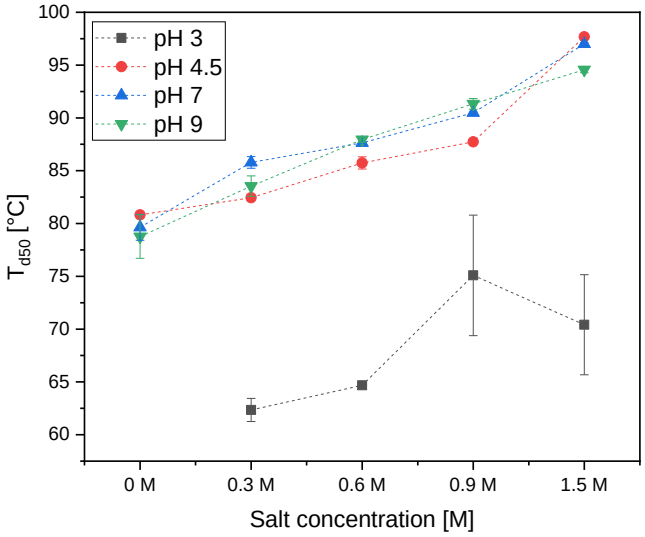

Figure 3-17: T_{d50} as function of pH and salt concentration measured by mDSC.

In general, denaturation temperature and T_{d50} increased with increasing salt concentration independent of pH. The effect of ionic strength between 0 M and 1.5 M NaCl was around 2.5 x bigger than the effect of pH in a pH range of 4.5 – 9. A bigger impact of ionic strength compared to pH on pea protein denaturation was found by Sun and Arntfield (2011), Shand et al. (2007) and Mession et al. (2013) for a smaller pH from 4 to 8 and ionic strength range of 0 M to 2.0 NaCl. The finding of a second peak and a lower denaturation temperature than reported by Sun and Arntfield (2011), Shand et al. (2007) and Mession et al. (2013) can be explained by the usage of a modulated DSC, usage of 15% protein solution and a lower heating ramp 2 K/min. This experimental setting increases sensitivity of the measurement and denaturation temperature is lower, because of temperature-time effect using a lower heating ramp of 2 K/min compared to 5 or 10 K/min. NaCl stabilizes the quaternary structure of pea protein and inhibits aggregation (Mession et al. 2013; Tanger et al. 2020). The denaturation temperature of pea protein at pH 3, independently of ionic strength, was always lowest compared to the other pH values. This can be explained by the additional chemical denaturation by acid (Sun and Arntfield 2011). Regarding the following thermal treatments, it can already be said, that the denaturation temperature of the second peak, which are above 95°C, will not be reached during thermal treatment in the rheometer.

The enthalpy change was smallest for samples at pH 3 and increased with ionic strength from 0.23 J/g to 1.05 J/g. This can also be explained by the denaturing effect of the acid and the stabilizing effect of salt on the protein structure. In contrast to the denaturation temperatures, the pH had a more pronounced effect on the enthalpy change than the ionic strength. Shand et al. (2007) found no effect of ionic strength on enthalpy change for samples in a smaller pH range of 6.4 - 6.5 and varying ionic strength of 0 – 2% NaCl. This study extends and deepens the current knowledge of

the thermal behaviour of pea protein by using a more sensitive DSC measurement a covering a wider pH and ionic strength range. At 0 M NaCl, the enthalpy change was the highest for pH 7 and lowest at pH 4.5. This could be explained by prior denaturation of the protein at acidic or alkaline pH values.

3.3.3.3 Effect of pH and ionic strength on gel stiffness and gel elasticity

The storage modulus is a measure of the stiffness of the formed gel. In Figure 3-18 the storage modulus ($G'_{25°C}$) and tan δ are shown for all produced gels during rheological measurement.

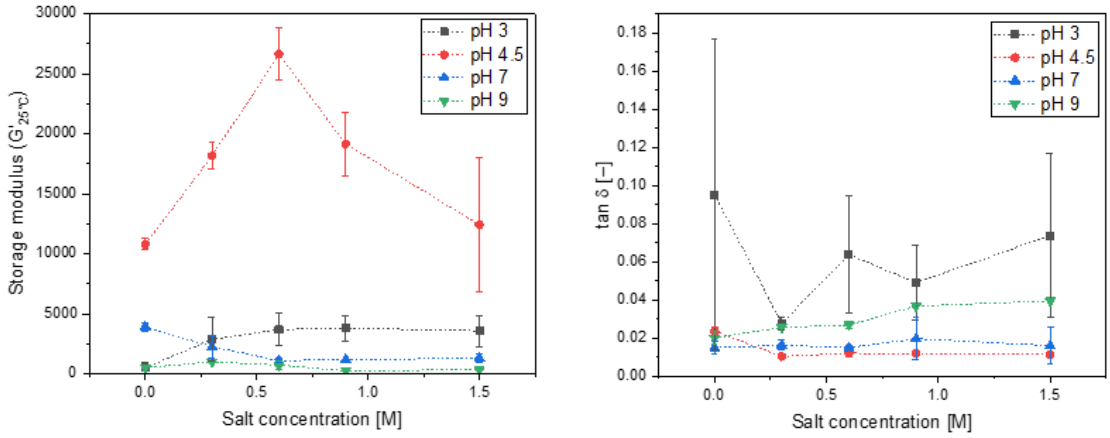

Figure 3-18: $G'_{25°C}$ and tan δ as function salt concentration for different pH values.

Tan δ represents G'/G''. The stiffness is highest for gels formed at pH 4.5 irrespectively of ionic strength. The stiffness is lowest for gels formed at pH 9 at all ionic strengths. For gels formed at pH 7, the stiffness decreases with increasing ionic strength and for gels formed at pH 3, the stiffness increases with increasing ionic strength. The elasticity (tan δ) was found to be highest for gels formed at pH 3 independent of ionic strength with 0.028 to 0.095. The elasticity of the gels formed in the pH range of 4.5 to 9 with 0 M NaCl varied only slightly between 0.015 and 0.024. However, with increasing ionic strength the elasticity varied in a wider range between the gels in the pH range of 4.5 and pH 9 between 0.010 and 0.040. By the addition of salt, the elasticity of gels formed at pH 4.5 decreased slightly leading to the lowest measured elasticity of 0.010. The elasticity of the gels formed at pH 9 increased slightly with increasing salt concentration from 0.020 to 0.040. The high stiffness and low elasticity of the gels formed at pH 4.5 indicate that active fillers are incorporated in the gel network (Ben-Harb et al. 2018; Klost and Drusch 2019). Pea protein is also most insoluble at pH 4.5 compared to pea protein samples at other pH values. The highest stiffness is obtained at pH 4.5/0.6 M NaCl. At pH 4.5 0.6 M NaCl the protein is 50% soluble. This leads to the assumption that 50% protein in the gel network and 50% insoluble protein aggregates incorporated in the gel network as active fillers lead to the stiffest gel. This would extend the findings of Sun and Arntfield (2011), who found a high G' and a low tan δ for pea protein gels formed at pH 3 to 4 at 0.3 M NaCl compared to other pH values at smaller ionic strength range of 0 M to 0.4 M NaCl than presented in this study. Sun

and Arntfield (2011)suggested, that the gels are rather particulate gels formed by aggregates rather than a continuous protein network, which would be in contrast to the statement made above by Ben-Harb et al. (2018) and Klost and Drusch (2019) that there are active fillers incorporated in the network. By taking the solubility of the protein into account this study would support the statement of active fillers incorporated in the gel network at pH 4.5. The high tan δ values between pH 7 to 9 were attributed to little protein-protein interaction. With this in mind, it can be said that there was a good protein network formed at pH 3 at all ionic strengths compared to gels formed at pH 7, 9 and 4.5. A denaturation temperature could not be found at pH 3 at 0 M NaCl, so protein were already fully denatured before heat treatment. With increasing ionic strength, a denaturation temperature far below 95°C was found and the stiffness of pea protein gels formed at pH 3 increased also with increasing ionic strength. This leads to the assumption that the protein could completely denature at pH 3 at NaCl concentrations above 0.3 M upon heat treatment and form a gel network. In contrast to protein, which is already denatured by the acid, protein, which denatures during heat treatment, form stiffer gels at pH 3. This is in contrast to gels formed at pH 7 and 9, where the gel stiffness decreased with increasing ionic strength from 3904 Pa to 1287 Pa and 512 Pa to 319 Pa, respectively. Tan δ increased with increasing ionic strength for gels formed at pH 9 and increased slightly for gels formed at pH 7 indicating a decrease in protein-protein interaction. With increasing ionic strength, the denaturation temperature of pea protein increases. At pH 7 and pH 9 and a high ionic strength, the denaturation temperature increases above 95°C. This means that the protein is not able to fully denature and expose all buried reactive groups during heat treatment. The decreased gel stiffness and increased elasticity of the gels at pH 7 and pH 9 with increasing ionic strength can be explained by the incomplete exposure of reactive groups of the protein and the resulting decrease in protein-protein interaction.

3.3.3.4 Effect of pH and ionic strength on the ratio G'25°C/G'95°C

The ratio of $G'_{25°C}$ to $G'_{95°C}$ is a value for the characterization of the formation of covalent and non-covalent bonds during cooling (Andlinger et al. 2021a; Martin et al. 2014). A higher value of the $G'_{25°C}/G'_{95°C}$ ratio is associated with a high amount of electrostatic interactions and hydrogen bond formation, whereas a low $G'_{25°C}/G'_{95°C}$ value is associated with a high amount of disulphide bonds and hydrophobic interactions. The strength of hydrophobic interactions decreases with decreasing temperature, whereas electrostatic interactions and hydrogen bonds increase in strength during cooling (Bowland et al. 1995; van Dijk et al. 2015). The $G'_{25°C}/G'_{95°C}$ for all salt concentrations and pH values can be found in Figure 3-19.

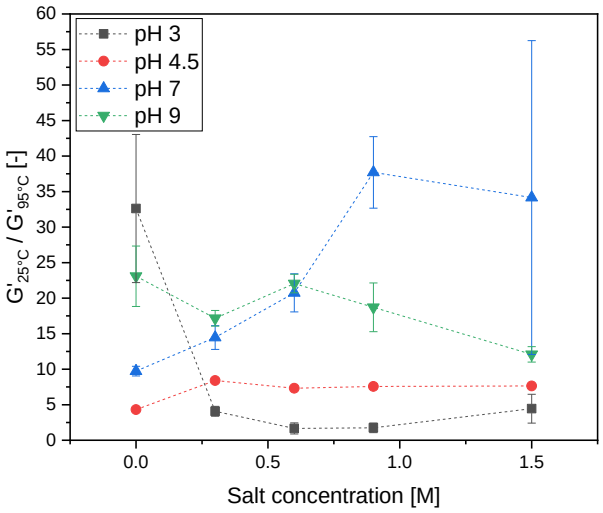

Figure 3-19: Ratio of G'$_{25°C}$/G'$_{95°C}$ for all gels over salt concentration.

The G'$_{25°C}$/G'$_{95°C}$ ratio varied between 1.6 for gels at pH 3 at 0.6 M NaCl and 37.7 for gels at pH 7 at 0.9 M NaCl. A value of around 3 has been found for a 17.5% pea protein gel made from pea protein extracted by alkali extraction and isoelectric precipitation (Martin et al. 2014). High values up to 30 have been found for alkali extracted and isoelectric precipitated 21.5% lupine protein gel. Low values of 2 were found for 15% whey and 10% and 12.5% egg white protein gels (Martin et al. 2014). Gels formed at pH 3 at 0 M NaCl had a G'$_{25°C}$/G'$_{95°C}$ value of 32.6. This indicates a high amount of non-covalent interactions mainly of electrostatic nature and hydrogen bonds. With increasing amount of NaCl at pH 3, the value decreased to 1.6 at 0.6 M NaCl indicating a higher amount of covalent bonds and/or hydrophobic interactions. This decrease in G'$_{25°C}$/G'$_{95°C}$ value led to the assumption that with increasing ionic strength at pH 3, more covalent bonds and hydrophobic interactions were formed. This would meaningfully add to the findings of the increasing stiffness of the protein gels at pH 3 with increasing ionic strength and the appearance of an endothermic peak at ionic strengths higher than 0.3 M NaCl at pH 3 during mDSC measurement. The statement derived from the increasing stiffness and the appearance of an endothermic peak during mDSC measurement was that at pH 3 without NaCl the protein is already denatured by the acid. With increasing salt concentration, the protein is not fully denatured by the acid, but completely denatures during heat treatment exposing all buried reactive groups. This complete exposure of reactive groups then leads to more protein-protein interaction, assumed to be of more covalent and hydrophobic nature than at pH 3 0 M NaCl. This adds meaningfully to the findings of a stiffer gel with increasing ionic strength. This also shows that the ionic strength has a large impact on the gelation of pea protein at acidic pH. At pH 7 the G'$_{25°C}$/G'$_{95°C}$ value increases from 9.7 to 37.7 with increasing ionic strength indicating more electrostatic interactions and hydrogen bond formation with increasing ionic strength from 0 M NaCl to 1 M NaCl. At pH 4.5 and pH 9, the G'$_{25°C}$/G'$_{95°C}$ value stays nearly constant around 20 indicating only slight changes in protein interactions with increasing ionic strength. Comparing the G'$_{25°C}$/G'$_{95°C}$ values between the pH values, it can be said that at 0 M NaCl gels at the isoelectric point

show more covalent bonds and / or hydrophobic interactions than pH-levels further away from the isoelectric point of pH 4.5. In general, pea protein have been found to mainly aggregate via hydrophobic interactions whereby disulphide bonds only play a minor role (Felix et al. 2017; Sun and Arntfield 2012). This study goes more in-depth that the dependence of ionic strength and pH on the $G'_{25°C}/G'_{95°C}$ value indicates that ionic strength and pH have an effect on the reactivity of the thiol groups and hydrophobic residues of the pea protein. This reactivity is connected with the denaturation temperatures. In contrast to pH 4.5, the samples at pH 7 and 9 cannot completely denature at 95°C at salt concentrations above 0.3 M NaCl. Because of this, the higher $G'_{25°C}/G'_{95°C}$ value of pH 7 and pH 9 gels and therefore higher amount of electrostatic interaction and hydrogen bonds can be explained by the incomplete denaturation and therefore decreased reactivity of reactive residues. At pH 4. all proteins can denature and interact in the gel network including thiol groups and exposed hydrophobic residues. However, $G'_{25°C}/G'_{95°C}$ values found for pH 4.5 gels were higher than values found for pH 3 gels above 0.3 M NaCl. Since denaturation temperatures of pH 3 samples at 0.3 to 1.5 M NaCl were around 20°C lower than the ones found for pH 4.5, denaturation is more complete at pH 3 0.3 – 1.5 M NaCl than at pH 4.5. Therefore, buried reactive residues become more exposed and are therefore also reactive.

3.3.3.5 Effect of pH and ionic strength on the frequency sweep

A frequency sweep after the complete heating cycle was used to determine the dependence of G' on the oscillatory frequency. The frequency dependence was analysed by calculating the slope (n) and intercept (K) of the curve of G' as function of frequency (from log(G') = n*log(ω)+K). For a gel network mainly formed by covalent (or elastic) bonds, the slope is closer to 0. Whereas, for a gel network mainly formed by more physical (or viscous) networks, the slope value is higher (Creusot et al. 2011; Sun and Arntfield 2011). The intercept (K) can be used as an indicator for the molecular interaction strength in the gel matrix (Kim and Yoo 2009). The calculated slopes (n) and intercept (K) for all gels can be found in Figure 3-20.

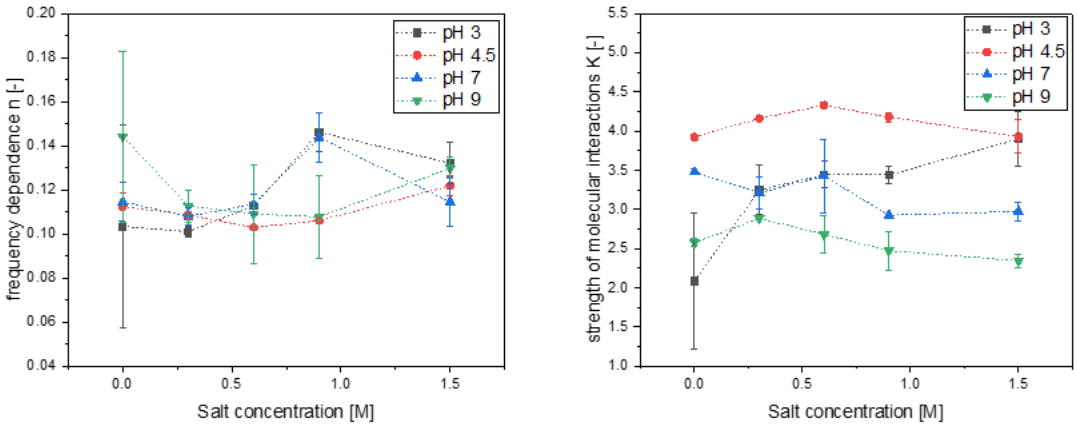

Figure 3-20: Frequency dependence n and strength of molecular interactions K of all gels formed at different pH over salt concentration.

The values found for n for thermally induced gelation in this study are in the same range as found for acid induced pea protein gels (Klost and Drusch 2019). The dependence of the G' on the frequency indicates a network that is mainly formed via non-covalent bonds, which is in line with the $G'_{25°C}/G'_{95°C}$ findings. At pH 9 at 0.9 M NaCl and at 1.5 M NaCl G'' became higher than G' at higher frequencies. This is shown in Figure 3-21.

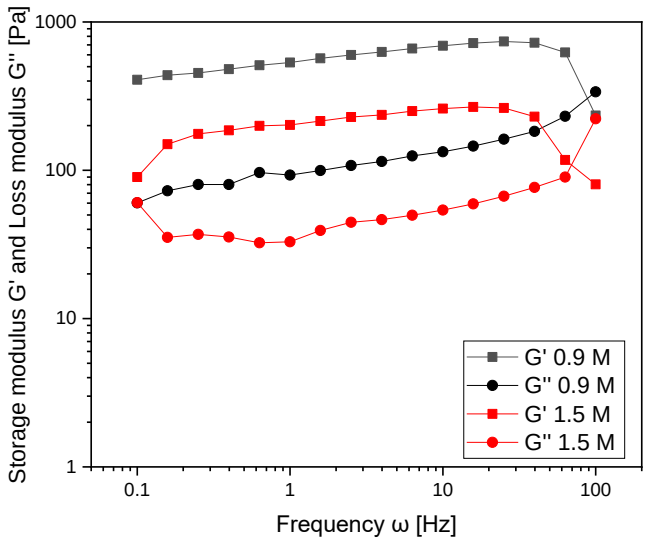

Figure 3-21: Frequency sweep of gels formed at pH 9 and 0.9 M NaCl and 1.5 M NaCl.

This crossover of G' and G'' indicates that the gels became more fluid-like with increasing frequency. This shift from gel to fluid suggests that the sample was an entangled solution rather than a true gel (Brighenti et al. 2020; Pai and Khan 2002). Entangled solutions are known from other polymers. Since the protein at pH 9 at 0.9 M and 1.5 M NaCl cannot fully denature (mDSC data) this is an indication that only aggregates are formed weakly interacting with each other, forming a gel network only at low frequencies and turning back into a fluid at higher frequencies.

The intercept (K) as indicator for the molecular interaction strength in the gel network is independent of ionic strength highest at pH 4.5 and decreases at more acidic or alkaline pH values. This is in line with the findings for the stiffness (G') of the gels. Additionally, charge repulsion is lowest at around the isoelectric point. This can explain the high molecular strength in the gel network.

3.3.3.6 Effect of pH and ionic strength on the yield stress

The yield stress gives the point at which the network structure is destroyed and G' decreases with increasing strain. The curve deviates from the LVE plateau at the yield stress. The yield stresses for all samples are depicted in Figure 3-22.

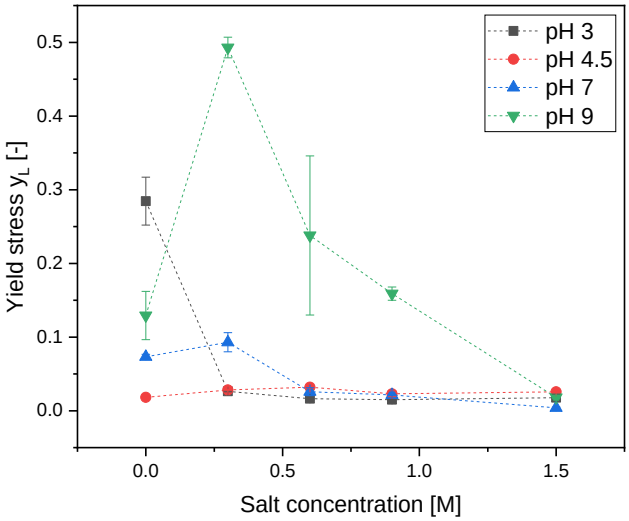

Figure 3-22: Yield stress of protein gels over salt concentration

It can be seen that the yield stress is highest for gels formed at pH 9 at 0.3 M NaCl to 0.9 M NaCl indicating a more elastic gel with 0.49 to 0.16 At pH 3 0 M NaCl yield stress is highest compared to all other gels at the same ionic strength with 0.28. Yield stress decreases with increasing ionic strength for pH 3 to 0.02. Gels formed at pH 4.5 show the lowest yield stress indicating a brittle gel. This is in agreement with the high G' and low tan δ of the gels formed at pH 4.5. The overall low yield stress indicates that only weak gels are formed, independently of ionic strength and pH value. T are mostly brittle and low in elasticity.

3.3.3.7 Effect of pH and ionic strength on stabilizing protein interactions

Stabilizing protein interactions were measured using a protein interaction assay and SDS-PAGE. The results of the protein interaction assay can be found in Figure 3-23.

It can be seen that the main protein interactions are non-covalent bonds regardless of pH and ionic strength, disulphide bonds only at a lower extent. These findings specifying the type of non-covalent interaction, amount of stabilizing protein interaction, and range of pH and ionic strength level extend the work of Sun and Arntfield (2012) who reported that pea protein interaction was mainly of non-covalent nature by using rheological analysis of gelation of pea protein at pH 5.65 and 0.3 M NaCl with the addition of blocking substances. Hydrophobic interactions are the major protein interaction for gels at pH 3 and pH 4.5 with 80% to 100%. At pH 7 and pH 9 also electrostatic interactions played a significant role with 51% to 80%.

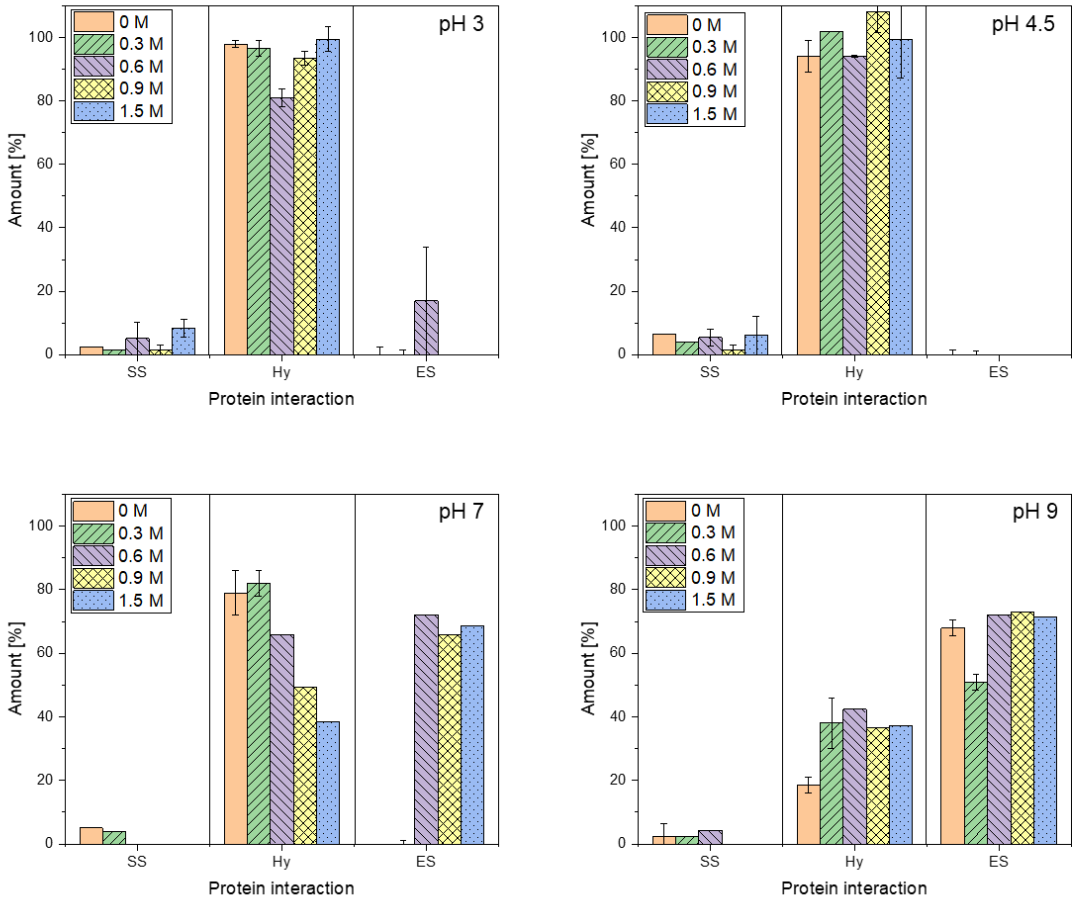

Figure 3-23: Protein interaction of the gels measured by protein interaction assay with disulphide bonds (SS), hydrophobic interactions (Hy) and electrostatic interactions (ES)

The amount of electrostatic interactions increased with increasing ionic strength at pH 7 from a minor amount of below 10% to around 79%. Hydrophobic interactions decreased with increasing salt concentration. The amount of electrostatic interactions for gels at pH 9 was independent of salt concentration around 70%. However, since the formed gels at pH 7 and pH 9 resembled rather a highly viscous fluid than a gel, the high amount of soluble protein in buffer B_1 could also indicate that instead of a continuous gel network only aggregates were formed during heat treatment small enough to stay soluble during centrifugation. This would be in line with the finding of the intercepting of G' and G'' during the frequency sweep at pH 9, which already indicated that rather an entangled solution was formed than a continuous gel network. In any case, the results of a high amount of electrostatic interactions at pH 7 at high ionic strength and at pH 9 would also be in line with the high $G'_{25°C}/G'_{95°C}$ value found during rheology measurements.

In order to detect, whether also small aggregates too small to be separated by centrifugation were formed via disulphide bonds, SDS-PAGE analysis of the supernatant of buffer B_2 was performed. Results are shown in Figure 3-24.

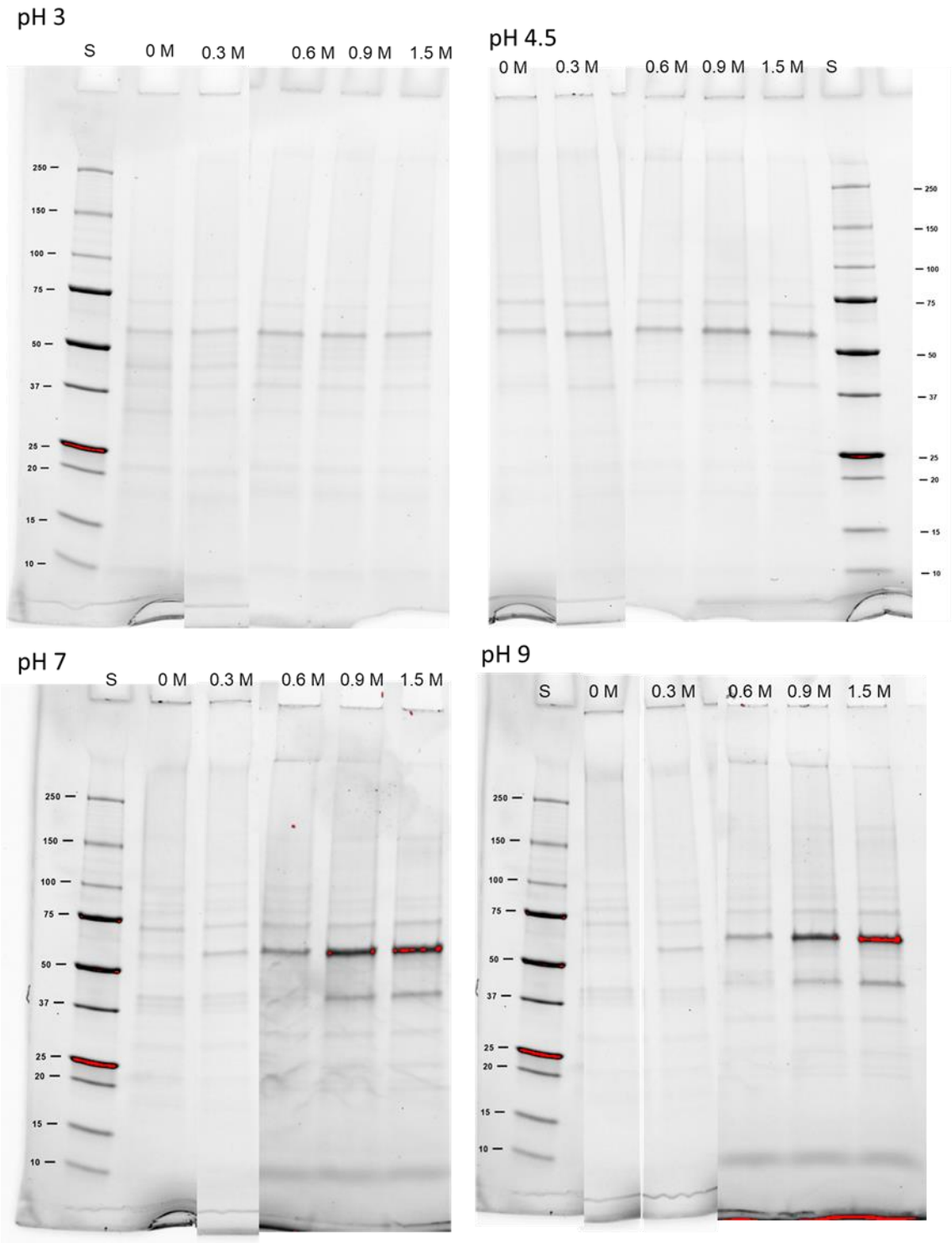

Figure 3-24: SDS-PAGE profile of supernatant of buffer B_2 of all gels. Lanes are labelled. Protein standard is labelled as S. Oligomers bound together by disulphide bonds can be seen as bands in the pocket above 250 kDa.

It can be seen that at all pH values and ionic strengths a band occurs in the pocket, where the sample was placed on the gel. This indicates that covalently bound aggregates were formed during heat treatment, which could not enter the gel. Therefore, it can be said that disulphide bond formation does occur during gelation. However, only few proteins are connected by disulphide bonds. These proteins connected by disulphide bonds do not form a continuous network as it is the case with whey protein

(Havea et al. 2009). This research shows that gel formation of pea protein does not only occur via hydrophobic interactions, but other interactions also play a role. The type and amount of protein interaction in pea protein gels can be manipulated by changing pH and ionic strength.

3.3.4 Conclusion

The effect of pH and ionic strength on gelation of pea protein has been studied. Both pH and ionic strength were shown to have an influence on denaturation and solubility of the pea protein and therefore also on the gelation of the protein. The impact of pH was more pronounced than that of ionic strength, which was only of minor effect at neutral and alkaline pH. However, ionic strength had a major influence on the gelation at acidic pH and pH around the isoelectric point. Pea protein gelation can therefore be modified by controlling the pH and ionic strength in a targeted manner.

Pea protein was least soluble at pH 4.5. At 0.6 M NaCl, the solubility was 50% and led to the stiffest gels. At pH 9 and high ionic strength rather an entangled solution was formed than a continuous gel network. With increasing ionic strength, the denaturation temperature increased, which was higher than 95°C, the gelation temperature used in this study. This led to an incomplete denaturation and lower intensity of protein interaction. Stabilizing protein interactions were mainly of non-covalent kind and also pH and ionic strength dependent. Disulphide bonds were not involved in forming a continuous network.

This study can serve as a base for gel formation application in pea protein-based novel vegan foods under variable salt and pH conditions. In future, it would be of interest to also study pea protein gelation at higher temperatures than 95°C.

Acknowledgements

We would like to acknowledge Julia Engel for her support during extraction of the pea protein. Annette Brümmer-Rolf and Christine Haas are thanked for Elementar measurement. We would like to thank Thomas Pruter from Emsland Stärke, Emlichheim, Germany, for providing the pea flour.

This project was executed as part of an Industrial Collective Research (IGF) project of the Forschungskreis der Ernährungsindustrie e.V., Bonn (FEI) supported by the German Ministry of Economics and Technology via AiF (AiF 20197N).

Compliance with ethical standards

This article does not contain any studies with human or animal subjects performed by any of the authors.

Conflict of interest

The authors declare that they have no conflict of interest.

3.3.5 Appendix

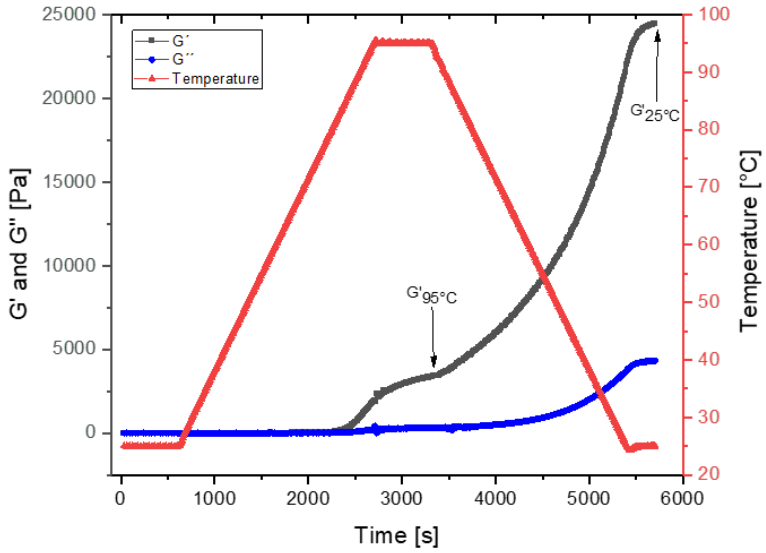

Figure A3-25: Typical G', G'' trend and during gel formation over time in the rheometer. $G'_{95°C}$ and $G'_{25°C}$ for calculation of the $G'_{25°C}/G'_{95°C}$ ration are labelled.

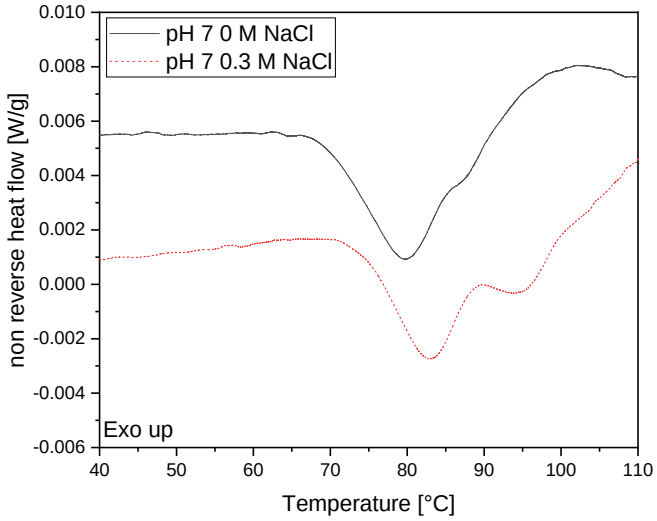

Figure A3-26: Typcial mDSC thermograph of a 15% solution of pea protein at pH 7 0 M NaCl and 0.3 M NaCl. The sample at pH 7 0 M NaCl depicts one peak and the sample at pH 7 0.3 M NaCl depicts two peaks.

3.4 Comparative assessment of thermal aggregation of whey, potato and pea protein under shear stress for microparticulation

Summary and contribution of the doctoral candidate

Little is known about the aggregation behaviour of pea and potato protein under shear stress in comparison to whey protein. In this study, thermal aggregation under shear stress using a rheometer of pea, potato and whey protein is compared with each other head-to-head. For whey protein, a whey protein concentrate, containing lactose, and a whey protein isolate without lactose was used. For pea protein, a commercial pea protein and a laboratory extracted pea protein was used. The differences between them were their 'nativity' and particle size in the starting material. From this, two different processes emerged, the top-down process and the bottom-up process. The bottom-up process was used for whey, potato and laboratory extracted pea protein, which had a high degree of 'nativity'. The protein denatured, aggregated, and increased in particle size during thermo-mechanical treatment. For commercial pea protein, the top-down process was used, which was already highly aggregated. Therefore, during thermo-mechanical treatment, the particles were decreased in size by the breakage of aggregates. Starting material was analysed on thermal stability. The resulting particles were analysed in particle size, morphology and protein-protein interaction. Potato protein was the protein with the lowest thermal stability of 63°C because of the absence of an intramolecular disulphide bridge. Laboratory extracted pea protein was highest in thermal stability with a denaturation temperature of 78°C because of its high complexity and intramolecular hydrophobic interactions. Due to the absence of lactose whey protein isolate formed aggregates in nanometre-scale at 10% protein concentration. All other protein formed aggregates between 0 and 250 µm. Aggregate size decreased with increasing shear rate because of the increased shear stress acting on the particle. Potato protein and laboratory extracted pea protein formed smaller particles than commercial pea protein and whey protein concentrate. Whey protein aggregates were mainly held together by covalent bonds, whereas the main protein-protein interaction in the plant protein were hydrophobic interactions. The number of covalent bonds was lowest in potato protein. For pea protein, covalent bonds were around 35% to 55%. However, in contrast to whey protein mostly small oligomers were bound together by disulphide bonds and they did not form a continuous network. Thiol-disulphide interchange reaction is possible in pea protein, however, might be stopped or inhibited by further aggregation via non-covalent interaction, which buried reactive thiol groups. The high amount of non-covalent bonds might make the plant-based protein particles softer.

The doctoral candidate substantially contributed to this manuscript by conceptualization and designing the experiments. Statistical data analysis and interpretation of the results were carried out by the doctoral candidate. The doctoral candidate wrote the original draft and included the reviewer's comments. Co-authors contributed to the experimental part and/or discussion of the results. They also provided input on the drafted publication before submission.

Adapted original manuscript[7]

Comparative assessment of thermal aggregation of whey, potato and pea protein under shear stress for microparticulation[8]

Caren Tanger*, Paola Quintana Ramos, Ulrich Kulozik

Chair of Food and Bioprocess Engineering, Technical University of Munich, Weihenstephaner Berg 1, Freising-Weihenstephan, Germany

Graphical Abstract

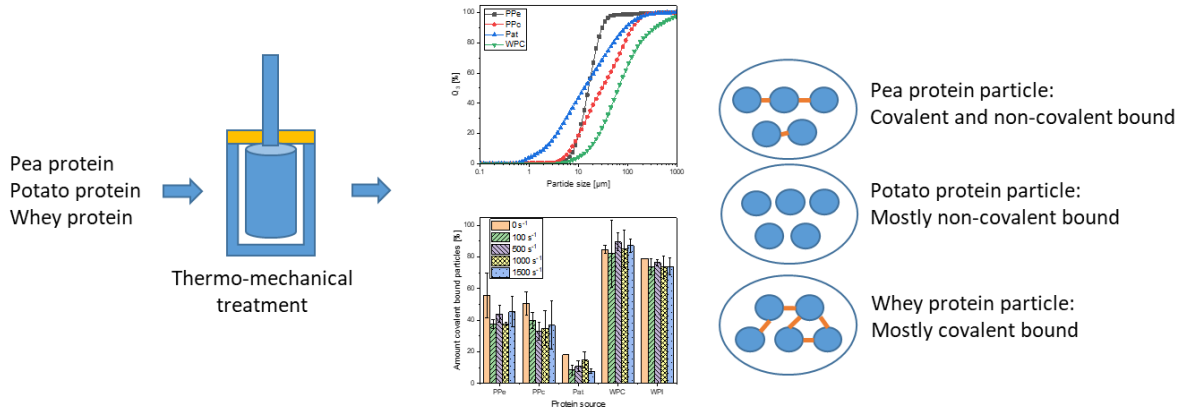

Abstract

The presented work investigates the aggregation behaviour of whey, pea and potato protein under shear stress using a rotational rheometer. Size, protein-interaction and morphology of the aggregates were analysed. Whey protein particles were cross-linked by disulphide bonds (75% - 90%). In contrast, potato protein particles were cross-linked by hydrophobic interaction (88% - 97%). High shear rates were needed to limit aggregate growth. Pea protein particles were stabilized in equal parts by hydrophobic interactions (40% - 62%) and disulphide bonds (37% - 56%) in equal parts. Aggregate size was dependent on the processing history of the protein. Native pea protein favoured a particle size of 5 – 30 µm and was independent of shear rate. Increasing shear rate decreased the aggregate size of pre-aggregated pea protein to a $d_{50,3}$ of 29 µm. A general prediction of the protein aggregation behaviour based on their molecular structure remains a challenging task. This research provides insights into the aggregation behaviour of pea and potato protein and helps to design microparticulated structures of plant proteins.

3.4.1 Introduction

Lower caloric, protein-rich and more sustainable diets are generally of increasing importance. Part of this trend is to apply or consider plant proteins as an alternative protein source in partial or full replacement of animal protein. Plant proteins, however, are

[7] Adaption refer to formatting issues: e.g., abbreviations, figure, table, equation and section numbering, citation style, notation of units, spelling, axis labelling. References of all chapters are merged at the end to avoid redundancies.

[8] Originally published in: ACS Food Science and Technology (2021), Vol. 5, 975 - 985 . Permission for reuse of this article was granted by ACS.

less well investigated in their functionality and processing behaviour, compared to whey proteins, in particular. Little is known about how to process plant protein to generate new functionalities for incorporation in foods. As an example, functionalization of whey proteins by a targeted thermally induced aggregation, controlled by simultaneous application of shear (`microparticulation´), was applied to replace fat in foods, provided the aggregates´ size and shape mimics fat droplets (Spiegel and Huss 2002). This can be explained by a ball-bearing effect of round shaped particles behaving like fat droplets between tongue and palate, which `lubricates´ the movement of tongue and palate thus creating a creamy mouthfeel (Liu et al. 2016b). The microparticulation process of whey protein was studied using a rheometer on small scale (Wolz et al. 2016b; Moakes et al. 2015) and twin-screw extruder (Wolz et al. 2016a) and a scraped-surface heat-exchanger (Spiegel and Huss 2002; Toro-Sierra et al. 2013) for large scale production. Next to size, also shape, structure and protein type have an impact on the perceived textural effect of microparticles (Liu et al. 2016a; Engelen et al. 2005). The size threshold, beyond which such microparticles create a gritty, mealy or sandy mouthfeel is dependent on the hardness of the particles (Engelen et al. 2005; Liu et al. 2016a) and also on the viscosity of the continuous phase. Protein-based microparticles can also be created for other purposes, for instance, to stabilize foams or emulsions. This application has been studied by Zhang et al. (2020a) for pea proteins, Destribats et al. (2014) and Dombrowski et al. (2016) for whey protein.

Whey protein microparticles have already been used as fat replacers in yoghurt (Sandoval-Castilla et al. 2004) and cheese (Sturaro et al. 2015; Sánchez-Obando et al. 2020; Steffl et al. 1999) or as functional particles for foam or emulsion stabilisation (Çakır-Fuller 2015) and mitigation of melting of ice cream (Koxholt et al. 1999).

For plant proteins, heat-induced aggregation has been studied extensively while shearing has been studied to a much lower extent. For a better understanding of the behaviour of different sources of protein under thermal and shear conditions, it is worthwhile to compare their molecular characteristics. Whey protein consists of the major fractions β-lactoglobulin and α-lactalbumin. The tertiary structure of β-lactoglobulin is stabilized by two disulphide bonds and is strongly dependent on pH, temperature and other milieu conditions. β-lactoglobulin also contains a free thiol group, in its native state normally hidden by an α-helix (Tolkach and Kulozik 2007). Whey protein aggregates and gels are primarily formed by disulphide bonds and hydrophobic interactions (Havea et al. 2004; Havea et al. 2009). Size and structure of the aggregates are dependent on processing conditions such as pH, temperature, heating time and shear stress (Tolkach and Kulozik 2007; Zúñiga et al. 2010).

The plant proteins investigated in this research are pea and potato protein. The main pea protein fractions can be divided into salt soluble globulins and the water-soluble albumins. The ratio of the two analytical determined groups depends on the extraction method(Tanger et al. 2020). Globulins contain the protein legumin, vicilin and convicilin. Legumin occurs as a hexamer, which is bound by hydrophobic interactions. The monomers (60 kDa) consist of an acidic (40 kDa) and an alkaline (20 kDa) side-chain bound by a disulphide bond (Shand et al. 2007). Vicilin occurs as a trimer (150 kDa)

of monomers of 50 kDa (Shand et al. 2007). Convicilin is a tetramer (280 kDa) of monomers of 70 kDa. Convicilin does not contain disulphide bonds (O'Kane et al. 2004a). Depending on the genotype, vicilin may also contain one or two cysteine residues, which may form disulphide bonds (Chihi et al. 2016). Bogahawaththa et al. (2019) studied the impact of shearing on the solubility and heat stability of pea protein isolates. They found that ionic strength, pH and shear stress affect both studied functionalities. Besides, shearing has an impact on the molecular structure of pea protein and therefore on protein-protein interactions of the resulting aggregates similar to other proteins (Bogahawaththa et al. 2019; Bekard et al. 2011). Zhang et al. (2020a) studied microgels produced from pea protein isolates using a top-down process. i.e. by mechanical destruction of large aggregates produced before to the desired size range of particles. The resulting microgel properties were dependent on ionic strength and pH. These microgels were able to stabilize emulsions for a few months. It has to be noted that all of the studies mentioned above used commercial pea protein with unknown or undeclared molecular states, which might have been different due to their individual processing histories.

To our knowledge, there is only one study on heating and shearing potato proteins (Schmidt et al. 2017). Patatin, the main protein of potato protein is a highly hydrophobic protein. In contrast to whey proteins and pea proteins, patatin does not contain a disulphide bridge stabilizing the molecule, but a free thiol group, rendering it reactive to form disulphide bonds (Creusot et al. 2011). However, a thiol-disulphide interchange creating a network of connected molecules like for whey proteins is not possible for patatin. Schmidt et al. (2017) heated laboratory extracted, i.e. mostly native, potato protein dried by spray drying or and freeze-drying at different pH levels and ionic strength. After heating and cooling the suspension was sheared with shear rates from 0.1 to 100 s^{-1}. The drying method, pH and ionic strengths influenced the gel structure formed. Creusot et al. (2011) studied the gelation of patatin compared to β-lactoglobulin, ovalbumin and glycinin. The insight was that patatin has unique aggregation properties due to its hydrophobic character. The quaternary structure is more similar to β-lactoglobulin and ovalbumin than to the soy protein glycinin. Therefore, the gelation behaviour of patatin was found to be more similar to the one of animal proteins than to other plant proteins.

In this study, the aggregate size and morphology and protein-protein interaction during heating and shearing of a whey protein isolate, a whey protein concentrate, a potato protein concentrate, a lab-scale produced native pea protein concentrate and a commercial pea protein concentrate were investigated. The starting materials were compared in solubility, heat stability and protein interactions resulting in gelation before investigating the generation of microparticles from plant proteins and their functionality as potential fat replacer material in comparison to whey protein microparticles. To our knowledge, there is only one study by Amagliani et al. (2020), which compares the effect of post-shearing of heat-treated alkali extracted pea and soy protein as well as commercially available potato and whey proteins with varying salt and oil content at a low protein content of 3% and only one shear rate. They found a great dependence of

the aggregate characteristics on the protein source. In contrast to the study of Amagliani et al. (2020) the heat and shear treatment in this study was simultaneous with varying shear rate, which is expected to result in different particle properties. Additionally, to the study of Amagliani et al. (2020) the protein interactions within the particles were investigated. This approach allowed us to compare the different proteins head-to-head to get a better understanding of the differences of these protein systems. It is postulated that plant protein can serve as fat replacer similar to whey protein or can be used to produce a clean label emulsion or foam stabilizer. However, due to differences in molecular structure and lower amount of reactive free thiol groups, protein interactions in plant-based microparticles are hypothesized to be more of hydrophobic nature compared to whey protein, which may result in other particle characteristics.

3.4.2 Material and Methods

3.4.2.1 Materials

Pea flour and pea protein concentrate (E86) was provided by Emsland Stärke (Emlichheim, Germany). Pea flour contained 18.27% protein on a dry basis and the pea protein isolate contained 70.8% protein on a dry basis. Potato protein concentrate (Solanic 200) was provided by Avebe (Veendam, Netherlands), It contained 75.52% protein on a dry basis. Patatin content was 60% of total protein determined by SDS-PAGE (data not shown). Whey protein isolate (WPI) (BiPRO^{TM}) was obtained from Agropur Dairy Cooperative (Saint-Hubert, Longueuil, Canada). It contained 92.91% protein on a dry basis, 1.9% ash and no lactose. Whey protein concentrate (WPC) was obtained from Germanprot Sachsenmilch (Leppersdorf, Germany). It contained 80% protein, 4.4% lactose and 3.2% ash, which may affect protein reactivity to heat, compared to WPI. The protein content of the protein powders was analyzed using Dumas method with a Vario MAX cube (Elementar Analysensysteme GmbH, Langenselbold, Germany). To calculate the protein content from the determining nitrogen content, a conversion factor of 5.4 was used for pea protein, 5.4 for potato protein and 6.35 for whey protein (Mariotti et al. 2008). Deionized water was used to prepare the dispersions (MilliQ Integral 3, Merck KGaA, Darmstadt, Germany). The mineral composition of the protein powders can be found in Table 3-5.

All other chemicals were of analytical grade and purchased from regular suppliers.

Table 3-5: Mineral composition (g/kg) of the protein powders.

	Na^+	K^+	Ca^{2+}
WPI	5.83	0.37	1.21
WPC	3.34	9.17	6.18
PPc	7.94	0.24	0.87
PPe	11.99	0.19	0.14
Pat	7.52	2.78	0.07

3.4.2.2 Extraction of pea protein

Pea protein was alkali extracted from pea flour and isoelectrically precipitated on a laboratory scale as described by Tanger et al. (2020). This extraction was chosen because it is widely used in literature. As described elsewhere (Tanger et al. 2020) the resulting protein concentrate contains “native” protein in contrast to the commercial pea protein. In short, 50 g pea flour was dispersed in 750 ml water at pH 9. The slurry was stirred for 1 h in a glass beaker at 35 °C. The dispersion was centrifuged at 4,500 g for 20 min at 4 °C. The pellet was discarded and the supernatant was set to pH 4.5 with 1 M HCl and stirred for 30 min at room temperature. The dispersion was then centrifuged at 4,500 g for 20 min at 4 °C. The supernatant was discarded and the pellet was dispersed 1:1 with water. The dispersion was set to pH 7 with 1 M NaOH and stirred for 30 min. Then, the dispersion was freeze-dried. The obtained protein product contained only globulins with 71.14% protein content on a dry basis.

3.4.2.3 Preparation of protein dispersions

The protein powders were dispersed in water to obtain a 10% (w/w) protein dispersion, which was the highest concentration at which commercial pea protein and potato protein, could be dissolved. The pH was not adjusted. It varied between pH 6.9 for potato protein and 7.5 as the upper level for commercial pea protein. The protein dispersions were stirred for at least 12 h at 4 °C to allow complete hydration and stored less than 24 h before use. In the following, commercial pea protein is referred to as PPc, laboratory extracted pea protein as PPe, patatin as Pat, whey protein concentrate as WPC and whey protein isolate as WPI.

3.4.2.4 Solubility of unheated dispersions

Solubility of the different proteins used was measured based on the method described previously (Tanger et al. 2020). In short, 0.2 g protein was dissolved in 20 g water and stirred for 1 h. Thereafter, the dispersion was centrifuged for 15 min at 6,000 g at 20 °C to remove big particles and 20 min at 10,000 g at 20 °C to let smaller particles sediment. The protein content of the supernatant was measured using Dumas method. The solubility was calculated by dividing the amount of protein in the supernatant by the amount of dissolved protein.

3.4.2.5 Determination of denaturation temperature

The denaturation temperature of a 10% protein dispersion (w/w) was determined using modulated dynamic scanning calorimetry (DSC Q1000, TA instruments, New Castle, USA) as described elsewhere (Tanger et al. 2020). Summarizing, indium was used as a reference to calibrate the heating ramp. 20 µl of a 10% protein dispersion was pipetted in an aluminium pan, which was hermetically sealed. An empty pan served as a reference. The pans were heated in modulated DSC mode with an underlying heating ramp of 2 K / min and a modulation amplitude of ± 0.5°C every 60 s from 25 °C to 100 °C. Denaturation temperature T_d, T_{onset} and enthalpy change was measured. Data was analyzed using TA universal Analysis 2000 software.

3.4.2.6 Thermal treatment

Samples were heat-treated with and without shear. Samples prepared without shear were heated in steel tubes at T_d + 10°C for 30 min in a water bath. Thus, the temperature was the same as in the thermo-mechanical treatment. Heating to and from 95°C took 1 min. The holding time at 95°C of 30 min was chosen to achieve complete aggregation.

3.4.2.7 Thermo-mechanical treatment

Thermo-mechanical treatment was performed based on the method reported by Wolz et al. (2016b). A rotational rheometer MCR 302 (AntonPaar, Graz, Austria) was used equipped with a Mooney-Ewart geometry ME 21 (cup diameter: 22.93 mm, bob diameter: 21.01 mm, angle: 4°, AntonPaar, Graz, Austria). The Mooney-Ewart geometry combines a cone-plate geometry and a cylindrical geometry to ensure the same shear rate in all places of the sample. 4 ml of sample was placed in the gap between bob and cylinder. Protein dispersions were heated to T_d + 10°C with a heat holding time of 10 min. Heating from room temperature to processing temperature took 15 min and cooling from processing temperature to room temperature took 20 min. Shear conditions were varied from 100 s^{-1} to 1500 s^{-1}. The samples were covered with a wet sponge and a lid to avoid evaporation of water during measurement. After processing the samples were poured into a plastic container and stored at 4°C for further characterization.

3.4.2.8 Particle size measurement

Particle size distribution of the produced aggregates was measured using a Malvern Mastersizer Hydro 2000S (Malvern Instruments Ltd, Malvern, Worcestershire, UK). Before measurement, the samples were diluted to a 1% protein dispersion with water. (Mie theory was applied to calculate the particle size distribution. A refractive index of 1.45 was used for the dispersed phase, a refractive index of 1.33 was used for the dispersant medium and absorbance of 0.001 for the protein dispersion was used (McCarthy et al. 2016). The $d_{50,3}$ as a specific result and the cumulative particle size distribution (Q_3) to show the whole multimodal distribution are shown in the results.

Because WPI particles were too small to be measured using a mastersizer, they were measured using a ZetaSizer Nano ZS (Malvern Instruments Ltd, Malvern, Worcestershire, UK). Measurements were performed at a fixed angle of 173 ° and a wavelength of 632.8 nm using a refractive index of 1.45. Z-Average are shown in the results.

3.4.2.9 Protein-protein interaction

The protein-protein interaction in the produced aggregates were analysed using a protein interaction assay based on the method used by Tanger et al. (2021a) with some modifications. 0.2 g of sample was dispersed in 10 g of a 50 mM phosphate buffer pH 7 (B_1), 50 mM phosphate buffer pH 7.5 with 2 g / l SDS (B_2) and 50 mM phosphate buffer pH 7.5 with 2 g / l SDS and 15 g / l DTT (B_3). Buffer B_1 should cleave all electrostatic interaction, buffer B_1 all electrostatic and hydrophobic interactions and buffer B_3 all electrostatic and hydrophobic interactions and disulphide bonds. The samples were dissolved overnight using a shaker (LAUDA-GFL Gesellschaft für Labortechnik mbH, Burgwedel, Germany) and then centrifuged at 10,000 g for 20 min at 20°C. The nitro-

gen content of the supernatant was determined using the Dumas method. The following equations were used to determine the contributions of different types of each type of chemical bonds:

$$C_{n,bond,Bi} = \frac{(m_S + m_{gel})}{m_{gel}} * C_{n,sup,Bi} \quad (3\text{-}21)$$

$$\frac{C_{n,bond,B1}}{C_{n,gel}} = P(ES) \quad (3\text{-}22)$$

$$\frac{C_{n,bond,B2}}{C_{n,gel}} = P(ES) + P(Hy) \quad (3\text{-}23)$$

$$\frac{C_{n,bond,B3}}{C_{n,gel}} = P(ES) + P(Hy) + P(SS) \quad (3\text{-}24)$$

$$P(Hy) = \frac{C_{n,bond,B2}}{c_{n,gel}} - \frac{C_{n,bond,B1}}{C_{n,gel}} \quad (3\text{-}25)$$

$$P(SS) = \frac{C_{n,bond,B3}}{C_{n,gel}} - \frac{C_{n,bond,B2}}{C_{n,gel}} \quad (3\text{-}26)$$

With m_S as the initial mass (10 g), m_{gel} as the mass of the gel (0.2 g) and $C_{n,sup,Bi}$ as dissolved nitrogen in the supernatant in [%], $C_{n,gel}$ as the nitrogen content of the microparticle in [%], ES for electrostatic interactions, Hy for hydrophobic interactions and SS as an acronym for disulphide bonds. $C_{n,bond,Bx}$ is the concentration of cleaved protein bonds by the respective buffer.

Because some of the produced aggregates were smaller than 0.45 µm, these aggregates stayed in the supernatant during centrifugation at 10,000 g. In order to get a better idea of whether these aggregates were formed by covalent or non-covalent bonds, the supernatant of buffer B_2 was analysed with an SDS-PAGE. SDS-PAGE was performed as described previously (Tanger et al. 2020). Band intensity was analysed using ImageLab Software (version 6.0) and served as a measurable amount of covalently bound aggregates, which were not detected by the protein interaction assay.

3.4.2.10 Optical microscopy

In order to display the morphology of the aggregates, the aggregates were visually inspected using an optical microscope (Axioskop, Carl Zeiss AG, Oberkochen, Germany). The aqueous dispersion was diluted to 1% protein dispersion. Pictures were taken using Motic Images Plus 3.0 (Motic, Barcelona, Spain).

3.4.2.11 Statistical analysis

All experiments were performed in at least duplicate from two different dispersions. Mean values are shown in the graphs and error bars indicate upper and lower values if not indicated otherwise. The dotted line serves as a guide to the eye. A one-way analysis of variance (ANOVA) for significant differences between samples was performed followed by a Tukey-Kramer (HSD) test. Minimum significance was set to 5% level ($p < 0.05$). For comparison of covalently bound particles between shear and no shear stress a Dunnett's test ($\alpha = 0.05$) was performed with the sample heated without shear stress as reference. All statistical analysis was executed using JMP Pro (SAS Institute Inc., Cary, USA/Version 14)

3.4.3 Results and discussion

3.4.3.1 Solubility of protein powders

The protein powders and their dispersions differed in their functionalities. The solubility of a protein greatly determines the gelling ability of the protein. It was reported that insoluble particles act as fillers in protein gels and weaken the gel structure (Klost et al. 2020; Britten and Giroux 2001). This may have an influence on particles formed under shear stress. Therefore, the solubility of the five different proteins was determined. The soluble protein contents in the supernatant obtained at 6,000 g and 10,000 g are depicted in Figure 3-27. It can be seen that whey protein was the most soluble protein. WPI was slightly more soluble (93%) than WPC (90%). Centrifugation speed had only a small effect on the amount of determined soluble protein. The commercial pea protein was the most insoluble protein powder with a solubility of 17%. Low solubility of commercial pea protein was also found in a previous study (Tanger et al. 2020). Laboratory extracted pea protein was found to be better soluble (75%) similar to potato protein isolates (80%). A better solubility of laboratory extracted pea protein compared to commercial pea protein was also reported by Tanger et al. (2020). A low solubility does not only indicate that a weak gel will be formed upon gelation but also indicates that the protein was already denatured and aggregated due to prior processing impact (Fuhrmeister and Meuser 2003). This was the case for the commercial pea protein. In general, comparable solubility's were found for pea, potato and whey protein at a protein concentration of 4% (Amagliani et al. 2020).

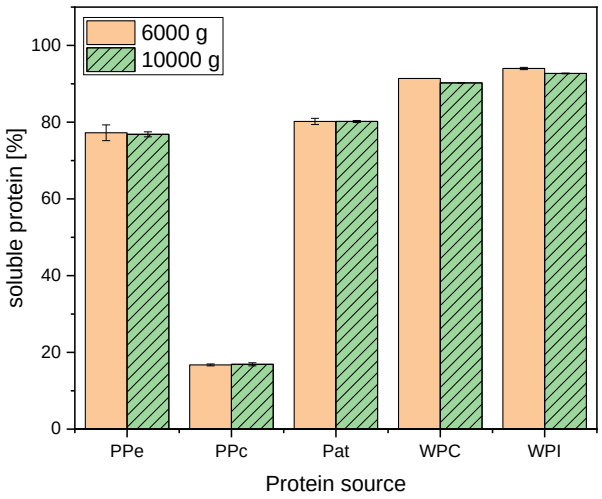

Figure 3-27: Solubility of different protein powders at 6,000 g and 10,000 g.

3.4.3.2 Thermal stability of the different dispersions

In order to analyse the thermal stability of the different proteins, the denaturation temperature, as well as T_{onset} and the enthalpy change, were measured using DSC. All thermograms showed one denaturation peak except for the commercial pea protein, where no denaturation peak was seen. The denaturation temperature (T_d) was defined as the peak maximum, T_{onset} described as the beginning of the reaction, and the enthalpy change (ΔH) was obtained by integration of the peak. The results for all protein isolates can be found in Table 3-6.

Table 3-6: Denaturation temperature (T_d), T_{onset} and enthalpy change (ΔH) for 10% dispersions dissolved in water for all protein powders measured by DSC.

	PPe	PPc	Pat	WPC	WPI
T_d (°C)	78.01 ± 0.09[a]	-	62.99 ± 0.05[b]	73.97 ± 0.06[c]	72.81 ± 0.11[d]
T_{onset} (°C)	70.55 ± 0.05[a]	-	54.46 ± 0.04[b]	68.75 ± 0.31[c]	68.23 ± 0.03[c]
ΔH	0.49 ± 0.02	-	0.74 ± 0.00	0.16 ± 0.02	0.12 ± 0.00

[a-s] Row values followed by the same letter are not significantly different (p > 0.05)
*Means ± SD of triplicate

Potato protein showed the lowest denaturation temperature of 63°C. Creusot et al. (2011) and Delahaije et al. (2015) reported a denaturation temperature of 60°C using a 1 K/min ramp for potato protein. The less steep heating ramp can explain the slightly lower denaturation temperature since denaturation is a temperature-time effect. The lack of a disulphide bond explains the low heat stability of potato protein (Creusot et al. 2011).

The denaturation temperature of both whey protein powders were similar, 73°C and 74°C, respectively. A denaturation temperature of 75.5°C was found for WPI using DSC measurement with a higher heating rate of 5 K/min (Nikolaidis and Moschakis 2018). The steeper heat ramp explains the higher denaturation temperature found. The higher denaturation temperature of WPC can be explained by the stabilizing effect of lactose by preferential exclusion. The higher denaturation temperature of WPC can be explained by the stabilizing effect of lactose by preferential exclusion (Spiegel 1999b). Wolz and Kulozik (2015) found a bend temperature of 80°C for the same WPC as used in this study. The bend temperature separates unfolding limited area and aggregation limited area from each other. This bend temperature is slightly higher than the denaturation temperature found in this study, but could also be explained by the low heating ramp of the mDSC. Delahaije et al. (2015) reported a denaturation temperature of 75°C for β-lactoglobulin as the major whey protein using a heating ramp of 1 K/min. Wit and Swinkels (1980) reported a denaturation temperature of 70.4 °C for β-lactoglobulin extrapolated to a zero heating rate. The denaturation temperature of α-lactalbumin is dependent on its form, apo or holo. Holo-α-lactalbumin was reported to have a denaturation temperature of 64.3°C and apo-α-lactalbumin of 35.0°C using a heating rate of 0.5 K/min. The presence of β-lactoglobulin increased the denaturation temperature of α-lactalbumin by 2.5°C (Boye and Alli 2000). Since only one peak was observed, it was concluded that the denaturation peak of β-lactoglobulin and α-lactalbumin overlapped at the heating rate used in this study.

The most heat-stable protein was laboratory extracted pea protein with a denaturation temperature of 78°C, Such high denaturation temperatures have also been found for soy protein (Shand et al. 2007). The high denaturation temperatures can be explained by the intramolecular disulphide bonds and possibly high inter- and intramolecular forces, such as hydrophobic interactions. In contrast to whey protein and patatin, pea proteins occur mainly multimeric and are high in conformational compactness (Mession et al. 2013) meaning before unfolding these multimers have to dissociate. β-

lactoglobulin dimers are very loosely associated and can easily be broken apart by the application of heat. How strong the multimers are bound together has not been investigated so far. Strong intermolecular interactions between the monomers can possibly add to the thermal stability of pea protein. Additionally, remaining sugars and salt in the pea protein powders could possibly enhance heat stability either by shielding effects of the salt or the preferential exclusion by sugars similar to whey protein.

3.4.3.3 Effect of protein source and shear rate on aggregate size

The size of the resulting aggregates was measured using laser diffraction. The WPI aggregates were too small to be assessed by laser diffraction. In order to see the effect of shear rate on the WPI aggregates, dynamic laser scattering was used instead. All other produced aggregates were large enough to be measured by laser diffraction. The $d_{50,3}$ for the remaining four protein dispersions at all shear rates[1] are shown in Figure 3-28.

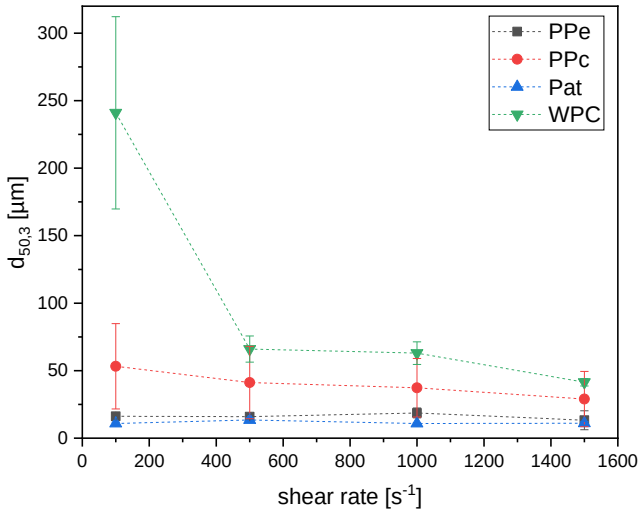

Figure 3-28: $D_{50,3}$ of PPe, PPc, Pat and WPC particle size distribution as function of shear rate.

It can be seen that treatment of WPC dispersion resulted in the largest aggregates compared to the other samples. The main difference between the WPI and the WPC is the lactose content in WPC. Spiegel (1999b) found that lactose has a decelerating effect on the unfolding of β-lactogobulin due to the better hydration of the protein molecules in an aqueous sugar solution by preferential exclusion Aggregate growth is stronger with increasing content of lactose leading to larger loosely packed aggregates. At low lactose concentration, the denaturation was reported to be fast, because the native protein structure was not stabilized by lactose. This fast denaturation led to dense and compact aggregates with a low amount of bound serum (Spiegel 1999b). Therefore, either protein concentration or lactose concentration has to be increased to form particles on a microscale for WPI. The plant protein aggregates had a smaller particle size than the WPC aggregates but were significantly larger than the WPI aggregates. Delahaije et al. (2015) already reported that patatin favours the formation of fewer, but larger aggregates compared to β-lactoglobulin and ovalbumin. However, the

aggregation behaviour could not be linked to a molecular property or the reaction kinetics. Creusot et al. (2011) stated that the formation of larger aggregates is attributed to their high exposed hydrophobicity. Chihi et al. (2016) reported that heated pea protein led to middle- to large-sized aggregates compared to β-lactoglobulin similar to soy protein and patatin. The authors explained the large aggregates by the dominant role of hydrophobic interactions involved in aggregate formation. In addition, the remaining sugars and salt in the plant protein concentrate can possibly affect particle formation. However, this has not been studied in detail so far, because this would have gone above the scope of this research. The particle size of pea and potato protein were slightly higher than found by Amagliani et al. (2020), heated at 95°C for 90 s and afterwards sheared with an Ultra-Turrax at 11,000 rpm for 1 min. The difference in particle size can be explained by the different, less defined thermo-mechanical process in the Ultra-Turrax.

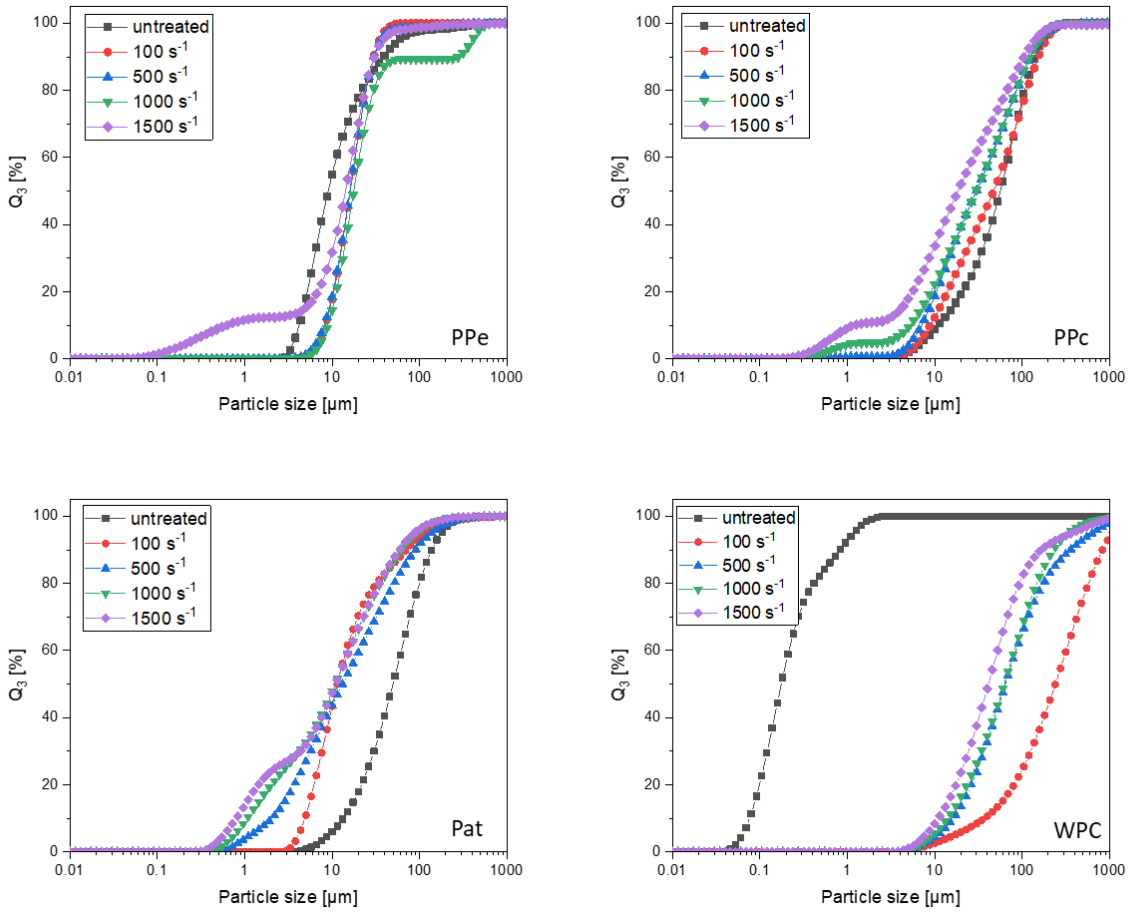

Figure 3-29: Cumulative particle size distribution (Q_3) of PPe, PPc. Pat and WPC at different shear rates and untreated.

The shear rate can have two effects on the aggregation of proteins. One effect would be that the collision probability increases and therefore larger or more aggregates can be formed. The second effect could be the shear stress, which destructs loosely bound aggregates into smaller aggregates(Wolz et al. 2016b). The particle size distributions in dependence of shear rate are depicted in Figure 3-29. Overall, the shear stress

predominated for WPC and all plant proteins and the size of the aggregates decreased with increasing shear rate. The particle size distribution for WPI aggregates was multimodal (data not shown). The Z-average is shown as a function of the shear rate in Figure 3-30.

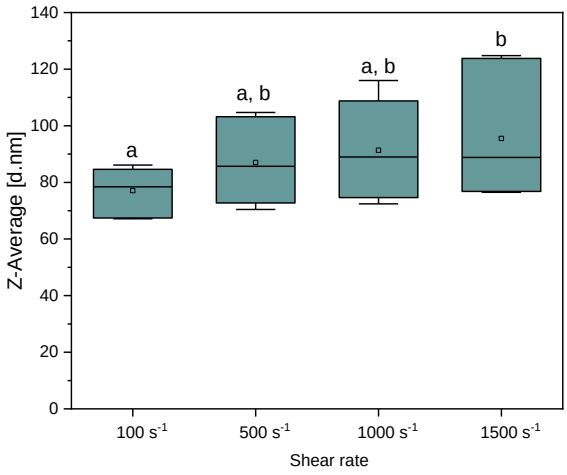

Figure 3-30: Z-average over shear rate for WPI protein sample. [a-b] same letters indicate no significant difference between samples ($p < 0.05$).

The Z-Average increased slightly with increasing shear rate indicating the formation of larger and/or denser aggregates (Delahaije et al. 2015). However, the effect is only significant between the lowest and the higher shear rates. A similar size increase with increasing shear stress has been reported for heating a 4 wt% WPI dispersion on in the presence of NaCl under shear (Vilotte et al. 2021). This effect can be explained by higher collision probability at higher shear rates leading to larger aggregates (Wolz et al. 2016b) or by differences in thermal history due to the different distribution of heat at different shear rates (Vilotte et al. 2021). It has to be noted that there was a small sediment in the sample for potato protein heated at low shear rates. A steep increase in viscosity in the first heating phase, which in the second phase dropped (data not shown) together with the sediment suggested that gel network was formed initially by potato protein, which eventually was disrupted by the shear stress. With increasing shear rate, no sediment could be found and the increase in viscosity was significantly lower (data not shown). This suggests that gel network formation and aggregate size was limited by the shear stress. With increasing shear rate, the number of particles around 0.5 to 4 µm increased. The same effect can be seen for laboratory extracted pea protein. At 1500 s^{-1} small particles around 0.1 to 5 µm were found. However, the effect of shear rate for laboratory extracted pea protein is smaller than for potato protein and the commercial pea protein. Aggregates around the size of 5 µm to 30 µm are favoured independently of shear rate at a protein concentration of 10% for laboratory extracted pea protein. Particle size in this range would render the laboratory extracted pea protein particles a suitable fat replacer (Cheftel and Dumay 1993). The aggregates produced in this study were much larger than the aggregates formed by Chihi et al. (2016) in a 2 wt% protein concentration 5 mM NaCl pH 7.2 dispersion heated at 85°C

for 60 min. This difference can be explained by the different heat treatments, protein concentrations and different protein concentrate used in this study. Particle formation of commercial pea protein was a top-down process. In this case, the particle size decreased with increasing shear rate. This can be explained by the increase in shear stress with increasing shear rate, which breaks the aggregates apart leading to smaller particles.

3.4.3.4 Effect of protein source and shear rate on protein interaction upon aggregation and gelation

Protein interactions are strongly dependent on the molecular structure and exposure of reactive groups of the protein. Without shear stress, whey proteins are known to mainly interact via disulphide bonds and hydrophobic interactions (Havea et al. 2004; Havea et al. 2009; Wijayanti et al. 2014). Potato protein is capable of forming disulphide bonds but mainly interacts by hydrophobic interactions (Creusot et al. 2011). It is similar to pea protein, where disulphide bonds are formed, but play a minor role in gelation. The main protein interactions are also non-covalent (Sun and Arntfield 2012; Chihi et al. 2016).

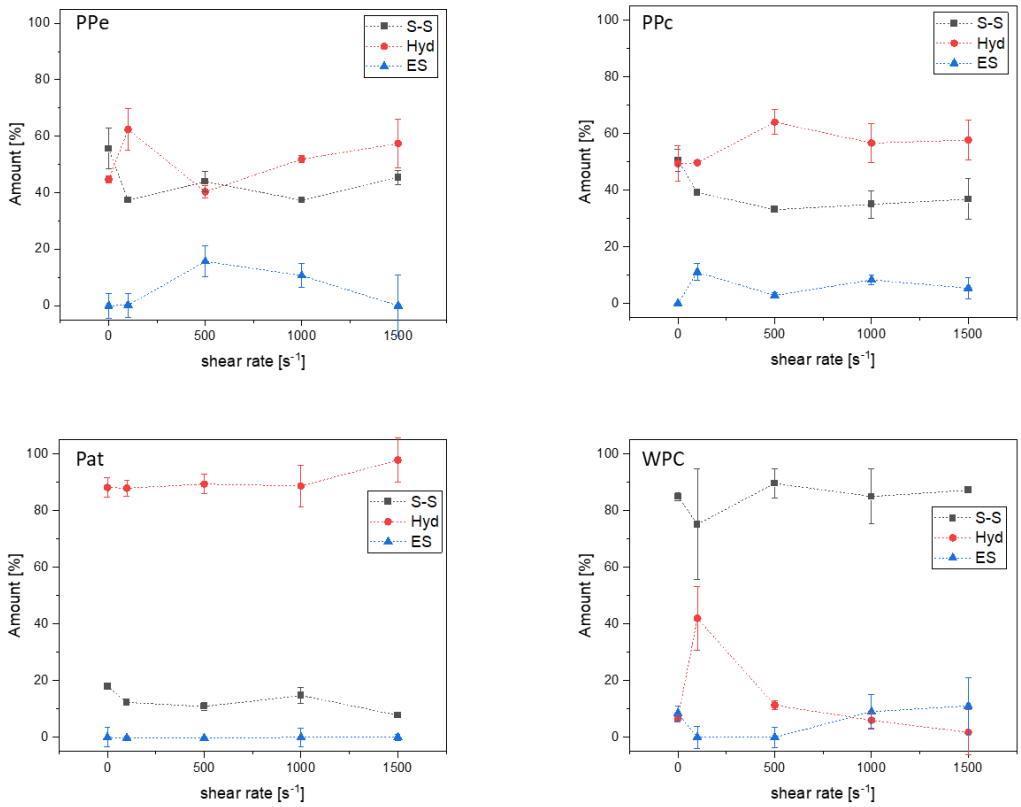

Figure 3-31: Contribution of various types of protein interactions for PPe, PPc, Pat and WPC for no shear rate applied and 100, 500, 1,000 and 1,500 s^{-1}, determined by protein interaction assay and SDS-PAGE.

In the following section, a difference is made between covalently bound large particles and covalently bound colloidal dispersed aggregates. For the sake of clarity, covalently bound particles include all particles cross-linked by disulphide bonds, calculated using equations (3-21) - (3-26) using the results of the protein interaction assay and SDS-PAGE. Colloidally dispersed covalently bound aggregates describe small particles,

which stay in the supernatant in buffer B_2 during centrifugation, which cleaves only hydrophobic and electrostatic interactions during centrifugation of the protein interaction assay. These soluble aggregates do not form a continuous network. The soluble covalently bound aggregates were only determined by SDS-PAGE of the supernatant of buffer B_2. As can be seen in Figure 3-32 and Figure 3-33, most particles (~ 70% - 90%) are covalently crosslinked in WPC and WPI, independently of the shear rate. Quevedo et al. (2020a) stated that most interactions were covalent bonds in pure β-lactoglobulin samples, simultaneously sheared and heated in a closed cavity rheometer at a protein concentration of 50% - 70% and that shearing accelerated denaturation.

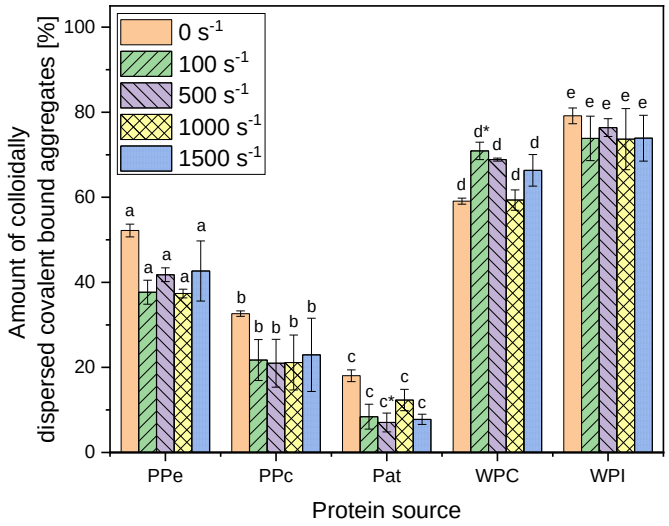

Figure 3-32: Amount of colloidally dispersed covalently bound aggregates at 10,000 g in PPe, PPc, Pat, WPC, WPI and without shear rate applied and 100, 500, 1,000 and 1,500 s^{-1}, assessed by SDS-PAGE of the supernatant of buffer B_2. [a-e] same letters indicate no significant difference between samples ($p < 0.05$). * indicate significant difference to the reference (0 s^{-1})

For WPI, the particles formed were small enough to stay in the supernatant at 10,000 g and therefore only SDS-PAGE results could be analysed. For WPC, it was found that small and larger particles mainly were connected by disulphide bonds, as can be seen in Figs. 5, 6 and 7. Hydrophobic interactions played a negligible role. The high amount of covalent bonds adds to the findings for gels and aggregates (Havea et al. 2004). Shear stress was found to increase the thiol-disulphide interchange reaction (Evans 2001). However, no significant difference between the sheared samples and those produced without shear stress was observed, but a significant difference between the protein sources was found. Except PPc and PPe samples were not significantly different in disulphide bridges stabilizations. A significant difference was found between WPI and WPC samples, which could be due to the presence of lactose in WPC.

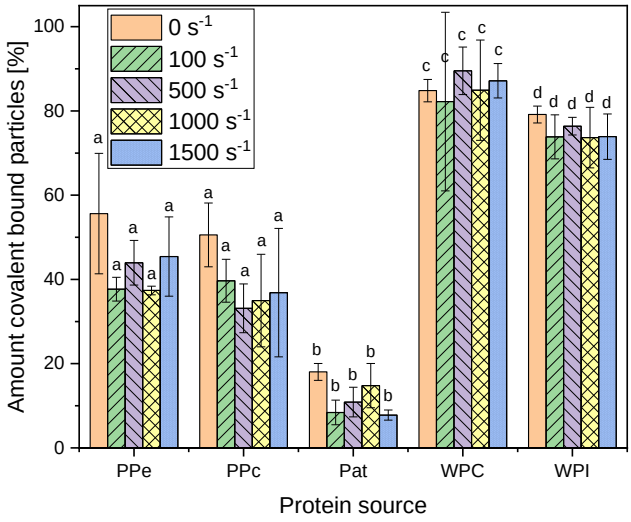

Figure 3-33: Amount of total covalently crosslinked particle in PPe, PPc, Pat, WPC and WPI without shear rate applied and 100, 500, 1000 and 1500 s^{-1}, assessed by SDS-PAGE of the supernatant of buffer B_2 and protein interaction assay. [a-d] same letters indicate no significant difference between samples ($p < 0.05$).

In contrast to whey protein aggregates, the potato protein aggregates were mainly stabilized by hydrophobic interactions, independently of the shear rate, as can be seen in Figure 3-31. Only a minor part of soluble particles was crosslinked by disulphide bonds (Figure 3-33). Without shear stress, fewer disulphide bonds were found in potato protein particles (Figure 3-33). However, this amount was not significantly lower than the sample without shear stress. Creusot et al. (2011) and Schmidt et al. (2019) explained the high amount of hydrophobic interaction in patatin gels with the molecular structure of patatin. Patatin contains only one free thiol group and no disulphide bond in its native molecular structure. Thus, there is a limited possibility to form a continuous network only by disulphide bonds Initial aggregation was suggested to occur via hydrophobic interactions (Pots et al. 1999) due to the high exposed hydrophobicity of the patatin, which also leads to a very low gelation concentration of 3% (Creusot et al. 2011; Schmidt et al. 2019). In addition, primary patatin aggregates were found to be formed independently of the protein concentration and their structure did not change upon further aggregation and gelation (Delahaije et al. 2016). The results in this study show that disulphide bonds are present in patatin aggregates. However, they do not form a continuous network and only add to a negligible amount to the stabilization of patatin aggregates. This is in contrast to the aggregation behaviour of β-lactoglobulin, where disulphide bond formation plays a major role in aggregation (Roefs and Kruif 1994; Zúñiga et al. 2010; Tolkach and Kulozik 2007).

In Figure 3-31 it can be seen that pea protein aggregates were neither formed mostly by hydrophobic interaction, as potato protein nor by disulphide bonds, as whey protein. Around 35% to 45% of the interactions in the particles were covalent and the rest was of hydrophobic and electrostatic character. Commercial pea protein was already denatured and aggregated before the treatment in this study. In other words, particle formation, in this case, was a top-down process, whereas for laboratory extracted pea

protein it was a bottom-up process. First, the bottom-up process of laboratory extracted pea protein is discussed in the following, then the top-down process of the commercial pea protein.

Legumin contains a disulphide bond and depending on genotype vicilin and legumin also contain a free thiol group (Chihi et al. 2016). A classic thiol-disulphide bond interchange is possible in contrast to patatin and is similar to whey protein. However, a continuous covalently cross-linked network is not formed. For pea protein gels it has been reported that protein interactions are mainly of non-covalent nature (Chihi et al. 2016; Sun and Arntfield 2012). The absence of a continuous covalently cross-linked network suggests that the thiol groups and disulphide bonds may not be as reactive or accessible in pea protein compared to whey protein. Similar to patatin the initial aggregation is suggested to occur via non-covalent bonds. O'Kane et al. (2004c) reported that in contrast to soy glycinin a pea protein gel network could still be formed even with the inhibition of disulphide bond formation. However, disulphide bonds enhanced the gel network.

Reheating a pea protein gel resulted in structural changes (O'Kane et al. 2004c). This leads to the microparticulation of commercial pea protein, where already denatured pea proteins are reheated. In contrast to laboratory extracted pea protein, disulphide bonds contribute more to the formation of a continuous network. The higher amount of disulphide bonds in the continuous network in commercial pea protein can be explained by either the denaturation process during extraction of the protein or the rearrangement and higher accessibility of thiol groups and intermolecular disulphide bonds during the second heat treatment leading to rearrangement in the particle structure. Pea proteins react rather quickly upon denaturation (O'Kane et al. 2004c). Pea proteins are also very heat stable and therefore might already start aggregation without complete denaturation. Thus, reactive groups as for example thiol groups are still buried within the core of the protein and only react during a second heat treatment resulting in more complete denaturation. Differences in remaining sugars and salt could possibly also influence the protein interactions. The high ratio of hydrophobic interactions in the pea and potato protein particles can be advantageous for usage as fat replacer since a high amount of hydrophobic interactions leads to high deformability of the aggregates (Sun and Arntfield 2012; Creusot et al. 2011). This can be beneficial for the ball-bearing effect, where the particle size threshold is also dependent on the hardness of the particles (Liu et al. 2016a). The harder and irregular the shape of the particles were, the lower was the particle size threshold. The particles size threshold is the size upon which the particles are perceived as rough and gritty. Soft and smooth particles can be larger than the hard particles and still be perceived as creamy (Engelen et al. 2005). Additionally, the deformability and protein interaction within the particles can affect the potential of these particles to stabilize emulsions and foams due to differences in interfacial properties and give hints about their heat stability (Dombrowski et al. 2016; Quevedo et al. 2020a). The protein source had a bigger impact on protein interaction than the application of shear stress.

3.4.3.5 Effect of protein source and shear rate on morphology of produced aggregates

A well-known application of microparticles is the fat replacement. The shape of the particles has an impact on the perceived creaminess of the product with such particles and, thus on their suitability as fat replacer (Engelen et al. 2005; Liu et al. 2016a). The more round-shaped the particles were, the lower was the size threshold of the perceived grittiness of the particles (Engelen et al. 2005). Next to the suitability as fat replacement, the shape of the protein particles are also important for the interfacial properties of the particles, where also a more round shape is more effective to stabilize emulsions and foams (Dombrowski et al. 2016; Quevedo et al. 2020a). It can be seen from the results presented here that varying the protein source and shear rate can generate different shapes and can be used to structure foods. Microscopic images show that the different protein aggregates differ in their shapes, as can be seen in Figure 3-34.

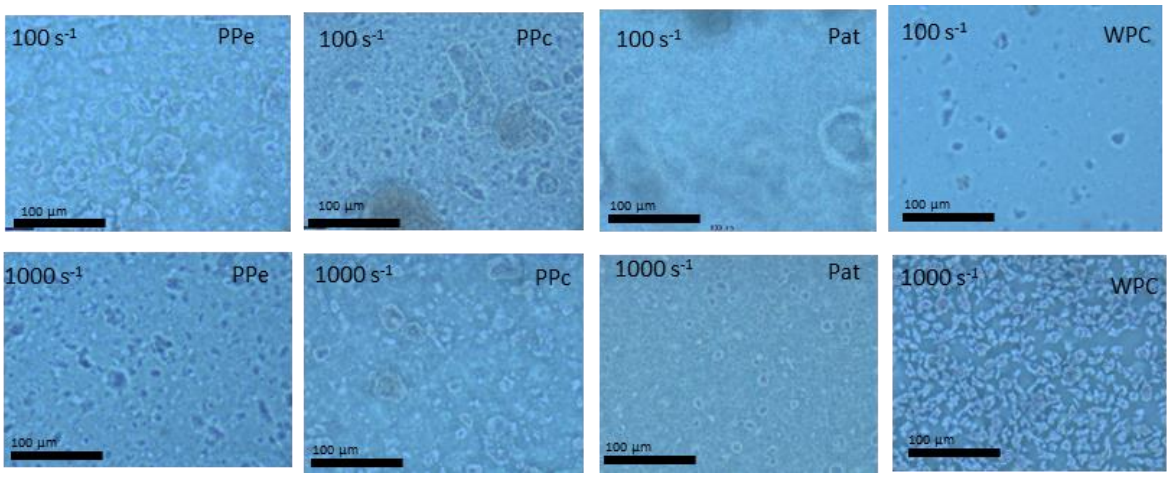

Figure 3-34: Light microscopy images of PPe, PPc, Pat and WPC at 100 s^{-1} (top row) and 1000 s^{-1} (bottom row)

Due to their small size, WPI aggregates could not be analysed using a light microscope. At low shear rates, all aggregates had sharp edges, especially patatin. With increasing shear rate the aggregates became rounder and more uniform in shape. This presumably resulted from the higher shear stress at higher shear rates. A higher shear stress can enhance the erosion at the surface of the aggregates and provide them with a more spherical shape (Wolz et al. 2016b). Wolz et al. (2016b) and Moakes et al. (2015) reported a similar trend for aggregates of whey protein at high protein concentration by increasing the shear rate. Amagliani et al. (2020) found that the shape of the particles was mainly dependent on the protein source by using confocal laser scanning microscopy. In our study difference in shape between the protein sources were also seen, the use of a light microscopy did not allow us to go further in the discussion of our results.

3.4.3.6 Hypothetical aggregation behaviour of pea and potato protein in comparison to whey proteins

The presented results show that the aggregation behaviour of pea, potato and whey protein is different. The aggregation mechanism of whey protein cannot be transferred to either pea or potato protein. In line with previous results of gelation of pea and potato

protein (Creusot et al. 2011; O'Kane et al. 2004c), these proteins were found to react quickly upon heating. Initially formed aggregates are postulated to be formed by hydrophobic interactions. Disulphide bonds play a minor role in aggregate formation of pea and potato protein in contrast to whey protein. Thiol-disulphide interchange is theoretically not possible in potato protein but pea proteins. Chihi et al. (2016) found a higher amount of free thiol groups and a reduced number of disulphide bonds upon heating pea protein. Heating cleaves disulphide bonds forming free thiol groups. However, these thiol groups also need to be exposed to react with another thiol group to form new disulphide bonds connecting two proteins. Quick random aggregation via hydrophobic interaction may hinder exposure of reactive free thiol groups and reduce the amount of aggregation via disulphide bonds. The exposure of reactive free thiol groups and therefore formation of a continuous network via covalent bonds is dependent on the denaturation process and degree of pre-denaturation. This influence can be seen in the different aggregation behaviour of laboratory extracted pea protein and commercial pea protein.

To summarize, a general aggregation model cannot be developed, as expected, due to the different molecular structures of the various proteins. This research provides more insight regarding the aggregation mechanism of pea and potato protein under shear stress, which is of high importance in the food industry, where both heat and shear are applied during processes and also heat stability of ingredients is of interest The new insights will help to characterize these proteins in further research and applying them in (innovative vegan) food. Application areas could be fat replacement or stabilizing foams and emulsions.

Funding Sources

This project was executed as part of an Industrial Collective Research (IGF) project of the Forschungskreis der Ernährungsindustrie e.V., Bonn (FEI) supported by the German Ministry of Economics and Technology via AiF (AiF 20197N).

Acknowledgement

We would like to acknowledge the help of Annette Brümmer-Rolf and Christine Haas for protein measurement. Special thanks to Julia Engel for laboratory help and David Andlinger for valuable discussion. We would like to thank Marc Laus from AVEBE, Veendam, The Netherlands, for providing the potato protein isolate and Thomas Pruter and Stephanie Schomaker from Emsland Stärke, Emlichheim, Germany, for providing the pea protein isolate and pea flour.

Abbreviations

PPe, laboratory extracted pea protein; PPc, commercial pea protein, Pat, potato protein isolate / patatin; WPC, whey protein concentrate; WPI, whey protein isolate.

3.5 Influence of extraction method on the aggregation of pea protein during thermo-mechanical treatment

Summary and contribution of the doctoral candidate

Since commercial pea protein was found to be highly denatured and aggregated, pea protein is extracted from pea flour for most research purposes. In literature, there are two extraction methods, which are used mostly for gelation and aggregation studies. These are salt extraction and alkali extraction. Even though both extraction methods render a protein powder of around 75% protein they were found to be different in the amount of native protein and protein profile leading to different functionalities (Tanger et al. 2020). Since they have different functionalities, it is of interest whether these also influence the microparticulation behaviour. To answer this question, two protein powders were produced. One was produced by salt extraction and the other one was produced by alkali extraction. From previous studies, it was already known that the salt extracted protein powder was much higher in legumin content than the alkali extracted one (Tanger et al. 2020), which was seen back in a higher denaturation temperature. It also contained a higher amount of native pea protein compared to the alkali extracted pea protein, which was seen back in a higher enthalpy change. Thermo-mechanical treatment was performed without adjusting pH, natural pH, and at pH 4 and varying shear rates. Natural pH was pH 6.5 for salt extracted pea protein and pH 6.9 for alkali extracted pea protein. At natural pH thermo-mechanical treatment led to dense and shear stable particles for salt extracted pea protein. Whereas for alkali extracted pea protein thermo-mechanical treatment led to worm-like, transparent and less shear-stable particles. At pH 4 particles resulting from thermo-mechanical treatment were dense and shear stable for both extracted pea proteins. Particles were also bigger at pH 4 due to the decreased repulsive forces between the proteins at this pH. The differences between the particles formed upon thermo-mechanical treatment proteins could be explained by the difference in protein profile, degree of nativity, and resulting solubility. Alkali extraction can lead to partially unfolded pea protein. Thus, already part of the reactive core is exposed, which then can lead to rapid aggregation by an increase in temperature and further unfolding. This aggregation before unfolding, can inhibit further unfolding due to steric hindrance and lead to loosely bound particles. The high legumin content in salt extracted pea protein might lead to more covalently bound and hydrophobic bound particles upon thermo-mechanical treatment at natural pH compared to alkali extracted pea protein. A shift in pH is likely to change the type of protein-protein interactions and therefore also more dense and bigger particles can be created. Summarizing, by controlling protein profile and the functionalities connected to it, particle size and structure can be manipulated.

The substantial contribution of the doctoral candidate to this manuscript included conceptualization and designing of the experiments based on literature review. Statistical data analysis and interpretation of the results were carried out by the doctoral candidate. The doctoral candidate wrote the original draft. Co-authors contributed to the experimental part and/or discussion of the results.

Adapted original manuscript[9]

Influence of extraction method on the aggregation of pea protein during thermo-mechanical treatment[10]

Caren Tanger*, Johannes Mertens, Ulrich Kulozik

Chair of Food and Bioprocess Engineering, Technical University of Munich, Weihenstephaner Berg 1, Freising-Weihenstephan, Germany

Graphical abstract

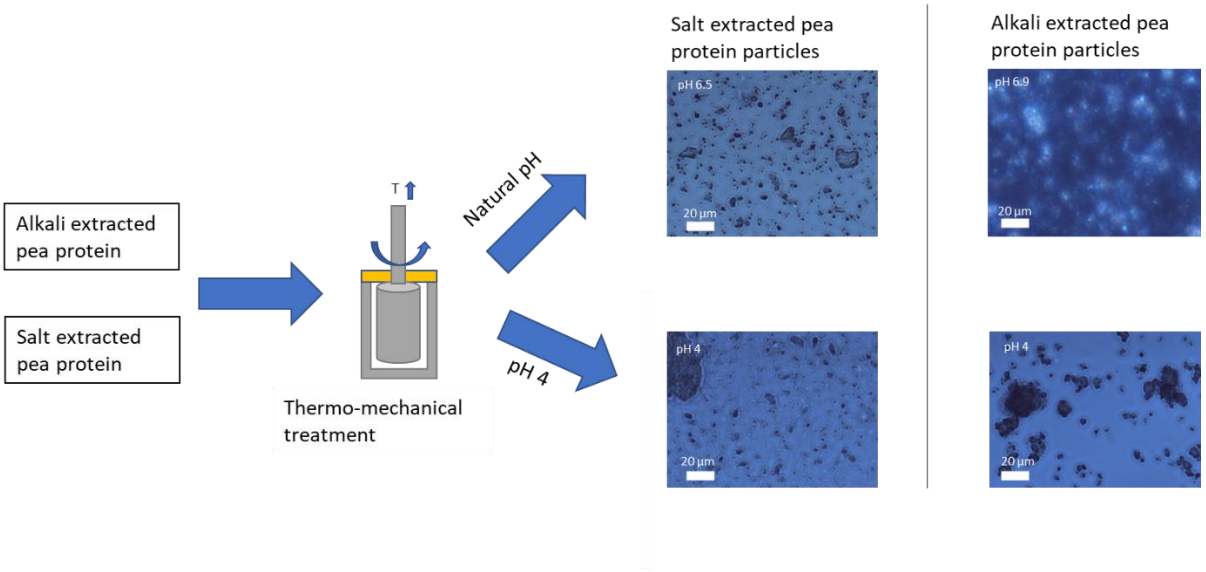

Highlights

- Alkali extracted and salt extracted pea protein was compared head-to-head with each other upon thermo-mechanical treatment
- Thermo-mechanical treatment led to dense particles for salt extraction and porous, transparent particles for alkali extraction
- A shift to pH 4 led to larger and denser particles
- Particle structure is most likely influenced by extraction and structural changes resulting from it

Abstract

Two methods to extract pea protein from pea flour, alkali extraction – isoelectric precipitation and salt extraction – dialysis, were compared regarding the functional behaviour of the resulting protein isolates upon thermo-mechanically induced aggregation to obtain microparticulates. In addition, the effects of pH and temperature during thermo-mechanical treatment were investigated. The resulting particles were analysed for size and morphology. Particles between 1 and 30 µm were formed. The biggest effect on

[9] Adaption refer to formatting issues: e.g., abbreviations, figure, table, equation and section numbering, citation style, notation of units, spelling, axis labeling. References of all chapters are merged at the end to avoid redundancies.

[10] Originally published in: Food Hydrocolloids (2022), Vol. 127, 107514. Permission for reuse of this article was granted by Elsevier.

the size and structure of the particle was the extraction method, followed by a variation of pH during heat treatment. Particles generated from pea protein obtained by salt extraction – dialysis were smaller and denser than particles produced from protein material obtained from alkali extraction – isoelectric precipitation. pH 4 during thermo-mechanical treatment resulted in larger and denser particles compared to particles at natural pH. Temperature variation between 88°C and 98°C had a minor influence. This study can serve as a base for further research on the thermal behaviour of pea protein and can help to manipulate aggregate structure for incorporation in novel innovative (vegan) food concepts.

3.5.1 Introduction

With the increasing problem of feeding the world with protein, pea proteins are gaining interest in food technology. However, commercial pea protein was found to be low in solubility and techno-functionality (Shand et al. 2007; Fuhrmeister and Meuser 2003), which results from destructive, untargeted processing stress during downstream processing. In order to analyse the functionalities of native pea protein, pea protein is extracted from pea flour with much lower processing stress on a laboratory scale.

Two dedicated laboratory extraction methods are currently mostly used for the production of pea protein with a high degree of nativity: Alkali extraction – isoelectric precipitation (in short referred to as `alkali extraction´ in the following) and salt extraction – dialysis / micellar precipitation (below referred to as `salt extraction´ method). During alkali extraction, the protein is solubilized at alkaline pH and then precipitated at its isoelectric point of pH 4.5. Before freeze-drying, the pH of the precipitated protein is set back to pH 7 (Mession et al. 2012). During salt extraction, the protein is solubilized at a high salt concentration and then precipitated by decreasing the salt content in the solution. Before freeze-drying, the solution is dialysed to remove the salt (Sun and Arntfield 2010). Even though both extraction methods by themselves were optimized in the above-mentioned studies and the obtained proteins were superior in solubility and techno-functionality compared to commercial pea protein, they were found to differ significantly in their protein composition and characteristics. This can partly be explained by the different cultivars used. In order to eliminate this aspect as a potential variable, Tanger et al. (2020) performed a comparative assessment of protein products from both extraction methods. This work reported that while the protein concentration in the resulting protein powder of both extraction methods was similar at 75%, the yield of protein during extraction was significantly lower for salt extraction compared to alkali extraction. Next to this, salt extracted protein powder contained 75% legumin and only minor amounts of vicilin and convicilin, whereas alkali extracted protein powder contains only 50% legumin and 30% vicilin and 20% convicilin (Tanger et al. 2020). Differences in protein profile were also seen back in different amino acid compositions of the extracted protein (Stone et al. 2015). Legumin is the most hydrophobic protein of the globulins (Gueguen 1989). These differences should affect the functionalities of the differently extracted proteins. In contrast to alkali extracted pea protein, salt extracted pea protein is poorly soluble at low salt concentration beneath 0.3 M NaCl at pH 7. The isoelectric point of the alkali extracted pea protein was found between pH 4 and

pH 4.5 and for salt extracted pea protein at pH 5 (Tanger et al. 2020). The higher legumin content in salt extracted pea protein resulted in a higher denaturation temperature compared to alkali extracted pea protein (Stone et al. 2015). The enthalpy change was determined as the area underneath the endothermic denaturation reaction curve during mDSC measurement. This was used for characterising the degree of nativity. In order to eliminate the different pH levels of the protein from the alkali and the salt extraction methods, Tanger et al. (2020) adapted the pH to the same level to assess the protein characteristics under the same conditions. However, despite the exclusion of pH differences as a potential reason for the different behaviour, a lower enthalpy change was found for alkali extracted pea protein indicating a lower amount of “native” proteins compared to salt extracted pea protein (Tanger et al. 2020). In other words, certain structural modifications of the pea protein remain from the conditions of the different extraction methods, even if the mildest conditions per respective method are applied.

Therefore, the extraction method has a significant influence on the functional behaviour of the resulting protein (Tanger et al. 2020; Stone et al. 2015), which is expected to also influence thermal and thermo-mechanical treatment. A high amount of convicilin was found to lead to transparent gels because this pea protein fraction contained a highly negatively charged N-terminal extension, which hinders gelation due to repulsive forces (O'Kane et al. 2004b). However, this study only focused on the vicilin and convicilin fractions. Limited to alkali extraction Kornet et al. (2021b) found that a limited fractionation without a precipitation step led to firmer gels with a more homogenous gel network structure. Yang et al. (2021) compared gel strength and structure of pea proteins extracted by different extraction methods and found that a more homogenous protein profile led to a uniform gel structure. This study was limited to analysis at pH 7 and the absence of a shear rate. It remains open, whether this knowledge can be transferred to a thermo-mechanical treatment. One such thermo-mechanical process is the microparticulation process, which results in aggregates in the size range of microns. The effect of an additional shear rate on a thermal process was extensively studied for whey proteins and was found to inhibit gel formation and control particle size (Wolz et al. 2016b). Such particles can be used as fat replacers in food (Kew et al. 2020) and can be analysed by common known methods. The purpose of this study, was to perform a comparison of aggregates obtained by the same thermo-mechanical treatment of alkali extracted and salt extracted pea protein from the same pea flour. The hypothesis was that the functional behaviour of the protein mixes from the alkali extraction and salt extraction methods should be different, due to their differences in protein profile and functionalities due to enduring effects of the extraction conditions. These might affect type and intensity of protein interactions within the produced aggregates, which then result in different aggregates sizes and structures. Due to the higher amount of legumin in salt extracted pea protein compared to alkali extracted pea protein, salt extracted pea protein would be hypothesized to rather react via covalent and hydrophobic interactions leading to denser particles. Alkali extracted pea protein would be hypothesized to rather react via hydrophobic and electrostatic interaction leading to smaller loosely bound particles.

3.5.2 Materials and methods

3.5.2.1 Materials

Pea flour was provided by Emsland Stärke (Emlichheim, Germany). The starting material contained 18.27% protein on a dry basis. For all extractions and analyses demineralized water (MilliQ Integral 3, Merck, Darmstadt, Germany) was used. All other materials and chemicals were purchased from regular suppliers and were of analytical grade.

3.5.2.2 Extraction of pea proteins

As briefly mentioned above, for the sake of better readability, the `salt extraction – dialysis and micellar precipitation´-method in the following is referred to as `salt extraction´. `Alkali extraction – isoelectric precipitation´ is shortened to alkali extraction. Two differently extracted pea protein concentrates were compared to each other, one was generated via alkali extraction as described in Tanger et al. (2020) and the other via salt extraction as described in Tanger et al. (2022). Both protein concentrates only contained globulins. Alkali extracted pea protein concentrate contained 51% legumin (Tanger et al. 2020) and salt extracted pea protein concentrate contained 63% legumin (Tanger et al. 2022) determined by SDS-PAGE. Before thermo-mechanical treatment, the protein powder was dissolved to a 10% protein solution in water. The original pH of this protein solution was pH 6.5 for salt extraction and 6.9 for alkali extraction after overnight stirring. This pH value is called natural pH in the following and was not changed to compare the extraction methods without changing the ion composition. For analysis of the influence of pH, the pH was set to pH 4 using 1 M HCl. After this, the solutions were stirred overnight at 4°C.

3.5.2.3 Determination of denaturation temperature

The denaturation temperature (T_d) of the two protein solutions at natural pH and pH 4 were analysed using modulated dynamic scanning calorimetry (DSC Q1000, TA Instruments, New Castle, USA) as described in Tanger et al. (2020). In short, the DSC was calibrated using indium and a sapphire. Twenty microliters of the samples were pipetted in an aluminium pan, which was hermetically sealed. An empty pan served as a reference. The pans were heated with a heating ramp of 2 K/min and modulation amplitude of ± 0.5°C every 60 s from 25°C to 120°C. The resulting thermograms were analysed using TRIOS software (Version: 5.1.1.46572; TA Instruments, New Castle, USA). Peak maximum represented the denaturation temperature and peak area of the enthalpy change. T_{onset} represents the temperature, where the denaturation reaction starts.

3.5.2.4 Thermo-mechanical treatment

Thermo-mechanical treatment was conducted in a rheometer MCR 302 (Anton Paar, Graz, Austria) equipped with a Mooney-Ewart ME21 measuring device (cup diameter: 22.93 mm, bob diameter: 21.01 mm, angle: 4°, AntonPaar, Graz, Austria) as described elsewhere (Tanger et al. 2021b). In short, 4 ml of the sample were placed between bob and cup. The cup was covered with a wet sponge to minimize evaporation during treatment. Samples were pre-sheared at 100 s^{-1} at 25°C for 10 s. Then, the sample was heated within 15 min from 25°C to 88°C or 98°C with a varying shear rate between 100

s^{-1} and 1500 s^{-1}. The temperatures 88°C and 98°C were chosen to ensure a high degree of aggregation after treatment and minimizing concentration of the sample by water evaporation. The temperature was held for 10 min while shearing and afterwards cooled down to 25°C while shearing. The last step was a viscosity measurement at 100 s^{-1} for 30 s at 25°C. After processing the samples were poured into a plastic container with a screw cap and stored at 4°C until analysis. For clear separation between particles generated by the thermo-mechanical treatment and aggregates formed during extraction the particles generated by the thermo-mechanical treatment of salt extracted pea protein are called ‘SE-P’ and of alkali extracted pea protein ‘AE-P’

3.5.2.5 Zeta potential

The charge of the starting protein solution at natural pH and pH 4 and the charge of the processed samples were analysed. For this, the solutions were dissolved to a 1% solution and measured with a ZetaSizer Nano ZS 2000S (Malvern Panalytical Ltd, Malvern, UK). Before the start of the measurement, samples were equilibrated at 20°C for 2 min. Each measurement comprised 3 runs with 1 – 100 required sub runs, which is part of the automated measuring routine of the method. Zetasizer Software 7.13 (Malvern Panalytical Ltd, Malvern, UK) was used to convert electrophoretic mobility to the zeta potential.

3.5.2.6 Particle size analysis

For particle size analysis the processed samples were diluted to a 1% protein solution with water to avoid multiple scattering events and analyzed with a Malvern Mastersizer Hydro 2000S (Malvern Panalytical Ltd, Malvern, UK). For calculation of the particle size an optical model (Mie theory), a refractive index of 1.45 for the dispersed phase, a refractive index of 1.33 for the dispersant medium, and an absorbance of 0.001 for the protein dispersion was used (McCarthy et al. 2016). The volume basedparticle size distribution (q_3) and $d_{50,3}$ are shown. The $d_{50,3}$ gives the particle size, where 50% of the particles are smaller and 50% of the particles are bigger.

3.5.2.7 Morphology

In order to analyze the shape of the particles, they were visually inspected using an optical microscope (Axioskop, Carl Zeiss AG, Jena, Germany). The processed samples were diluted with water to a 1% protein solution or lower and inspected. Pictures were taken with a camera and analyzed using Motic Image Plus 3.0 (Motic, Barcelona, Spain)

3.5.2.8 Statistical analysis

Each thermo-mechanical treatment was performed at least twice from two different protein solutions from two different extractions. Analysis of the samples was conducted in at least duplicate. A one-way analysis of variance (ANOVA) for significant differences between the extraction types and pH value of the solution was conducted with JMP Pro (SAS Institute Inc., Cary, USA / Version 14). Minimum significance was set to 5% ($p < 0.05$) and the ANOVA was followed by a Tukey-Kramer HSD test. Graphs were plotted using OriginPro 2019 (originLab Corporation, Northhampton, USA).

3.5.3 Results and discussion

3.5.3.1 Determination of denaturation temperature by differential scanning thermal analysis (DSC)

In order to analyse the thermal stability of the two different protein powders at natural and acidic pH, mDSC measurement was performed. Denaturation temperature (T_d), T_{onset}, and the enthalpy change of the four different samples are shown in Table 3-7.

Table 3-7: Tonset, denaturation temperature (T_d), and enthalpy change (ΔH) for 10% protein solution of alkali extraction and salt extraction at natural pH and pH 4.

	pH	T_{onset} (°C)	T_d (°C)	ΔH
Alkali extraction	natural	$69.8^{a} \pm 0.2$	$79.1^{b} \pm 0.2$	$1.9^{a} \pm 0.3$
Alkali extraction	4	$70.2^{a, b} \pm 0.0$	$79.0^{b} \pm 0.4$	$1.0^{a} \pm 0.1$
Salt extraction	natural	$73.5^{a, b} \pm 0.8$	$82.4^{b} \pm 0.0$	$2.9^{a} \pm 0.9$
Salt extraction	4	$66.4^{b} \pm 2.0$	$78.1^{b} \pm 0.7$	1.5^{a}

$^{a-b}$ Column values followed by the same letter are not significantly different ($p < 0.05$)
*Means ± SD of duplicate

The denaturation temperature varied from 78.1°C for salt extracted protein at pH 4 to 82.4°C at the natural pH, which can be explained by conformational changes of the protein with changes in pH-level. For alkali extraction, no significant change was found for pH 4 and the natural pH. The higher denaturation temperature of salt extraction compared to alkali extraction at natural pH can be explained by a higher legumin to vicilin ratio of salt extraction. Vicilin trimers are lower in conformational compactness and therefore easier to unfold than legumin (Tanger et al. 2020; Marcone et al. 1998; Mession et al. 2012). Sun and Arntfield (2010) found slightly higher denaturation temperatures of 86.21°C for salt extracted pea protein at pH 7. Mession et al. (2013) found higher values for alkali extracted pea protein of 87.4°C at pH 7. The higher denaturation temperatures found by these latter two works can be explained by the higher heating ramp of 10 K/min and usage of an unmodulated DSC system. The enthalpy change was always higher for salt extraction compared to alkali extraction indicating a higher amount of native protein at both pH levels. The drop in enthalpy change from natural pH to pH 4 can be explained by pre-denaturation during hydration overnight by the acid and conformational changes in protein structure and colloidal behaviour near the isoelectric point (Sun and Arntfield 2011).

3.5.3.2 Zeta potential of proteins in the starting solutions

To determine the repulsive and attractive forces between the proteins in solution the zeta potential of the starting solutions was measured. The measured charge of the proteins is depicted in Table 3-8.

Table 3-8: Zeta potential of pea proteins in the starting solutions at natural pH and pH 4.

	pH	Zeta potential (mV)
Alkali extraction	natural	-30.4 ± 2.3[a]
Alkali extraction	4	10.3 ± 1.3[b]
Salt extraction	natural	-10.2 ± 1.2[c]
Salt extraction	4	20.1 ± 3.8[d]

[a-d] Columns values with same letter indicate no significant difference ($p < 0.05$)
*Means ± SD of duplicates

All starting solutions showed a significant difference in zeta potential. Starting solutions at natural pH were negatively and at pH 4 positively charged. The isoelectric point for alkali extraction was found to be between pH 4 and pH 4.5 and for salt extraction around pH 5 (Tanger et al. 2020). At the natural pH, the charge and therefore repulsive forces between proteins were higher for alkali extracted protein than for the salt extracted counterpart. At pH 4, charge and repulsive forces are higher for salt extracted protein compared to alkali extraction.

3.5.3.3 Viscosity of microparticulated samples

Immediately after cooling down of the thermo-mechanical treated sample, the viscosity was measured at 100 s^{-1}. The results gave first hints about the particles built during treatment and are shown in Figure 3-35.

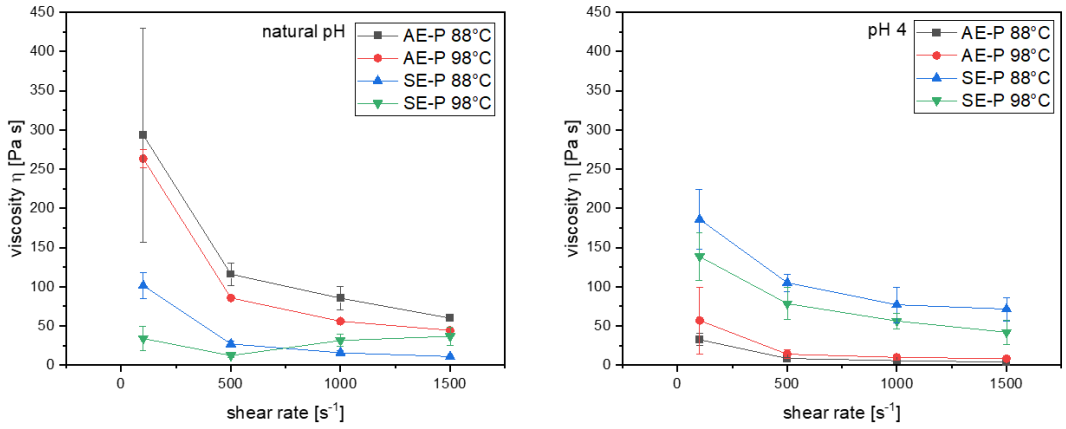

Figure 3-35: Measured viscosity after thermo-mechanical treatment at 100 s^{-1} for all analysed samples.

A higher shear rate during thermo-mechanical treatment led to a lower viscosity after treatment. At natural pH, AE-P were higher in viscosity than SE-P and at pH 4 vice versa indicating differences in particle structure and interactions. The pH drop to pH 4 resulted in a decrease in viscosity for AE-P and an increase in viscosity for SE-P. A higher viscosity indicates stronger interactions between the particles. Therefore, lower viscosity indicates stronger interactions within the particles. A lower viscosity also stands for more round particles, which do not get entangled (Brighenti et al. 2020). Therefore, these results indicate that a higher shear rate during thermo-mechanical treatment decreased interactions between the particles inhibiting gel network formation

(Wolz et al. 2016b). In addition, the results indicate that SE-P are more round particles compared to AE-P at natural pH. The same applies to the pH drop to pH 4 for AE-P. AE-P particles at pH 4 are expected to be more round than at natural pH according to the viscosity results.

3.5.3.4 Microparticulation at natural pH

An important characteristic for particulation is the resulting particle size, which was measured using laser diffraction. The q_3 particle size distribution is shown in Figure 3-36 for particles formed at natural pH at 88°C and 98°C at varying shear rates for both extraction methods.

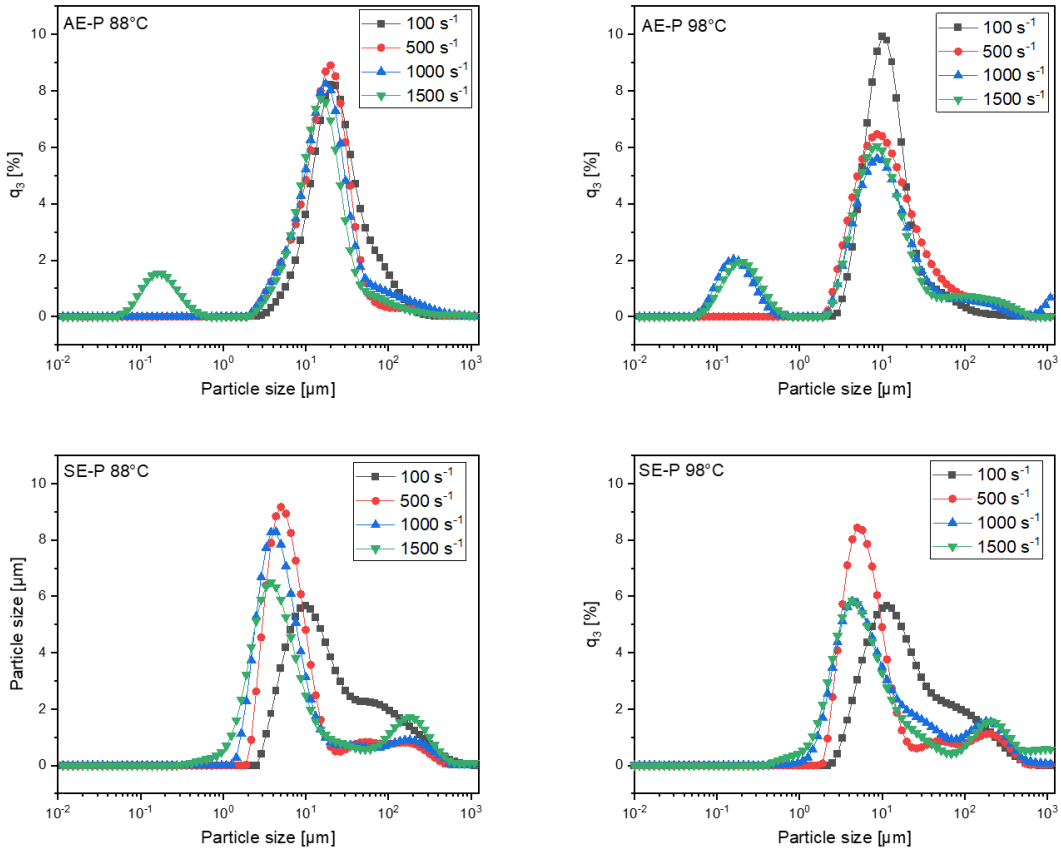

Figure 3-36:Particle size distribution of particles formed during treatment at 88°C and 98°C at shear rates varying from 100 s^{-1} to 1500 s^{-1} for AE-P and SE-P.

For a better overview, the $d_{50,3}$ of the resulting particles is also shown in Table 3-9. From Figure 3-36, it can be seen that the treatments result in different particle size distributions for the two extractions and that the microparticulation temperature had a different effect. $D_{50,3}$ varied from 5 - 24 µm. The particle size distribution showed a multimodal size distribution for all samples. $D_{50,3}$ was higher for AE-P compared to SE-P. Alkali extracted pea protein had a higher charge at natural pH with -30 mV than salt extracted pea protein with -10 mV (Table 3-8). The higher $D_{50,3}$ of AE-P compared to SE-P would, therefore, contradict the common knowledge that lower repulsive forces in the starting material lead to larger aggregates.

Table 3-9: D50,3 of particle formed during thermo-mechanical treatment at 88°C and 98°C at varying shear rates from 100 s^{-1} to 1500 s^{-1} for AE-P and SE-P.

Shear rate (s^{-1})	$d_{50,3}$ (µm)			
	AE-P 88°C	AE-P 98°C	SE-P 88°C	SE-P 98°C
100	24.3 ± 6.3^{a}	$10.4 \pm 0.6^{d,e,f}$	16.7 ± 6.3^{b}	$15.8 \pm 1.4^{b,c}$
500	$15.7 \pm 3.3^{b,c}$	$10.8 \pm 2.7^{c,d,e}$	$5.8 \pm 0.3^{e,f,g}$	$7.0 \pm 2.1^{d,e,f,g}$
1000	$15.8 \pm 1.2^{b.c}$	$8.6 \pm 3.7^{d,e,f,g}$	5.0 ± 0.6^{g}	$7.5 \pm 1.1^{d,e,f,g}$
1500	$11.4 \pm 3.6^{c,d}$	$7.4 \pm 3.2^{d,e,f,g}$	$5.3 \pm 1.2^{f,g}$	$6.8 \pm 2.1^{d,e,f,g}$

$^{a-g}$ Columns values with the same letter indicate no significant difference ($p < 0.05$)
*Means ± SD of duplicates

In SE-P a minor amount of large particles above 100 µm was found. Since salt extracted pea protein had a low charge at natural pH, the formation of these large particles during thermo-mechanical treatment can be explained by the lower repulsive forces between the proteins. The differences is particle size between low shear rates of 100 s^{-1} and 500 s^{-1} was bigger than between the higher shear rates of 500 s^{-1} to 1500 s^{-1}. Thus, indicating that structure building forces as aggregation and structure destroying forces as mechanical forces are in equilibrium at these shear rates during thermo-mechanical treatment. AE-P contained a minor amount of small particles below 1 µm at high shear rates above 1000 s^{-1}. Increased shear stress was found to break loosely bound aggregates in smaller aggregates (Wolz et al. 2016b; Vilotte et al. 2021). This showed that the SE-P were more stable against shear stress than the AE-P at high shear rates. For whey protein microparticles it has been found that similar to SE-P a plateau of particle size was reached at shear rates between 500 s^{-1} and 1500 s^{-1} and high resistance against shear stress at high shear rates with the same thermo-mechanical treatment (Tanger et al. 2021b). In contrast to the non-covalent bound pea protein microparticles, whey protein microparticles were found to be bound together by mostly disulphide bonds (Tanger et al. 2021b). With increasing temperature, the intensity of disulphide bonds and hydrophobic interaction was found to increase (van Dijk et al. 2015), whereas electrostatic interactions decrease in intensity (Bowland et al. 1995). Even though hydrophobic interactions are non-covalent, they can be very strong with 50 – 100 kj/mol (Nakai and Li-Chan 1988) and therefore, a SE-P particle held together by hydrophobic interaction can also appear similar in shear stability as a covalently cross-linked whey protein particle for the analysed shear rates. A difference in covalently cross-linked whey protein particles and hydrophobic cross-linked SE-P might be seen at extremely high shear rates outside the area analysed in this research. The lower shear stability of AE-P indicates a loosely bound particle structure and weaker protein interactions holding the particle together for example electrostatic interactions compared to SE-P. Microscopic pictures of the aggregates produced gave more information about the aggregates formed.

The pictures of the particles formed at 1000 s^{-1} at 88°C and 98°C for alkali extraction and salt extraction at natural pH are shown in Figure 3-37.

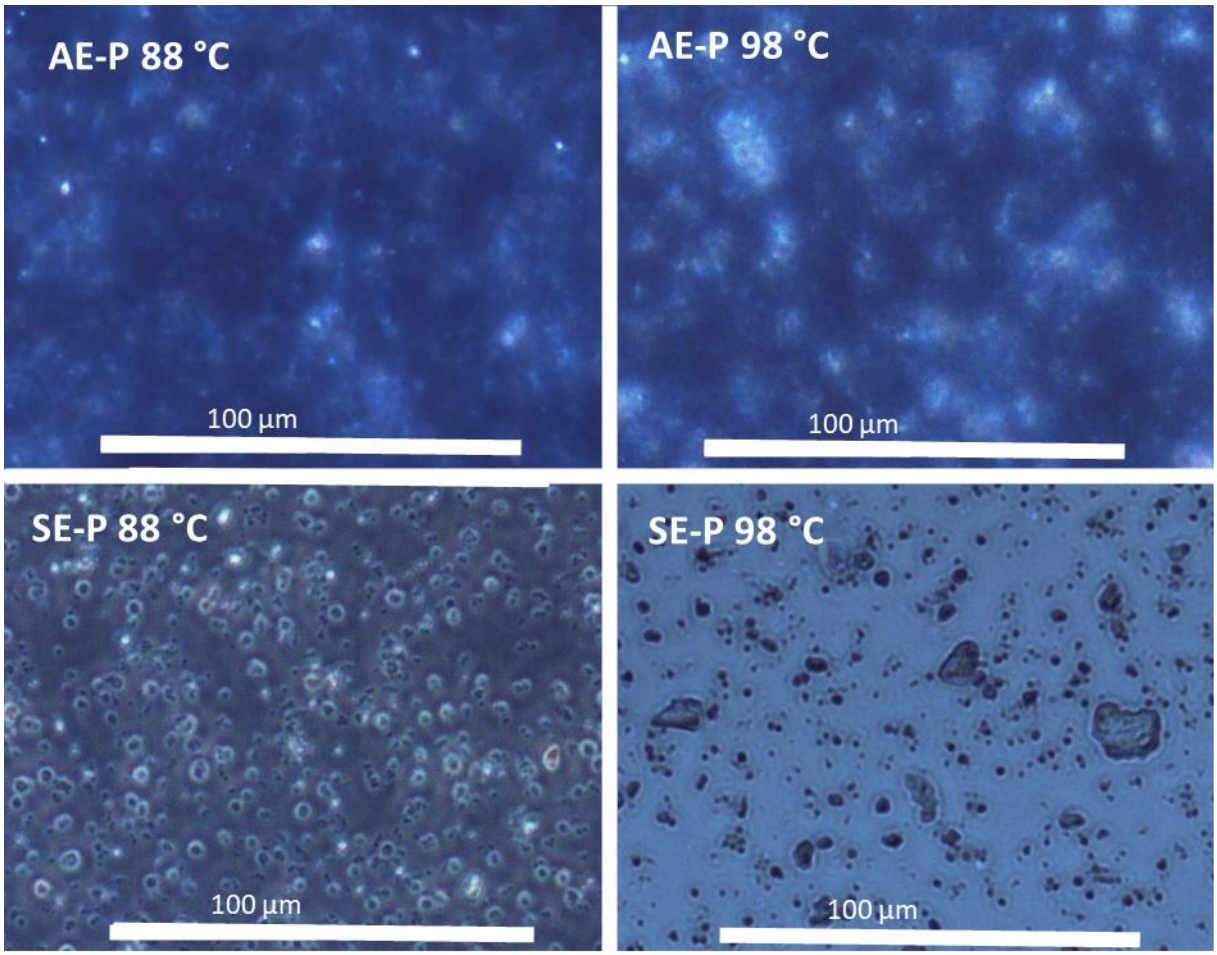

Figure 3-37: Light microscope images of AE-Pat 88°C and 98°C and SE-Pat 88°C and 98°C. All particles were produced at a shear rate of 1000 s^{-1}.

From the microscopic images, it can be seen that the particles have different structures. AE-P are more transparent compared to SE-P, where the edges are less round-shaped. The transparent and porous appearance of AE-P indicates that the structure of the particles is more open or loose, which would also explain why AE-P are less shear stable than SE-P. SE-P appear to have a dense structure with clear edges. Also, some big particles are visible within a crowd of small particles. The shape of SE-P are spherical. The particle structure suggests a better protein-protein interaction in SE-P than AE-P. This phenomenon can be explained by the high legumin content of the salt extracted protein and the higher nativity. Legumin, in contrast to the other globulins vicilin and convicilin, is a sulphur-containing protein (Mession et al. 2015; O'Kane et al. 2005). Thus, legumin can react via disulphide bond formation and non-covalent bonds, whereas vicilin and convicilin can only aggregate via non-covalent interaction. Covalently bound particles can be denser in structure than non-covalently bound particles. Homogenous protein composition was also found to lead to gels, which are densely interconnected leading to high mechanical strength (Yang et al. 2021). Another factor is the assumed lower degree of the nativity of alkali extracted pea protein. Alkali extracted pea protein was found to have a loose conformation with exposed interior structure compared to pea proteins extracted by other extraction methods. This conformation

and the exposed interior structure can lead to rapid aggregation upon thermal treatment. This rapid aggregation upon thermal treatment, however, can inhibit complete unfolding due to steric hindrance (Yang et al. 2021) The incomplete unfolding and rapid aggregation of AE-P could explain the porous and loosely bound particles with a transparent appearance of AE-P.

Another explanation for the difference in particle structure between AE-P and SE-P is the low solubility of salt extracted pea protein between pH 6 and 7 at low salt concentrations in comparison with high solubility of alkali extracted pea protein at pH 7 at low salt concentrations (Tanger et al. 2020). The low solubility is explained by reversible micelle formation with a hydrophobic core at low salt concentrations. With increasing solubility, the gel strength was found to decrease and protein-protein interaction shifted from hydrophobic interactions to electrostatic interactions upon thermal treatment (Tanger et al. 2022). Combining this information with the worm-like transparent appearance of AE-P and the dense structure of SE-P, we would suggest that in AE-P electrostatic interactions are dominant and in SE-P, covalent and hydrophobic interactions are dominant at natural pH due to the difference in solubility and protein profile.

3.5.3.5 Microparticulation at pH 4

pH 4 is much closer to the isoelectric point of pea proteins at pH 4 – 4.5 for alkali extracted pea protein and pH 5 for salt extracted pea protein. Therefore, acidic conditions are expected to accelerate thermally induced aggregation. The resulting particles sizes at shear rate 1000 s^{-1} are shown as an example at natural pH and pH 4 in Figure 3-38.

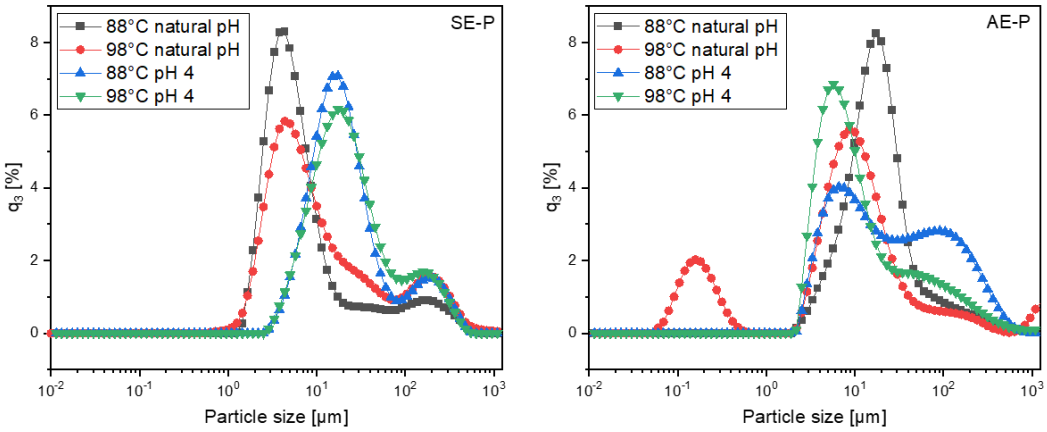

Figure 3-38: Particles size distribution of AE-P and SE-P at natural pH and pH 4 at 88°C and 98°C at a shear rate of 1000 s^{-1}.

In order to get a better overview of the particles size, the $d_{50,3}$ is shown in Table 3-10. For both extraction types, the particles became bigger with pH shifting towards acidic pH, which can be explained by the closeness of the isoelectric point and reduced protein charge for alkali extracted pea protein. AE-P also did not show a small number of small particles below 1 µm at high shear rates as was the case at natural pH. Thus, the particles became more shear stable at pH 4.

Table 3-10: $D_{50,3}$ of particle formed during thermo-mechanical treatment at 88°C and 98°C and pH 4 and natural pH at shear 1000 s^{-1} for AE-P and SE-P.

	$d_{50,3}$ (µm)			
pH	AE-P88°C	AE-P98°C	SE-P88°C	SE-P98°C
4	27.4 ± 18.7^{a}	10.6 ± 6.7^{a,b,c}	18.2 ± 4.6^{a,b,c}	19.9 ± 1.9^{a,b}
Natural pH	15.8 ± 1.2^{b,c,d}	8.6 ± 3.7^{c,d}	5.0 ± 0.6^{d}	7.5 ± 1.1^{c,d}

$^{a-d}$ Columns values with same letter indicate no significant difference ($p < 0.05$)
*Means ± SD of duplicates

The charge, however, cannot explain the increase in particle size for salt extraction because with a charge of 20 mV the repulsive forces are bigger than at natural pH with a charge of -10 mV. However, an increase in particle size with decreasing pH has also been found for commercial pea protein (Bogahawaththa et al. 2019). Thus, also other factors as for example structural changes of the protein due to pH change must explain the increase in particle size.

Similar to natural pH, microscopic images have been taken from the particles at pH 4. The images are shown in Figure 3-39.

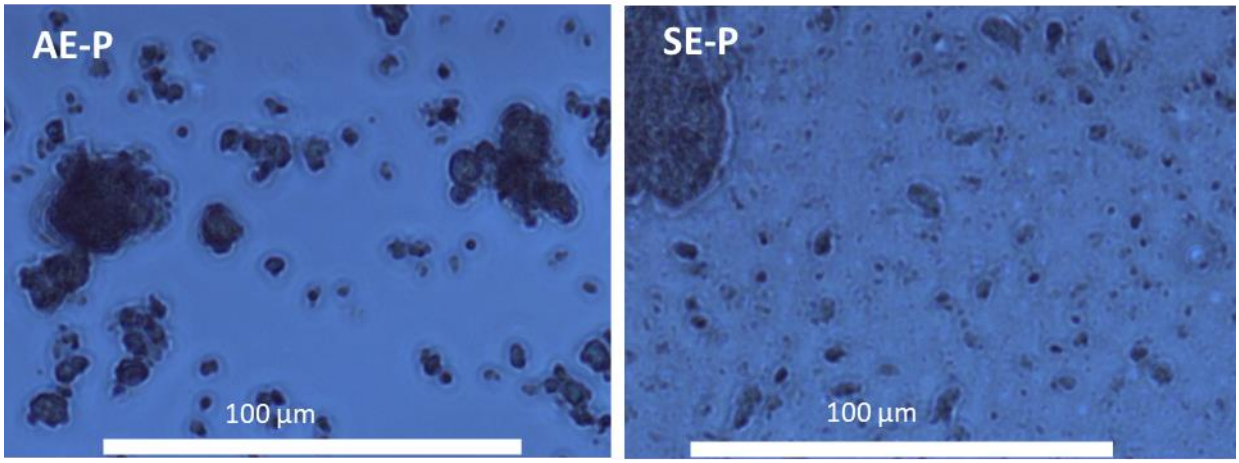

Figure 3-39: Light microscope images AE-P and SE-P at 88°C at pH 4 and a shear rate of 1000 s^{-1}.

From the pictures, it can be seen that even though the pH is the same, the particles have a different appearance. AE-P are very compact and dense with sharp edges and are spherical. They differ significantly from the particles at natural pH. SE-P are also round in shape and have sharp edges. However, they are slightly more transparent than at natural pH. Similiar to our findings, for β-lactoglobulin it has been found that the pH has a major influence on the structure of the thermally produced aggregates. Around the isoelectric point, aggregates are spherical and dense and at pH 7 they form small worm-like aggregates (Jung et al. 2008), which resulted from the dominating bond type between the protein, which is dependent on the pH (Zúñiga et al. 2010). Since the particle size for both extraction methods increase it can be assumed that non-covalent protein-protein interaction increase in intensity with decreasing pH. Since the particles get more shear stable and become compacter and denser in structure, this is likely due to increased hydrophobic interactions. As already described above,

hydrophobic interactions lead to more shear stable particles due to the high strength of hydrophobic interactions and increase of them with increasing temperature. The shift to more hydrophobic interactions upon thermo-mechanical treatment might be explained by the low solubility of both extracted pea protein and the change in protein conformation due to pH change (Tanger et al. 2020).

3.5.4 Conclusion

In this research, the effects of extraction method, pH, shear rate, and temperature on microparticulation of pea protein were analysed. The biggest impact of the above named parametes were extraction type and pH concerning particle size and structure. This study shows that there are differences in morphology of AE-P and SE-P. The extraction method was shown to have a significant effect on the thermal aggregation kinetics of pea proteins concerning their particle size, and structure. Two pH values, four different shear rates and two different temperatures were tested. At natural pH, AE-P are worm-like and transparent, whereas the SE-P are dense and spherical. With the decrease in pH AE-P became bigger and denser. SE-P became more uniform in size and overall bigger. The particle structure is most likely influenced by the different protein profiles, solubility, and the number of native proteins, which is likely to influence protein-protein interaction during thermo-mechanical treatment. SE-P are suggested to be covalently and hydrophobically cross-linked at natural pH and pH 4. AE-P are suggested to be cross-linked via electrostatic interactions at natural pH and via hydrophobic interactions at pH 4. This knowledge can be used to produce aggregates for different kinds of applications in structuring food gels, foams or emulsions. Based on the findings reported here, it would be beneficial to study the reaction kinetics and aggregation mechanisms at a broader range of thermal conditions, pH and ionic strengths.

Acknowledgements

We would like to thank Thomas Pruter and Stephanie Schomaker from Emsland Stärke, Emlichheim, Germany, for providing the pea flour. Priska Pröll and David Andlinger are thanked for the valuable discussion and Michaela Müller is thanked for support in the laboratory.

This project was executed as part of an Industrial Collective Research (IGF) project of the Forschungskreis der Ernährungsindustrie e.V., Bonn (FEI) supported by the German Ministry of Economics and Technology via AiF (AiF 20197N).

Compliance with ethical standards

This article does not contain any studies with human or animal subjects performed by any of the authors.

Conflict of interest

The authors declare that they have no conflict of interest.

3.6 Pea protein microparticulation using extrusion cooking: Influence of extrusion parameters and drying on microparticle characteristics and sensory by application in a model milk dessert

Summary and contribution of the doctoral candidate

Currently, there is a wide knowledge about microparticulation using extrusion cooking for whey protein. Extrusion cooking for pea proteins is currently limited to expanded snacks and meat analogues. In contrast to whey protein, commercial pea protein is denatured and aggregated. Therefore, pea protein microparticulation is a top-down process, where big particles get reduced in size. This research shows a method for pea protein microparticulation for fat-replacement using extrusion cooking. To achieve a suitable particle size of 1 – 20 µm for fat replacement, extrusion cooking parameters were varied. Protein concentration was set to 20% because higher protein concentrations were not feasible. High extruder barrel temperatures above 100°C were found to increase microparticle particle size possibly due to increased intensity in hydrophobic interaction between the proteins. Extruder barrel temperature did not affect the type of protein-protein interaction similar to a change in screw speed. Screw speeds above 200 rpm were found to not affect particle size. Most suitable particle sizes were found at a powder mass flow of 4 kg h^{-1}. Higher or lower mass flows led to bigger particles and/or uncontinuous product flow through the extruder. Most suitable particle characteristics were found at a powder mass flow of 4 kg h^{-1}, a screw speed of 600 rpm, and an extrusion barrel temperature of 100°C with a $d_{50,3}$ of 15.31 µm. These particles were produced in a big batch. The produced fresh microparticles were compared in size with the same microparticles spray-dried and freeze-dried. Drying did not affect particle size negatively. Dried microparticles resulted in a powder, whereas fresh microparticles were a peanut butter-like mass. For further analysis, dried microparticles were rehydrated. The three microparticle samples were compared with each other on suitability as a fat-replacer in a model milk dessert. For this, a full-fat milk dessert was developed. In the fat-reduced milk desserts, 50% of the fat was replaced by one of the microparticle samples. The milk desserts were compared sensorically with each other. The attributes creamy and grassy/beany were of the highest interest. Even though 50% of the fat was replaced the fat-reduced milk desserts were not significantly different to the full-fat reference. Therefore, all three microparticle samples were assumed to be suitable as a fat-replacer. Due to the incorporation of pea protein, the grassy/beany aroma increased in the fat-reduced milk desserts compared to the full-fat reference. However, both dried microparticle samples showed a lower grassy/beany aroma. Sensory data showed that drying was beneficial for the aroma of the fat-reduced milk dessert.

The doctoral candidate substantially contributed to this manuscript by conceptualization and designing the experiments. Statistical data analysis and interpretation of the results were carried out by the doctoral candidate. The doctoral candidate wrote the original draft and included the reviewer's comments. Co-authors contributed to the experimental part and/or discussion of the results. They also provided input on the drafted publication before submission and helped answer the reviewer's comments.

Adapted original manuscript[11]

Pea protein microparticulation using extrusion cooking: Influence of extrusion parameters and drying on microparticle characteristics and sensory by application in a model milk dessert[12]

Caren Tanger*[a], Florian Schmidt[a], Florian Utz[b], Johanna Kreissl[c], Corinna Dawid[b], Ulrich Kulozik[a]

[a]Chair for Food and Bioprocess Engineering TUM School of Life Sciences, Technical University of Munich, Weihenstephaner Berg 1, Freising-Weihenstephan, Germany

[b]Chair of Food Chemistry and Molecular Sensory, TUM School of Life Sciences, Technical University of Munich, Lise-Meitner-Straße 34, Freising-Weihenstephan, Germany

[c]Leibniz-Institute for Food Systems Biology at the Technical University of Munich, Lise-Meitner-Straße 34, Freising-Weihenstephan, Germany

Highlights

- Extrusion cooking can be used to produced pea protein microparticles
- Particle size can be controlled by extruder barrel temperature, screw speed and mass flow
- Drying of extruded particles has no negative effect on the size
- Drying reduced grassy/beany off-flavour
- The produced microparticles can be used to inhibit a decreased creaminess in fat-reduced food

Abstract

Microparticulated proteins are potential fat replacers to reduce the caloric value of foods. In contrast to whey protein, knowledge on the formation of microparticles based on pea protein using extrusion cooking is limited. This research aimed at evaluating the impact of extrusion parameters and subsequent effects of spray- and freeze-drying on the physico-chemical and sensorical characteristics of the resulting `functionalized´ pea protein microparticles. A method for pea protein microparticulation is presented. Extrusion parameters could be varied such that particles suitable for fat replacement in terms of size range were formed. Particle size was mainly dependent on extrusion temperature and residence time. The screw speed was of negligible influence. Post-extrusion spray- or freeze-drying did not affect the particle size. To assess the aggregation mechanism of particulation, the stabilizing forces were investigated by applying a protein interaction assay. It was found that pea protein microparticles were mainly stabilized by hydrophobic interactions. The ability of functionalized pea proteins to replace fat while maintaining authentic dairy flavour was tested sensorically in a model milk dessert. The incorporation of microparticles in a fat-reduced milk dessert resulted

[11] Adaption refer to formatting issues: e.g., abbreviations, figure, table, equation and section numbering, citation style, notation of units, spelling, axis labelling. References of all chapters are merged at the end to avoid redundancies.

[12] Originally published in: Innovative Food Science and Emerging Technologies (2021), Vol. 5, 975 - 985 . Permission for reuse of this article was granted by Elsevier.

in almost the same creamy perception compared to the full-fat milk dessert as control. An important finding was that drying of the microparticles lowered undesired grassy/beany off-flavours, which are currently typical disadvantages of pea protein usage within food.

3.6.1 Introduction

Attempts to lower the caloric content of foods by fat replacement often results in lower sensorical acceptance scores due to reduced creaminess (Frøst and Janhøj 2007). Proteins are lower in energy density (4 kcal/g) than fat (9 kcal/g) and they produce a higher satiation effect compared to fat and carbohydrates (Simpson and Raubenheimer 2005; Weigle et al. 2005). One way to reduce high calory fat while still generating a creamy mouthfeel is to add particulated protein. Round-shaped protein particles were reported to induce a ball-bearing effect between the palate and tongue, which lubricates the mouth, thus generating a creamy mouthfeel (Cheftel and Dumay 1993; Liu et al. 2016b). Decisive particle properties are size and shape. If particles are below a certain threshold size, they are perceived as empty, too large particles as mealy, gritty or sandy (Kew et al. 2020; Singer and Dunn 1990). A size of around 10 µm was identified as a suitable target level to induce the desired creaminess effect (Spiegel and Huss 2002; Spiegel 1999b; Wolz et al. 2016a; Kew et al. 2020; Yan et al. 2021). However, also larger, but soft, non-covalently stabilized spherical particles could still be perceived as creamy (Engelen et al. 2005). Such particles can be created by the microparticulation of proteins. Microparticulation of proteins is referred to as a heat-induced aggregation process, controlled by shearing, sequentially or simultaneously, to limit aggregation and particle growth (Singer and Dunn 1990). Microparticulation can be performed in a scraped-surface heat exchanger (Toro-Sierra et al. 2013; Spiegel and Huss 2002), an extruder (Quéguiner et al. 1992; Wolz et al. 2016a) or by post-heat shear treatment using a homogenizer (Liu et al. 2018a; Liu et al. 2018b; Sánchez-Obando et al. 2020; Zhang et al. 2020b). Most works so far focus on microparticulation of whey proteins, which are known to be covalently crosslinked by disulfide bonds. Only two studies report on non-dairy proteins by post-heat shear treatment. Liu et al. (2018b) microparticulated egg white protein for application in salad dressing, Zhang et al. (2020b) microparticulated a blend of soy protein and egg white protein. The extraction of lupin protein from lupin flakes resulted in a protein isolate suitable for fat replacement (Sussmann et al. 2013a). The application of plant proteins is of increasing interest because it is considered more sustainable than whey proteins (Fasolin et al. 2019). Pea plants can be locally grown in central Europe (Fuhrmeister and Meuser 2003), which is another aspect related to sustainability from a European perspective. Pea protein, like other plant proteins, are also of interest as meat replacing material after extrusion to produce fibre-like structures resembling the textural sensorial impression of meat, (Osen et al. 2015; Cornet et al. 2021) or expanded snacks (Beck et al. 2017), which, however, are other fields of application. Nano- and micrometre-sized particles were already created by using post-heat shear treatment of pea protein to stabilise emulsions and as structuring agents (Zhang et al. 2020a; Amagliani et al. 2020). It seems there is lacking knowledge on the microparticulation of plant protein,

produced by applying heat and shear simultaneously. In our earlier research, microparticulation using simultaneous heat and shear treatment of pea protein was studied on small scale in a rheometer (Tanger et al. 2021b). This approach was scaled up in this research from batch production of 4 ml product in a rheometer to a continuous process with a throughput of 15 kg h^{-1} product using an extruder.

In contrast to whey protein, commercially available pea protein is already denatured, aggregated, and low in functionality (Tanger et al. 2020), because currently, it is a processing side stream of starch production. This research aims to functionalize non-functional pea protein by microparticulation. Since the starting material already contains too large aggregates, the aggregate size has to be decreased during the microparticulation process. This means in contrast to whey protein, where microparticulation is a bottom-up process, it here is a top-down process (Tanger et al. 2021b). Protein-protein interaction in pea protein particles is known to be mostly non-covalent (Chihi et al. 2016). These interactions can be broken apart during heat and shear treatment. It is hypothesized that functional particles can be created similar to the bottom-up process of whey protein with the top-down process using a non-functional processing side stream as starting material. Milling would be a possible method to reduce particle size, however, developing heat during the process cannot be controlled. An advantageous process, where heat and shear can be controlled, is extrusion cooking. O'Kane et al. (2004c) found that pea protein gelation was not complete after the first heat treatment and that protein conformation can change during the second heat treatment. However, it is still unclear, whether this is also the case for particulation as investigated in this study. To solve this problem, extrusion cooking parameters such as extruder barrel temperature, screw speed and mass flow were varied and resulting microparticles were analyzed on size and protein-protein interactions, newly created after breaking down the previous protein-protein interactions in the starting material. The functionality to enhance creaminess in fat-reduced food of the microparticles to reduce fat was tested sensorically. Apart from the aspect of creamy mouthfeel, a disadvantage of using pea protein in contrast to whey protein is the bitter taste and grassy-beany off-flavour. Octacosa- 6,9,19,22-tetraen was found to be one of the key bitter compounds in pea proteins (Gläser et al. 2020). The bitter taste was found to be dependent on the degree of hydrolysis (García Arteaga et al. 2020). The mentioned bitter compound and other secondary plant metabolites responsible for the off-flavour were proposed to bind to the protein by non-covalent interactions, which can be cleaved and removed by processing for example fermentation (Klotzbücher 2009; Schindler et al. 2012) or solid dispersion-based spray drying (Lan et al. 2019; Pang et al. 2015). Two methods of post-processing of the microparticles, which are of industrial relevance, are spray-drying and freeze-drying. Both can alter the protein structure and thereof, are hypothesized to also alter the protein-flavour binding (Zhan et al. 2019). During spray-drying, oxidation can occur due to the presence of air and temperatures of 40°C - 50°C. Freeze-drying is performed at very low temperatures, under vacuum and exclusion of air and free water. Therefore, the drying is postulated to have a positive effect on the

aroma and taste profile of the fat-reduced milk dessert produced with the dried microparticles. However, the drying could also affect the particle size, which will be monitored.

3.6.2 Materials and methods

3.6.2.1 Materials

Pea protein isolate was provided by Emsland Stärke (Emlichheim, Germany). Pea protein isolate (E86) contained 71.4% protein on a dry basis. All other materials were purchased from regular suppliers and were of analytical grade. The particle size of the commercial pea protein isolate used before microparticulation is shown in Figure 3-40.

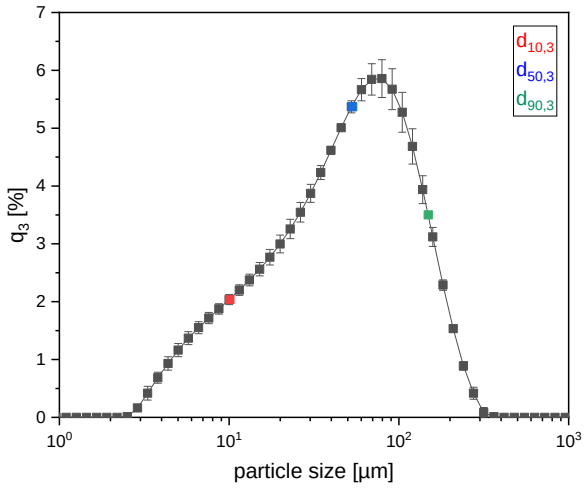

Figure 3-40: Volume based particle size distribution of commercial pea protein isolate before microparticulation. $D_{10,3}$, $d_{50,3}$ and $d_{90,3}$ are labelled in red, blue and green.

The initial particles are in the range of 3 – 300 µm with $d_{10,3}$ of 10,1 ± 0,7 µm, a $d_{50,3}$ of 53,4 ± 3,2 µm and a $d_{90,3}$ of 149,0 ± 1,9 µm. Microparticles suitable for fat replacementare smaller and range from 1 – 20 µm (Cheftel and Dumay 1993), thus particle size needs to be reduced during extrusion and is created via a top-down process.

3.6.2.2 Extrusion process

Commercial pea protein isolate was extruded using an intermeshing twin-screw extruder (ZSK25, Coperion, Stuttgart, Germany) with a screw diameter of 25 mm, a smooth barrel, and a total length of the screw of 28D. The extruder barrel contained 9 segments. Each of the segments was equipped with an independent temperature control except the first segment. The segments could be heated by an electric cartridge heating system and cooled with water. The second and the third segment were set to 30°C and 50°C / 60°C respectively. The last two segments were used for cooling and were set to 60 °C and 30°C. The fourth to seventh segments were variably set to the respective extruder temperature, which was varied from 30°C to 150°C. The extruder temperatures mentioned in the results section refer to the barrel temperature between the fourth and the seventh segment. A schematic overview is found in Figure 3-41.

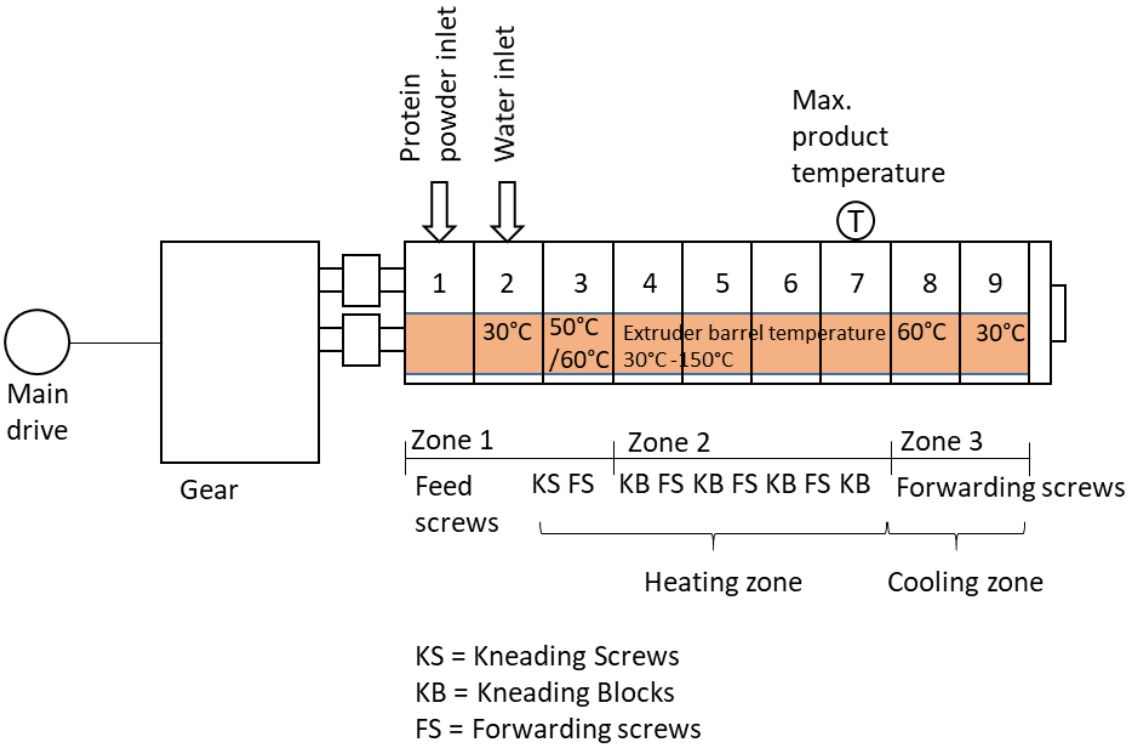

Figure 3-41: Schemeatic overview of the extrusion process.

The actual maximum product peak temperature was up to 20°C lower than the set extruder barrel temperature, as shown in Figure 3-42. The lower the set temperature was, the lower was the difference.

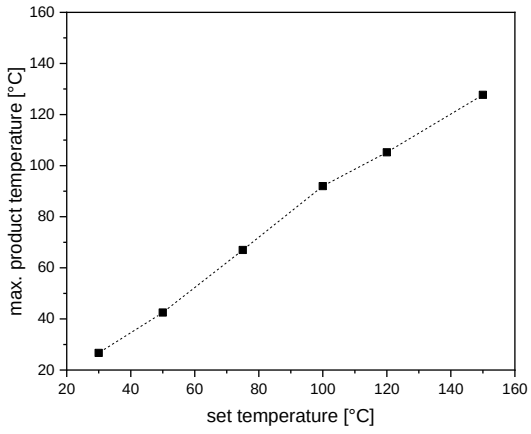

Figure 3-42: Set extruder barrel temperature versus actual maximum product temperature measured in segment 7.

The screw speed was varied from 200 rpm to 1200 rpm. The screw profile used was the same as described for microparticulation of whey proteins (Wolz et al. 2016a). Briefly, it was comprised of a feeding zone 1 (L = 366 mm) equipped with forwarding screw elements with a pitch of 36 mm, intercepted by 2 kneading blocks (5 disks, L = 2 mm, offset of 45°). Zone 2 (L = 336 mm) consisted of 4 alternating kneading blocks (5 disks, L = 36 mm, 45°) and a 48 mm forwarding screw element with a pitch of 24

mm. Cooling zone 3 (L = 256 mm) was comprised of a forwarding screw element to avoid friction and energy conversion into heat. The endplate had one hole of 10 mm diameter to avoid pressure build-up. The texture of the extruded product was comparable to a soft particulate gel, which easily falls apart under pressure.

Powder mass flow ($\dot{m}_P$) was varied from 3.0 to 4.5 kg h^{-1} in 0.5 kg h^{-1} steps. Water mass flow was varied from 7.7 to 11.6 kg h^{-1}, such that the protein concentration of the product (c_{end}) set to 20%. The water mass flow ($\dot{m}_W$) was calculated by the following equation:

$$\dot{m}_W = \frac{\dot{m}_P \times P}{c_{end}} - \dot{m}_P \tag{3-27}$$

3.6.2.3 Sample collection

Samples were collected in plastic containers with a screw lid when the product temperature reached a steady state. After collection, they were rapidly cooled and stored on ice.

3.6.2.4 Particle size measurement

For particle size measurement the samples were dissolved with water to a 1% protein solution. The particle size of the samples was measured using laser diffraction with a mastersizer. The mastersizer was equipped with a Malvern Mastersizer Hydro 2000S measurement unit (Malvern Panalytical, Malvern, Worcestershire, UK). For the calculation of the particle size, an optical model (Mie theory (Eremin 2005)) was applied. For the dispersed phase, a refractive index of 1.45 was used and for the dispersant medium, a refractive index of 1.33 was used. An absorbance of 0.001 was used for the protein solution (McCarthy et al. 2016). Cumulative particle size distribution (Q_3) is shown as well as $d_{10,3}$, $d_{50.3}$, and $d_{90,3}$ 10%, 50%, and 90% of the particles are smaller than the $d_{10,3}$, $d_{50.3}$, and $d_{90,3}$, respectively.

3.6.2.5 Particle stabilizing chemical interactions

Particle stabilizing interaction analysis was performed as described by Tanger et al. (2021a), with slight modifications. The collected samples were pressed through a garlic press to increase the surface. 0.2 g (m_S) of the sample was dispersed in 20 g (m_{gel}) 50 mM phosphat buffer pH 7.5 (B_1), 50 mM phosphate buffer pH 7.5 with 2 g / l sodium dodecyl sulfate (SDS) (B_2), and 50 mM phosphate buffer pH 7.5 with 2 g / l SDS and 15 g / l dithiothreitol (DTT) (B_3). SDS cleaved all hydrophobic interactions and DTT cleaved all disulphide bridges. The samples were dissolved over night at room temperature in a shaker (LAUDA-GFL, Burgwedel, Germany). On the next day, insoluble protein aggregates were separated from soluble protein aggregates by centrifugation at 10,000 g for 20 min at 20°C. The soluble nitrogen content was determined by Dumas method using a Vario MAX cube (Elementar Analysensysteme GmbH, Langenselbold, Germany) (Ebeling 1968). The following set of equations was used to calculate the distribution of the various kinds of protein interactions.

$$C_{n,bond,Bi} = \frac{(m_S + m_{gel})}{m_{gel}} * C_{n,sup,Bi} \tag{3-28}$$

$$\frac{C_{n,bond,B1}}{C_{n,gel}} = P(ES) \quad (3\text{-}29)$$

$$\frac{C_{n,bond,B2}}{C_{n,gel}} = P(ES) + P(Hy) \quad (3\text{-}30)$$

$$\frac{C_{n,bond,B3}}{C_{n,gel}} = P(ES) + P(Hy) + P(SS) \quad (3\text{-}31)$$

$$P(Hy) = \frac{C_{n,bond,B2}}{c_{n,gel}} - \frac{C_{n,bond,B1}}{C_{n,gel}} \quad (3\text{-}32)$$

$$P(SS) = \frac{C_{n,bond,B3}}{C_{n,gel}} - \frac{C_{n,bond,B2}}{C_{n,gel}} \quad (3\text{-}33)$$

With $C_{n,sup,Bi}$ as the dissolved nitrogen in the supernatant in [%], $C_{n,gel}$ as the nitrogen content of the sample in [%], P for the amount of (), ES for electrostatic interactions, Hy for hydrophobic interactions and SS for disulphide bonds. $C_{n,bond,Bx}$ is the concentration of cleaved protein bonds by the respective buffer.

3.6.2.6 Drying of the microparticulate

From the results, optimal extrusion cooking parameters were obtained. Only these were used further for drying. Spray- and freeze-drying of the microparticulates were compared. Before drying, the microparticulate was diluted 1:1 with water, to decrease viscosity and avoid clogging the tubes. Spray-drying was performed using a pilot-scale spray-dryer NIRO ATOMIZER (GEA, Copenhagen, Denmark). A T_{inlet} of 190°C, a T_{outlet} of 80°C, a drying airflow of 20 m / s, atomisation of 15,000 rpm and a feed flow of 0.26 l / min. Before freeze-drying, the microparticulate was frozen at -80°C for at least 2 h. Freeze-drying was performed using a pilot-scale freeze dryer (Christ, Model: Alpha 1–4 LSC; Osterode, Germany). Shelf temperature was set to 15°C and chamber pressure was set to 0.370 mbar.

3.6.2.7 Application in model milk dessert

The suitability of the microparticles for fat replacement was tested in a model milk dessert. The reference full-fat product contained 227 g dairy cream, 33 g sugar, 233 g 0.1 % fat yoghurt and 7 g stabilizer. The ingredients were whipped and mixed. For the fat reduced model milk dessert, 50% of the cream was substituted by (rehydrated) microparticles. Freshly extruded microparticles, freeze-dried, and spray-dried microparticles were compared with each other like a fat replacement in the model milk dessert. Thus, three fat-reduced milk desserts, one containing freshly extruded microparticles (fresh MP MD), one containing spray-dried microparticles (spray-dried MP MD), and one containing freeze-dried microparticles (freeze-dried MP MD), were compared with the full-fat milk dessert (MD w/o MP). Freshly extruded microparticles did not need rehydration for application in the model milk dessert, but spray- and freeze-dried microparticles did. 22 g dried microparticles were rehydrated with 91 g demineralized water at room temperature for 30 min. Dry matter was the same for rehydrated and fresh microparticles. After production, the model milk dessert was stored at 4°C.

3.6.2.8 Sensory analysis – General conditions and panel training

Three fat-reduced model milk desserts were evaluated using comparative flavour profile analysis with the full-fat model milk dessert, which served as a reference, to see the sensory effect of fat replacement and incorporation of pea protein microparticles on taste and aroma. Sensory analysis and panel training was performed according to Utz et al. (2021). For taste analysis, 14 panellists (eight women and six men, age 22-32 years) were recruited from the Chair of Food Chemistry and Molecular Sensory Science, for aroma analysis, 16 assessors (nine women and seven men, 22-58 years) were consulted from the Chair of Food Chemistry and Molecular Sensory Science and the Leibniz-Institute for Food Systems Biology at the Technical University of Munich. Each panellist joined a weekly training session for at least two years to become familiar with taste and aroma terminology and had no history of known disorders. Using the sip-and-spit method the panellists were trained to evaluate the taste of aqueous solutions (2 ml) for taste attributes of the following reference compounds: sucrose (50 mmol / l) for sweet taste, lactic acid (20 mmol / l) for sour taste, monosodium glutamate (3 mmol / l) for umami taste, NaCl (20 mmol / l) for salty taste, and caffeine (1 mmol / l) for bitter taste. For creaminess, a water/sunflower oil emulsion (4/6, w/w; containing 0.5% Span 65) and for astringency, tannic acid (0.05%) were used (Schlutt et al. 2007; Scharbert and Hofmann 2005). The activity of mouthfullness enhancement and complexity increase was trained by comparison of a blank model broth (control) with a solution of reduced glutathione (5 mmol / l) in model broth (Brehm et al. 2019). Reference odorants (20 ml) for aroma evaluation used for sensory training were: trans,trans-2,4-decadienal (0.32 µg / l) for fatty aroma, acetic acid (60 mg / l) for sour aroma, hexanoic acid (48 mg / l) for rancid aroma, vanillin (530 µg / L) for vanilla-like aroma, commercial milk for milklike aroma, and a mixture of hexanal and 3-isopropyl-2-methoxypyrazine (25 µg / l, 0.1 µg / l) for grassy/green/bean-like notes. All sensory analyses were performed in an air-conditioned room at 20 − 25 °C in a sensory panel room with single booths. The single booths were under yellow (set to 60%) and white (set to 60%) light conditions. Data was acquired by the FIZZ sensory analysis software (Biosystems, Dijon, France).

3.6.2.9 Comparative flavour profile analysis

To characterize taste and aroma profiles of three fat reduced model milk desserts, comparative quantitative descriptive analysis (QDA) was conducted according to Stone and Sidel (2012) and Utz et al. (2021). To avoid cross-modal interactions with odorants nose clips were used during taste profile analysis. After rinsing their mouth with bottled water, the intensities of the taste attributes (sweet, sour, umami, salty, bitter, astringent, creamy, mouthfullness, and kokumi) were judged by all panellists on a linear five-point scale from 0 (not detectable) to 5 (very intense) in comparison to the full-fat milk dessert reference as a control. To evaluate the aroma profiles of all fat reduced prototypes, the panellists were asked to compare the intensities of the aroma attributes fatty, sour, rancid, vanilla-like, milk-like, and grassy/green/bean-like on a linear five-point scale from 0 (not detectable) to 5 (very intense). Thereby, the intensities of all attributes were evaluated for the fat-reduced model milk desserts in comparison to the full-fat model milk dessert reference.

3.6.2.10 Statistical analysis

All experiments were carried out in at least duplicate. Data points show the average and error bars show the upper and the lower value as not indicated otherwise. Graphs were plotted using OriginPro 2019 (originLAb Coorperation, Northampton, USA). A one-way analysis of variance (ANOVA) for significant difference between groups followed by a Dunnett's test with the full-fat milk dessert as reference was performed for sensorical results. The ANOVA was followed by a Tukey-Kramer (HSD) test for particle size and protein interaction measurement. Minimum significant difference was set to a 5% level ($p < 0.05$). Statistical analysis was performed using JMP Pro (SAS Institute Inc., Cary, USA/Version 14)

3.6.3 Results and discussion

3.6.3.1 Influence of extruder barrel temperature

The impact of the extruder barrel temperature on the resulting particle size and stabilizing protein interaction was analysed. First, the impact on particle size is discussed and second the stabilizing protein interactions. The $d_{50,3}$ of microparticles produced at all analyzed extrusion cooking parameters can be found in Table A3-11 – Table A3-14. In Figure 3-43 the particle size of the microparticles at varying temperatures for low, medium and high screw speed at a mass flow of 4 kg h^{-1} is shown.

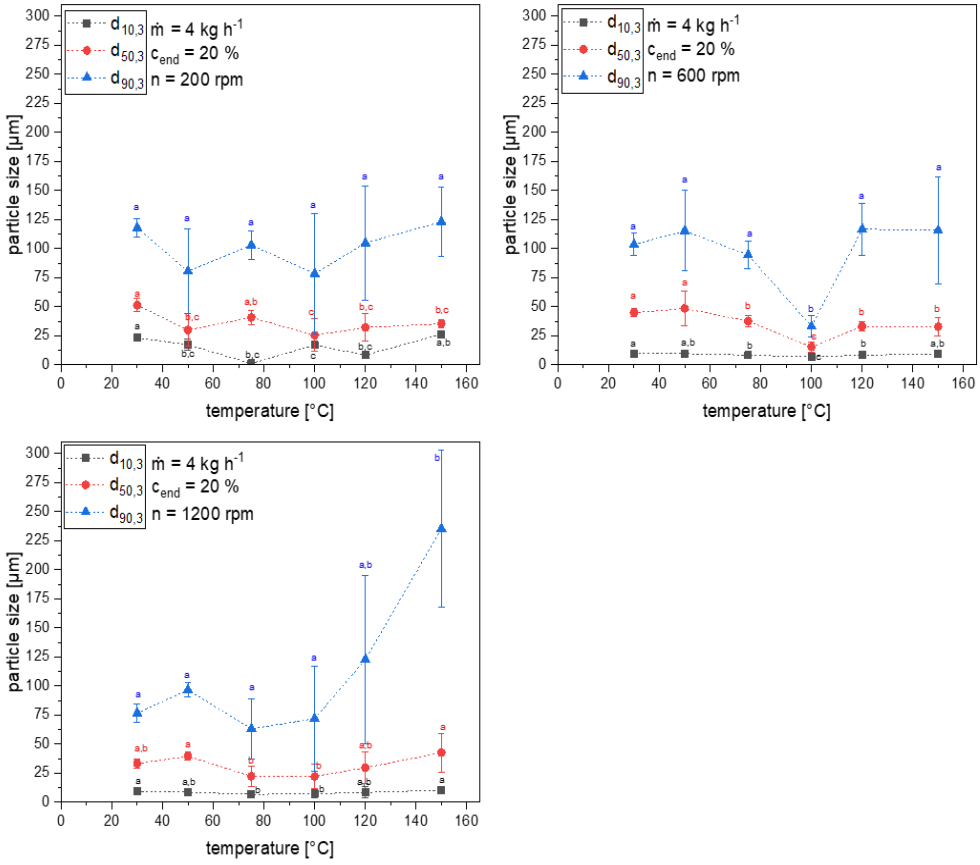

Figure 3-43: Particle size $d_{10,3}$, $d_{50,3}$ and $d_{90,3}$ of pea protein microparticles at 200 rpm, 600 rpm and 1200 rpm at 4 kg h-1 as a function of set extruder barrel temperature in segment 4 - 7. $^{a-c}$ $d_{10,3}$, $d_{50,3}$ and $d_{90,3}$ values with the the same letter indicate no significant difference ($p < 0.05$)

Particle size was reduced compared to the starting product. The temperature influences microparticulation. In contrast to the bottom-up process of whey protein, a trend is only seen at high screw speeds from 600 rpm (Wolz et al. 2016a). This is because the pea protein is already denatured contrary to the whey protein used in the study of Wolz et al. (2016a). In their study, the protein first needed to be heated above denaturation temperature to denature to aggregate during microparticulation. This is not the case in our study. However, at screw speeds from 600 rpm, particle size increases with increasing temperature. This is especially seen for the d_{90}. At high screw speeds and high temperatures, big particles are formed or the initial aggregates are not torn apart by theshear stress, which can be explained by the high amount of hydrophobic interaction between the proteins, which is discussed below. The aggregates in the starting material were stabilized by 20% disulphide bonds, 64% hydrophobic interactions and 16% electrostatic interaction. In Figure 3-44, the distribution of the stabilizing protein interactions is shown at low and high screw speeds.

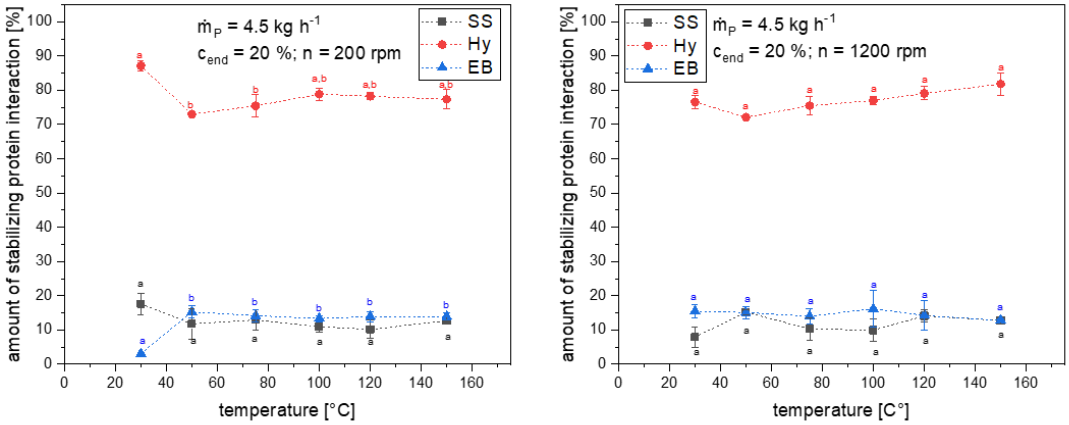

Figure 3-44: Amount of stabilizing protein interaction of microparticles produced at 200 rpm and 1200 rpm, 4.5 kg h^{-1} as a function of set extrder barrel temperature in segments 4 - 7. SS being short for disulphide bonds, Hy being short for hydrophobic interaction and EB being short for electrostatic interactions. $^{a-b}$ SS, Hy and EB values with the the same letter indicate no significant difference ($p < 0.05$)

The temperature does not affect the type of stabilizing protein interaction. Hydrophobic interactions are the major protein interaction stabilizing the particles. Disulphide bonds and electrostatic interaction play a minor role. A high amount of non-covalent interaction of pea protein has been found for pea protein gels (O'Kane et al. 2004a; Sun and Arntfield 2012) and aggregates (Chihi et al. 2016). In earlier research, a higher amount of disulphide bonds was found for microparticulation using a rotational rheometer (Tanger et al. 2021b). This research adds to the protein interaction assay an SDS-PAGE was performed also detecting small covalently cross-linked oligomers. In the presented research an additional SDS-PAGE was relinquished due to the high amount of samples and because the precise amount of disulphide bonds was not of interest. The focus lies on stabilizing protein interactions forming a continuous network. The temperature, however, affects the intensity of the protein interactions. Hydrophobic interactions increase in intensity with increasing temperature (van Dijk et al. 2015). Therefore, at high temperatures, the hydrophobic interactions may get so strong that the

shear cannot tear the proteins apart and form smaller particles. The most suitable extruder barrel temperature was found to be from 75°C to 120°C to produce particles with a $d_{50,3}$ closest to the targeted size range of 1-20 µm for whey proteins (Wolz et al. 2016a), which indicate that heating is necessary to reduce particle size.

3.6.3.2 Influence of screw speed

The influence of the screw speed on particle size and stabilizing protein interaction has been analysed. Figure 3-45 shows the particle size at varying screw speeds.

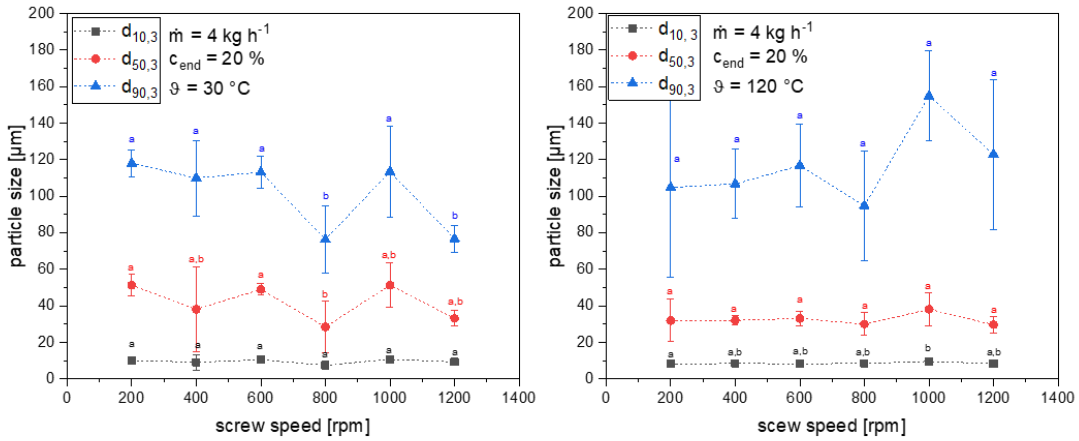

Figure 3-45: Particle size $d_{10,3}$, $d_{50,3}$ and $d_{90,3}$ of pea protein microparticles at 30 °C and 120°C with a mass flow of 4 kg h^{-1} as a function of screw speed. $^{a-b}$ $d_{10,3}$, $d_{50,3}$ and $d_{90,3}$ values with the the same letter indicate no significant difference ($p < 0.05$)

The particle size varies with varying screw speed. For whey protein, it has been found that an increasing screw speed leads to a reduction in particle size (Wolz et al. 2016a). This was not found for pea protein microparticulation. The screw speed can have two effects on the aggregation of proteins. The aggregates can break up due to the shear stress or aggregation is increased, because of a higher collision probability (Wolz et al. 2016b). Quéguiner et al. (1992) found that an increase in a screw speed decreased the size of whey protein during microparticulation using an extruder at acidic pH. However, they only analysed screw speeds between 100 – 200 rpm, which is lower than used in this study. Thus, the effect of shear rate might be highest for low screw speeds. Lower screw speeds could not be analyzed in this study, because extrusion at shear rates below 200 rpm led to a discontinuous product flow. At high screw speeds, a variation in screw speed does not impact the particle size or only slightly. The screw speeds used in this study are high enough to lead to suitable particle size for fat replacement. Most suitable were screw speeds between 600 rpm and 800 rpm.

Next to particle size, shear stress was found to promote thiol-disulphide interchange reaction (Evans 2001; Choi et al. 2007). However, if a high and a low screw speed are compared with each other, as is shown in Figure 3-44, no difference was found for the distribution of protein interactions. There are four hypotheses to explain this finding. First, as already mentioned the used pea protein isolate contained already denatured protein. Due to this, no further thiol groups get exposed upon heating and thiol-disulphide interchange might occur but does not change the relative amount of disulphide

bonds. Second, the newly build disulphide bonds do not form continuous networks but only connect small oligomers. Small oligomers connected via covalent bonds, cannot be separated by the protein interaction assay used in this study. Third, the screw speeds used in this study are too high to distinguish between the effect of screw speed on thiol-disulphide interchange reaction. The third argument is weakened by the fact that the amount of covalent bonds between the starting product and the resulting microparticles does not increase. Fourth, pea proteins native structure is held together by hydrophobic interactions, which only get stronger with increasing temperature. For complete denaturation and complete exposure of the thiol groups, a high amount of energy is needed. At low heat holding times, as is the case during extrusion, the pea protein may only partly unfold and aggregate via that unfolded exposed, reactive group. However, other parts of the protein might still be folded. Upon aggregation of the unfolded part, other reactive groups in the still folded part might never get exposed.

3.6.3.3 Influence of mass flow

The influence of mass flow was analysed with a constant end protein concentration of 20%. Powder mass flows of 3 to 4.5 kg h^{-1} were compared. With increasing powder mass flow the water mass flow increased from 7.7 kg h^{-1} and therefore also the total mass flow increased from 10.7 kg h^{-1} to 16.1 kg h^{-1}. The water flow is limited to 14.7 kg h^{-1} due to the capacity of the used pump. Therefore, higher mass flows cannot be analysed without changing the protein end concentration. Figure 3-46 shows the particle size distribution of the microparticles at different powder mass flows.

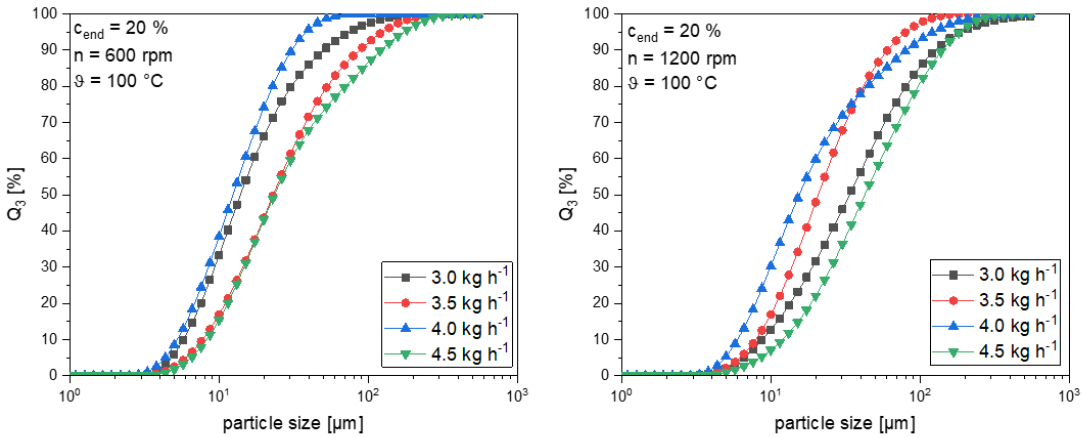

Figure 3-46: Cumulative particle size distribution of pea protein microparticles at 600 rpm and 1200 rpm at 10°C for varying powder mass flows.

At 600 rpm the biggest particles were produced at 3.5 kg h^{-1} and 4.5 kg h^{-1}. The size distribution was narrowest for 4 kg h^{-1}. At 1200 rpm biggest particles were produced at 3 kg h^{-1} and 4.5 kg h^{-1}. For microparticulation of whey protein, a higher mass flow resulted in lower degrees of denaturation (Wolz et al. 2016a). This was explained by an increase in screw filling level. At higher screw filling levels the contact between the product and heated extruder barrel wall is reduced (Yeh et al. 1992). This then leads to a lower product temperature. However, an increase in screw filling can also increase product temperature due to friction. With the pea protein already denatured used in

this study, the maximum product temperature does not affect denaturation. However, as described above temperature does affect the particle size (Figure 3-43). Wolz et al. (2016a) found that an increasing mass flow decreased the shear stress because the resulting mechanical input per mass unit decreased. This would explain, why at the highest analysed powder mass flow of 4.5 kg h^{-1} the biggest particles are produced. The shear stress is lower and therefore cannot effectively reduce particle size.

3.6.3.4 Effect of drying on the microparticles

One of the most optimal process parameters to produce microparticles in the size range suitable for fat replacement were a powder mass flow of $\dot{m}_P$ = 4 kg h^{-1}; a temperature of ϑ = 100°C; and a screw speed of n = 600 rpm. Particles produced at this extrusion cooking parameter had a $d_{10,3}$ of 6.71 µm, a $d_{50,3}$ of 15.31 µm, and a $d_{90,3}$ of 33.03 µm. Based on the $d_{50,3}$ these were the smallest particles, which could be produced in this study. In order to produce products with a longer shelf-life, the particles were dried. Drying can influence particles size, because of concentration and heat treatment. The effect of freeze-drying and spray-drying were evaluated. Figure 3-47 displays the effect of drying on particle size.

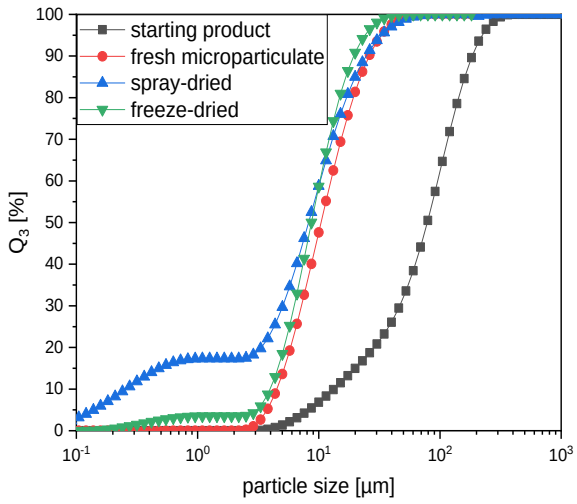

Figure 3-47: Cumulative particle size distribution of dried and fresh microparticles.

Microparticulation reduced the particle size of the starting product. Drying had a neglectable effect on particle size. Similar to our findings, spray-drying increased the particle size of whey protein microparticles slightly. However, with dissolution in water the size shrank to the same size of the aggregates before drying (Toro-Sierra et al. 2013). Some particles (15% - 20%) also decreased in size after drying and solubilisation, which might be due to additional shear stress during spray drying. For rice protein, it was found that spray-dried rice protein isolate was smaller in particle size than freeze-dried rice protein isolate (Zhao et al. 2013), which would be similar to our findings. Next to size, the two different drying methods were shown to affect protein conformation and can induce structural transformation in secondary structure in proteins (Zhao et al. 2013). These protein conformations can affect flavour binding, which is discussed in the following.

3.6.3.5 Incorporation of microparticles in model food product

To not solely rely on measurable characteristics of the produced microparticles to conclude, whether they are suitable for fat replacement, the fresh and the dried microparticles were incorporated as a fat replacement in a model food. The effect on taste and aroma was sensorically evaluated. A model milk dessert was chosen as a test matrix because it was easy to produce and a creamy taste and mouthfeel is expected. The flavour blueprint of this milk dessert was already investigated (Utz et al. 2021). A fat replacement of 50% in the model milk dessert should have a measurable influence on the perceived creaminess of the product without the incorporation of a fat replacer. Figure 3-48 displays the results of the taste and aroma profile of the three fat-reduced milk desserts and the reference full-fat milk dessert.

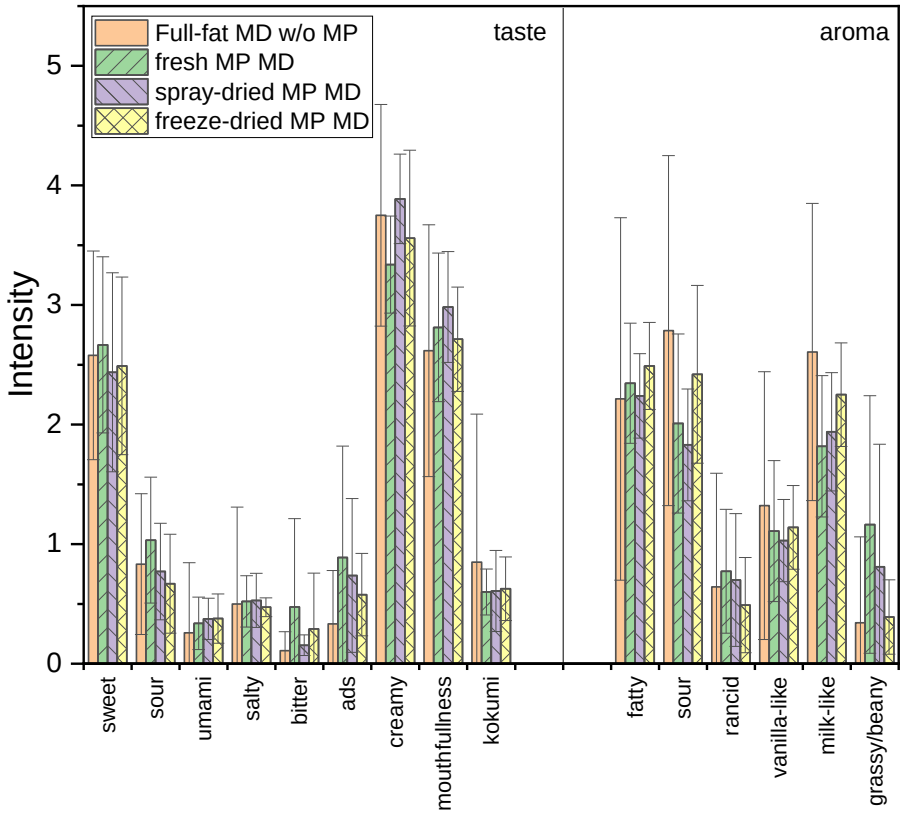

Figure 3-48: Intensity ratings of aroma and taste of the full-fat milk dessert without microparticles and the three fat-reduced milk desserts with microparticles. In the fat-reduced milk desserts fat was 50% substituted by fresh microparticles (fresh MP MD), spray-dried microparticles (spray-dried MP MD) and freeze-dried microparticles (freeze-dried MP MD). *indicates significant difference to the reference

There is no significant difference between the four milk desserts regarding sweetness, sourness, umami, mouthfullness and kokumi. Bitterness and astringency are slightly higher in the fat-reduced milk desserts due to the incorporation of pea protein. However, all values remain below 1 meaning they are nearly not detectable and thus, did not affect negatively taste profiles. Even though 50% of the fat has been replaced in the milk dessert the intensity of perceived creaminess was not halved. The creaminess

was not significantly different between the three milk desserts. Therefore, microparticles were able to produce comparable creamy perceptions such as fat as expected from the size and protein interaction analysis measurement.

Regarding aroma, there was no significant difference in fatty, rancid, and vanilla-like aroma. The fat-reduced milk desserts scored lower in sourness and milk-likeness and higher in grassy/beany aroma. It was shown that the usage of pea protein microparticles had a stronger effect on aroma than taste. This was expected because plant proteins were shown to have a grassy/beany aroma, which in most products is unwanted. With the drying of the microparticles, the grassy/beany aroma was reduced compared to the fresh MP MD. In another study, it was shown that solid dispersion-based spray-drying reduced the grassy/beany off-flavour in pea protein isolate (Lan et al. 2019). This reduction of off-flavour can be explained by the loss of volatile aroma compounds during evaporation of water and lower binding to the protein. The higher temperature (40°C – 50°C) and low water content of the product during spray-drying might inactivate lipoxygenase, which is responsible for the oxidation of fatty acids leading to a green beany off-flavour. It has been found that freeze-drying changes the tertiary structure of pea protein and pea protein-polysaccharide complexes, which alters the flavour binding to the protein, leading to a loss of the volatile aroma compounds (Zhan et al. 2019). Therefore, drying had no significant effect on particle size, but it had a significant effect on aroma profiles. This would increase consumer acceptance of products focusing on plant proteins with pea proteins as the main source.

3.6.4 Conclusions

The influence of varying extrusion parameters on the microparticulation of pea proteins was studied. Suitable particle size and stabilizing protein interaction was found by using a powder mass of $\dot{m}_P$ = 4 kg h^{-1}; a temperature of ϑ = 100°C; and a screw speed of n = 600 rpm. Both spray and freeze-drying did not affect the particle size negatively for microparticles produced at optimal extrusion cooking parameters but affected taste and aroma positively. Fresh and dried microparticles were incorporated in a fat-reduced model milk dessert. It was shown that the reduced-fat model milk dessert was perceived nearly the same regarding creaminess compared to the full-fat milk dessert. Drying of the microparticulates could reveal that especially undesired grassy/beany off-flavours could be advantageously reduced. Therefore, the microparticulation process of a pea protein isolate, which is lower in food protein functionality than most whey protein isolates, using extrusion cooking offers a possibility for fat replacement using plant proteins, similar to what was shown for microparticulated whey proteins. These pea protein microparticles can be applied in innovative vegan food for example vegan cheese, ice cream and yoghurt or as shown in dairy products to replace fat and add to a creamy mouthfeel. For future research, it would be of interest to also study the microparticulation of other plant proteins.

Acknowledgements

We would like to acknowledge the help of Franz Kuhnert, Andreas Matyssek and Günther Unterbuchberger for help during extrusion cooking and spray drying.

This project was executed as part of an Industrial Collective Research (IGF) project of the Forschungskreis der Ernährungsindustrie e.V., Bonn (FEI) supported by the German Ministry of Economics and Technology via AiF (AiF 20197 N).

Conflict of interest

The authors declare that they have no conflict of interest.

Abbreviations

n	screw speed
ϑ	temperature
q_3	volume based particle size distribution
Q_3	cumulative particle size distribution
MP	microparticle
MD	milk dessert
MD w/o MP	full-fat milk dessert without microparticles
Fresh MD MP	fat-reduced milk dessert with fresh microparticles
Spray-dried MD MP	fat-reduced milk dessert with spray-dried microparticles
Freeze-dried MD MP	fat-reduced milk dessert with freeze-dried microparticles

3.6.5 Appendix

Table A3-11: $D_{50,3}$ values of microparticles produced at 3 k h^{-1} powder mass flow.

Screw speed (rpm)	Set extruder barrel temperature (°C)					
	30	50	75	100	120	150
200	41 ± 22	36 ± 19	16 ± 6	36 ± 3	17 ± 6	38 ± 25
400	45 ± 25	36 ± 16	27 ± 8	37 ± 9	16 ± 5	17 ± 5
600	36 ± 29	35 ± 15	23 ± 4	16 ± 6	31 ± 3	32 ± 21
800	41 ± 23	30 ± 20	20 ± 3	32 ± 4	54 ± 11	48 ± 28
1000	43 ± 29	31 ± 15	23 ± 2	40 ± 9	40 ± 16	34 ± 20
1200	43 ± 23	34 ± 17	14 ± 1	39 ± 17	35 ± 8	50 ± 26

*Means ± SD values

Table A3-12: $D_{50,3}$ values of microparticles produced at 3.5 k h^{-1} powder mass flow.

Screw speed (rpm)	Set extruder barrel temperature (°C)					
	30	50	75	100	120	150
200	32 ± 7	25 ± 3	28 ± 5	9 ± 5	59 ± 25	35 ± 19
400	30 ± 8	18 ± 6	33 ± 14	23 ± 2	38 ± 23	36 ± 25
600	30 ± 9	18 ± 5	41 ± 10	24 ± 2	38 ± 14	27 ± 13
800	32 ± 10	18 ± 3	39 ± 15	31 ± 18	46 ± 27	17 ± 2
1000	23 ± 3	19 ± 2	23 ± 5	40 ± 12	38 ± 6	19 ± 7
1200	30 ± 3	17 ± 4	23 ± 13	23 ± 6	26 ± 9	32 ± 18

*Means ± SD values

Table A3-13: $D_{50,3}$ values of microparticles produced at 4 k h^{-1} powder mass flow

Screw speed (rpm)	Set extruder barrel temperature (°C)					
	30	50	75	100	120	150
200	51 ± 6	30 ± 6	41 ± 6	25 ± 13	32 ± 12	35 ± 3
400	38 ± 23	24 ± 8	40 ± 4	27 ± 15	32 ± 2	39 ± 4
600	49 ± 3	49 ± 14	25 ± 5	15 ± 1	33 ± 4	33 ± 7
800	28 ± 14	35 ± 17	30 ± 9	23 ± 12	30 ± 6	28 ± 9
1000	51 ± 12	40 ± 3	22 ± 10	25 ± 2	38 ± 9	40 ± 4
1200	33 ± 4	39 ± 3	22 ± 8	22 ± 12	30 ± 4	43 ± 15

*Means ± SD values

Table A3-14: $D_{50,3}$ values of microparticles produced at 4.5 k h^{-1} powder mass flow

Screw speed (rpm)	Set extruder barrel temperature (°C)					
	30	50	75	100	120	150
200	34 ± 10	29 ± 9	30 ± 20	29 ± 15	21 ± 3	25 ± 12
400	34 ± 4	29 ± 3	33 ± 24	29 ± 19	21 ± 1	24 ± 3
600	18 ± 1	31 ± 5	22 ± 10	35 ± 19	26 ± 7	20 ± 4
800	25 ± 3	52 ± 6	23 ± 18	32 ± 16	36 ± 4	16 ± 2
1000	24 ± 7	30 ± 16	14 ± 10	43 ± 20	37 ± 16	25 ± 2
1200	34 ± 5	25 ± 13	40 ± 34	52 ± 22	28 ± 2	44 ± 4

*Means ± SD values

3.7 Influence of pea and potato protein microparticles on texture and sensory properties in a fat-reduced model milk dessert

Summary and contribution of the doctoral candidate

Microparticles in general can be used as a fat-replacer in food due to the ball-bearing effect, which generates a creamy mouthfeel. Currently, there is a lot of knowledge about the application of whey protein-based microparticles in food. However, less is known how plant-based microparticles, such as pea and potato, alter the food structure and flavour. Therefore, in this research paper, pea and potato protein microparticles were produced and applied in a model milk dessert. Three milk desserts were compared with each other texturally and sensorically. One milk dessert was the full-fat reference, which did not contain any microparticles. The other two milk desserts were 50% fat reduced. The fat was replaced in one milk dessert with pea protein microparticles and in the other one with potato protein microparticles. Overall the milk dessert containing pea protein microparticles was harder and higher in adhesiveness compared to the full-fat reference and the milk dessert containing potato protein microparticles. The milk dessert containing potato microparticles was softer in texture and lower in adhesiveness compared to the full-fat reference and the milk dessert containing pea protein microparticles. Thus, even though pea and potato microparticles are both plant-based they affected the texture differently. Sensory profile analysis revealed that the full-fat milk dessert and the milk dessert containing pea protein microparticles were not significantly different in terms of creaminess. Thus, pea protein microparticles could inhibit a loss in creaminess upon fat reduction. Milk desserts containing potato protein microparticles were significantly lower in creaminess compared to the full-fat reference. This might not only be due to particle characteristics but also to an increased amount of decanoic and dodecanoic acid, which leads to a scratchy mouthfeel. The bitter and adstringent taste was also significantly higher in milk desserts containing potato protein compared to the other milk desserts. Grassy, bean-like aroma was increased significantly in both fat-reduced milk desserts, which can be explained by the increased amount of hexanal, acetaldehyde, and 2-/3-methylbutyric acids compared to the full-fat reference. For milk desserts containing potato protein microparticles, the bitter and astringent taste can be explained by the high amount of short-chain fatty acids. Patatin, the main potato protein, exhibits a lipase activity and can cleave short-chain fatty acids from triglycerides, when not fully inactivated. Thus, the challenge of reducing the off-flavour in plant-based microparticles remains. However, it has to be tackled differently for pea and potato microparticles.

This manuscript was shared first authorship. Both first authors, including the doctoral candidate, contributed substantially to the conceptualisation and method development. Statistical data analysis and interpretation were carried out by both first authors. The original draft was written by both first authors. The doctoral candidate covered the food engineering and food structure part, whereas the other first author covered the sensorical and food chemistry part. Co-authors contributed to experimental work and/or discussion.

Adapted original manuscript[13]

Influence of pea and potato protein microparticles on texture and sensory properties in a fat-reduced model milk dessert[14]

Caren Tanger*[a], Florian Utz*[b], Andrea Spaccasassi[b], Johanna Kreissl[c], Jannika Dombrowski[a,d], Corinna Dawid[b], Ulrich Kulozik[a]

[a]Chair for Food and Bioprocess Engineering TUM School of Life Sciences, Technical University of Munich, Weihenstephaner Berg 1, Freising-Weihenstephan, Germany

[b]Chair of Food Chemistry and Molecular Sensory, TUM School of Life Sciences, Technical University of Munich, Lise-Meitner-Straße 34, Freising-Weihenstephan, Germany

[c]Leibniz-Institute for Food Systems Biology at the Technical University of Munich, Lise-Meitner-Straße 34, Freising-Weihenstephan, Germany

[d]Nestlé Research, Société des Produits Nestlé SA, Route du Jorat 57, 1000 Lausanne 26, Switzerland

Graphical Abstract

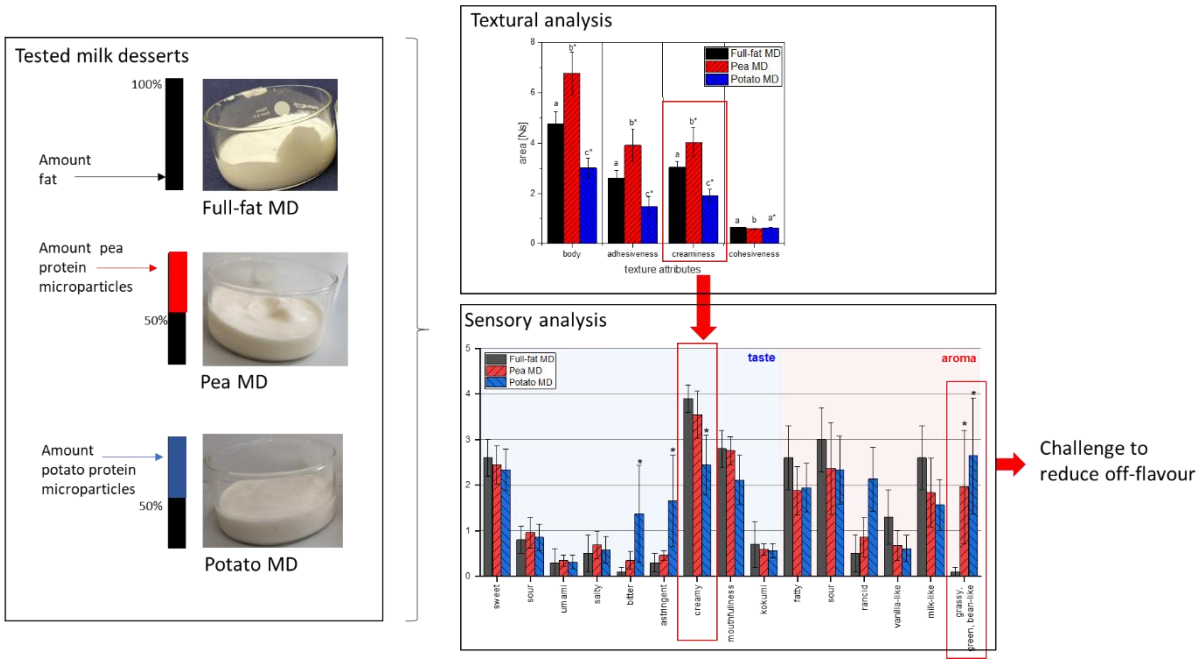

Abstract

With increasing diet-related health issues and awareness of climate change, the demand for sustainable protein-based fat replacer increases. In this study, the impact of the incorporation of pea and potato protein microparticles in fat-reduced (-50%) milk desserts was tested texturally and sensorically. The incorporation of pea protein microparticles led to a harder texture and higher adhesiveness and creaminess, whereas

[13] Adaption refer to formatting issues: e.g., abbreviations, figure, table, equation and section numbering, citation style, notation of units, spelling, axis labelling. References of all chapters are merged at the end to avoid redundancies.

[14] Originally published in: ACS Food Science and Technology (2021), Vol. 2,1, 169-179. Permission for reuse of this article was granted by ACS.

these attributes were decreased by the incorporation of potato protein microparticles. Nevertheless, in both pea and potato milk desserts an unwanted grassy, green, bean-like aroma was additionally perceived. For the potato milk dessert also further taste attributes such as bitter and astringent were disadvantageously impacted, very likely correlating with higher concentrations of short-chain fatty acids released by residual lipase activity in the potato protein isolate, which was not fully deactivated by extrusion cooking. Even though both potato and pea proteins are plant proteins, they have to be processed differently to obtain the desired results and are suitable for different food applications.

3.7.1 Introduction

With increasing wealth and food accessibility in industrial countries, diet-related health issues such as diabetes and cardiovascular diseases increase. Overconsumption of sugar and fat is postulated to be responsible for weight gain and diet-related health issues. Proteins are lower in energy density than fat and have higher satiation compared to fat and carbohydrates (Simpson and Raubenheimer 2005, 2014; Weigle et al. 2005). However, central sensorical attributes of food products are linked with sugar and fat. One of these characteristics of fat is creaminess. The creamy perception of food is complex and difficult to recreate in fat-reduced food. Creaminess has been described as the interaction of aroma, taste and texture (Mela 1988; Tournier et al. 2007). Creamy aroma, for instance, can arise from different volatiles such as octanoic acid, 3-methylbutyric acid, and dimethyl sulfide and it was revealed that especially distinct concentrations of methanethiol can positively or negatively influence creamy perception (Hernández 2007). In milk fat, semi-volatile long-chain *δ*-tetradecalactone, *δ*-hexadecalactone, and *δ*-octadecalactone affect sensory creamy taste (Schlutt et al. 2007). The aroma and taste of a fat-containing milk dessert could be re-engineered as complete flavour recombinant in a triacylglyceride-free lipid-like matrix (Utz et al. 2021). From a texture point of view, the melting and lubrication behaviour between the palate and tongue of fat in foods add to the creamy mouthfeel (Liu et al. 2016b; Cheftel and Dumay 1993). The lubrication behaviour can be generated by microparticles made of proteins. Protein microparticles are protein aggregates produced by heating and shearing in the size range of micrometres. These microparticles, with the right size and structural characteristics, can generate a ball-bearing effect (Liu et al. 2016b; Kew et al. 2020). To generate this ball-bearing effect a particle size between 1 – 10 µm is targeted for whey proteins (Wolz et al. 2016a; Yan et al. 2021; Spiegel 1999b). Next to size, also hardness and shape play an important role. The softer and rounder the particles, the bigger the particles can be to be still perceived as creamy and not as gritty (Engelen et al. 2005). A number of studies have dealt with the incorporation of whey protein microparticles in fat-reduced food (Aggarwal et al. 2016; Temiz and Kezer 2015; Schädle et al. 2020; Torres et al. 2011; Akin and Kirmaci 2015; El-Aidie et al. 2019; Steffl et al. 1999). Egg white protein microparticles have been incorporated in salad dressing (Liu et al. 2018a) and also soy protein egg white mixture microparticles have been analysed in a model liquid (Zhang et al. 2020b). Those microparticles showed promising results regarding the impact on the sensory and texture performance of the food product.

With increasing awareness of sustainability, plant proteins are of high interest (Janssen et al. 2016). Sussmann et al. (2013b) analysed the suitability of lupin protein micelles from extraction from lupin flakes as a fat replacement. There is a lack of knowledge concerning the application of plant protein microparticles, such as pea and potato. In an earlier study, pea and potato protein microparticulation was compared with whey protein microparticulation using a rheometer (Tanger et al. 2021b). In contrast to the well-described whey protein microparticulation process starting from native, individual proteins, commercial pea protein microparticulation followed a top-down process, where larger aggregates stemming from the effects of previous processing history, were broken down into smaller pieces. These larger aggregates were then recombined into newly created particles. Potato protein microparticulation followed a similar bottom-up process compared to whey protein. However, the process resulted in smaller aggregate size and more than 60% fewer covalent protein bonds within the aggregate. From these results, it could be hypothesized that both potato and pea protein microparticles could induce a ball-bearing effect and add a supporting creamy texture to a food product. However, pea and potato protein microparticles differ in structure and therefore are hypothesized to have different effects on food structure. In another study (Tanger et al. 2021c), pea protein microparticles were generated using extrusion cooking and applied in a model milk dessert. It could be shown that fat reduction of 50% did not result in a decrease in creamy perception. However, one of the challenges arising was the increased grassy, green, bean-like off-flavour in the milk dessert by incorporation of pea protein microparticles. Drying of the microparticles prior to integration in the dessert formula was shown to decrease the grassy, green, bean-like off-flavour, but could not fully remove the off-flavour. Textural analysis of the incorporation of pea protein microparticles on the texture of the milk dessert compared to the full-fat milk dessert was not addressed in this work. Potato protein microparticles were not studied regarding the sensorical performance of compensating the effect fat reduction by adding potato protein microparticles. To summarize, there is knowledge about the microparticulation process and microparticle characteristics of pea and potato protein. In addition, there is no study on their impact on food texture. For potato protein microparticles as a fat replacer, it is unclear how flavour and aroma are affected.

This study tries to close these knowledge gaps. Therefore, pea and potato protein microparticles were produced using extrusion cooking to generate sufficient amounts of sample material. The resulting microparticles were incorporated in a model milk dessert and their influence on texture was tested rheologically and using a texture analyser. No drying step was included to compare pea and potato protein microparticles head-to-head without the additional influence of drying. Since pea and potato protein both resulted in different microparticle characteristics, their impact on texture was hypothesized to alter the original texture of the milk dessert and potato and pea protein milk desserts are significantly different in texture. Pea protein microparticles were shown to induce a grassy, green, bean-like off-flavour (Tanger et al. 2021c), which is compared in this study head-to-head to the flavour profile of the potato protein milk dessert. Since potato does not belong to the family of leguminosae, the flavour profile is hypothesized to deviate to the one of pea protein microparticle milk dessert. For a

detailed explanation of the flavour profile of pea and potato protein milk dessert, an quantification of important dairy odorants and tastants (Utz et al. 2021) was added.

3.7.2 Material and Methods

3.7.2.1 Materials

Pea protein isolate (E86) was kindly donated by Emsland Stärke (Emsland Stärke, Emlichheim, Germany). It contained 70.8% protein on a dry basis. Potato protein isolate (Solanic 200) was kindly donated by Avebe (Avebe, Veendam, Netherlands) and contained 75.5% protein on a dry basis. Patatin content was 60% of total protein determined by SDS-PAGE (data not shown). The protein content of the protein powders was analysed using the Dumas method with a Vario MAX cube (Elementar Analysensysteme GmbH, Langenselbold, Germany). A conversion factor of 5.4 was used for both pea protein and potato protein (Mariotti et al. 2008). The mineral composition of the two protein powders can be found in Table 3-15. Mineral composition was analysed using flame photometry.

Table 3-15: Mineral composition (g/kg) of the protein powders used (Tanger et al. 2021b).

	Na^+	K^+	Ca^{2+}
Pea protein isolate	7.94	0.24	0.87
Potato protein isolate	7.52	2.78	0.07

Water used was demineralized or for chromatography purified using a Milli-Q water advantage A10 water system (Millipore, Molsheim, France). The following compounds were purchased from Sigma Aldrich (Steinheim, Germany), if not specified in brackets: 3-nitrophenylhydrazine hydrochloride (3-NPH), pyridine, N-(3-(dimethylamino)-propyl)-N′-ethylcarbodiimide hydrochloride (EDC), formic acid, D2O, N-ethylmaleimide (NEM), triethylamine (TEA), methanol, ethanol, ethyl acetate, hexanal, hexanal-d12, trans-2-octenal, acetaldehyde, acetaldehyde-d3, diacetyl, diacetyl-d6 (CDN Isotopes, Pointe-Claire, Canada), acetoin, butyric acid, sodium butyrate-13C4, 2-methylbutyric acid (Fluorochem, Hadfield, UK), 3-methylbutyric acid, pentanoic acid, hexanoic acid (Merck KGaA, Darmstadt, Germany), hexanoic acid-d3, octanoic acid, octanoic acid-d15, nonanoic acid, decanoic acid, decanoic acid-13C, dodecanoic acid, tetradecanoic acid, phenylacetic acid, phenylacetic acid-13C2, benzaldehyde, vanillin, vanillin-d3, δ-dodecalactone-d2 (aromaLAB, Martinsried, Germany), δ-tetradecalactone, δ-hexadecalactone (aromaLAB), δ-octadecalactone (aromaLAB), sodium thiomethoxide, dimethyl sulfide, dimethyl sulfide-d6, acetic acid, and sodium acetate-13C2. Solvents (acetonitrile, isopropyl alcohol) used for UHPLC-MS/MS analysis were of LC-MS grade (Honeywell, Seelze, Germany). All other chemicals were of analytical grade and purchased from regular suppliers.

3.7.2.2 Microparticulation of pea and potato protein

Protein microparticles were produced using a twin-screw extruder (ZSK25, Coperion, Stuttgart, Germany) with a screw diameter of 25 mm, a smooth barrel, and a total

length of the screw of 28D. The screw profile was the same as for whey protein microparticulation (Wolz et al. 2016a). A powder mass flow of 4 kg / h, a water mass flow of 14 kg / h was used and a screw speed of 800 rpm. For pea protein, extruder barrel temperature was set to 130°C and for potato protein, extruder barrel temperature was set to 80°C. The pH value of the pea protein mixture was 7.5 and for potato protein, it was pH 6.9.

3.7.2.3 Analysis of protein particles

The particle size of the microparticles was measured using a mastersizer equipped with a Malvern Mastersizer Hydro 2000S measurement unit (Malvern Panalytical, Malvern, Worcestershire, UK). Before measurement, the samples were diluted to a 1% solution. Particle size was calculated using the Mie theory. A refractive index of 1.45 was used for the dispersed phase and a refractive index of 1.33 was used for the dispersant medium. For the protein solution, an absorbance of 0.001 was used (McCarthy et al. 2016).

Additionally to the size, the protein-protein interactions were analysed based on the protein interaction assay described by Tanger et al. (2021a). In short, 0.5 g of microparticulated samples was disperesed in 20 g of 50 mM phosphate buffer at pH 7.5 (B_1), 50 mM phosphate buffer at pH 7.5 with 2 g/l sodium dodecl sulfate (SDS) (B_2), and 50 mM phosphate buffer at pH 7 with 2g/l SDS and 15 g/l dithiothreitol (DTT) (B_3). Buffer B_1 cleaves all electrostatic interactions, B_2 cleaves additionally all hydrophobic interactions, and B_3 cleaves all interactions including disulfide bonds. The samples were dissolved overnight in a shaker (LAUDA-GFL Gesellschaft für Labortechnik GmbH). After that the soluble proteins were separated from the unsoluble and uncleaved microparticles by centrifugation at 10 000 g for 20 min at 20°C. The nitrogen content of the supernatant was determined using the Dumas method with the Vario MAX cube (Elementar Analysensysteme GmbH, Langenselbold, Germany), which was used to calculate the amount of stabilizing protein interactions. The following equations were used to determine electrostatic (ES), disulfide (SS) and hydrophobic (Hy) interactions:

$$C_{n,bond,Bi} = \frac{(m_S + m_{mp})}{m_{mp}} * C_{n,sup,Bi} \tag{3-34}$$

$$\frac{C_{n,bond,B1}}{C_{n,mp}} = P(ES) \tag{3-35}$$

$$\frac{C_{n,bond,B2}}{C_{n,mp}} = P(ES) + P(Hy) \tag{3-36}$$

$$\frac{C_{n,bond,B3}}{C_{n,mp}} = P(ES) + P(Hy) + P(SS) \tag{3-37}$$

$$P(Hy) = \frac{C_{n,bond,B2}}{c_{n,mp}} - \frac{C_{n,bond,B1}}{C_{n,mp}} \tag{3-38}$$

$$P(SS) = \frac{C_{n,bond,B3}}{C_{n,mp}} - \frac{C_{n,bond,B2}}{C_{n,mp}} \tag{3-39}$$

With m_S being the initial mass (20 g), m_{mp} being the mass of the sample (0.5 g) and $C_{n,sup,Bi}$ being dissolveld nitrogen in the supernatant in [%], $C_{n,mp}$ being the nitrogen

content of the microparticle in [%] . $C_{n,bond,Bx}$ is the concentration of cleaved protein bonds by the respective buffer.

3.7.2.4 Milk dessert production

The resulting microparticles were applied in a model milk dessert (MD) for testing their functionality as a fat replacer. The application of microparticles has mostly been studied in dairy products (Kew et al. 2020). The reference model milk dessert contained 45% full-fat cream, 47% 0.1% fat yoghurt, 7% sugar and 1% HAMULSION® stabilizer system (Tate & Lyle, London, UK). The calculated amount of fat, protein, carbohydrates, and energy density from the specifications of the used ingredients are shown in Table 3-16. For fat 9 kcal/g and for protein and carbohydrates 4 kcal/g were assumed.

Table 3-16: Nutritional value of the full-fat milk dessert and the two fat-reduced milk desserts.

	Energy density [kcal / g]	Fat [g / 100 g]	Protein [g / 100 g]	Carbohydrates [g / 100 g]
Full- fat milk dessert	1.89	15	3.42	10
Fat reduced Pea	1.34	7.84	6.60	9.30
Fat reduced Potato	1.35	7.84	6.83	9.30

Ingredients were whipped and mixed using a household kitchen machine KitchenAid (Whirlpool Corporation, Benton Harbor, USA) at the highest power. Two fat-reduced milk desserts were tested. One where 50% of the cream was substituted with pea protein microparticles (Pea MD) and the other one where 50% of the cream was substituted by potato protein microparticles (Potato MD). 50% fat reduction was chosen to test a measurable fat reduction of the food. The fat reduction of 50% led to a decrease in energy density of 30%. The milk desserts were stored at 4°C and produced on the same day of analysis.

3.7.2.5 Texture profile analysis (TPA)

The textural properties of the milk dessert were analysed using a texture profile analyzer TA.XT plus (Stable Micro Systems Ltd, Godalmin, UK) with a 500 g load cell. 35 g of the milk desserts were scooped in a glass dish with a 7 cm diameter and stored at 4°C and were taken from the cooling chamber at least 1 h before measurement. An acrylic glass cylindrical probe (diameter: 25 mm) compressed the milk dessert to a depth of 8 mm with a test speed of 0.5 mm/s and a trigger force of 0.05 N. In the pretest, no breakage force was detected. The firmness, adhesiveness, rebuild structure and cohesiveness are documented. Measurement was performed in 5 fold from two milk desserts.

3.7.2.6 Rheological analysis of the milk desserts

The rheological properties of the three different milk desserts were tested rheologically using an MCR 702 (AntonPaar, Graz, Austria) with a plate-plate geometry (PP50 diameter: 50 mm). The temperature was set to 20°C during the whole measurement. For temperature equilibration samples were stored at room temperature for at least 1 h.

Samples were scooped on the plate and then trimmed. The gap between plate and plate was set to 1 mm. After 1 min of equilibration time rheological measurement started. A frequency sweep was performed followed by an amplitude sweep. The frequency sweep was applied over a range of 0.1 to 100 rad / s with an amplitude strain of 0.02. Between frequency sweep and amplitude sweep a resting phase of 5 min was set. The amplitude strain was performed over a range of 0.01 to 100% with a frequency of 10 Hz. Storage modulus (G') and loss modulus (G'') were determined for each measurement. Measurement was performed in 3 fold from two milk desserts.

3.7.2.7 Sensory analysis

3.7.2.7.1 General Conditions and Panel Training

Eight female and seven male panellists (23 – 38 years old), who had given their informed consent to participate in the sensory tests of the present investigation and had no history of known disorders, participated in this study. Each panellist joined a weekly training session for at least two years to become familiar with aroma and taste terminology and the methodologies used. Panel training was conducted according to Utz et al. (2021). All sensory analyses were performed in an air-conditioned room at 22 − 25 °C.

3.7.2.7.2 Comparative Flavor Profile Analysis

To characterize the (orthonasal) aroma and taste profiles of plant-based microparticles (pea, potato) within the milk desserts, a comparative quantitative descriptive analysis (QDA) was conducted according to Stone and Sidel (2012) and Utz et al. (2021). Taste: To avoid cross-modal interactions with odorants nose clips were used during taste profile analysis. After rinsing their mouth with bottled water, the intensities of the taste attributes (sweetness, sourness, umami, saltiness, bitterness, astringency, creaminess, mouthfullness, and kokumi) were judged by all panellists on a linear scale from 0 (not detectable) to 5 (very intense) in comparison to the milk dessert reference as a control. Aroma: To evaluate the aroma profiles off all products, the panellists were asked to compare the intensities of the aroma attributes fatty, sour, rancid, vanilla-like, milk-like, and grassy/green/bean-like on a linear scale from 0 (not detectable) to 5 (very intense). Thereby, the intensities of all attributes were evaluated for the fat-reduced prototypes (7.5% potato/pea protein) in comparison to the reference (the milk dessert bearing a native fat content of 15%). Data was acquired by the FIZZ sensory analysis software (Biosystems, Dijon, France) and evaluated with Excel 2016 (Microsoft, Redmond, US) and Origin 2018b 9.55 (OriginLab Corporation, Northampton, US).

3.7.2.8 Quantification of important dairy odorants and tastants

By using recently published UHPLC-MS/MS, HS-SPME-GC-MS and qHNMR methods,(Utz et al. 2021) the presence and concentrations of potentially important dairy odorants, semi-volatiles and tastants could be analysed:

3-NPH-UHPLC-MS/MS analysis: For stable isotope dilution analysis (SIDA), the following isotopically labeled internal standard (IS) mixture was diluted in acetonitrile/water (50:50, v/v): hexanal-d_{12} (0.9 µg/mL), acetaldehyde-d_3 (2.1 µg/mL), diacetyl-d_6 (22.2 µg/mL), sodium butyrate-$^{13}C_4$ (14.0 µg/mL), hexanoic acid-d_3 (6.2 µg/mL),

octanoic acid-d_{15} (8.1 µg/mL), decanoic acid-^{13}C (44.3 µg/mL), phenylacetic acid-$^{13}C_2$ (3.0 µg/mL), vanillin-d_3 (0.6 µg/mL), and sodium acetate-$^{13}C_2$ (4.3 µg/mL). Aliquots (40 mg) of the milk dessert samples were equilibrated with 20 µL of the IS mixture and derivatized with a solution of 3-NPH (20 µL, 200 mmol/L) in acetonitrile/water (50:50, v/v) and a solution of EDC (20 µL, 120 mmol/L) in acetonitrile/water (50:50, v/v, 6% pyridine) for 30 min at 40 °C. After dilution to a volume of 1 mL with acetonitrile/water (50:50, v/v), 1 µL of the membrane-filtered samples were analyzed via UHPLC-MS/MS. To calculate IS calibration curves, stock solutions of hexanal (89 µg/mL), *trans*-2-octenal (78 µg/mL), acetaldehyde (1.2 mg/mL), diacetyl (76 µg/mL), acetoin (2.0 mg/mL), butyric acid (182 µg/mL), 2-methylbutyric acid (82 µg/mL), 3-methylbutyric acid (83 µg/mL), pentanoic acid (98 µg/mL), hexanoic acid (199 µg/mL), octanoic acid (177 µg/mL), nonanoic acid (104 µg/mL), decanoic acid (1.0 mg/mL), dodecanoic acid (1.1 mg/mL), tetradecanoic acid (1.1 mg/mL), phenylacetic acid (96 µg/mL), benzaldehyde (88 µg/mL), vanillin (93 µg/mL), and acetic acid (207 µg/mL) in acetonitrile/water (50:50, v/v) were diluted one-to-two resulting in 15 calibration solutions. Each calibration solution (40 µL) was spiked with 20 µL of the IS mixture and further prepared as described above.

UHPLC-MS/MS analysis of *δ*-lactones: The milk dessert samples (5 g) were analyzed via SIDA and equilibrated with 80 µL of a solution of *δ*-tetradecalactone-d_2 (IS, 28.9 µg/mL) in ethyl acetate. After centrifugation (10,000 rpm; 10 min) the aqueous phase was disposed and the residue was extracted with ethyl acetate (3×5 mL) The filtered extracts were separated from solvent in vacuum, re-collected in 4 mL of ethyl acetate and freezed for 2 h at – 20 °C. After triacylglyceride removal (10,000 rpm; - 11 °C; 10 min) 1 µL of the membrane-filtered supernatants were analyzed by UHPLC-MS/MS. For quantitation, IS calibration curves were calculated diluting the stock solutions of *δ*-tetradecalactone (4.1 mg/mL), *δ*-hexadecalactone (0.3 mg/mL) and *δ*-octadecalactone (1.0 mg/mL) in ethyl acetate by one-to-two steps (15 calibration solutions) and mixing each calibration solution (735 µL) with the IS (15 µL).

HS-SPME-GC-MS analysis: The milk dessert samples (1-2 g) were diluted with water (6 mL) for methanethiole quantitation (standard addition approach) and for dimethyl sulfide quantitation spiked with 1.5 mL of dimethyl sulfide-d_6 (IS, 0.01 µg/mL; SIDA). After an equilibration periode of 2 h the samples were measured by means of HS-SPME-GC-MS. Methanethiole was extracted via on-fiber derivatization using *N*-ethylmaleimide and triethylamine (NEM/TEA; 30:70, w/w),(Frerot et al. 2014) while dimethyl sulfide could be directly extracted from the headspace. Based on final concentrations of 0.01 µg/mL of methanethiole or dimethyl sulfide in water, five calibration solutions were produced at ratios of 0.2-5.

qHNMR analysis: For an exhausting extraction of sucrose, lactose, galactose, citric and lactic acid, the milk dessert samples (2 g) were extracted with 0.1% formic acid in water (3×2.5 mL) using the Precellys Super Homogenizer (Precellys® Evolution, bertin Technologies, Montigny-le-Bretonneux, France). The solutions were centrifugated (4,400 rpm; 5 min), the supernatant collected and adjusted to an end volume of 100 mL with 0.1% formic acid in water. 540 µL of the membrane-filtered supernatant was

mixed with 60 µL of D_2O in a qNMR tube and analysed by quantitative ^1H NMR analyses according to literature (Frank et al. 2014).

Detailed sample preparations, validation and UHPLC-MS/MS, GC-MS and qHNMR parameters can be taken from the original work of Utz et al. (2021).

All qFor heatmap visualisation all quantified concentrations were finally divided by their odour or taste thresholds, recorded in oil,(Utz et al. 2021; Neugebauer et al. 2020; Welke et al. 2014; Zhou et al. 2019; Dunkel and Hofmann 2009; Stark et al. 2006) and expressed as odour activity values (OAV) or dose over thresholds (DoT). The odour threshold of nonaoic acid had to be determined first in commercially available, odorless sunflower oil, as reported recently (Czerny et al. 2008; Kreissl et al. 2019).

3.7.2.9 Statistical analysis

All experiments were performed in at least triplicate from two different milk desserts. Curves were plotted using OriginPro 2019 (originLAb Coorperation, Northampton, USA). Mean values are shown in the graphs. Error bars indicate the upper and lowest value as not indicated otherwise. The dotted line serves as a guide to the eye. A one-way analysis of variance (ANOVA) for the significant difference was performed using JMP Pro (SAS Institute Inc., ver. 14). The ANOVA was followed by a Tukey-Kramer (HSD) test and a Dunnett's test with the full-fat milk dessert as reference. Minimum significance was set to 5% level ($p < 0.05$). The OAV/DoT heatmap was performed using R (version 4.0.4) and the package "ComplexHeatmap" (R Core Team 2021; Gu et al. 2016).

3.7.3 Results and discussion

3.7.3.1 Particle size and protein-protein interaction of microparticles

The particle size of the used pea protein and potato protein particles are shown in Figure 3-49.

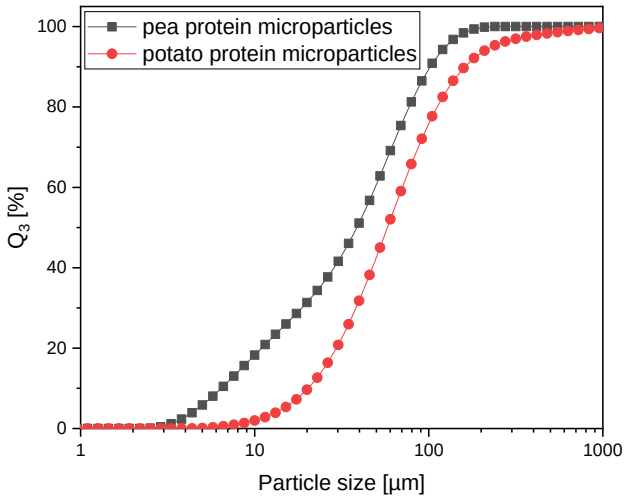

Figure 3-49: Cumulative particle size distribution of pea and potato protein microparticles.

Particle size ranged from 3 µm to 100 µm for pea protein microparticles and 9 µm to 110 µm for potato protein microparticles. This is similar to the particle sizes found in the thermo-mechanical treatment of pea and potato protein using a rheometer (Tanger et al. 2021b). For potato protein, the particle size was slightly higher than the one of the small scale experiments. This can be explained by the higher reactivity of the potato protein and higher protein concentration necessary for extrusion (17%) compared to thermo-mechanical treatment using a rheometer (10%) (Schmidt et al. 2019; Creusot et al. 2011).

Besides size also the protein-protein interaction in the particles is of interest. Figure 3-50 shows the protein-protein interaction within the microparticles found by the protein interaction assay.

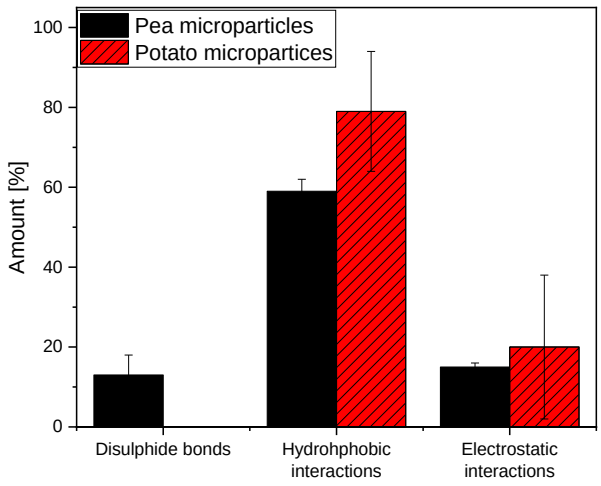

Figure 3-50: Protein-protein interactions within pea and potato protein microparticles.

The particles were mainly held together by hydrophobic interactions. Potato protein did not show any covalent bonds, whereas pea protein did show a minor part of 10-20% disulfide bonds. This is in line with findings in an earlier study, where microparticles were created using a rheometer (Tanger et al. 2021b). Microparticles from whey protein were found to be mainly stabilized via covalent bonds (Tanger et al. 2021b). The high amount of non-covalent bonds, also makes the pea and potato protein microparticles softer than the covalently bound whey protein microparticles. Therefore, pea and potato protein microparticles can be bigger than whey protein microparticles and still be perceived as creamy. The particle size threshold from which the particles are perceived as gritty is dependent on the hardness of the particle (Engelen et al. 2005). The particle size and the protein-protein interaction in the particles would render the created pea and potato protein a suitable fat replacer in theory. In the following, the effect of the application of the pea and potato protein in a milk dessert is tested texturally and sensorically.

3.7.3.2 Impact of replacement of fat by pea and potato protein microparticles on textural properties

Pea and potato protein microparticles were used to replace 50% cream in a milk dessert and therefore also 50% fat. Textural properties of the three milk desserts were analysed using a texture profile analysis with a texture analyser and a frequency sweep and amplitude sweep using a rheometer. Analysis with the texture analyser gives information about macroscopic deformation, whereas rheological measurements give more information about non-perceptible deformation, which give hints about the molecular interactions (Schmidt et al. 2019). The hardness of the milk dessert is defined as the maximum peak force during compression in a texture analyser. The hardnesses of the three milk desserts are shown in Figure 3-51.

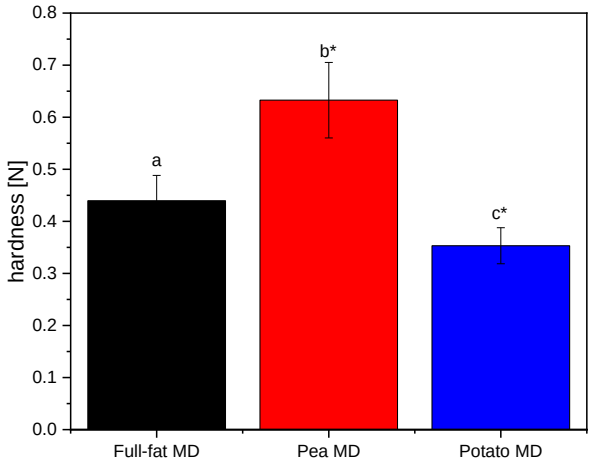

Figure 3-51: Hardness of the full-fat milk dessert and the fat-reduced milk desserts containing pea protein microparticles and potato protein particles. [a-c] different letters indicate significant difference($p < 0.05$) * indicates significant difference to the full-fat milk dessert.

By the reduction of fat and incorporation of microparticles, hardness is affected. The hardness is lowest for potato protein milk dessert and highest for pea protein milk dessert. Akin and Kirmaci (2015) also found a lower hardness, with the incorporation of Simplesse100 and Maltrin M040, two whey protein-based microparticles. In line with our findings for potato protein milk dessert, the incorporation of fat replacers based on aggregated whey protein in Edam cheese manufactured from buffalo's milk led to a decreased firmness (El-Aidie et al. 2019). The decreased hardness and firmness was explained by the high water holding capacity and moisture content of the fat replacer used. Baune et al. (2021) found that the protein type had a significant impact on the hardness of a protein emulsion. In their study, potato protein emulsions exhibited a higher hardness compared to pea protein. However, they used the protease inhibitor fraction of potato protein, whereas in this study mainly the patatin fraction is used.

Other texture attributes as body, adhesiveness, creaminess and cohesiveness are shown in Figure 3-52.

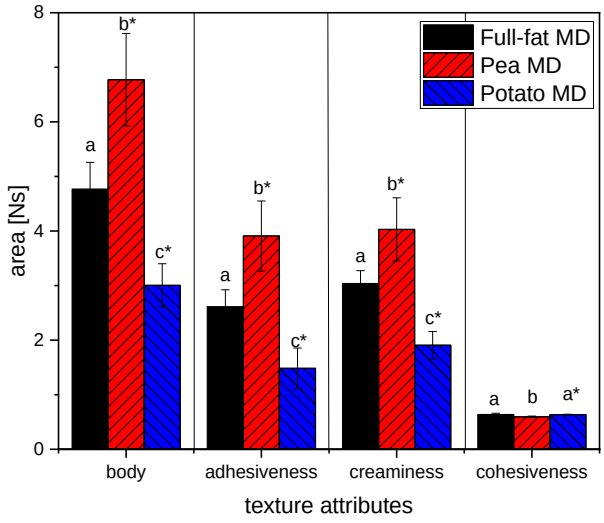

Figure 3-52: Body, adhesiveness, creaminess and cohesiveness of the full-fat milk dessert and the two fat-reduced milk desserts. [a-c] different letters indicate significant differences within one attribute ($p < 0.05$) * indicates significant difference to the full-fat milk dessert within one attribute.

It can be seen that there are significant differences in texture between the full-fat milk dessert and the fat-reduced milk dessert, but also between the two different fat-reduced milk desserts. The body, adhesiveness and creaminess increased for pea protein milk dessert and decreased for potato protein milk dessert. Cohesiveness only changed significantly for pea protein milk dessert. Both protein sources impacted the texture differently. An influence on fat replacement type on the change in texture has also been seen in cheese products (Akin and Kirmaci 2015; El-Aidie et al. 2019) and can be explained by their different building structure.

To get a better insight into the molecular interactions, the three milk desserts have been analysed rheologically using a frequency sweep and an amplitude sweep. The frequency sweep is shown in Figure 3-53.

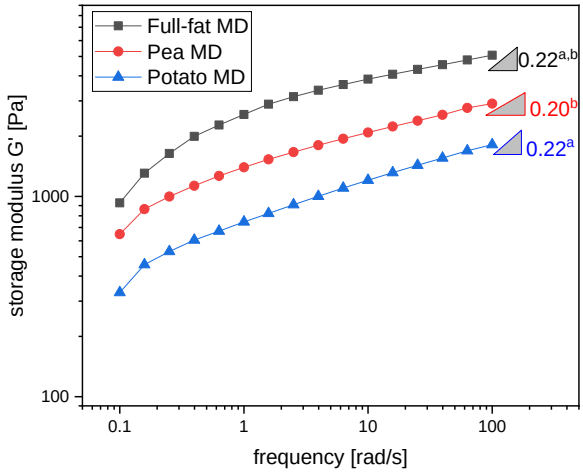

Figure 3-53: Storage modulus as a function of frequency for the three milk desserts. The slope of the curve is given behind the triangle. [a-b] different letters indicate significant difference ($p < 0.05$)

The storage modulus is significantly higher for full-fat milk desserts than for fat-reduced milk desserts. There is no significant difference in the dependence of the frequency between the full-fat milk dessert and the two-fat reduced milk dessert. However, the two fat-reduced milk desserts were significantly different in frequency dependence. Potato milk dessert shows a significantly higher frequency dependence than the pea milk dessert. A lower frequency dependence and a higher storage modulus G' indicate that the full-fat milk dessert and the pea milk dessert are more gel-like than the potato milk dessert meaning that stabilizing interactions are higher. Zhang et al. (2020b) found that soy and egg white protein microparticles showed a frequency dependency and therefore acted as viscous liquids. They also found the higher the number of disulphide bonds within the particle the more heat-stable the particles. Potato protein microparticles have a very low amount of disulphide bonds, which might lead to interactions of the microparticles with other ingredients in the milk dessert. Urgu et al. (2019) found that the incorporation of whey protein microparticles reduced the firmness and viscosity of cheese emulsions using rheological measurements. In addition, they also found that the amount of incorporated microparticles impacted the texture. Baune et al. (2021) also found a higher frequency dependence for potato protein emulsions than pea protein emulsions.

For a complete view of the texture of the three milk desserts, the amplitude sweep is shown in Figure 3-54.

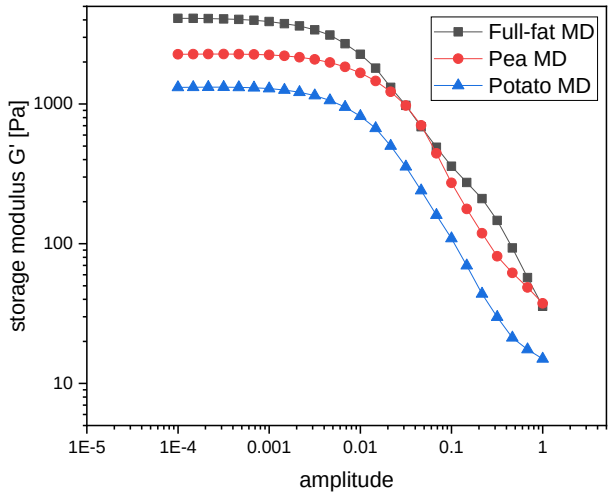

Figure 3-54: Storage modulus G' as a function of amplitude for the full-fat milk dessert and the two fat-reduced milk desserts.

Disregarding the higher storage modulus of the full-fat milk dessert, the course of the storage modulus with increasing amplitude is quite similar between the full-fat milk dessert and the two fat-reduced milk desserts. The end of the linear viscoelastic region is significantly different, however only has a small range from 0.0106 for the full-fat milk dessert and 0.0185 for pea milk dessert. There is also no significant difference in the yield point (G' = G''), which varies between 0.1056 and 0.1400.

Summarizing, the results show that the replacement of fat with pea and potato microparticles changes the texture of the milk dessert significantly. This impact of fat reduction by whey protein microparticles has also been found in cheese products (Akin and Kirmaci 2015; El-Aidie et al. 2019; Urgu et al. 2019) and yoghurt (Sandoval-Castilla et al. 2004). In ice cream, the fat replacement of whey protein led also to a decrease in melting time and stability of the ice cream (Koxholt et al. 1999). Soy protein microparticles have also been found to enhance foam and emulsion stability (Matsumiya and Murray 2016). In fat-reduced yoghurt small particles ($d_{90,3}$ < 50 µm), a high viscosity (τ < 100 s^{-1} > 80 s^{-1}), and a low friction (µ < 1 mm s^{-1} < 0.3) could generate a similar creamy mouthfeel than full-fat yoghurt (Sonne et al. 2014). There is also a significant difference between pea and potato protein microparticles. Pea protein microparticles have more disulphide bonds than potato protein microparticles. The higher the number of disulphide bonds the more stable is the particle (Zhang et al. 2020b). For β-lactoglobulin particles, it has been found that a high degree of covalent cross-links increases foam stability (Kurz et al. 2021). In another study, it has been found that pea protein forms a protein-stabilized emulsion gel in comparison to the protease inhibitors of potato protein, which form an emulsion-filled protein gel, which could also explain the results found in this study (Baune et al. 2021). However, also other parameters such as charge and surface hydrophobicity, which are influenced by the ionic environment and pH, have an impact on foam stability and emulsion stability. In addition, also moieties of sugars and other plant extracts might influence the foaming behaviour and interactions in the milk dessert, which have not been analysed in this research.

Even though 50% of the fat has been replaced the milk dessert did not lose its complete texture. The textural analysis gives us some information on the impact of the replacement of fat by pea and potato protein microparticles. From the textural results, it could be hypothesized that pea protein milk dessert will rate higher in creaminess compared to potato protein milk dessert in sensory evaluation. However, as already mentioned also flavour and aroma play an important role in perceived creaminess, which cannot be measured texturally. In addition, for plant protein also off-flavours are of interest, which is discussed in the following.

3.7.3.3 Comparative Flavor Profile Analysis

To get a better sensory understanding of flavour changes arising by the introduction of pea and potato protein into the milk dessert, comparative flavour profile analyses were conducted. Figure 3-55 shows the sensory results of the full-fat reference and the two fat-reduced milk desserts.

The fat-reduced pea and potato milk desserts were presented to trained sensory panels, which were asked to rate the intensities of the different taste (sweet, sour, umami, salty, bitter, astringent, creamy, mouthfullness, kokumi) and aroma modalities (fatty, sour, rancid, vanilla-like, milk-like, grassy, green, bean-like) on a linear 5-point intensity scale in comparison to the full-fat milk dessert. The highest taste intensities were judged as centring around the creamy, mouthful and sweet sensations.

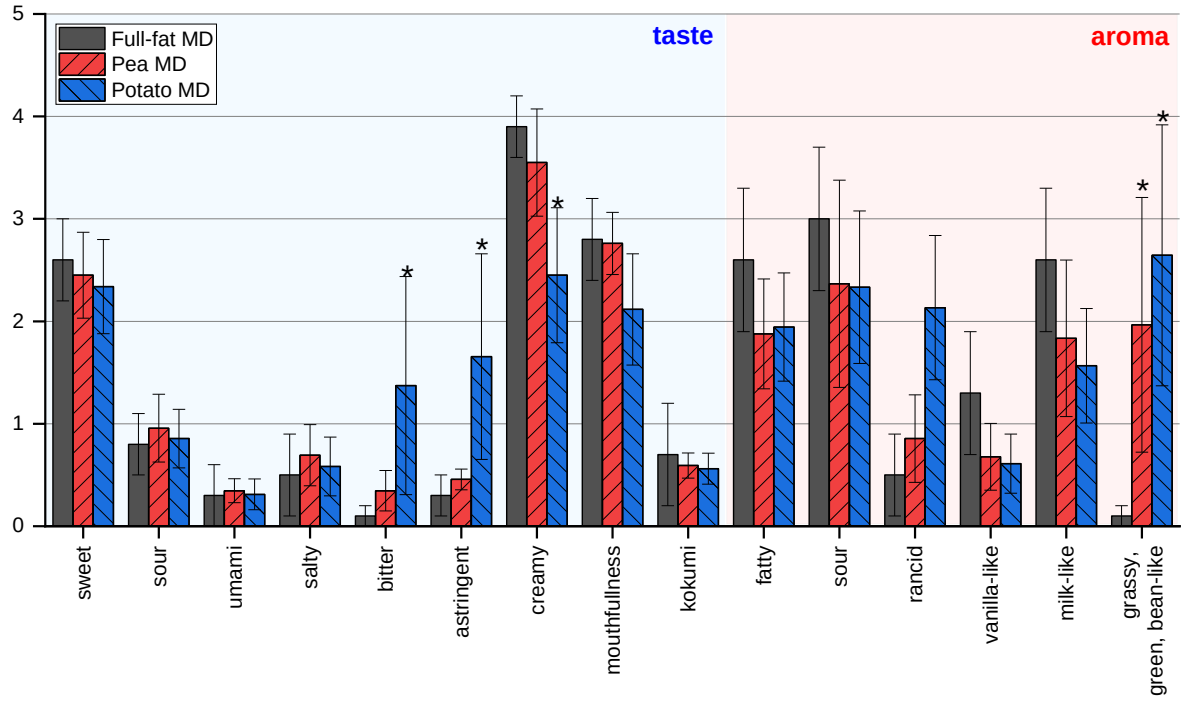

Figure 3-55: Comparative flavour profile analysis of the full-fat milk dessert and the two fat-reduced milk desserts containing pea protein microparticles (Pea MD) and potato protein microparticles (Potato MD). *symbolises a significant difference to the full-fat milk dessert.

In this context, the replacement of 50% fat by pea and potato protein microparticles, had no significant influence on the sweet, sour, umami, salty and kokumi quality. In contrast, undesired bitter and astringent notes increased in the potato milk dessert (Potato MD), while important dairy attributes such as creaminess and mouthfullness simultaneously decreased. In both cases, the effects for the pea milk dessert (Pea MD) were less distinctive and insignificant, and more pronounced when Potato MD was tested in comparison to the full-fat MD finally leading to significant differences in bitterness, astringency, and creamy taste. In addition, on the one hand, aroma profile analysis revealed an intensity decrease for the attributes fatty, sour, vanilla- and milk-like for both prototypes containing plant-based proteins (Pea and Potato MD). On the other hand, rancidity and grassy, green, bean-like off-flavours increased, especially when potato proteins were used. The perceived grassy, green, bean-like aroma, however, resulted for both cases in significant differences compared to the full-fat MD.

In summary, it could be highlighted that in comparison to the full-fat MD, the overall taste of Pea MD remained the same, and Potato MD showed clearly adverse differences in bitterness, astringency, and creaminess, respectively. The perception of grassy, green, bean-like off-notes in Pea and Potato MD seemed to be the most challenging problem. Nevertheless, microparticulated pea protein showed promising sensory results. The flavour profiles of milk desserts using microparticulated potato proteins have still to be improved. Besides comparative flavour profile analysis, creaminess was also detected to be decreased during textural measurement in potato milk dessert. As the creamy taste of the pea milk dessert (compared to the full-fat milk dessert) was slightly, but not significant lower, it may be a consequence of the discussed ball-bearing effect (Liu et al. 2016b). Thus, pea protein microparticles may also

enhance the creamy taste. Potato protein microparticles could enhance creamy taste perception to a lower extent, which might be explained by a reduced ball-bearing effect compared to pea protein microparticles and a bigger impact on textural properties of the milk dessert.

3.7.3.4 Quantification of important dairy odorants, semi-volatiles and tastants

Besides sensory experiments, further quantitations were performed in order to explain observed flavour changes and thus, to provide a toolbox for flavour optimization of functional food, produced by microparticulated plant-based proteins.The list of the following dairy volatiles, semi-volatiles and non-volatiles was checked regarding their presence in the full-fat, pea and potato protein milk desserts and identified analytes were consequently quantified by means of stable isotope dilution analyses, standard addition or external calibration with the help of validated LC-MS/MS, HS-SPME-GC-MS or qHNMR measurements (Utz et al. 2021): hexanal, methional, *cis*-3-hexenal, *trans*-2-octenal, *cis*-2-nonenal, *trans*-2-nonenal, *trans,trans*-2,4-nonadienal, *trans,cis*-2,6-nonadienal, *trans,trans*-2,4-decadienal, *trans*-4,5-epoxy-(*E*)-2-decenal, *trans*-2-undecenal, *trans*-2-dodecenal, acetaldehyde, diacetyl, acetoin, 1-hexen-3-one, 1-octen-3-one, butyric acid, 2-methylbutyric acid, 3-methylbutyric acid, pentanoic acid, hexanoic acid, octanoic acid, nonanonic acid, decanoic acid, dodecanoic acid, tetradecanoic acid, phenylacetic acid, benzaldehyde, phenylpropanoic acid, vanillin, 2-aminoacetophenone, sotolon, 2-acetyl-1-pyrroline, 2-acetyl-2-thiazoline, δ-tetra- (δ-C14L), δ-hexa- (δ-C16L), δ-octadecalactone (δ-C18L), methanethiole, dimethyl sulfide, lactose, galactose, sucrose, acetic acid, lactic acid, and citric acid. In the next step, odour activity values (OAV) for odorants and dose over thresholds (DoT) for tastants were calculated by dividing the quantified concentration by its concrete threshold. Doing so, aroma- and taste-active compounds exceeding their thresholds in various extents could be highlighted in one OAV / DoT heatmap (Figure 3-56)

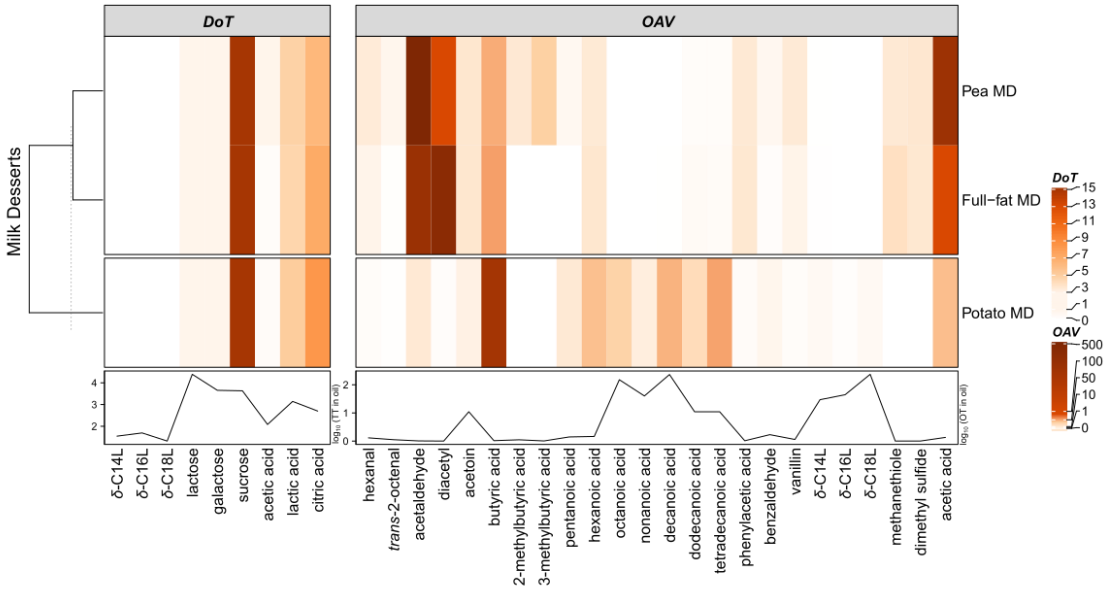

Figure 3-56: Activity-guided heatmap of the full-fat MD, Pea and Potato MD. The left part represents taste- and the right part aroma-activities. Line charts below show taste and odour thresholds of individual analytes used for DoT and OAV calculations.

This also helped to draw conclusions on which analytes might be responsible for the flavour changes of pea and potato MD in comparison to the full-fat reference. Regarding the examined tastants (*δ*-C14L, *δ*-C16L, *δ*-C18L, lactose, galactose, sucrose, acetic acid, lactic acid, and citric acid), the heatmap and cluster analysis revealed that none of them were decisively up- and/or downregulated to each other. Nevertheless, preliminary sensory evaluations highlighted significantly increased bitter-astringent off-taste for Potato MD, while the taste attributes of Pea MD were not perceived significantly different in comparison to the full-fat MD (Figure 3-55). Therefore, it is obvious that the bitter-astringent off-taste and intensified rancidity in potato MD might correlate with increased concentrations and consequently higher OAVs of free fatty acids (FFA) such as the short- and medium-chained butyric, pentanoic, hexanoic, decanoic, dodecanoic, and tetradecanoic acids. According to literature, too high concentrations of decanoic and dodecanoic acid elicited a scratchy instead of fatty taste impression (Galindo et al. 2012). The presence of these high FFA concentrations of can be explained by a still active lipase effect of patatin. The glycoprotein patatin is known for its hydrolase activity towards various substrates such as fatty acids (Spelbrink et al. 2015). As especially milk fat shows high amounts of short-chain triacylglycerides, the in-situ liberation by the still active patatin leads to the detected off-flavour and high short-chain FFA concentrations (Figure 3-57).

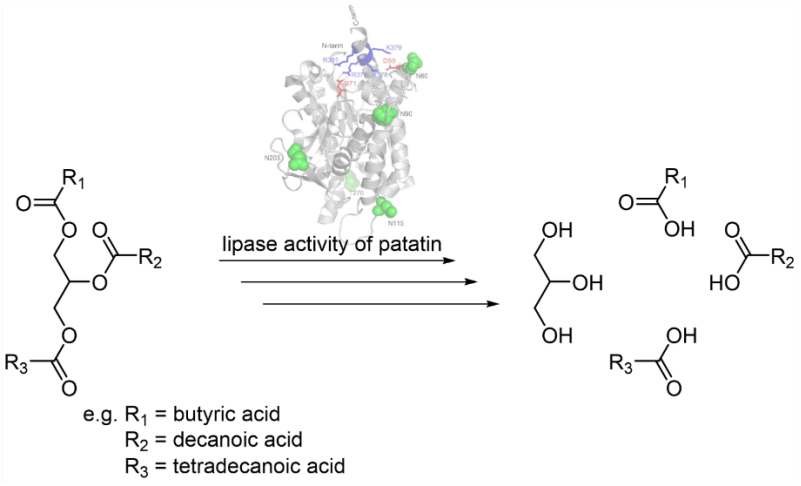

Figure 3-57: In-situ liberation of short-chain free fatty acids such as butyric, decanoic or tetradecanoic acids by still active patatin. Atomic Strucutre of patatin taken from Welinder and Jørgensen (2009).

To counteract the fatty acid liberation, the lipase activity of patatin must be inactivated completely by heat treatment (Spelbrink et al. 2015). However, from the results presented here, it becomes clear that heat-treatment during the extrusion process was not sufficient and there was still some residual lipase activity. If this formation of short-chain fatty acid is controlled, the flavour formation might also be beneficial for the development of cheeses and other fermented products. Another option to inactivate the lipase activity could be an adjustment of the extrusion process or an additional pasteurisation step. Finally, diacetyl, acetaldehyde and methanethiole were reported as important creamy odorants in dairy products (Utz et al. 2021; Hernández 2007) and decreased concentrations thereof might explain lower fatty and milk-like aroma perception of pea and potato MD. Moreover, increased OAVs of hexanal, acetaldehyde,

and 2-/3-methylbutyric acids could be responsible for the grassy, green, bean-like off-flavours. Nevertheless, an entire Sensomics approach has to be performed to clearly explain grassy, green, bean-like aroma changes introduced by microparticulated plant-based proteins and thus, to optimize the overall flavour of functional food.

3.7.4 Influence of pea and potato microparticles on texture and sensory in a fat-reduced milk dessert

This research shows that the incorporation of pea and potato protein microparticles affects the texture and sensory properties of a fat-reduced model milk dessert. Whereas the incorporation of pea protein microparticles led to an increase in hardness, adhesiveness and textural measured creaminess, these attributes were decreased in a potato protein milk dessert. While for the pea protein milk dessert only the grassy, greeny, bean-like aroma was increased, compared to the full-fat reference, the potato protein milk dessert showed additionally more pronounced astringent and bitter taste. This off-taste could be explained by the still active lipase effect of the potato protein resulting in high short-chain free fatty acid concentrations. From a texture point of view, no conclusion can be drawn regarding whether pea or potato protein microparticles are “better” fat replacers. From a sensorical point of view, it can be concluded that the pea protein microparticles were a better fat-replacer in the milk dessert. However, still valuable information about the application of potato protein microparticles was gathered and they might be of interest for other non-dairy food applications, where short-chain fatty acids are released out of triacylglycerides only to a limited extent. Moreover, the microparticulation process could be improved for more sufficient heat treatment or additional processing inactivating lipase activity of the potato protein but also to change protein-flavour binding of pea protein. By doing so, it could beneficially result in a decreased off-flavour and consequently increased consumer acceptability.

Acknowledgements

We would like to acknowledge the help of Annette Brümmer-Rolf and Christine Haas for Elementar measurement. Special thanks to Julia Engel and Michaela Müller for laboratory help and David Andlinger and Marius Reiter for valuable discussion. We would like to thank Marc Laus from AVEBE, Veendam, The Netherlands, for providing the potato protein isolate and Thomas Pruter and Stephanie Schomaker from Emsland Stärke, Emlichheim, Germany, for providing the pea protein isolate and pea flour.

This project was executed as part of an Industrial Collective Research (IGF) project of the Forschungskreis der Ernährungsindustrie e.V., Bonn (FEI) supported by the German Ministry of Economics and Technology via AiF (AiF 20197N).

Conflict of interest

The authors declare that they have no conflict of interest.

3.7.5 Appendix

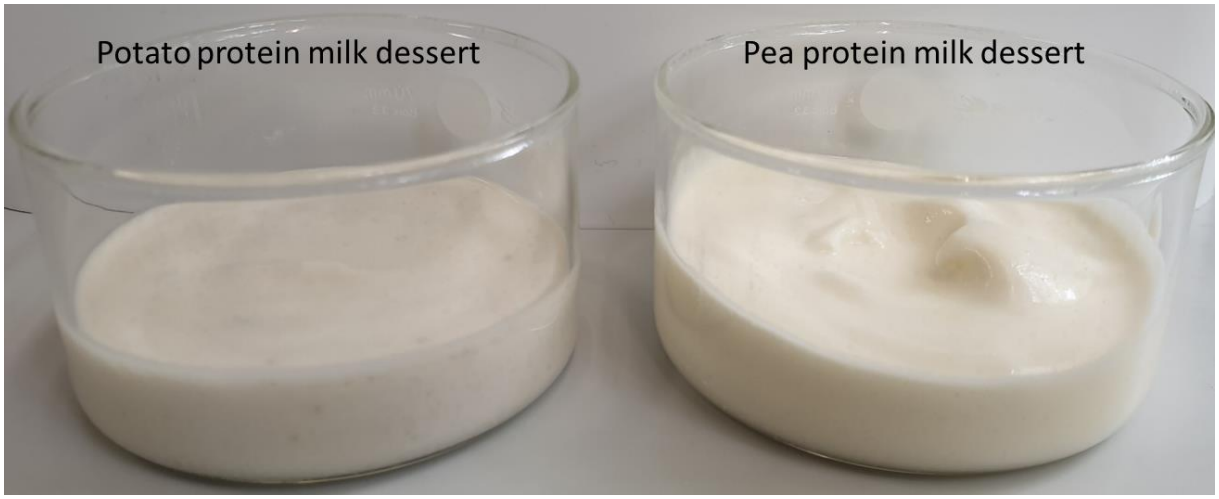

Figure A3-58: Picture of pea and potato protein milk dessert in glass beaker used for texture analysis

3.7.6 Supporting information

MRM transitions of analyzed dairy flavor molecules, IS calibration curves, and raw data of OAV/DoT heatmap.

Table S3-17: MRM transitions of analyzed 3-NPH derivates (adapted from Utz et al. (2021)).

Analyte (number) *qt./ql.*	Ionization	Q1 [*m/z*]	Q3 [*m/z*]	t_R [min]	DP [V]	EP [V]	CE [V]	CXP [V]
hexanal *qt*.	ESI^+	236.1	119.0	8.9	46	10	19	14
hexanal *ql.*	ESI^+	236.1	137.0	8.9	46	10	23	14
(IS) hexanal-d_{12} *qt.*	ESI^+	248.1	120.0	8.9	41	10	21	14
(IS) hexanal-d_{12} *ql.*	ESI^+	248.1	137.0	8.9	41	10	23	16
methional *qt*.	ESI^+	240.1	75.0	7.0	6	10	17	8
methional *ql.*	ESI^+	240.1	139.0	7.0	6	10	11	14
cis-3-hexenal *qt*.	ESI^+	234.1	152.0	8.5	106	10	19	16
cis-3-hexenal *ql.*	ESI^+	234.1	98.1	8.5	106	10	21	14
trans-2-octenal *qt.*	ESI^+	248.1	126.0	10.2	121	10	23	14
trans-2-octenal *ql.*	ESI^+	248.1	137.0	10.2	121	10	25	16
cis-2-nonenal *qt*.	ESI^+	276.2	139.9	10.4	156	10	25	18
cis-2-nonenal *ql.*	ESI^+	276.2	229.1	10.4	156	10	27	16
trans-2-nonenal *qt*.	ESI^+	276.2	140.1	10.5	86	10	23	22
trans-2-nonenal *ql.*	ESI^+	276.2	118.9	10.5	86	10	39	12
trans,trans-2,4-nonadienal *qt.*	ESI^+	274.1	152.0	10.1	1	10	21	16
trans,trans-2,4-nonadienal *ql.*	ESI^+	274.1	207.2	10.1	1	10	15	12
trans,cis-2,6-nonadienal *qt.*	ESI^+	274.1	119.2	9.8	1	10	27	12
trans,cis-2,6-nonadienal *ql.*	ESI^+	274.1	138.2	9.8	1	10	19	10

trans,trans-2,4-decadienal *qt.*	ESI^+	288.1	152.1	10.5	1	10	25	20
trans,trans-2,4-decadienal *ql.*	ESI^+	288.1	221.1	10.5	1	10	17	14
trans-4,5-epoxy-*trans*-2-decenal *qt.*	ESI^+	304.1	286.2	10.3	36	10	15	16
trans-4,5-epoxy-*trans*-2-decenal *ql.*	ESI^+	304.1	158.2	10.3	36	10	31	14
trans-2-undecenal *qt.*	ESI^+	304.2	118.9	11.3	1	10	31	20
trans-2-undecenal *ql.*	ESI^+	304.2	168.0	11.3	1	10	27	20
trans-2-dodecenal *qt.*	ESI^+	318.2	182.2	11.7	1	10	27	8
trans-2-dodecenal *ql.*	ESI^+	318.2	271.1	11.7	1	10	33	16
acetaldehyde *qt.*	ESI^+	180.0	137.0	5.0	1	10	17	16
acetaldehyde *ql.*	ESI^+	180.0	119.1	5.0	1	10	15	12
(IS) acetaldehyde-d_3 *qt.*	ESI^+	183.0	136.8	5.0	6	10	17	18
(IS) acetaldehyde-d_3 *ql.*	ESI^+	183.0	118.9	5.0	6	10	15	12
diacetyl *qt.*	ESI^-	219.9	136.9	5.8	-105	-10	-24	-17
diacetyl *ql.*	ESI^-	219.9	122.0	5.8	-105	-10	-24	-15
(IS) diacetyl-d_6 *qt.*	ESI^-	226.0	137.8	5.7	-10	-10	-26	-21
(IS) diacetyl-d_6 *ql.*	ESI^-	226.0	91.7	5.7	-10	-10	-30	-11
acetoin *qt.*	ESI^-	222.0	136.9	3.6	-70	-10	-20	-13
acetoin *ql.*	ESI^-	222.0	203.9	3.6	-70	-10	-18	-19
1-hexen-3-one *qt.*	ESI^+	234.1	165.0	8.8	156	10	21	18
1-hexen-3-one *ql.*	ESI^+	234.1	118.9	8.8	156	10	31	14
1-octen-3-one *qt.*	ESI^+	262.1	165.2	9.9	56	10	27	20

1-octen-3-one *ql.*	ESI^+	262.1	119.0	9.9	56	10	29	14
butyric acid *qt.*	ESI^-	222.0	136.8	2.2	-85	-10	-26	-15
butyric acid *ql.*	ESI^-	222.0	151.9	2.2	-85	-10	-22	-23
(IS) butyric acid-$^{13}C_4$ *qt.*	ESI^-	226.0	136.7	2.2	-100	-10	-28	-17
(IS) butyric acid-$^{13}C_4$ *ql.*	ESI^-	226.0	151.9	2.2	-100	-10	-22	-19
(IS) butyric acid-$^{13}C_4$ *qt.*	ESI^+	228.1	137.9	2.2	86	10	23	20
(IS) butyric acid-$^{13}C_4$ *ql.*	ESI^+	228.1	91.9	2.2	86	10	23	10
2-methyl butyric acid *qt.*	ESI^+	238.1	137.0	3.1	101	10	23	16
2-methyl butyric acid *ql.*	ESI^+	238.1	101.8	3.1	101	10	23	10
3-methyl butyric acid *qt.*	ESI^+	238.1	138.2	3.2	1	10	23	12
3-methyl butyric acid *ql.*	ESI^+	238.1	102.0	3.2	1	10	23	12
pentanoic acid *qt.*	ESI^+	238.1	136.9	3.4	1	10	23	16
pentanoic acid *ql.*	ESI^+	238.1	102.0	3.4	1	10	23	16
hexanoic acid *qt.*	ESI^-	250.0	137.0	4.9	-125	-10	-36	-15
hexanoic acid *ql.*	ESI^-	250.0	151.8	4.9	-125	-10	-24	-21
(IS) hexanoic acid-d_3 *qt.*	ESI^-	253.1	136.7	4.8	-100	-10	-26	-35
(IS) hexanoic acid-d_3 *ql.*	ESI^-	253.1	151.8	4.8	-100	-10	-24	-37
octanoic acid *qt.*	ESI^-	278.0	136.9	7.2	-150	-10	-30	-17
octanoic acid *ql.*	ESI^-	278.0	151.9	7.2	-150	-10	-26	-17
(IS) octanoic acid-d_{15} *qt.*	ESI^-	293.1	136.7	7.1	-120	-10	-34	-11
(IS) octanoic acid-d_{15} *ql.*	ESI^-	293.1	152.9	7.1	-120	-10	-30	-7

nonanoic acid *qt.*	ESI^-	292.0	136.9	7.9	-110	-10	-30	-19
nonanoic acid *ql.*	ESI^-	292.0	151.9	7.9	-110	-10	-26	-21
decanoic acid *qt.*	ESI^-	306.0	137.0	8.5	-130	-10	-34	-15
decanoic acid *ql.*	ESI^-	306.0	152.0	8.5	-130	-10	-28	-17
(IS) decanoic acid-^{13}C *qt.*	ESI^-	307.1	136.9	8.5	-120	-10	-32	-9
(IS) decanoic acid-^{13}C *ql.*	ESI^-	307.1	151.7	8.5	-120	-10	-28	-21
dodecanoic acid *qt.*	ESI^-	334.0	136.9	9.5	-155	-10	-36	-15
dodecanoic acid *ql.*	ESI^-	334.0	151.9	9.5	-155	-10	-30	-19
tetradecanoic acid *qt.*	ESI^-	362.1	136.9	10.5	-160	-10	-38	-17
tetradecanoic acid *ql.*	ESI^-	362.1	152.0	10.5	-160	-10	-34	-17
phenylacetic acid *qt.*	ESI^+	272.1	91.0	3.8	1	10	23	10
phenylacetic acid *ql.*	ESI^+	272.1	136.0	3.8	1	10	23	16
(IS) phenylacetic acid-$^{13}C_2$ *qt.*	ESI^+	274.1	91.9	3.8	76	10	23	10
(IS) phenylacetic acid-$^{13}C_2$ *ql.*	ESI^+	274.1	138.1	3.8	76	10	23	16
benzaldehyde *qt.*	ESI^+	241.9	106.0	8.1	61	10	21	12
benzaldehyde *ql.*	ESI^+	241.9	137.0	8.1	61	10	23	14
phenylpropanoic acid *qt.*	ESI^+	286.1	105.0	5.0	1	10	23	48
phenylpropanoic acid *ql.*	ESI^+	286.1	90.8	5.0	1	10	53	16
vanillin *qt.*	ESI^+	288.0	151.0	6.4	1	10	21	18
vanillin *ql.*	ESI^+	288.0	105.0	6.4	1	10	35	12
(IS) vanillin-d_3 *qt.*	ESI^+	291.0	154.2	6.4	41	10	27	18

(IS) vanillin-d_3 *ql.*	ESI^+	291.0	108.9	6.4	41	10	55	12
aminoacetophenone *qt.*	ESI^+	270.9	133.9	6.6	1	10	21	14
aminoacetophenone *ql.*	ESI^+	270.9	92.9	6.6	1	10	45	10
sotolon *qt.*	ESI^-	262.0	136.9	4.4	-5	-10	-26	-5
sotolon *ql.*	ESI^-	262.0	106.8	4.4	-5	-10	-32	-19
2-acetyl-1-pyrroline *qt.*	ESI^-	398.2	137.0	6.1	-200	-10	-38	-8
2-acetyl-1-pyrroline *ql.*	ESI^-	398.2	203.0	6.1	-200	-10	-38	-8
2-acetyl-2-thiazoline *qt.*	ESI^+	265.0	138.0	3.9	1	10	29	16
2-acetyl-2-thiazoline *ql.*	ESI^+	265.0	131.9	3.9	1	10	31	12
acetic acid *qt.*	ESI^-	193.9	152.0	1.1	-100	-10	-18	-17
acetic acid *ql.*	ESI^-	193.9	137.0	1.1	-100	-10	-26	-17
(IS) acetic acid-$^{13}C_2$ *qt.*	ESI^-	195.9	151.9	1.1	-30	-10	-18	-17
(IS) acetic acid-$^{13}C_2$ *ql.*	ESI^-	195.9	136.9	1.1	-30	-10	-24	-15

qt. = quantifier MRM. *ql.* = qualifier MRM. Q1 = precursor ion. Q3 = selected product ion. t_R = retention time. DP = declustering potential.
EP = entrance potential. CE = collision energy. CXP = cell exit potential.

Table S3-18: MRM transitions of δ-lactones and the corresponding 5-hydroxy acids (Utz et al. 2021).

Analyte (number) *qt./ql.*	Ioniza-tion	Q1 [*m/z*]	Q3 [*m/z*]	t_R [min]	DP [V]	EP [V]	CE [V]	CXP [V]
(IS) *δ*-dodecalactone-d_2 *qt.*	ESI^+	201.0	165.0	1.7	91	10	13	10

(IS) δ-dodecalactone-d_2 *ql.*	ESI^+	201.0	55.0	1.7	91	10	37	8
5-hydroxy dodecanoic acid-d_2 *qt.*	ESI^+	219.1	184.1	1.7	61	10	15	6
5-hydroxy dodecanoic acid-d_2 *ql.*	ESI^+	219.1	166.0	1.7	61	10	19	8
δ-tetradecalactone *qt.*	ESI^+	227.2	209.1	1.9	51	10	9	26
δ-tetradecalactone *ql.*	ESI^+	227.2	69.0	1.9	51	10	23	8
5-hydroxy tetradecanoic acid *qt.*	ESI^+	245.2	210.2	1.9	1	10	15	12
5-hydroxy tetradecanoic acid *ql.*	ESI^+	245.2	192.2	1.9	1	10	17	10
δ-hexadecalactone *qt.*	ESI^+	255.2	55.0	2.0	46	10	45	8
δ-hexadecalactone *ql.*	ESI^+	255.2	41.0	2.0	46	10	65	18
5-hydroxy hexadecanoic acid *qt.*	ESI^+	273.3	256.2	2.0	1	10	9	16
5-hydroxy hexadecanoic acid *ql.*	ESI^+	273.3	238.2	2.0	1	10	15	14
δ-octadecalactone *qt.*	ESI^+	283.2	69.0	2.2	51	10	33	8
δ-octadecalactone *ql.*	ESI^+	283.2	97.1	2.2	51	10	23	12
5-hydroxy octadecanoic acid *qt.*	ESI^+	301.3	266.2	2.2	1	10	15	16
5-hydroxy octadecanoic acid *ql.*	ESI^+	301.3	248.3	2.2	1	10	19	16

qt. = quantifier MRM. *ql.* = qualifier MRM. Q1 = precursor ion. Q3 = selected product ion. t_R = retention time. DP = declustering potential.
EP = entrance potential. CE = collision energy. CXP = cell exit potential

Table S3-19: Used isotopically labeled internal standards (IS), calibration curves and coeffi-cients of determination (R2) of the quantified analytes (adapted from Utz et al. (2021)).

odorants	IS	calibration curve	R^2
hexanal	hexanal-d_{12}	y = 6.73533x + 0.76115	0.99977
trans-2-octenal	hexanal-d_{12}	y = 0.44980x + 0.00122	0.99984
acetaldehyde	acetaldehyde-d_3	y = 0.00109x + 0.00523	0.99977
diacetyl	diacetyl-d_6	y = 0.22772x + 0.00490	0.99935
acetoin	diacetyl-d_6	y = 0.27767x + 0.00297	0.99959
butyric acid	butyric acid-$^{13}C_4$	y = 0.37437x + 0.00699	0.99916
2-methyl butyric acid	butyric acid-$^{13}C_4$	y = 0.32659x − 0.02073	0.99956
3-methyl butyric acid	butyric acid-$^{13}C_4$	y = 0.81690x − 0.01772	0.99974
pentanoic acid	butyric acid-$^{13}C_4$	y = 0.58184x + 0.00666	0.99894
hexanoic acid	hexanoic acid-d_3	y = 0.50083x + 0.04289	0.99920
octanoic acid	octanoic acid-d_{15}	y = 0.31739x + 0.01858	0.99941
nonanoic acid	octanoic acid-d_{15}	y = 1.40377x + 0.18264	0.99973
decanoic acid	octanoic acid-d_{15}	y = 0.15123x + 0.01375	0.99988
dodecanoic acid	decanoic acid-^{13}C	y = 0.12564x + 0.00176	0.99968
tetradecanoic acid	decanoic acid-^{13}C	y = 0.11727x + 0.00489	0.99858
phenylacetic acid	phenylacetic acid-$^{13}C_2$	y = 2.53632x + 0.00487	0.99902
benzaldehyde	phenylacetic acid-$^{13}C_2$	y = 0.36952x – 0.00010	0.99906
vanillin	vanillin-d_3	y = 32.8480x + 0.02129	0.99966
acetic acid	acetic acid-$^{13}C_2$	y = 0.32377x + 0.26738	0.99939
δ-C14L	*δ*-C12L-d_2	y = 0.23241x + 0.12251	0.99618
δ-C16L	*δ*-C12L-d_2	y = 0.35681x + 0.08428	0.99921
δ-C18L	*δ*-C12L-d_2	y = 0.56428x + 0.04695	0.99845
methanethiole	- (standard addition)	y = 56312x – 9137	0.98894
dimethyl sulfide	dimethyl sulfide-d_6	y = 0.34645x – 0.02631	0.99854

4 OVERALL DISCUSSION

The concept of using the microparticulation process on plant proteins and to use the resulting microparticles as fat replacers in foods was based on a similar process used for microparticulation of whey proteins. With the increasing world population and the need to feed the world with protein, plant-based alternatives for animal-based protein are increasing. Plant-based proteins are more sustainable than animal-based proteins and can also be used for vegan food. The used proteins in this study, pea proteins, come from plants that can be locally grown in central Europe. Currently, pea protein is known for its emerging application in meat alternatives. Meat alternatives are also extruded products from pea protein that are increasing in consumer acceptance. Introducing pea protein microparticles as fat replacers or as a structuring agent to enhance creaminess in a product, consumer acceptance is likely to be high. Especially replacing dairy fats in food products would make the products also interesting for vegan consumers.

Based on the microparticulation process used in previous studies (Wolz et al. 2016a; Wolz et al. 2016b) for whey protein the process was developed to microparticulate pea protein. Overall microparticulated pea protein could be produced on a small scale using a rheometer and on a large scale using an extruder in a size range of 1 – 20 µm, which was found to be the optimum size range for whey protein microparticles as fat replacer (Spiegel 1999b). However, the process deviated significantly from the well-known microparticulation process of whey protein, which also led to different particle characteristics. In addition, little is known about the aggregation mechanism of pea protein compared to whey protein. Therefore, the focus of this thesis laid on analysing the aggregation behaviour of pea protein with and without shear. An overall and more detailed discussion of the findings is carried out in the following.

4.1 Extraction of pea protein from pea flour

In contrast to whey protein concentrate and isolate, commercial pea protein was found to be highly denatured and aggregated. This was shown in a low solubility and absence of a denaturation peak in mDSC measurements. In order to obtain ‘native’ pea protein, the pea protein had to be extracted from pea flour on a laboratory scale. Three different extraction methods were compared with each other: Alkali extraction – isoelectric precipitation, micellar precipitation, and salt extraction. Stone et al. (2015) found a significant difference between the three extraction methods regarding their functionality at pH 7. Adding to that, also their response to changes in pH and ionic strength and protein profile was found to be influenced by the extraction method. Functionalities were found to be dependent on the protein profile, the type of co-extracted plant substances, and the conformational changes during extraction. Each step that affects the resulting protein product is shown in Figure 4-1. The conformational changes were mainly dependent on the pH used during extraction and precipitation. The protein profile depended on the precipitation step. For this aspect, it is important to know that the isoelectric point of globulins is pH 4.5 and that of albumins is pH 6 (Swanson 1990). Thus, during precipitation at pH 4.5, the albumins stay soluble and end up in the waste

stream. In addition, the albumins are water-soluble and globulins are salt soluble (Osborne 1909). Legumin is the most hydrophobic pea protein and forms micelles at low salt concentrations by non-covalent possibly hydrophobic interactions between the proteins (Arntfield et al. 1985). This also explains the term 'micellar precipitation'. The less hydrophobic vicilin and the albumins can stay soluble at lower salt concentrations, which explains the high amount of legumin and low yield in micellar precipitated pea protein. Salt extraction was not comprised of a precipitation step and therefore, contained both globulins and albumins.

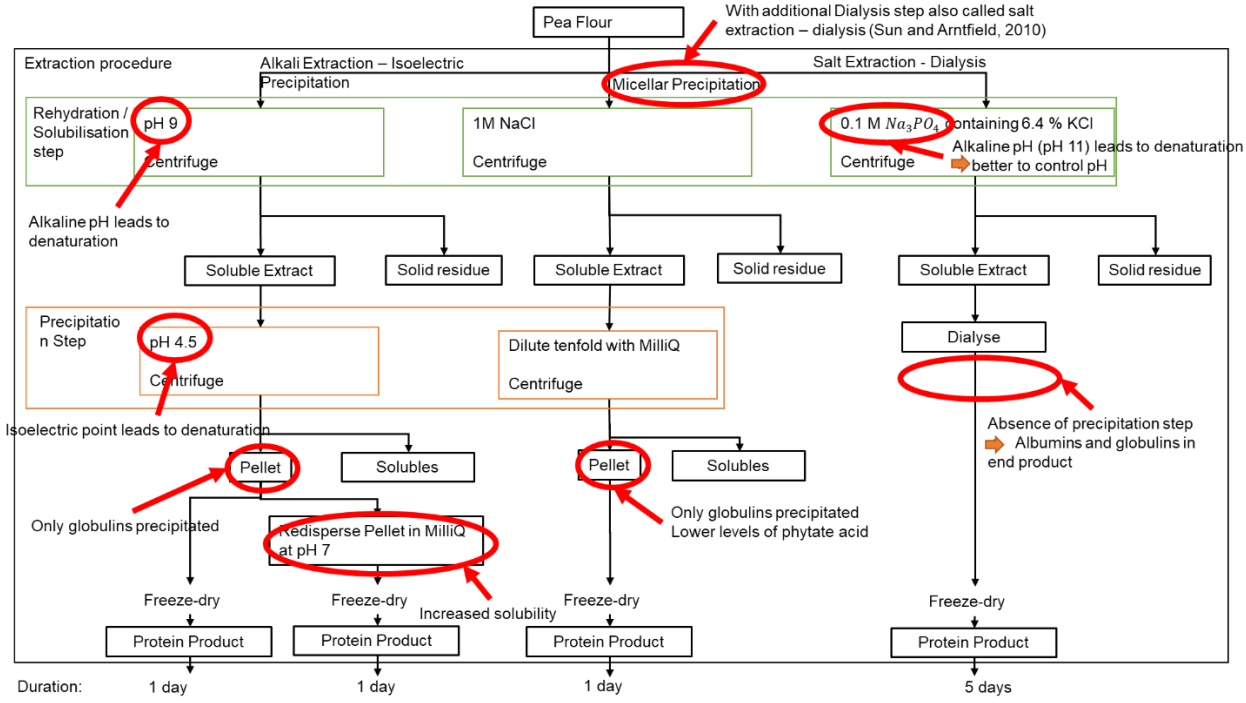

Figure 4-1: Schematic overview of the influence of extraction type on the protein product.

A difference in solubility and isoelectric point was found between alkali extracted – isoelectric precipitated, salt extracted – dialysed and micellar precipitated pea protein. The isoelectric point for alkali extracted – isoelectric precipitated and salt extracted – dialysed pea protein was between pH 4 and 4.5, whereas the isoelectric point for micellar precipitated pea protein was around pH 5. The lowest solubility was found between pH 2 and pH 4.5 for alkali extracted – isoelectric precipitated and salt extracted – dialysed pea protein and between pH 5 and pH 6. This difference can be explained by the amount of co-extracted phytate acid. The amount of phytate acid is high for alkali extracted – isoelectric precipitated pea protein and salt extracted – dialysed pea protein because phytate acid decreases solubility at low pH levels (Ali et al. 2010). Micellar precipitation was found to decrease the amount of phytate acid (Cordero-de-los-Santos et al. 2005; Rahma et al. 2000). Interesting to note is that phytate acid also decreases digestibility (Fredrikson et al. 2001). Therefore, a reduction in phytate acid during extraction might increase the value of a pea protein ingredient in food application.

Solubility at pH levels above pH 6 was higher for alkali extraction – isoelectric precipitation with adjusted pH to neutral pH before freeze-drying compared to freeze-drying

at pH 4.5, which would indicate a higher degree of the nativity for samples freeze-dried at pH 7. Currently, there is no chromatographic or any other method available to determine the absolute amount of “native” pea protein due to the lack of a protein analytical standard. Therefore, ‘nativity’ could only be assessed in relative amounts. In this research, the amount of enthalpy change during mDSC measurements was used to compare the degree of nativity between the different extraction methods. A higher enthalpy change indicated a higher degree of the nativity. The enthalpy change during mDSC measurements was not significantly different between alkali extraction – isoelectric precipitation freeze-dried at pH 7 and pH 4.5. Therefore, no difference in the amount of ‘native’ pea protein was found between the two. Micellar precipitation was found to be the mildest extraction leading to the highest amount of enthalpy change and therefore the highest amount of ‘native’ protein. The enthalpy change of salt extracted pea protein was found to be lowest due to the strong alkaline pH of 11 during the solubilisation step. By adjusting the pH during solubilisation to pH 7 a higher enthalpy change was found and therefore, a higher degree of nativity.

From this, it becomes clear that the extraction method can be used to control the protein product. Based on this, the extraction method can be chosen and modified to one’s need for example if a special protein profile or a high degree “native” pea protein is desired. Another factor, which is of interest is the duration time of the extraction. Extraction time varied from 1 to 5 days. Alone the addition of a dialysis step takes approximately three extra days. Additionally, the protein yield differed between the extractions. The yield varied between 25% and 50% of the possible protein that can be extracted from pea flour. This means that 50% to 75% of protein ended up in the waste stream during extraction. Stone et al. (2015) could achieve a yield varying between 30% and 75%. This is slightly higher compared to our findings, which might be explained by the difference in cultivar. However, it still means that 25% to 70% of protein ended up in the waste stream. This is quite a high amount, especially keeping in mind that pea flour contains ‘only’ 18% protein. Thus, even though 100 g of pea flour is used during extraction, it only results in around 10 g of the protein product. Handling higher volumes would require an approach on a pilot plant scale.

For further experiments, alkali extraction – isoelectric precipitation with freeze-drying at pH 7 and a combination of salt extraction – dialysis and micellar precipitation was used. The combination followed the approach of micellar precipitation with lower salt contents of only 0.3 M NaCl and an additional dialysis step before freeze-drying. Protein profile and functionalities were identical to the ones of micellar precipitation. In the following alkali extraction – isoelectric precipitation is shortened to ‘alkali extraction’ and the combination of salt extraction – dialysis and micellar precipitation is shortened to ‘salt extraction’.

4.2 Thermal aggregation behaviour of pea protein

The thermal aggregation behaviour of pea protein was found to differ from that of the well-known whey protein. Similar to whey protein the aggregation and gelation of pea protein were dependent on pH and ionic strength (Sun and Arntfield 2011; Nicolai et al. 2011b). However, in contrast to whey protein, also the extraction method was found

to affect gelation and aggregation of pea protein. Each of the analysed influencing factors is discussed in detail below.

4.2.1 Influence of pH

The extraction method was found to determine the natural pH, and, thus, the charge of the pea proteins. Around the isoelectric point of pH 4.5, the charge was close to 0, meaning repulsive forces were lowest at this point. Aggregation of proteins already occurred without heat treatment, which is already reflected in the low solubility at this pH and also the use of the isoelectric point to precipitate pea protein (Stone et al. 2015; Tanger et al. 2020). Figure 4-2 shows an alkali extracted and salt extracted untreated protein solution at natural pH of 6.9 / 6.4 and pH 4.

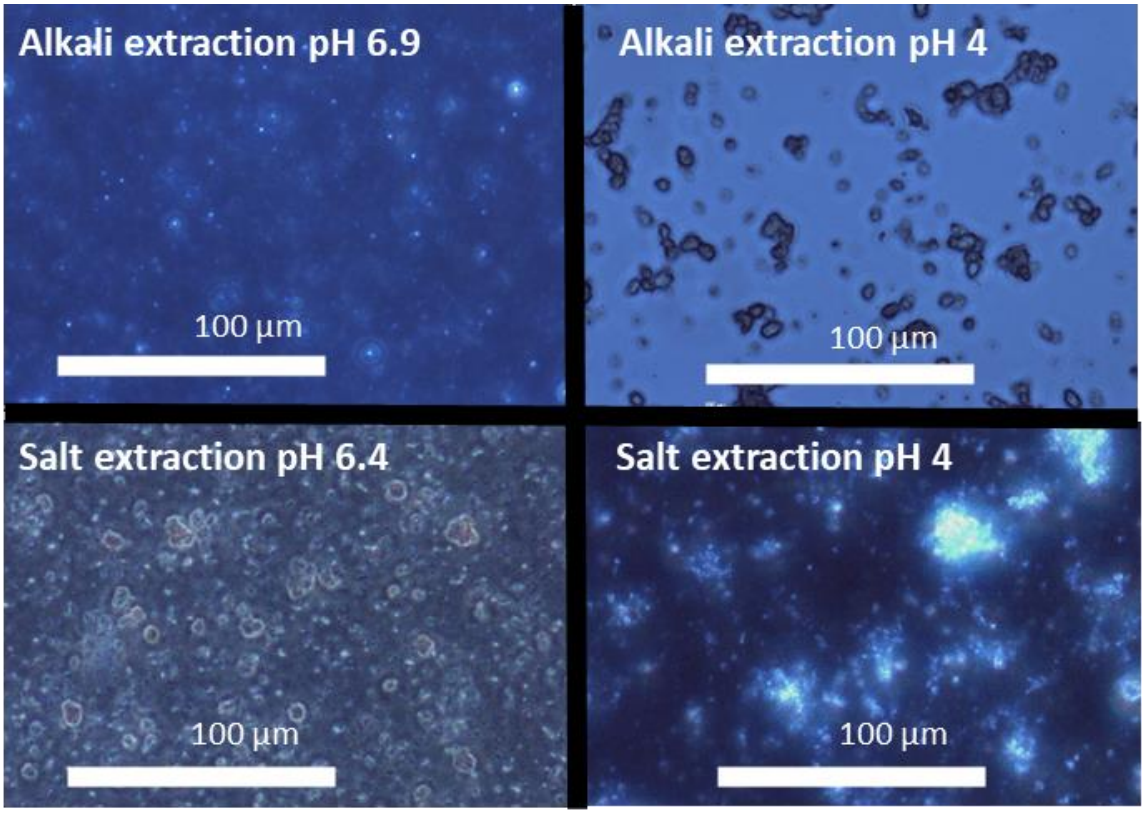

Figure 4-2: Alkali extracted and salt extracted untreated protein solution at pH 4 and natural pH of pH 6.9 and 6.4.

At natural pH, only the micelles of the salt extracted protein are visible, whereas the protein of alkali extracted protein are transparent. At pH 4 however, the aggregates formed without heat treatment of both extracted pea proteins are clearly visible under the microscope. Whey proteins were found to form oligomers at their isoelectric points, however, these oligomers were too small to sediment or being visible under the light microscope**.** This means that pea protein undergoes conformational changes upon changing the pH, which enables them to form big aggregates without thermal treatment. By the conformational changes upon pH change part of the hidden hydrophobic core could be exposed and lead to attractive forces between the proteins leading to aggregates. These formed aggregates before heat treatment could affect denaturation and aggregation of the pea protein with increasing temperature (Yang et al. 2021).

For whey protein, the importance of electrostatic interactions and hydrophobic interactions increased with pH values closer to the isoelectric point (Zúñiga et al. 2010). A similar behaviour of pea protein could not be determined. It rather seemed that electrostatic interaction increased in importance with more alkaline pH and hydrophobic interactions increased with pH closer to the isoelectric point. This might be explained by the lower charge near the isoelectric point of pH 4.5 and therefore decreased repulsive forces between the protein enabling exposed hydrophobic patches between proteins to interact with each other. The importance of covalent bonds increased with more alkaline pH for whey proteins (Zúñiga et al. 2010). However, this cannot be confirmed or rejected, since pea proteins form no continuous covalently bound gel network and this aspect, therefore, was not possible to be analysed. Another factor is that the salt concentration has a major influence on solubility and also the gelation of pea protein in contrast to whey protein. Thus, results with different solubilities as it is the case for pH 7 and pH 9 cannot be compared for pea protein gels and aggregates.

The pea protein gels showed a high stiffness and low tanδ especially at pH 4.5. This indicated active fillers (Ben-Harb et al. 2018; Sun and Arntfield 2011). This could be insoluble protein aggregates, which are incorporated in a gel network of soluble protein. Only at pH 3 and at pH 9 more than 50% of the pea protein was soluble at 0 M NaCl. At these two pH values also the stiffness was lower with similar or even higher tanδ to pH 4.5 and pH 7, which would support the above named hypothesis. An explanation could be that there are rather interactions between the aggregates and a particulate gel is formed at conditions leading to low solubility of pea proteins similar to whey protein around their isoelectric point (Nicolai et al. 2011b). Advanced microscopic imaging such as transmission electron microscopy might be able to give more information about the gel structures. However, it has to be kept in mind that sample preparations could change the gel structure.

A major finding that could be shown in this research, was the influence of solubility on the gelation behaviour of pea protein. This is significantly different to whey protein and should be taken into account for further analysis.

4.2.2 Influence of ionic strength

Due to the fact that globulins, the main pea proteins, are salt soluble the ionic strength influences the thermal behaviour of pea protein by impacting their solubility. Legumin forms micelles at low ionic strength, which were shown to be solubilized by the addition of at least 0.3 M NaCl using the salting-in effect (Melander and Horváth 1977). Therefore, the addition of salt does change the protein conformation and with that the thermal behaviour. Interesting to note is that the addition of salt could prevent acid denaturation at pH 3. With an increase of NaCl concentration the thermal stability of the pea protein increased. Still, thermal stability at pH 3 was lower with a denaturation temperature of 61°C to 68°C compared to 75°C to 95°C at higher pH levels. The increase of ionic strength also led to stiffer gels with possibly increased intensity of hydrophobic interactions at pH 3. At neutral pH, an increase in ionic strength led to an increase in electrostatic interaction and a decrease in hydrophobic interactions. At pH 9 and high NaCl

concentrations of 0.9 M and 1.5 M the frequency sweep showed a cross-over of G' and G'' indicating rather an entangled solution than a gel (Brighenti et al. 2020; Pai and Khan 2002), which is known from polysaccharide gels. Sun and Arntfield (2011) found that no gel was formed at pH 5.65 and 2 M NaCl. This combined with our findings could indicate that the minimum gelation concentration increased with increasing ionic strength. In contrast, Pouzot et al. (2005) found an increase in aggregate size by the addition of NaCl in β-lactoglobulin aggregates. The difference between whey and pea protein aggregation might be explained by the different solubility. Whey protein is highly soluble (> 80%), whereas pea protein is low in solubility because of the micelle formation in the absence of salt at neutral pH. Using a pea protein product, which is higher in solubility in the absence of salt, alkali extraction, only minor effect of the addition of NaCl were found (Shand et al. 2007). Combining this knowledge with our findings, it could be confirmed that the salt addition affects gelation by changing the solubility of the pea protein.

Salt addition also led to higher denaturation temperatures of pea protein at all pH levels. This can be explained by the stabilizing effect of NaCl on the complex quarternary structure of pea protein (Mession et al. 2013; Sun and Arntfield 2011). The charge shielding effect of NaCl can reduce inter- and/or intra-molecular chain repulsion (Damodaran 1988). The addition of salt into a protein solution also changes the electrostatic and hydrophobic interaction of the water molecules with the protein (Choi and Ma 2005; Hippel and Schleich 1969), which leads to higher thermal stability of the protein. Overall, the influence of the pH was more significant than the influence of the ionic strength. However, the ionic strength influence should not be underestimated for pea proteins since it also affects solubility.

4.2.3 Influence of extraction method

The extraction method was found to have a significant influence on the aggregation of pea protein. This was best visible in aggregate structure but also the size was influenced. Particles formed upon thermo-mechanical treatment of salt extracted pea protein led to denser particles at natural pH. Particles formed upon thermo-mechanical treatment of alkali extracted pea protein led to transparent, porous, and worm-like aggregates at natural pH. The differences in particle structure can be explained by the resulting differences in protein powder by the extraction method as explained in 4.1. These differences concern protein profile, solubility, and the number of native proteins. The dense structure of the particles formed upon thermo-mechanical treatment of salt extracted pea protein can be explained by the low solubility at natural pH in the absence of salt. Alkali-extracted protein is much higher in solubility at natural pH but low in solubility at pH 4, where it also forms dense spherical particles. Thus, a low solubility seems to lead to dense spherical particles.

Particle structure may also be influenced by the protein profile. As mentioned above, alkali extracted pea protein and salt extracted pea protein differ significantly in their protein profile. Salt extracted pea protein is more homogenous in its protein profile with 75% legumin. Since legumin is the only globulin that contains sulphur, it is the only globulin, which can theoretically react via a thiol-disulphide interchange reaction and

form covalent bonds. The higher the legumin content in the protein product, the higher the chance of a thiol-disulphide interchange reaction, which would be the case for salt extracted pea protein.

Next, the particle structure can be linked to the degree of nativity of the pea protein used. Pre-denaturation can lead to quicker aggregation because reactive groups are already exposed or need less energy to be exposed and aggregate. This quick aggregation can inhibit further denaturation and exposure of reactive groups (Yang et al. 2021) due to steric hindrance, which could be the case for alkali extracted pea protein. This could explain the porous structure of the particles formed upon thermo-mechanical treatment from alkali extracted pea protein.

4.2.4 Influence of shear stress

Similar to whey protein an increase in shear stress was found to decrease the particle size (Wolz et al. 2016b). This could be explained by inhibition of further aggregation of pea protein aggregates under shear stress or breakage of already existing aggregates due to the shear stress. The effect was most profound at lower shear rates up to 500 s^{-1} using a rheometer. At higher shear rates the structure building forces, aggregation, and the structure destruction forces, the shear stress, were in equilibrium. Thus, increasing the shear rate did not result in even smaller particles. For extrusion-based microparticulation, no significant effect on particle size by the shear rate was found for shear rates higher than 200 rpm. Lower shear rates could not be analysed due to the limitations of the extruder used. Shear stress did not affect protein-protein interaction. Thus, shear stress above 500 s^{-1} for rheometer based microparticulation and 200 rpm for extrusion-based microparticulation was found to be sufficient to inhibit gel formation and generate suitable microparticles. The difference between shear stress during extrusion cooking and rheometer treatment is explained in more detail in 4.3.2.

4.2.5 Protein-protein interaction in pea protein aggregates

In contrast to whey protein, protein-protein interactions in pea protein aggregates and gels were found to be mostly non-covalent. This supports the findings of other studies (Sun and Arntfield 2012; Felix et al. 2017; Chihi et al. 2016). Non-covalent bonds were dominant at each pH and ionic strength and also during thermo-mechanical treatment. However, using an additional SDS-PAGE and quantification of the bands larger than 250 kDa indicating covalently bound oligomers, resulted in the finding of 40% to 50% covalent bonds in total at natural pH. These covalently bound oligomers were also found in pea protein gels at all pH levels. This is much lower than reported for whey protein gels and microparticles with 70% to 90% covalent bonds, however, should not be underestimated even though they did not form a continuous network, but only connected small oligomers. Chihi et al. (2016) found a slight increase of exposed hydrophobicity during heating for 60 min at 85°C, which was a lower increase compared to β-lactoglobulin. Additionally, they found an increase in free thiol groups and a decrease in disulphide bonds, whereas for β-lactoglobulin, the number of free thiol groups decreased and the number of disulphide bonds increased. In contrast to β-lactoglobulin with one free thiol group and one intermolecular disulphide bridge, legumin contains several disulphides and free thiol groups in one protein molecule (Shand et al. 2007).

A legumin monomer is also four times bigger than a β-lactoglobulin monomer. In addition, β-lactoglobulin can be analysed separately from all other whey proteins, whereas this is not possible for legumin. Legumin is mostly analysed in combination with the two other globulins vicilin and convicilin, which do not contain an intermolecular disulphide bridge or a free thiol group. This is also the case in our study because legumin could not be isolated from the other globulins efficiently. From our results, it could be hypothesized that legumin does undergo thiol-disulphide interchange reactions and forms small oligomers via covalent bonds. However, the interchange reaction is stopped by further reaction with vicilin and convicilin via non-covalent bonds. Reaction via non-covalent bonds before full unfolding is completed can also lead to inhibition of further unfolding or to burying of reactive groups during aggregation (Yang et al. 2021). This could be the case for globulins meaning that legumin reacts with another globulin via non-covalent interactions. By that aggregation, a free thiol group is buried and is not accessible anymore for reaction with another free thiol group or a disulphide bridge. This leads to the end of the thiol-disulphide interchange reaction or inhibits the start of it. A schematic overview of the pea globulin aggregation mechanism is shown in Figure 4-3.

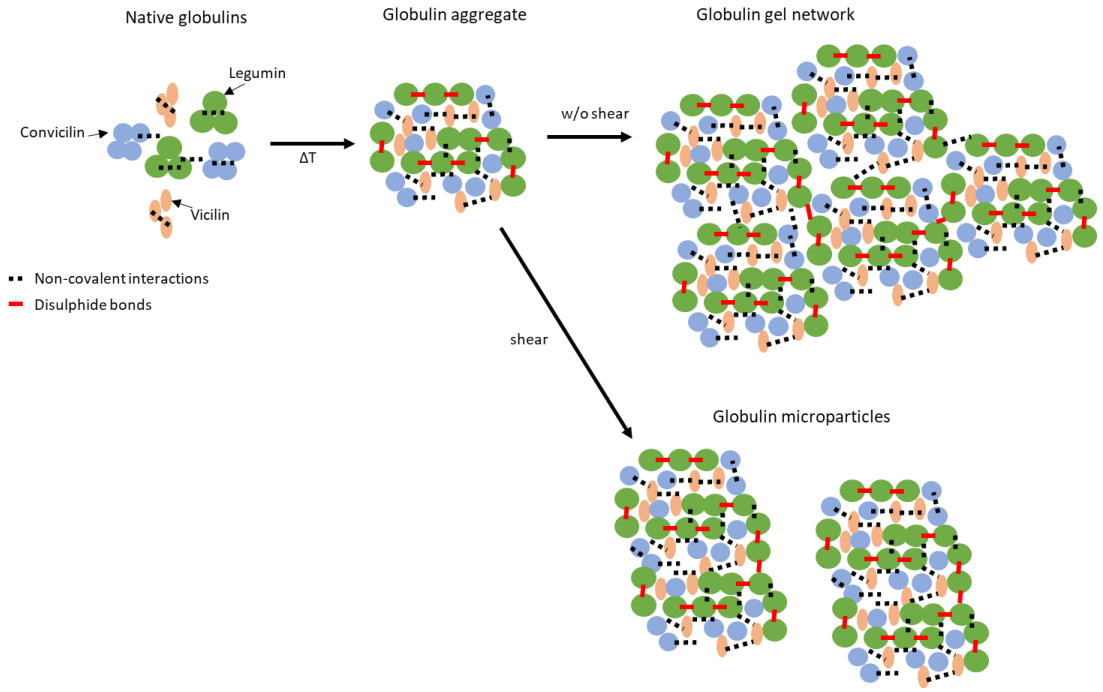

Figure 4-3: Schematic representation of pea globulin aggregation based on Chihi et al. (2016).

In the globulin aggregate, the inhibition of further thiol-disulphide interchange reaction of legumin (green) is shown by the end of a vicilin (pink) or convicilin (blue), which is bound non-covalently. The increase in free thiol groups can simply be explained by the heat treatment, which leads to the breakage of intermolecular disulphide bonds, which cannot react further due to the above described steric hindrance. In Figure 4-3 also the effect of shear is shown. Shear stress can easily break non-covalent interactions apart, however, breakage of covalent bonds needs more energy. Shear stress was reported to increase thiol-disulphide interchange reaction (Evans 2001). However, this was not seen in this work. This can be explained by the complex structure of the pea protein

and by the fact that thiol-disulphide interchange is also inhibited by quick aggregation via non-covalent bonds.

Another aspect that is of interest for the aggregation of pea protein is the presence of other plant metabolites, which make about 20% – 30% of the protein powder. Small sugar molecules could interact with the pea proteins and alter the gelation mechanism. Da Chen et al. (2021) found that the addition of green tea polyphenols decreased the gel stability of pea proteins extracted by alkali extraction. X-ray measurements showed that large protein aggregates were present in the gel and the gel network was disrupted by the green tea polyphenols. This could indicate that the remaining 20% – 30% plant metabolites could also interact with the pea proteins and disrupt gel network formation. This could especially be the case for hydrophobic molecules, which interact with the hydrophobic sites of the pea proteins and by doing so inhibiting the proteins to interact with each other.

4.3 Microparticulation of pea protein

Microparticles from extracted and commercial pea protein could be generated on a small scale, in a rheometer, and a large scale, by an extruder.

4.3.1 Bottom-up and Top-down approach

As already stated above, in contrast to whey protein concentrate and isolate, commercial pea protein was already denatured and aggregated. Laboratory extracted pea protein was high in ‘nativity’ but only small amounts could be extracted. This means that for large scale experiments commercial pea protein needed to be used. From that, a different microparticulation process from the one described in 1.6 deviates. The process for commercial pea protein was a top-down process instead of the bottom-up process of “native” protein. A schematic representation of the two processes side by side is shown in Figure 4-4.

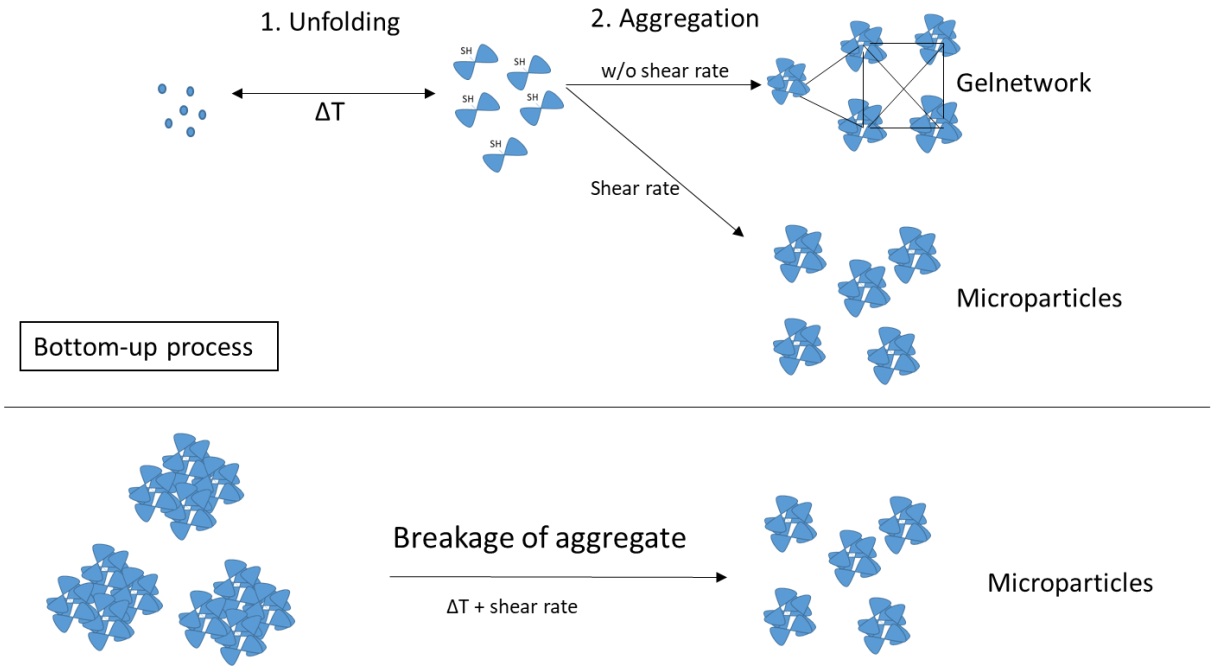

Figure 4-4: Schematic overview of the bottom-up process of "native" protein and the top-down process for aggregates protein systems during microparticulation.

For the bottom-up process, the start material is ‘native’ and has a small particle size. The size increased during thermo-mechanical treatment due to denaturation and aggregation resulting in bigger particles. The shear rate inhibits the gel formation. For the top-down process, the starting material already contains denatured and aggregates particles. These particles get crushed and decrease in size during thermo-mechanical treatment. The bottom-up process of whey protein has been studied extensively (Wolz et al. 2016a; Wolz et al. 2016b; Toro-Sierra 2016; Spiegel 1999b). For commercial pea protein, this process is not possible and the top-down process is used. O'Kane et al. (2005) found that pea protein reacted quickly upon heating and rearranged during second heat treatment. This leads to the conclusion that not only the shear stress is responsible for breaking down aggregates but also the heating has an effect on the breakage of pea protein aggregates. This hypothesis was supported by the finding in this thesis that particle size of the produced microparticles was temperature-dependent.

4.3.2 Rheometer vs. Extruder

The rheometer was used as a shearing device for small-scale experiments, whereas the extruder was used for large-scale experiments. Due to the small sample volume laboratory extracted pea protein and commercial pea protein could be analysed during thermo-mechanical treatment using a rheometer. For extrusion cooking experiments, only commercial pea protein was used. In addition, changes in the ionic environment or pH value were not possible to be applied with the extruder used in this work due to material instability issues at extreme chemical conditions. Thus, only the top-down process at natural pH could be analysed using extrusion cooking. This makes it difficult to compare the resulting particles using a rheometer and extrusion cooking. The effect of decreasing particle size with increasing shear rate could not be found in extrusion cooking but thermo-mechanical treatment using a rheometer. However, with the rheometer low shear rates of 100 s^{-1} were possible. These low shear rates were not possible in the extruder, because the extrusion process was not constant anymore in contrast to the same process with whey protein (Wolz et al. 2016a). For whey protein microparticulation, an increase of particle size at these low shear rates of 100 s^{-1} was found (Wolz et al. 2016a). Thus, the limitation of the constant process could be the reason, why the effect of shear rate was not observed for pea protein microparticulation during extrusion cooking but during thermo-mechanical treatment using a rheometer. Overall, similar particle sizes could be achieved for rheometer and extrusion cooking treatment. $D_{50,3}$ values of microparticles generated with an extruder and a rheometer are shown in Figure 4-5.

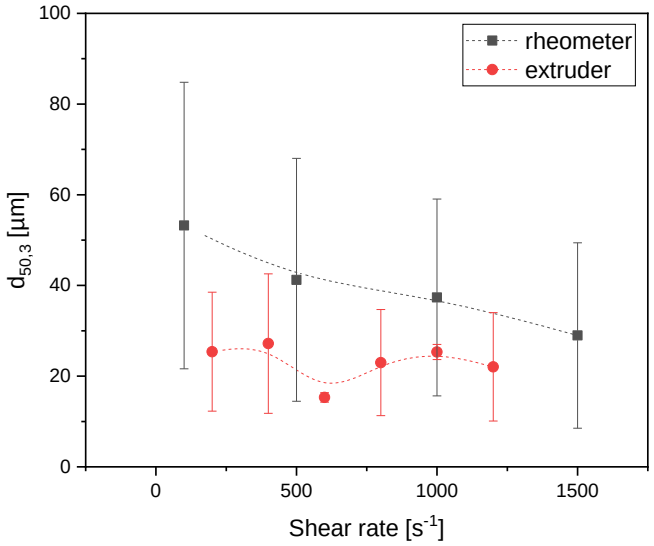

Figure 4-5: Comparison of $d_{50,3}$ values of pea protein microparticles generated with an extruder (Extruder barrel temperature: 100°C; powder mass flow: 4 kg h^{-1}) and rheometer (Temperature: 88°C, Processing time: 10 min).

The overall particle size of extruded microparticles is slightly lower. This can be explained by the additional pressure that is induced during extrusion cooking, which cannot be simulated in a rheometer. In order to also introduce the pressure to the small scale thermo-mechanical treatment, a closed cavity rheometer would be needed (Quevedo et al. 2020a). In addition, during extrusion cooking, a higher protein concentration of 20% was possible instead of only 10% in a rheometer. For rheological thermo-mechanical treatment, a solution needed to be prepared beforehand. Only 10% protein concentration was possible to dissolve for commercial pea protein. Higher protein concentration led to incomplete hydration of the protein powder. During extrusion cooking, powder and water mixing occurred in the extruder barrel under high pressure. With the addition of shear stress and pressure, it was possible to hydrate 20% protein. A closed cavity rheometer would give the possibility analysing highly concentrated protein systems as done by Quevedo et al. (2020a). However, a closed cavity rheometer was not accessible in this study for the amount of experiments. Higher protein concentrations than 20% were also not feasible during extrusion cooking because the extrusion product was burned and could not be diluted in the water anymore.

4.3.3 Effect of spray- and freeze-drying on pea protein microparticles

Spray- and freeze-drying of the pea protein microparticles was shown to not affect particle size. This behaviour is similar to whey protein microparticles (Toro-Sierra et al. 2013). However, drying affects the protein conformation and can induce structural changes (Zhao et al. 2013). This is of great importance for protein-flavour binding. Our results showed that the grassy/beany aroma could be reduced by both spray- and freeze-drying of the pea protein microparticles. A reduction of off-flavour in pea proteins has also been found by using solid dispersion-based spray-drying (Lan et al. 2019). The reduction in water and changes in tertiary structure can lead to an altered and less intense protein-flavour binding leading to a loss of volatile off-flavour (Zhan et

al. 2019). Therefore, drying is less interesting in changing particle size but it is of interest to reduce off-flavour in pea protein.

4.3.4 Microparticle functionalities

One of the most important microparticle functionalities is fat replacement. Whey protein microparticles are often used to replace fat because particles with the right characteristics can induce a ball-bearing effect, which leads to a creamy perception (Kew et al. 2020). In this thesis, it has been shown that the replacement of 50% fat with pea protein microparticles inhibited a decrease in creaminess. Because a fat reduction would lead to a significant decrease of perceived creaminess without the incorporation of microparticles it can be assumed that the produced pea protein microparticles have the right characteristics to induce a ball-bearing effect and generate a creamy mouthfeel. It was shown that pea protein microparticles were better in inhibiting a loss in creaminess compared to potato protein microparticles, which could be due to their superior structure. Similar to whey protein microparticles in ice cream, pea protein microparticles could enhance the structure of a model milk dessert (Koxholt et al. 1999).

Other functionalities of interest for microparticles would be foam and emulsion stabilising via the Pickering concept (Zhang et al. 2020a) because Pickering emulsions generated with suitable particles are more resistant to Ostwald ripening compared to emulsions stabilized with surfactants and biopolymers (Schmitt et al. 2021). Foaming and emulsion experiments have been performed with the fresh and dried microparticles and the untreated protein isolate and an extracted ‘native’ protein concentrate as a comparison. The results for the foam experiments are shown in Figure 4-6.

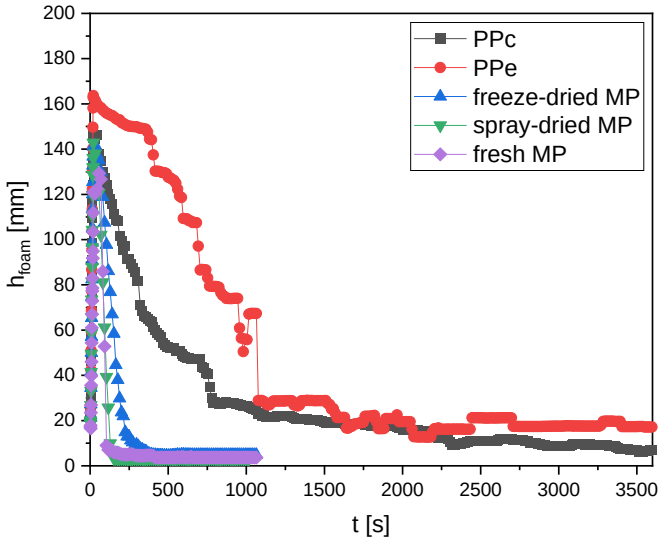

Figure 4-6: Foam height over time for commercial pea protein (PPc), extracted "native" pea protein (PPe), fresh microparticulate (MP) and dried microparticulate.

For the foam, it can be seen that the foam height decreased the slowest for the extracted “native” pea protein, which means that it was able to stabilize the foam better compared to the commercial pea protein and the microparticulated pea protein. However, it has to be noted that for Pickering foams particles with a particle size in the

submicron are used and the microparticles and the commercial pea protein have a particle size far above 1 µm (Schmitt et al. 2021). Thus, they might be too big in particle size to stabilize a foam via the Pickering concept. In addition, the solubility of the microparticles and the commercial pea protein was very low with a maximum of 30%, which is not ideal for foams due to sedimentation (Schmitt et al. 2021). Other factors such as charge and surface hydrophobicity play a major role in foam stability (Dombrowski et al. 2016). The zeta potential of the microparticles was highly negative ranging from -22 mV to 29 mV. The high charge would lead to repelling of the particles, which would also inhibit bubble coalescence. However, the high charge also would inhibit dense packing of the particle at the interface (Dombrowski et al. 2016). Reliable measurement for surface hydrophobicity could not be performed, because of the turbidity of the samples, which results in unreliable results during spectrophotometric measurements.

Next to foaming experiments also the emulsion stability has been tested for the microparticles compared to the untreated pea protein isolate and an extracted ‘native’ pea protein. The results are shown in Figure 4-7. The emulsion stability value is a measure for phase separation. It describes the height of the visually stable sample after 30 min and 60 min. The difference to 100% stands for the height of the oil phase at the top of the sample, relative to the total sample height.

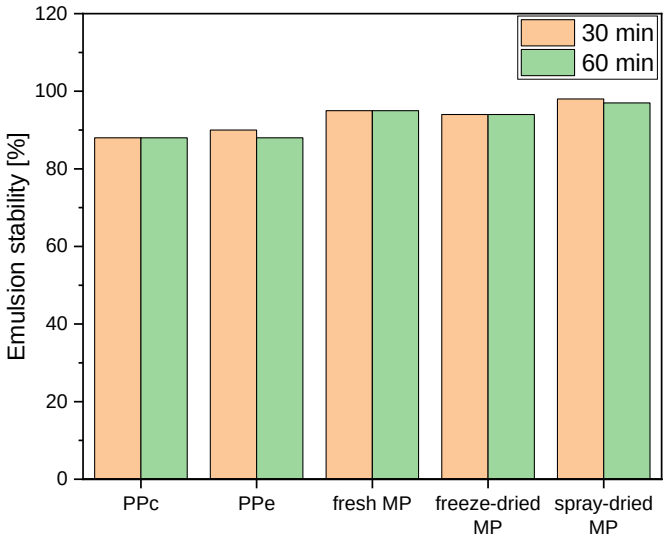

Figure 4-7: Emulsion stability after 30 min and 60 min for commercial pea protein (PPc), extracted "native" pea protein (PPe), fresh microparticulate (MP) and dried-microparticulate

From these results, it becomes clear that the emulsion stability after 30 min and 60 min is slightly higher for the microparticles compared to the untreated pea protein and the extracted ‘native’ pea protein. Stone et al. (2015) found that emulsion stability was dependent on extraction method and cultivar. Micellar precipitated pea protein, which forms micelles in the absence of salt (Tanger et al. 2020), had the highest emulsion stability on average with 99.5% compared to salt extracted with 97 – 99.6% and alkali extracted and isoelectric precipitated pea protein with 96.7 – 99-9%. The extracted

‘native’ pea protein used in this work was alkali extracted and isoelectrically precipitated pea protein. From this, it can be seen that the microparticles were better in stabilizing emulsions than stabilizing foams.

5 OVERALL CONCLUSION AND PERSPECTIVE

The overall aim of this thesis was to use the microparticulation process for functionalising pea protein as well as acquiring new insights into the aggregation process of pea protein. Thermo-mechanical treatment using extrusion cooking and a rheometer could both be used to produce pea protein microparticles from commercial pea protein via a top-down process and from laboratory extracted pea protein via a bottom-up process. Microparticles in the desired size range of 1 – 20 µm were generated. Microparticles generated by extrusion cooking from commercial pea protein were shown to suitable as fat replacers with no significant decrease in creaminess in a model milk dessert.

For ‘native’ pea protein, the following factors were found to influence aggregation in order of impact starting with the highest impact: extraction method, pH, ionic strength, and temperature (when above 88°C). Particle size during thermo-mechanical treatment could additionally be controlled by varying the shear stress. The extraction method had the biggest impact, because it controlled protein profiles, solubility, and amount of native pea protein in the protein powder. In general, small oligomers were found to be crosslinked by covalent bonds; however, no continuous covalent network was formed between the pea proteins. Interactions via non-covalent bonds inhibited further thiol-disulphide interchange reaction. Therefore, in contrast to whey protein, non-covalent interactions were of main importance during aggregation upon thermal treatment. The type of non-covalent bond interaction was found to be dependent on extraction type, pH, and salt concentration. These three variables also influenced solubility. Therefore, controlling the solubility of the pea protein is likely to have a major impact on the type of protein interaction upon thermal treatment.

This thesis presents a deeper insight into the aggregation mechanism of pea proteins and shows a method to functionalize pea protein by microparticulation. The microparticulation process using extrusion cooking offers a possibility to incorporate a waste stream, commercial pea protein, meaningful and valuable in a food application by simulating the creamy mouthfeel of fat. The insights gained by studying the extrusion process of commercial pea protein in this thesis can be used as a base for the development of other extrusion processes for food application of pea protein and as a base for industrial handling of commercial pea proteins.

This study also forms a basis for a better understanding of pea protein aggregation and the importance of the extraction method. Significant differences in aggregation between pea and whey protein were shown. This together can be a base for further development of extraction processes of pea protein on a larger scale as industrial-scale or pilot plant scale. This can help to improve the quality and functionality of commercial pea protein in the future. The obtained knowledge about the aggregation of pea protein can also be used to control and manipulate aggregate and gel formation for food application. The work in this thesis can serve as a base for further research on pea protein and its functionalisation.

From this work, it becomes clear that pea protein is a promising food ingredient. However, there is still limited knowledge about pea protein available. Even though this work

is a step forward in the research field of pea protein technology, there is still plenty of room for more research. Next to pea protein, also other plant-based proteins for example chickpea, sun flower, and oat, which have not been studied in detail, yet. This thesis work can also serve as a base for studies concerning other Leguminosae proteins as beans, lupine, and lentils because of similar protein profiles.

6 SUMMARY/ZUSAMMENFASSUNG

6.1 Summary

Extensive research has been performed on the microparticulation process of whey protein using different thermo-mechanical treatments such as a rheometer, scraped surface heat exchanger or extrusion cooking. These particles were found to generate a ball-bearing effect and therefore be suitable as a fat replacer. However, with increased interest in more sustainable food ingredients and the exploitation of new plant proteins, other proteins come to the fore. A more sustainable alternative to whey protein, which can be grown in central Europe, is pea protein. Limited knowledge is available about pea proteins especially concerning thermo-mechanical treatment.

The current industrial extraction of pea proteins leads to highly denatured and aggregated pea proteins. One of the reasons for this is that those pea proteins are regarded as a waste stream of starch extraction and therefore less attention is paid to keep a high quality of pea proteins. However, with the increasing demand for pea proteins, this might change. Therefore, investigation on which treatment can denature and aggregate pea proteins during extraction on a laboratory scale is important. Currently, there are several methods to extract pea protein on a laboratory scale reported in the literature. Thus, the first aim was to compare current laboratory extraction methods and identify crucial steps during extraction. This resulted in a portfolio of extraction methods and their resulting protein material. From this, suitable extraction methods could be chosen for further analysis on aggregation with and without shear stress. Parameters of interest during aggregation with and without shear stress were changes in pH value, ionic environment, the protein profile of protein material, and shear stress.

Next to the classical bottom-up process, also the top-down process was of interest. The top-down process involves the commercial pea protein, which is highly denatured and aggregated, to become smaller in particle size during thermo-mechanical treatment and could thus be used as a functional ingredient despite its change in nativity and loss of functionality, which was reconstituted to provide added value to already “lost” protein. This way, high efforts in establishing complex extraction methods or compromising established processes for starch production could be avoided.

Thermo-mechanical treatment was performed on small scale using a rheometer and on large scale during extrusion cooking. For large-scale experiments, only commercial pea protein was used due to the lack of material of laboratory extracted ‘native’ pea protein. Thus, microparticulation using extrusion cooking was only performed via the top-down process. Using extrusion cooking has several advantages compared to a scraped surface heat exchanger or sequential processes using a homogenizer or dispersion unit after heating. Extrusion cooking is a simultaneous microparticulation process meaning heating and shearing occurs simultaneously. It is an energy-efficient technique, where process parameters such as temperature, screw speed and mass flow can be changed in a wide range. In comparison to a scraped surface heat exchanger, it can handle high viscosities, which allows high protein concentrations.

For identification of crucial extraction steps three commonly used extraction methods were compared with each other in terms of yield, protein profile, solubility at pH ranging from 3 to 8 and ionic strength ranging from 0.1 M NaCl to 2 M NaCl. The protein products were also compared upon thermal treatment using an mDSC. It could be identified that the precipitation step mainly influenced the protein profile. Protein profile influenced solubility and denaturation temperature. High amounts of legumin in the protein product led to micelle formation and low solubility at low salt concentrations. The usage of alkaline or acidic pH led to conformational changes and slight denaturation in the protein product, which could be seen back in a lower enthalpy change of alkali extracted pea protein.

The aggregation of pea protein was studied in a gel system using oscillatory rheology and during microparticulation using a rheometer and analysing particles on size, morphology and protein-protein interaction. Aggregation was influenced by extraction type, pH and ionic strength. Small oligomers were found to be bound together by covalent bonds. However, no continuous network of covalent bonds was formed. Protein-protein interaction was mostly non-covalent, dominated by hydrophobic interactions. Extraction type influenced the accessibility of protein and dominant protein interaction upon thermal treatment by influencing the degree of pre-denaturation, protein profile, and solubility of the protein material before thermal treatment.

Microparticulation of commercial pea protein was studied using extrusion cooking. Extruder barrel temperature, screw speed and mass flow were varied and resulting particle size and protein-protein interactions within the particles were analyzed. Even though commercial pea protein has a high degree of denatured and aggregated protein, by varying the process parameter the particle size could be manipulated. Protein-protein interaction did not change and was mainly non-covalent. Pea protein particles in the size range between 1 and 20 µm could be produced. Drying of these did not alter particle size. However, upon application of these microparticles in a 50% fat reduced milk dessert dried microparticles showed a lower green, beany off-flavour than undried particles. All pea protein microparticles could inhibit a loss in creaminess by the replacement of 50% fat with pea protein microparticles. Pea protein microparticles were also shown to increase the strength of the milk dessert. Microparticles could increase emulsion stability, but could not add to foam stability.

In conclusion, the microparticulation process of whey proteins was successfully transferred to pea proteins even though the two proteins differ in their aggregation behaviour. A deeper understanding of functionalising pea protein and fundamental knowledge about pea protein has been gathered.

6.2 Zusammenfassung

Die Mikropartikulierung von Molkenproteinen wurde mit Hilfe verschiedener thermomechanischer Verfahren wie Rheometer, Schabewärmetauscher oder Extrusion eingehend untersucht. Es wurde festgestellt, dass diese Partikel einen Kugellagereffekt erzeugen und daher als Fettersatzstoff geeignet sind. Mit dem zunehmenden Interesse an nachhaltigeren Lebensmittelzutaten und der Nutzung neuer Pflanzenproteine rücken andere Proteine in den Vordergrund. Eine u.U. nachhaltigere Alternative zu Molkenprotein, die in Mitteleuropa angebaut werden kann, ist Erbsenprotein. Über Erbsenproteine liegen nur begrenzte Kenntnisse vor, insbesondere was die thermomechanische Behandlung betrifft.

Die derzeitige industrielle Extraktion von Erbsenproteinen führt zu stark denaturierten und aggregierten Erbsenproteinen. Einer der Gründe dafür ist, dass diese Erbsenproteine als Abfallprodukt der Stärkeextraktion angesehen werden und daher weniger darauf geachtet wird, eine hohe Qualität der Erbsenproteine zu erhalten. Mit der steigenden Nachfrage nach Erbsenproteinen könnte sich dies jedoch ändern. Daher ist es wichtig zu untersuchen, durch welche Behandlung Erbsenproteine während der Extraktion im Labormaßstab denaturiert und aggregiert werden können. Derzeit sind in der Literatur mehrere Methoden zur Extraktion von Erbsenprotein im Labormaßstab beschrieben. Daher bestand das erste Ziel darin, die derzeitigen Laborextraktionsmethoden zu vergleichen und die entscheidenden Schritte während der Extraktion zu ermitteln. Dies führte zu einem Portfolio von Extraktionsmethoden und dem daraus resultierenden Proteinmaterial. Daraus konnten geeignete Extraktionsmethoden für die weitere Analyse der Aggregation mit und ohne Scherbeanspruchung ausgewählt werden. Die Parameter, die während der Aggregation mit und ohne Scherbeanspruchung von Interesse waren, waren Änderungen des pH-Werts, der ionischen Umgebung, des Proteinprofils des Proteinmaterials und der Scherbeanspruchung.

Neben dem klassischen Bottom-up-Verfahren war auch das Top-down-Verfahren von Interesse. Beim Top-down-Verfahren wird das kommerzielle Erbsenprotein, das stark denaturiert und aggregiert ist, durch eine thermomechanische Behandlung in eine kleinere Partikelgröße gebracht. Die thermomechanische Behandlung wurde in kleinem Maßstab mit einem Rheometer und in großem Maßstab mittels Extrusion durchgeführt. Für die Experimente im großen Maßstab wurde nur kommerzielles Erbsenprotein verwendet, da zu wenig Material des laborextrahiertem Erbsenprotein vorhanden war. Daher wurde die Mikropartikulation mittels Extrusionskochen nur im Top-down-Verfahren durchgeführt. Die Anwendung der Extrusion hat mehrere Vorteile im Vergleich zu einem Schabewärmetauscher oder zu sequentiellen Prozessen, in dem thermisch hergstellte Gele oder große Partikel zerkleinert werden mittels einem Homogenisator oder einer Dispergiereinheit. Beim Extrudieren handelt es sich um ein simultanes Mikropartikulationsverfahren, d. h. Erhitzung und Scherung erfolgen gleichzeitig. Es handelt sich um eine energieeffiziente Technik, bei der Prozessparameter wie Temperatur, Schneckendrehzahl und Massenstrom in einem weiten Bereich verändert werden können. Im Vergleich zu einem Schabewärmetauscher können hohe Viskositäten gehandhabt werden, was hohe Proteinkonzentrationen ermöglicht.

Zur Identifizierung der entscheidenden Extraktionsschritte wurden drei gängige Extraktionsmethoden hinsichtlich Ausbeute, Proteinprofil, Löslichkeit bei einem pH-Wert von 3 bis 8 und einer Ionenstärke von 0,1 M NaCl bis 2 M NaCl miteinander verglichen. Die Proteinprodukte wurden thermisch analysiert mit einer mDSC. Es konnte festgestellt werden, dass der Fällungsschritt das Proteinprofil am stärksten beeinflusst. Das Proteinprofil beeinflusste die Löslichkeit und die Denaturierungstemperatur. Ein hoher Anteil an Leguminosen im Proteinprodukt führte zu Mizellenbildung und geringer Löslichkeit bei niedrigen Salzkonzentrationen. Die Verwendung eines alkalischen oder sauren pH-Wertes führte zu Konformationsänderungen und einer leichten Denaturierung des Proteinprodukts, was sich in einer geringeren Enthalpieänderung des alkaliextrahierten Erbsenproteins widerspiegelte.

Die Aggregation von Erbsenprotein wurde in einem Gelsystem mit Hilfe der Oszillationsrheologie und während der Mikropartikulation mit einem Rheometer untersucht und die Partikel auf Größe, Morphologie und Protein-Protein-Interaktion analysiert. Die Aggregation wurde durch die Art der Extraktion, den pH-Wert und die Ionenstärke beeinflusst. Es wurde festgestellt, dass kleine Oligomere durch kovalente Bindungen miteinander verbunden sind. Es wurde jedoch kein kontinuierliches Netzwerk kovalenter Bindungen gebildet. Die Protein-Protein-Wechselwirkung war meist nicht kovalent und wurde von hydrophoben Wechselwirkungen dominiert. Die Art der Extraktion beeinflusste die Zugänglichkeit des Proteins und die vorherrschende Proteinwechselwirkung bei der thermischen Behandlung, indem sie den Grad der Vordenaturierung, das Proteinprofil und die Löslichkeit des Proteinmaterials vor der thermischen Behandlung beeinflusste.

Die Mikropartikulation von handelsüblichem Erbsenprotein wurde mittels Extrusion untersucht. Die Temperatur des Extruderzylinders, die Schneckendrehzahl und der Massenstrom wurden variiert und die daraus resultierende Partikelgröße sowie die Protein-Protein-Wechselwirkungen innerhalb der Partikel wurden analysiert. Obwohl handelsübliches Erbsenprotein einen hohen Anteil an denaturiertem und aggregiertem Protein aufweist, konnte die Partikelgröße durch Variation der Prozessparameter beeinflusst werden. Die Protein-Protein-Wechselwirkung änderte sich nicht und war hauptsächlich nicht kovalent. Es konnten Erbsenproteinpartikel in einem Größenbereich zwischen 1 und 20 µm hergestellt werden. Deren Trocknung veränderte die Partikelgröße nicht. Bei der Anwendung dieser Mikropartikel in einem 50% fettreduzierten Milchdessert zeigten die getrockneten Mikropartikel jedoch einen geringeren grünen, bohnigen Beigeschmack als die ungetrockneten Partikel. Alle Erbsenprotein-Mikropartikel konnten einen Verlust an Cremigkeit durch den Ersatz von 50% Fett durch Erbsenprotein-Mikropartikel verhindern. Es zeigte sich auch, dass Erbsenprotein-Mikropartikel die Festigkeit des Milchdesserts erhöhen. Mikropartikel konnten die Emulsionsstabilität erhöhen, aber nicht zur Schaumstabilität beitragen.

Zusammenfassend lässt sich sagen, dass der Mikropartikulationsprozess von Molkenproteinen erfolgreich auf Erbsenproteine übertragen wurde, obwohl sich die beiden Proteine in ihrem Aggregationsverhalten unterscheiden. Ein tieferes Verständnis der

Funktionalisierung von Erbsenproteinen und grundlegende Kenntnisse über Erbsenproteine wurden gewonnen.

7 PUBLICATION BIBLIOGRAPHY

Aggarwal, Dipesh; Sabikhi, Latha; Sathish Kumar, M. H. (2016): Formulation of reduced-calorie biscuits using artificial sweeteners and fat replacer with dairy–multigrain approach. In *NFS Journal* 2, pp. 1–7. DOI: 10.1016/j.nfs.2015.10.001.

Akin, Musa Serdar; Kirmaci, Zuhal (2015): Influence of fat replacers on the chemical, textural and sensory properties of low-fat Beyaz pickled cheese produced from ewe's milk. In *International Journal of Dairy Technology* 68 (1), pp. 127–134. DOI: 10.1111/1471-0307.12164.

Ako, Komla; Nicolai, Taco; Durand, Dominique; Brotons, Guillaume (2009): Microphase separation explains the abrupt structural change of denatured globular protein gels on varying the ionic strength or the pH. In *Soft Matter* 5 (20), p. 4033. DOI: 10.1039/b906860k.

Akyol, Çağdaş; Alpas, Hami; Bayındırlı, Alev (2006): Inactivation of peroxidase and lipoxygenase in carrots, green beans, and green peas by combination of high hydrostatic pressure and mild heat treatment. In *European Food Research and Technology* 224 (2), pp. 171–176. DOI: 10.1007/s00217-006-0303-3.

Ali, Fadi; Ippersiel, Denis; Lamarche, François; Mondor, Martin (2010): Characterization of low-phytate soy protein isolates produced by membrane technologies. In *Innovative Food Science & Emerging Technologies* 11 (1), pp. 162–168. DOI: 10.1016/j.ifset.2009.08.004.

Amagliani, Luca; Ben Sassi, Elyes; Buczkowski, Johann; Schmitt, Christophe (2020): Influence of protein source on the morphology, physicochemical and flow properties of protein-based emulsion particles to be used as texture modulators. In *Food Hydrocolloids* 101, p. 105581. DOI: 10.1016/j.foodhyd.2019.105581.

Andlinger, David Julian; Bornkeßel, Alina Claire; Jung, Isabella; Schröter, Baldur; Smirnova, Irina; Kulozik, Ulrich (2021a): Microstructures of potato protein hydrogels and aerogels produced by thermal crosslinking and supercritical drying. In *Food Hydrocolloids* 112, p. 106305. DOI: 10.1016/j.foodhyd.2020.106305.

Andlinger, David Julian; Rampp, Lena; Tanger, Caren; Kulozik, Ulrich (2021b): Viscoelasticity and Protein Interactions of Hybrid Gels Produced from Potato and Whey Protein Isolates. In *ACS Food Science & Technology* 1 (7), pp. 1304–1315. DOI: 10.1021/acsfoodscitech.1c00163.

Andlinger, David Julian; Röscheisen, Pauline; Hengst, Claudia; Kulozik, Ulrich (2021c): Influence of pH, Temperature and Protease Inhibitors on Kinetics and Mechanism of Thermally Induced Aggregation of Potato Proteins. In *Foods* 10 (4), p. 796. DOI: 10.3390/foods10040796.

Arêas, J. A. (1992): Extrusion of food proteins. In *Critical Reviews in Food Science and Nutrition* 32 (4), pp. 365–392. DOI: 10.1080/10408399209527604.

Arntfield, Susan D.; Ismond, M. Anne H.; Murray, E. Donald (1985): The fate of antinutritional factors during the preparation of a fababean protein isolate using a

micellization technique. In *Canadian Institute of Food Science and Technology Journal* 18 (2), pp. 137–143. DOI: 10.1016/S0315-5463(85)71771-3.

Arntfield, Susan D.; Maskus, H. D. (2011): 9 - Peas and other legume proteins. In Glyn O. Philips (Ed.): Handbook of food proteins. Oxford: Woodhead Publ (Woodhead Publishing series in food science, technology and nutrition, 222), pp. 233–266. Available online at https://www.sciencedirect.com/science/article/pii/B9781845697587500095.

Arntfield, Susan D.; Murray, E. Donald; Ismond, M. Anne H. (1991): Role of disulfide bonds in determining the rheological and microstructural properties of heat-induced protein networks from ovalbumin and vicilin. In *Journal of Agricultural and Food Chemistry* 39 (8), pp. 1378–1385. DOI: 10.1021/jf00008a005.

Bacon, James R.; Noel, Timothy R.; Lambert, N. (1990): Preparation of transparent pea protein gels: a comparison of isolation procedures. In *International Journal of Food Science & Technology* 25 (5), pp. 527–537. DOI: 10.1111/j.1365-2621.1990.tb01112.x.

Baldwin, Alan J. (2010): Insolubility of milk powder products – A minireview. In *Dairy Science & Technology* 90 (2-3), pp. 169–179. DOI: 10.1051/dst/2009056.

Barac, Miroljub; Cabrilo, Slavica; Pesic, Mirjana; Stanojevic, Sladjana; Zilic, Sladjana; Macej, Ognjen; Ristic, Nikola (2010): Profile and functional properties of seed proteins from six pea (Pisum sativum) genotypes. In *International Journal of Molecular Sciences* 11 (12), pp. 4973–4990. DOI: 10.3390/ijms11124973.

Baune, Marie-Christin; Schroeder, Sarah; Witte, Franziska; Heinz, Volker; Bindrich, Ute; Weiss, Jochen; Terjung, Nino (2021): Analysis of protein-network formation of different vegetable proteins during emulsification to produce solid fat substitutes. In *Journal of Food Measurement and Characterization* 15 (3), pp. 2399–2416. DOI: 10.1007/s11694-020-00767-9.

Beck, Svenja M.; Knoerzer, Kai; Arcot, Jayashree (2017): Effect of low moisture extrusion on a pea protein isolate's expansion, solubility, molecular weight distribution and secondary structure as determined by Fourier Transform Infrared Spectroscopy (FTIR). In *Journal of Food Engineering* 214, pp. 166–174. DOI: 10.1016/j.jfoodeng.2017.06.037.

Bekard, Innocent B.; Asimakis, Peter; Bertolini, Joseph; Dunstan, Dave E. (2011): The effects of shear flow on protein structure and function. In *Biopolymers* 95 (11), pp. 733–745. DOI: 10.1002/bip.21646.

Ben-Harb, S.; Panouillé, M.; Huc-Mathis, D.; Moulin, G.; Saint-Eve, Anne; Irlinger, F. et al. (2018): The rheological and microstructural properties of pea, milk, mixed pea/milk gels and gelled emulsions designed by thermal, acid, and enzyme treatments. In *Food Hydrocolloids* 77, pp. 75–84. DOI: 10.1016/j.foodhyd.2017.09.022.

Bhandari, Bhesh (2013): Handbook of food powders. Processes and properties. Cambridge: Woodhead (Woodhead Publishing series in food science, technology

and nutrition, 255). Available online at http://gbv.eblib.com/patron/FullRecord.aspx?p=1574962.

Blond, Genevieve; Roudaut, Gaelle; Simatos, Denise; Champion, Dominique; Le Meste, Martine (2005): Interaction of Water with Food Components. In : Food Science and Technology: CRC Press, pp. 87–138.

Bogahawaththa, Dimuthu; Chau, Nguyen Hoang Bao; Trivedi, Jigar; Dissanayake, Muditha; Vasiljevic, Todor (2019): Impact of controlled shearing on solubility and heat stability of pea protein isolate dispersed in solutions with adjusted ionic strength. In *Food Research International* 125, p. 108522. DOI: 10.1016/j.foodres.2019.108522.

Boland, M. (2011): 3 - Whey proteins. In Glyn O. Philips (Ed.): Handbook of food proteins. Oxford: Woodhead Publ (Woodhead Publishing series in food science, technology and nutrition, 222), pp. 30–55. Available online at https://www.sciencedirect.com/science/article/pii/B9781845697587500034.

Bon, Christel; Nicolai, Taco; Durand, Dominique (1999): Growth and structure of aggregates of heat-denatured beta-Lactoglobulin. In *International Journal of Food Science & Technology* 34 (5-6), pp. 451–465. DOI: 10.1046/j.1365-2621.1999.00310.x.

Böttcher, S.; Steinhäuser, U.; Drusch, S. (2015): Off-flavour masking of secondary lipid oxidation products by pea dextrin. In *Food Chemistry* 169, pp. 492–498. DOI: 10.1016/j.foodchem.2014.05.006.

Bowland, Eilene L.; Foegeding, Allen E.; Hamann, Donald D. (1995): Rheological analysis of anion-induced matrix transformations in thermally induced whey protein isolate gels. In *Food Hydrocolloids* 9 (1), pp. 57–64. DOI: 10.1016/S0268-005X(09)80194-X.

Boye, J. I.; Aksay, S.; Roufik, S.; Ribéreau, S.; Mondor, Martin; Farnworth, E.; Rajamohamed, S. H. (2010): Comparison of the functional properties of pea, chickpea and lentil protein concentrates processed using ultrafiltration and isoelectric precipitation techniques. In *Food Research International* 43 (2), pp. 537–546. DOI: 10.1016/j.foodres.2009.07.021.

Boye, J. I.; Alli, I. (2000): Thermal denaturation of mixtures of α-lactalbumin and β-lactoglobulin: a differential scanning calorimetric study. In *Food Research International* 33 (8), pp. 673–682. DOI: 10.1016/S0963-9969(00)00112-5.

Brehm, Laura; Jünger, Manon; Frank, Oliver; Hofmann, Thomas (2019): Discovery of a Thiamine-Derived Taste Enhancer in Process Flavors. In *Journal of Agricultural and Food Chemistry* 67 (20), pp. 5857–5865. DOI: 10.1021/acs.jafc.9b01832.

Brighenti, M.; Govindasamy-Lucey, S.; Jaeggi, J. J.; Johnson, M. E.; Lucey, J. A. (2020): Behavior of stabilizers in acidified solutions and their effect on the textural, rheological, and sensory properties of cream cheese. In *Journal of Dairy Science* 103 (3), pp. 2065–2076. DOI: 10.3168/jds.2019-17487.

Britten, Michel; Giroux, Hélène J. (2001): Acid-induced gelation of whey protein polymers: effects of pH and calcium concentration during polymerization. In *Food Hydrocolloids* 15 (4-6), pp. 609–617. DOI: 10.1016/S0268-005X(01)00049-2.

Çakır-Fuller, Esra (2015): Enhanced heat stability of high protein emulsion systems provided by microparticulated whey proteins. In *Food Hydrocolloids* 47, pp. 41–50. DOI: 10.1016/j.foodhyd.2015.01.003.

Casey, Roderick (1982): The genetics of pea seed storage proteins. In *Plant Foods for Human Nutrition* 31 (3), pp. 281–295. DOI: 10.1007/BF01108636.

Casey, Roderick; Short, Margaret N. (1981): Variation in amino acid composition of legumin from Pisum. In *Phytochemistry* 20 (1), pp. 21–23. DOI: 10.1016/0031-9422(81)85210-7.

Cavallieri, Angelo Luiz Fazani; Costa-Netto, Antonio Paulino; Menossi, Marcelo; Da Cunha, Rosiane Lopes (2007): Whey protein interactions in acidic cold-set gels at different pH values. In *Le Lait* 87 (6), pp. 535–554. DOI: 10.1051/lait:2007032.

Chao, Dongfang; Aluko, Rotimi E. (2018): Modification of the structural, emulsifying, and foaming properties of an isolated pea protein by thermal pretreatment. In *CyTA - Journal of Food* 16 (1), pp. 357–366. DOI: 10.1080/19476337.2017.1406536.

Chaudhari, Nirupa; Roper, Stephen D. (2010): The cell biology of taste. In *The Journal of Cell Biology* 190 (3), pp. 285–296. DOI: 10.1083/jcb.201003144.

Cheftel, Jean Claude (1986): Nutritional effects of extrusion-cooking. In *Food Chemistry* 20 (4), pp. 263–283. DOI: 10.1016/0308-8146(86)90096-8.

Cheftel, Jean Claude; Dumay, Eliane (1993): Microcoagulation of proteins for development of “creaminess”. In *Food Reviews International* 9 (4), pp. 473–502. DOI: 10.1080/87559129309540975.

Cheftel, Jean Claude; Kitagawa, M.; Quéguiner, C. (1992): New protein texturization processes by extrusion cooking at high moisture levels. In *Food Reviews International* 8 (2), pp. 235–275. DOI: 10.1080/87559129209540940.

Chihi, Mohammed Lazhar; Mession, Jean-Luc; Sok, Nicolas; Saurel, Rémi (2016): Heat-Induced Soluble Protein Aggregates from Mixed Pea Globulins and β-Lactoglobulin. In *Journal of Agricultural and Food Chemistry* 64 (13), pp. 2780–2791. DOI: 10.1021/acs.jafc.6b00087.

Choi, Hiuwan; Aboulfatova, Khatira; Pownall, Henry J.; Cook, Richard; Dong, Jing-fei (2007): Shear-induced disulfide bond formation regulates adhesion activity of von Willebrand factor. In *Journal of Biological Chemistry* 282 (49), pp. 35604–35611. DOI: 10.1074/jbc.M704047200.

Choi, Siu-Mei; Ma, Ching-Yung (2005): Conformational study of globulin from common buckwheat (Fagopyrum esculentum Moench) by Fourier transform infrared spectroscopy and differential scanning calorimetry. In *Journal of Agricultural and Food Chemistry* 53 (20), pp. 8046–8053. DOI: 10.1021/jf051040v.

Choi, Siu-Mei; Ma, Ching-Yung (2007): Structural characterization of globulin from common buckwheat (Fagopyrum esculentum Moench) using circular dichroism and Raman spectroscopy. In *Food Chemistry* 102 (1), pp. 150–160. DOI: 10.1016/j.foodchem.2006.05.011.

Cleland, W. W. (1964): Dithiothreitol, a New Protective Reagent for SH Groups *. In *Biochemistry* 3 (4), pp. 480–482. DOI: 10.1021/bi00892a002.

Cordero-de-los-Santos, M. Y.; Osuna-Castro, J. A.; Borodanenko, A.; Paredes-López, Octavio (2005): Physicochemical and Functional Characterisation of Amaranth (Amaranthus hypochondriacus) Protein Isolates Obtained by Isoelectric Precipitation and Micellisation. In *International Journal of Food Science & Technology* 11 (4), pp. 269–280. DOI: 10.1177/1082013205056491.

Cornet, Steven H. V.; Snel, Silvia J. E.; Schreuders, Floor K. G.; van der Sman, Ruud G. M.; Beyrer, Michael; van der Goot, Atze Jan (2021): Thermo-mechanical processing of plant proteins using shear cell and high-moisture extrusion cooking. In *Critical Reviews in Food Science and Nutrition*, pp. 1–18. DOI: 10.1080/10408398.2020.1864618.

Creusot, Nathalie; Wierenga, Peter A.; Laus, Marc C.; Giuseppin, Marco L. F.; Gruppen, Harry (2011): Rheological properties of patatin gels compared with β-lactoglobulin, ovalbumin, and glycinin. In *Journal of the science of food and agriculture* 91 (2), pp. 253–261. DOI: 10.1002/jsfa.4178.

Croy, R. R.; Gatehouse, J. A.; Tyler, M.; Boulter, D. (1980): The purification and characterization of a third storage protein (convicilin) from the seeds of pea (Pisum sativum L.). In *Biochemical Journal* 191 (2), pp. 509–516. DOI: 10.1042/bj1910509.

Croy, R. R.; Hoque, M. S.; Gatehouse, J. A.; Boulter, D. (1984): The major albumin proteins from pea (Pisum sativum L). Purification and some properties. In *Biochemical Journal* 218 (3), pp. 795–803. DOI: 10.1042/bj2180795.

Cui, Leqi; Kimmel, Jennifer; Zhou, Leon; Rao, Jiajia; Chen, Bingcan (2020): Combining solid dispersion-based spray drying with cyclodextrin to improve the functionality and mitigate the beany odor of pea protein isolate. In *Carbohydrate Polymers* 245, p. 116546. DOI: 10.1016/j.carbpol.2020.116546.

Czerny, Michael; Christlbauer, Martin; Christlbauer, Monika; Fischer, Anja; Granvogl, Michael; Hammer, Michaela et al. (2008): Re-investigation on odour thresholds of key food aroma compounds and development of an aroma language based on odour qualities of defined aqueous odorant solutions. In *European Food Research and Technology* 228 (2), pp. 265–273. DOI: 10.1007/s00217-008-0931-x.

Da Chen; Zhu, Xiao; Ilavsky, Jan; Whitmer, Tanya; Hatzakis, Emmanuel; Jones, Owen G.; Campanella, Osvaldo H. (2021): Polyphenols Weaken Pea Protein Gel by Formation of Large Aggregates with Diminished Noncovalent Interactions. In *Biomacromolecules* 22 (2), pp. 1001–1014. DOI: 10.1021/acs.biomac.0c01753.

Damodaran, Srinivasan (1988): Refolding of thermally unfolded soy proteins during the cooling regime of the gelation process: effect on gelation. In *Journal of Agricultural and Food Chemistry* 36 (2), pp. 262–269. DOI: 10.1021/jf00080a007.

Dannenberg, Frank; Kessler, Heinz-Gerhard (1988): Reaction Kinetics of the Denaturation of Whey Proteins in Milk. In *Journal of Food Science* 53 (1), pp. 258–263. DOI: 10.1111/j.1365-2621.1988.tb10223.x.

Delahaije, Roy J. B. M.; Gruppen, Harry; van Eijk Boxtel, Evelien L.; Cornacchia, Leonardo; Wierenga, Peter A. (2016): Controlling the Ratio between Native-Like, Non-Native-Like, and Aggregated β-Lactoglobulin after Heat Treatment. In *Journal of Agricultural and Food Chemistry* 64 (21), pp. 4362–4370. DOI: 10.1021/acs.jafc.6b00816.

Delahaije, Roy J. B. M.; Wierenga, Peter A.; Giuseppin, Marco L. F.; Gruppen, Harry (2015): Comparison of heat-induced aggregation of globular proteins. In *Journal of Agricultural and Food Chemistry* 63 (21), pp. 5257–5265. DOI: 10.1021/acs.jafc.5b00927.

Derbyshire, E; Wright, David J.; Boulter, D. (1976): Legumin and Vicilin, Storage Proteins of Legume Seeds. In *Phytochemistry* 15 (1), pp. 3–24. DOI: 10.1016/S0031-9422(00)89046-9.

Destribats, Mathieu; Rouvet, Martine; Gehin-Delval, Cécile; Schmitt, Christophe; Binks, Bernard P. (2014): Emulsions stabilised by whey protein microgel particles: towards food-grade Pickering emulsions. In *Soft Matter* 10 (36), pp. 6941–6954. DOI: 10.1039/c4sm00179f.

Djoullah, Attaf; Djemaoune, Yanis; Husson, Florence; Saurel, Rémi (2015): Native-state pea albumin and globulin behavior upon transglutaminase treatment. In *Process Biochemistry* 50 (8), pp. 1284–1292. DOI: 10.1016/j.procbio.2015.04.021.

Dombrowski, Jannika; Johler, F.; Warncke, M.; Kulozik, Ulrich (2016): Correlation between bulk characteristics of aggregated β-lactoglobulin and its surface and foaming properties. In *Food Hydrocolloids* 61, pp. 318–328. DOI: 10.1016/j.foodhyd.2016.05.027.

Dunkel, Andreas; Hofmann, Thomas (2009): Sensory-directed identification of beta-alanyl dipeptides as contributors to the thick-sour and white-meaty orosensation induced by chicken broth. In *Journal of Agricultural and Food Chemistry* 57 (21), pp. 9867–9877. DOI: 10.1021/jf900948r.

Dziuba, Jerzy; Szerszunowicz, Iwona; Natecz, Dorota; Dsiuba, Marta (2014): Proteomic Analysis of Albumin and Globulin Fractions of Pea (Pisum Sativum L.) Seeds. In *Acta Scientiarum Polonorum - Technologia Alimentaria* 13 (2), pp. 181–190. DOI: 10.17306/J.AFS.2014.2.7.

Ebeling, Melvin E. (1968): The Dumas Method for Nitrogen in Feeds. In *Journal of AOAC INTERNATIONAL* 51 (4), pp. 766–770. DOI: 10.1093/jaoac/51.4.766.

El-Aidie, Safaa A.M.; Ghita, Ebtisam I.; El-Dieb, Samia M.; El-Garhi, Hosam-Eddin M. (2019): Physicochemical, Microstructural and Sensory Impact of Fat Replacers on Low-fat Edam Cheese Manufactured from Buffalo's Milk. In *International Journal of Advancement in Life Sciences Research* 2 (3), pp. 11–21.

Elofsson, Ulla M.; Dejmek, Petr; Paulsson, Marie A. (1996): Heat-induced aggregation of β-lactoglobulin studied by dynamic light scattering. In *IDF Symposium on Science and Technology of Fermented MilkIDF Symposium on Microstructure of Dairy Products* 6 (4), pp. 343–357. DOI: 10.1016/0958-6946(95)00019-4.

Engelen, Lina; van der Bilt, Andries; Schipper, M.; Bosman, Frits (2005): Oral size perception of particles: Effect of size, type, viscosity and method. In *Journal of Texture Studies* 36 (4), pp. 373–386. DOI: 10.1111/j.1745-4603.2005.00022.x.

Eremin, Y. A. (2005): SCATTERING | Scattering Theory. In B. D. Guenther (Ed.): Encyclopedia of modern optics. Amsterdam: Elsevier, pp. 326–330. Available online at https://www.sciencedirect.com/science/article/pii/B0123693950006825.

Evans, E. (2001): Probing the relation between force--lifetime--and chemistry in single molecular bonds. In *Annual Review of Biophysics and Biomolecular Structure* 30, pp. 105–128. DOI: 10.1146/annurev.biophys.30.1.105.

Fasolin, L. H.; Pereira, R. N.; Pinheiro, A. C.; Martins, J. T.; Andrade, C. C. P.; Ramos, O. L.; Vicente, A. A. (2019): Emergent food proteins - Towards sustainability, health and innovation. In *Food Research International* 125, p. 108586. DOI: 10.1016/j.foodres.2019.108586.

Felix, M.; Perez-Puyana, V.; Romero, Alberto; Guerrero, A. (2017): Development of thermally processed bioactive pea protein gels: Evaluation of mechanical and antioxidant properties. In *Food and Bioproducts Processing* 101, pp. 74–83. DOI: 10.1016/j.fbp.2016.10.013.

Foegeding, Allen E.; Luck, P. J. (2003): MILK PROTEINS | Whey Protein Products. In Hubert Roginski (Ed.): Encyclopedia of dairy sciences. Amsterdam: Academic Press, pp. 1957–1960. Available online at https://www.sciencedirect.com/science/article/pii/B0122272358003266.

Frank, Oliver; Kreissl, Johanna Karoline; Daschner, Andreas; Hofmann, Thomas (2014): Accurate determination of reference materials and natural isolates by means of quantitative (1)h NMR spectroscopy. In *Journal of Agricultural and Food Chemistry* 62 (12), pp. 2506–2515. DOI: 10.1021/jf405529b.

Fredrikson, M.; Biot, P.; Alminger, M. L.; Carlsson, N. G.; Sandberg, A. S. (2001): Production process for high-quality pea-protein isolate with low content of oligosaccharides and phytate. In *Journal of Agricultural and Food Chemistry* 49 (3), pp. 1208–1212. DOI: 10.1021/jf000708x.

Frerot, Eric; Bagnoud, Alain; Cicchetti, Esmeralda (2014): Quantification of Hydrogen Sulfide and Methanethiol and the Study of Their Scavenging by Biocides of the Isothiazolone Family. In *ChemPlusChem* 79 (1), pp. 77–82. DOI: 10.1002/cplu.201300234.

Frøst, Michael Bom; Janhøj, Thomas (2007): Understanding creaminess. In *IDF Symposium on Science and Technology of Fermented MilkIDF Symposium on Microstructure of Dairy Products* 17 (11), pp. 1298–1311. DOI: 10.1016/j.idairyj.2007.02.007.

Fuhrmeister, H; Meuser, Friedrich (2003): Impact of processing on functional properties of protein products from wrinkled peas. In *Journal of Food Engineering* 56 (2-3), pp. 119–129. DOI: 10.1016/S0260-8774(02)00241-8.

Gaiani, C; Morand, Marion; Sánchez, C. C.; Tehrany, E; Jacquot, M; Schuck, P et al. (2010): How surface composition of high milk proteins powders is influenced by spray-drying temperature. In *undefined*. Available online at https://www.semanticscholar.org/paper/How-surface-composition-of-high-milk-proteins-is-by-Gaiani-Morand/41c9c93698e0246081dea3f4eeba6b9350c8c6dc.

Galindo, M. M.; Voigt, Nadine; Stein, Julia; van Lengerich, Jessica; Raguse, Jan-Dirk; Hofmann, Thomas et al. (2012): Protein–coupled receptors in human fat taste perception. In *Chemical Senses* 37 (2), pp. 123–139.

García Arteaga, Verónica; Apéstegui Guardia, Marijose; Muranyi, Isabel; Eisner, Peter; Schweiggert-Weisz, Ute (2020): Effect of enzymatic hydrolysis on molecular weight distribution, techno-functional properties and sensory perception of pea protein isolates. In *Innovative Food Science & Emerging Technologies* 65, p. 102449. DOI: 10.1016/j.ifset.2020.102449.

Gläser, Peter; Dawid, Corinna; Meister, Stefanie; Bader-Mittermaier, Stephanie; Schott, Michael; Eisner, Peter; Hofmann, Thomas (2020): Molecularization of Bitter Off-Taste Compounds in Pea-Protein Isolates (Pisum sativum L.). In *Journal of Agricultural and Food Chemistry* 68 (38), pp. 10374–10387. DOI: 10.1021/acs.jafc.9b06663.

Gómez-Guillén, M. C.; Borderías, A. Javier; Montero, P. (1997): Chemical Interactions of Nonmuscle Proteins in the Network of Sardine (Sardina pilchardus) Muscle Gels. In *LWT - Food Science and Technology* 30 (6), pp. 602–608. DOI: 10.1006/fstl.1997.0239.

Gruen, Clem; Guthrie, Robin; Blagrove, Robert (1987): Structure of a major pea seed albumin: Implication of a free sulphydryl group. In *Journal of Agricultural and Food Chemistry* 1987 (41), pp. 167–178.

Gu, Zuguang; Eils, Roland; Schlesner, Matthias (2016): Complex heatmaps reveal patterns and correlations in multidimensional genomic data. In *Bioinformatics* 32 (18), pp. 2847–2849. DOI: 10.1093/bioinformatics/btw313.

Gueguen, Jacques (1989): Relation between conformation and surface hydrophobicity of pea (Pisum sativum L.) globulins. In *Journal of Agricultural and Food Chemistry* 37 (5), pp. 1236–1241. DOI: 10.1021/jf00089a008.

Gueguen, Jacques; Vu, Anh T; Schaeffer, Francois: Large-scale purification and characterisation of pea globulins.

Harper, James M. (1986): Extrusion texturization of foods. In *Food Technology* 40, pp. 70–76.

Havea, Palatasa; Carr, Alistair J.; Creamer, Lawrence K. (2004): The roles of disulphide and non-covalent bonding in the functional properties of heat-induced whey protein gels. In *The Journal of dairy research* 71 (3), pp. 330–339. DOI: 10.1017/s002202990400024x.

Havea, Palatasa; Watkinson, Philip; Kuhn-Sherlock, Barbara (2009): Heat-induced whey protein gels: protein-protein interactions and functional properties. In *Journal of Agricultural and Food Chemistry* 57 (4), pp. 1506–1512. DOI: 10.1021/jf802559z.

Hernández, N. M. (2007): Aroma compounds responsible for the creamy aroma of milk products. Dissertation. Technische Universität München, München.

Hippel, Peter H. von; Schleich, Thomas (1969): Ion effects on the solution structure of biological macromolecules. In *Accounts of Chemical Research* 2 (9), pp. 257–265. DOI: 10.1021/ar50021a001.

Hoffmann, Marion A. M.; van Mil, Peter J. J. M. (1997): Heat-Induced Aggregation of β-Lactoglobulin: Role of the Free Thiol Group and Disulfide Bonds. In *Journal of Agricultural and Food Chemistry* 45 (8), pp. 2942–2948. DOI: 10.1021/jf960789q.

Hua, Yufei; Cui, Steve W.; Wang, Qi; Mine, Yoshinori; Poysa, Vaino (2005): Heat induced gelling properties of soy protein isolates prepared from different defatted soybean flours. In *Food Research International* 38 (4), pp. 377–385. DOI: 10.1016/j.foodres.2004.10.006.

Ipsen, Richard (2017): Microparticulated whey proteins for improving dairy product texture. In *IDF Symposium on Science and Technology of Fermented MilkIDF Symposium on Microstructure of Dairy Products* 67, pp. 73–79. DOI: 10.1016/j.idairyj.2016.08.009.

Janssen, Meike; Busch, Claudia; Rödiger, Manika; Hamm, Ulrich (2016): Motives of consumers following a vegan diet and their attitudes towards animal agriculture. In *Appetite* 105, pp. 643–651. DOI: 10.1016/j.appet.2016.06.039.

Jiang, Shanshan; Ding, Junzhou; Andrade, Juan; Rababah, Taha M.; Almajwal, Ali; Abulmeaty, Mahmoud M.; Feng, Hao (2017): Modifying the physicochemical properties of pea protein by pH-shifting and ultrasound combined treatments. In *Ultrasonics Sonochemistry* 38, pp. 835–842. DOI: 10.1016/j.ultsonch.2017.03.046.

Jiang, Zhong-qing; Pulkkinen, Marjo; Wang, Yu-jie; Lampi, Anna-Maija; Stoddard, Fred L.; Salovaara, Hannu et al. (2016): Faba bean flavour and technological property improvement by thermal pre-treatments. In *LWT - Food Science and Technology* 68, pp. 295–305. DOI: 10.1016/j.lwt.2015.12.015.

Jung, Jin-Mi; Savin, Gabriela; Pouzot, Matthieu; Schmitt, Christophe; Mezzenga, Raffaele (2008): Structure of heat-induced beta-lactoglobulin aggregates and their complexes with sodium-dodecyl sulfate. In *Biomacromolecules* 9 (9), pp. 2477–2486. DOI: 10.1021/bm800502j.

Karaca, Asli Can; Low, Nicholas H.; Nickerson, Michael T. (2011): Emulsifying properties of chickpea, faba bean, lentil and pea proteins produced by isoelectric precipitation and salt extraction. In *Food Research International* 44 (9), pp. 2742–2750. DOI: 10.1016/j.foodres.2011.06.012.

Keim, Susanne (2005): Hydrostatisch, thermisch, säure- und labinduzierte Casein- und Molkenprotein-Gele. Stabilisierende Bindungen und Textureigenschaften. Zugl.: Hohenheim, Univ., Diss., 2005. Aachen: Shaker (Berichte aus der Lebensmitteltechnologie).

Keim, Susanne; Hinrichs, Jörg (2004): Influence of stabilizing bonds on the texture properties of high-pressure-induced whey protein gels. In *International Dairy Journal* 14 (4), pp. 355–363. DOI: 10.1016/j.idairyj.2003.10.010.

Keim, Susanne; Kulozik, Ulrich; Hinrichs, Jörg (2006): Texture and stabilizing bonds in pressure-induced, heat-induced and rennet-induced milk protein gels. In *Milchwissenschaft* 61 (4), pp. 363–366.

Kennel, Regula (1994): Hitzeinduzierte Aggregatbildung von Molkenproteinen -Größenbestimmung und Strukturanalyse -. Dissertation. Technical University Munich, Freising, Germany. Lehrstuhl für Lebensmittelverfahrenstechnik und Molkereitechnologie.

Kessler, Heinz-Gerhard (2002): Food and bio process engineering. Dairy technology ; 109 tables. 5th revised and extended edition. München: A. Kessler. Available online at http://worldcatlibraries.org/wcpa/oclc/607055573.

Kew, Ben; Holmes, Melvin; Stieger, Markus; Sarkar, Anwesha (2020): Review on fat replacement using protein-based microparticulated powders or microgels: A textural perspective. In *Trends in Food Science & Technology* 106, pp. 457–468. DOI: 10.1016/j.tifs.2020.10.032.

Kim, Won-Woo; Yoo, Byoungseung (2009): Rheological behaviour of acorn starch dispersions: effects of concentration and temperature. In *International Journal of Food Science & Technology* 44 (3), pp. 503–509. DOI: 10.1111/j.1365-2621.2008.01760.x.

Klost, M.; Brzeski, C.; Drusch, S. (2020): Effect of protein aggregation on rheological properties of pea protein gels. In *Food Hydrocolloids* 108, p. 106036. DOI: 10.1016/j.foodhyd.2020.106036.

Klost, M.; Drusch, S. (2019): Structure formation and rheological properties of pea protein-based gels. In *Food Hydrocolloids* 94, pp. 622–630. DOI: 10.1016/j.foodhyd.2019.03.030.

Klotzbücher, Björn Christof (2009): Milchsaure Fermentation von Leguminosenproteinextrakten mit dem Ziel geschmacklicher Verbesserung. Available online at https://opacplus.bsb-muenchen.de/search?id=11723122&View=default&db=100.

Kornet, Remco; Shek, Carol; Venema, Paul; van der Goot, Atze Jan; Meinders, Marcel B. J.; van der Linden, Erik (2021a): Substitution of whey protein by pea protein is facilitated by specific fractionation routes. In *Food Hydrocolloids* 117, p. 106691. DOI: 10.1016/j.foodhyd.2021.106691.

Kornet, Remco; Veenemans, Justus; Venema, Paul; van der Goot, Atze Jan; Meinders, Marcel B. J.; Sagis, Leonard M.C.; van der Linden, Erik (2021b): Less is more: Limited fractionation yields stronger gels for pea proteins. In *Food Hydrocolloids* 112, p. 106285. DOI: 10.1016/j.foodhyd.2020.106285.

Kornet, Remco; Venema, Paul; Nijsse, Jaap; van der Linden, Erik; van der Goot, Atze Jan; Meinders, Marcel B. J. (2020): Yellow pea aqueous fractionation increases the specific volume fraction and viscosity of its dispersions. In *Food Hydrocolloids* 99, p. 105332. DOI: 10.1016/j.foodhyd.2019.105332.

Koxholt, M.; McIntosh, B.; Eisenmann, B. (1999): Enhanced stability of ice-cream by using particulated whey proteins. In *European Dairy Magazine* 10 (1), pp. 14–15.

Koyoro, H; Powers, J R (1987): Functional Properties of Pea Globulin Fractions. In *Cereal Chemistry* 67 (2), pp. 97–101.

Kreissl, Johanna Karoline; Mall, V; Steinhaus, P; Steinhaus, M (2019): M. Leibniz-LSB@TUM odorant database. Available online at https://www.leibniz-lsb.de/en/databases/leibniz-lsbtum-odorant-database.

Kurz, Franziska; Hengst, Claudia; Kulozik, Ulrich (2020): RP-HPLC method for simultaneous quantification of free and total thiol groups in native and heat aggregated whey proteins. In *MethodsX* 7, p. 101112. DOI: 10.1016/j.mex.2020.101112.

Kurz, Franziska; Reitberger, Vera; Hengst, Claudia; Bilke-Krause, Christine; Kulozik, Ulrich; Dombrowski, Jannika (2021): Correlation between Physico-Chemical Characteristics of Particulated β-Lactoglobulin and Its Behavior at Air/Water and Oil/Water Interfaces. In *Foods* 10 (6), p. 1426. DOI: 10.3390/foods10061426.

Lam, A. C. Y.; Can Karaca, A.; Tyler, Robert T.; Nickerson, Michael T. (2018): Pea protein isolates: Structure, extraction, and functionality. In *Food Reviews International* 34 (2), pp. 126–147. DOI: 10.1080/87559129.2016.1242135.

Lampart-Szczapa, E (1996): Preparation of protein from lupin seeds. In *Molecular Nutrition & Food Research* 40 (2). DOI: 10.1002/food.19960400205.

Lan, Yang; Xu, Minwei; Ohm, Jae-Bom; Chen, Bingcan; Rao, Jiajia (2019): Solid dispersion-based spray-drying improves solubility and mitigates beany flavour of pea

protein isolate. In *Food Chemistry* 278, pp. 665–673. DOI: 10.1016/j.food-chem.2018.11.074.

Leeb, Elena; Haller, Nicole; Kulozik, Ulrich (2018): Effect of pH on the reaction mechanism of thermal denaturation and aggregation of bovine β-lactoglobulin. In *IDF Symposium on Science and Technology of Fermented MilkIDF Symposium on Microstructure of Dairy Products* 78, pp. 103–111. DOI: 10.1016/j.idairyj.2017.09.006.

Liang, Han-Ning; Tang, Chuan-he (2013): pH-dependent emulsifying properties of pea [*Pisum sativum* (L.)] proteins. In *Food Hydrocolloids* 33 (2), pp. 309–319. DOI: 10.1016/j.foodhyd.2013.04.005.

Liu, Kun (2016): Lubrication and perception of foods. Tribological, rheological and sensory properties of particle-filled food systems. Wageningen University, Wageningen, Netherlands.

Liu, Kun; Stieger, Markus; van der Linden, Erik; van de Velde, Fred (2016a): Effect of microparticulated whey protein on sensory properties of liquid and semi-solid model foods. In *Food Hydrocolloids* 60, pp. 186–198. DOI: 10.1016/j.foodhyd.2016.03.036.

Liu, Kun; Tian, Yujie; Stieger, Markus; van der Linden, Erik; van de Velde, Fred (2016b): Evidence for ball-bearing mechanism of microparticulated whey protein as fat replacer in liquid and semi-solid multi-component model foods. In *Food Hydrocolloids* 52, pp. 403–414. DOI: 10.1016/j.foodhyd.2015.07.016.

Liu, Rui; Tian, Zhaojie; Song, Yingshi; Wu, Tao; Sui, Wenjie; Zhang, Min (2018a): Optimization of the Production of Microparticulated Egg White Proteins as Fat Mimetic in Salad Dressings Using Uniform Design. In *Food Science and Technology Research* 24 (5), pp. 817–827. DOI: 10.3136/fstr.24.817.

Liu, Rui; Wang, Liguo; Liu, Yan; Wu, Tao; Zhang, Min (2018b): Fabricating soy protein hydrolysate/xanthan gum as fat replacer in ice cream by combined enzymatic and heat-shearing treatment. In *Food Hydrocolloids* 81, pp. 39–47. DOI: 10.1016/j.foodhyd.2018.01.031.

Liu, Shuanghui; Low, Nicholas H.; Nickerson, Michael T. (2009): Effect of pH, salt, and biopolymer ratio on the formation of pea protein isolate-gum arabic complexes. In *Journal of Agricultural and Food Chemistry* 57 (4), pp. 1521–1526. DOI: 10.1021/jf802643n.

Loveday, Simon M. (2016): β-Lactoglobulin heat denaturation: A critical assessment of kinetic modelling. In *International Dairy Journal* 52, pp. 92–100. DOI: 10.1016/j.idairyj.2015.08.001.

Lukesh, John C.; Palte, Michael J.; Raines, Ronald T. (2012): A potent, versatile disulfide-reducing agent from aspartic acid. In *Journal of the American Chemical Society* 134 (9), pp. 4057–4059. DOI: 10.1021/ja211931f.

Lv, Yan-Chun; Song, Huan-Lu; Li, Xin; Wu, Liang; Guo, Shun-Tang (2011): Influence of blanching and grinding process with hot water on beany and non-beany flavor in

soymilk. In *Journal of Food Science* 76 (1), S20-5. DOI: 10.1111/j.1750-3841.2010.01947.x.

Marcone, Massimo F; Kakuda, Yukio; Yada, Rickey Y (1998): Salt-soluble seed globulins of dicotyledonous and monocotyledonous plants II. Structural characterization. In *Food Chemistry* (63), pp. 265–274. DOI: 10.1016/S0308-8146(97)00159-3.

Mariotti, Francois; Tome, Daniel; Mirand, Philippe Patureau (2008): Converting nitrogen into protein--beyond 6.25 and Jones' factors. In *Critical Reviews in Food Science and Nutrition* 48 (2), pp. 177–184. DOI: 10.1080/10408390701279749.

Martin, Anneke H.; Nieuwland, Maaike; Jong, Govardus A. H. de (2014): Characterization of heat-set gels from RuBisCO in comparison to those from other proteins. In *Journal of Agricultural and Food Chemistry* 62 (44), pp. 10783–10791. DOI: 10.1021/jf502905g.

Matsumiya, Kentaro; Murray, Brent S. (2016): Soybean protein isolate gel particles as foaming and emulsifying agents. In *Food Hydrocolloids* 60, pp. 206–215. DOI: 10.1016/j.foodhyd.2016.03.028.

McCarthy, Noel A.; Kennedy, Deirdre; Hogan, Sean A.; Kelly, Philip M.; Thapa, Krishtina; Murphy, Kevin M.; Fenelon, Mark A. (2016): Emulsification properties of pea protein isolate using homogenization, microfluidization and ultrasonication. In *Food Research International* 89 (Pt 1), pp. 415–421. DOI: 10.1016/j.foodres.2016.07.024.

Mela, David J. (1988): Sensory assessment of fat content in fluid dairy products. In *Appetite* 10 (1), pp. 37–44. DOI: 10.1016/S0195-6663(88)80031-X.

Melander, Wayne; Horváth, Csaba (1977): Salt effects on hydrophobic interactions in precipitation and chromatography of proteins: An interpretation of the lyotropic series. In *Archives of Biochemistry and Biophysics* 183 (1), pp. 200–215. DOI: 10.1016/0003-9861(77)90434-9.

Mession, Jean-Luc; Assifaoui, Ali; Cayot, P.; Saurel, Rémi (2012): Effect of pea proteins extraction and vicilin/legumin fractionation on the phase behavior in admixture with alginate. In *Food Hydrocolloids* 29 (2), pp. 335–346. DOI: 10.1016/j.foodhyd.2012.03.003.

Mession, Jean-Luc; Chihi, Mohammed Lazhar; Sok, Nicolas; Saurel, Rémi (2015): Effect of globular pea proteins fractionation on their heat-induced aggregation and acid cold-set gelation. In *Food Hydrocolloids* 46, pp. 233–243. DOI: 10.1016/j.foodhyd.2014.11.025.

Mession, Jean-Luc; Sok, Nicolas; Assifaoui, Ali; Saurel, Rémi (2013): Thermal denaturation of pea globulins (Pisum sativum L.)-molecular interactions leading to heat-induced protein aggregation. In *Journal of Agricultural and Food Chemistry* 61 (6), pp. 1196–1204. DOI: 10.1021/jf303739n.

Mezger, Thomas G. (2019): Das Rheologie Handbuch. Hannover, Germany: Vincentz Network.

Mitchell, J R (1980): The rheology of gels. In *Journal of Texture Studies* 11, pp. 315–337.

Moakes, R.J.A.; Sullo, A.; Norton, I. T. (2015): Preparation and characterisation of whey protein fluid gels: The effects of shear and thermal history. In *Food Hydrocolloids* 45, pp. 227–235. DOI: 10.1016/j.foodhyd.2014.11.024.

Monahan, Frank J.; German, J. Bruce; Kinsella, John E. (1995): Effect of pH and temperature on protein unfolding and thiol/disulfide interchange reactions during heat-induced gelation of whey proteins. In *Journal of Agricultural and Food Chemistry* 43 (1), pp. 46–52. DOI: 10.1021/jf00049a010.

Mounsey, John S.; O'Kennedy, Brendan T. (2007): Conditions limiting the influence of thiol–disulphide interchange reactions on the heat-induced aggregation kinetics of β-lactoglobulin. In *International Dairy Journal* 17 (9), pp. 1034–1042. DOI: 10.1016/j.idairyj.2006.12.008.

Munialo, Claire Darizu; Martin, Anneke H.; van der Linden, Erik; Jongh, Harmen H. J. de (2014): Fibril formation from pea protein and subsequent gel formation. In *Journal of Agricultural and Food Chemistry* 62 (11), pp. 2418–2427. DOI: 10.1021/jf4055215.

Munialo, Claire Darizu; van der Linden, Erik; Ako, Komla; Jongh, Harmen H. J. de (2015): Quantitative analysis of the network structure that underlines the transitioning in mechanical responses of pea protein gels. In *Food Hydrocolloids* 49, pp. 104–117. DOI: 10.1016/j.foodhyd.2015.03.018.

Nakai, Shuryo; Li-Chan, Eunice (1988): Hydrophobic interactions in food systems. Boca Raton Fla.: CRC Press.

Neugebauer, Anja; Granvogl, Michael; Schieberle, Peter (2020): Characterization of the Key Odorants in High-Quality Extra Virgin Olive Oils and Certified Off-Flavor Oils to Elucidate Aroma Compounds Causing a Rancid Off-Flavor. In *Journal of Agricultural and Food Chemistry* 68 (21), pp. 5927–5937. DOI: 10.1021/acs.jafc.0c01674.

Nicolai, Taco; Britten, Michel; Schmitt, Christophe (2011a): β-Lactoglobulin and WPI aggregates. Formation, structure and applications. In *Food Hydrocolloids* 25 (8), pp. 1945–1962. DOI: 10.1016/j.foodhyd.2011.02.006.

Nicolai, Taco; Britten, Michel; Schmitt, Christophe (2011b): β-Lactoglobulin and WPI aggregates: Formation, structure and applications. In *Food Hydrocolloids* 25 (8), pp. 1945–1962. DOI: 10.1016/j.foodhyd.2011.02.006.

Nicolai, Taco; Chassenieux, Christophe (2019): Heat-induced gelation of plant globulins. In *Current Opinion in Food Science* 27, pp. 18–22. DOI: 10.1016/j.cofs.2019.04.005.

Nicolai, Taco; Durand, Dominique (2013): Controlled food protein aggregation for new functionality. In *Current Opinion in Colloid & Interface Science* 18 (4), pp. 249–256. DOI: 10.1016/j.cocis.2013.03.001.

Nikolaidis, Athanasios; Moschakis, Thomas (2018): On the reversibility of ethanol-induced whey protein denaturation. In *Food Hydrocolloids* 84, pp. 389–395. DOI: 10.1016/j.foodhyd.2018.05.051.

Oakenfull, David; Fenwick, Dorothy E (1977): Thermodynamics and mechanism of hydrophobic interaction 1977 (30), pp. 741–752. DOI: 10.1071/CH9770741.

O'Kane, Francesca E.; Happe, Randolph P.; Vereijken, Johan M.; Gruppen, Harry; van Boekel, Martinus A. J. S. (2004a): Characterization of pea vicilin. 1. Denoting convicilin as the alpha-subunit of the Pisum vicilin family. In *Journal of Agricultural and Food Chemistry* 52 (10), pp. 3141–3148. DOI: 10.1021/jf035104i.

O'Kane, Francesca E.; Happe, Randolph P.; Vereijken, Johan M.; Gruppen, Harry; van Boekel, Martinus A. J. S. (2004b): Characterization of pea vicilin. 2. Consequences of compositional heterogeneity on heat-induced gelation behavior. In *Journal of Agricultural and Food Chemistry* 52 (10), pp. 3149–3154. DOI: 10.1021/jf035105a.

O'Kane, Francesca E.; Happe, Randolph P.; Vereijken, Johan M.; Gruppen, Harry; van Boekel, Martinus A. J. S. (2004c): Heat-induced gelation of pea legumin: comparison with soybean glycinin. In *Journal of Agricultural and Food Chemistry* 52 (16), pp. 5071–5078. DOI: 10.1021/jf035215h.

O'Kane, Francesca E.; Vereijken, Johan M.; Gruppen, Harry; van Boekel, Martinus A. J. S. (2005): Gelation Behavior of Protein Isolates Extracted from 5 Cultivars of Pisum sativum L. In *Journal of Food Science* 70 (2), C132-C137. DOI: 10.1111/j.1365-2621.2005.tb07073.x.

Oldfield, D. J.; Taylor, M. W.; Singh, H. (2005): Effect of preheating and other process parameters on whey protein reactions during skim milk powder manufacture. In *IDF Symposium on Science and Technology of Fermented MilkIDF Symposium on Microstructure of Dairy Products* 15 (5), pp. 501–511. DOI: 10.1016/j.idairyj.2004.09.004.

Onwulata, Charles I.; Smith, P W; Konstance, R P; Holsinger, V H (2001): Incorporation of whey products in extruded corn, potato or rice snacks. In *Food Research International* 2001 (34), pp. 679–687.

Osborne, Thomas B. (1909): The vegetable proteins. London: New York [etc.] Longmans, Green (Monographs on biochemistry). Available online at //catalog.hathitrust.org/Record/001034229.

Osen, Raffael; Toelstede, Simone; Eisner, Peter; Schweiggert-Weisz, Ute (2015): Effect of high moisture extrusion cooking on protein-protein interactions of pea (Pisum sativum L.) protein isolates. In *International Journal of Food Science & Technology* 50 (6), pp. 1390–1396. DOI: 10.1111/ijfs.12783.

Osen, Raffael; Toelstede, Simone; Wild, Florian; Eisner, Peter; Schweiggert-Weisz, Ute (2014): High moisture extrusion cooking of pea protein isolates: Raw material

characteristics, extruder responses, and texture properties. In *Journal of Food Engineering* 127, pp. 67–74. DOI: 10.1016/j.jfoodeng.2013.11.023.

Pai, Vandita B.; Khan, Saad A. (2002): Gelation and rheology of xanthan/enzyme-modified guar blends. In *Carbohydrate Polymers* 49 (2), pp. 207–216. DOI: 10.1016/S0144-8617(01)00328-9.

Pang, Shintaro; Ma, Changchu; Zhang, Naijie; He, Lili (2015): Investigation of the solubility enhancement mechanism of rebaudioside D using a solid dispersion technique with potassium sorbate as a carrier. In *Food Chemistry* 174, pp. 564–570. DOI: 10.1016/j.foodchem.2014.11.113.

Paquin, P.; Lebeuf, Y.; Richard, J. P.; Kaláb, M. (Eds.) (1992): Microparticulation of milk proteins by high pressure homogenization to produce a fat substitute. IDF Seminar.

Paredes-López, Octavio; Ordorica-Falomir, César (1986): Production of safflower protein isolates: Composition, yield and protein quality. In *Journal of the science of food and agriculture* 37 (11), pp. 1097–1103. DOI: 10.1002/jsfa.2740371107.

Plock, Jörn (1994): Zum Einfluß von Lactose auf die Denaturierung von Molkenproteinen in Molkenkonzentrat und auf die Ausbildung thermisch induzierter Gelstrukturen. Dissertation. Technical University Munich, Freising, Germany.

Pots, André M.; Grotenhuis, Erik ten; Gruppen, Harry; Voragen, Alphons G. J.; Kruif, Kees G. de (1999): Thermal Aggregation of Patatin Studied in Situ. In *Journal of Agricultural and Food Chemistry* 47 (11), pp. 4600–4605. DOI: 10.1021/jf9901901.

Pots, André M.; Jongh, Harmen H. J. de; Gruppen, Harry; Hamer, R. J.; Voragen, Alphons G. J. (1998a): Heat-induced conformational changes of patatin, the major potato tuber protein. In *European Journal of Biochemistry* 252 (1), pp. 66–72. DOI: 10.1046/j.1432-1327.1998.2520066.x.

Pots, André M.; Jongh, Harmen H. J. de; Gruppen, Harry; Hessing, Martin; Voragen, Alphons G. J. (1998b): The pH Dependence of the Structural Stability of Patatin. In *Journal of Agricultural and Food Chemistry* 46 (7), pp. 2546–2553. DOI: 10.1021/jf980034e.

Pouzot, M.; Nicolai, Taco; Visschers, R. W.; Weijers, M. (2005): X-ray and light scattering study of the structure of large protein aggregates at neutral pH. In *Food Hydrocolloids* 19 (2), pp. 231–238. DOI: 10.1016/j.foodhyd.2004.06.003.

Quaglia, G. B.; Gravina, R.; Paperi, R.; Paoletti, F. (1996): Effect of High Pressure Treatments on Peroxidase Activity, Ascorbic Acid Content and Texture in Green Peas. In *LWT - Food Science and Technology* 29 (5-6), pp. 552–555. DOI: 10.1006/fstl.1996.0084.

Quéguiner, C.; Dumay, Eliane; Salou-Cavlier, C.; Cheftel, Jean Claude (1992): Microcoagulation of a Whey Protein Isolate by Extrusion Cooking at Acid pH. In *Journal of Food Science* 57 (3), pp. 610–616. DOI: 10.1111/j.1365-2621.1992.tb08054.x.

Quevedo, Maria; Kulozik, Ulrich; Karbstein, Heike P.; Emin, M. Azad (2020a): Effect of thermomechanical treatment on the aggregation behaviour and colloidal functionality of β-Lactoglobulin at high concentrations. In *IDF Symposium on Science and Technology of Fermented MilkIDF Symposium on Microstructure of Dairy Products* 104, p. 104654. DOI: 10.1016/j.idairyj.2020.104654.

Quevedo, Maria; Kulozik, Ulrich; Karbstein, Heike P.; Emin, M. Azad (2020b): Influence of Thermomechanical Treatment and Ratio of β-Lactoglobulin and α-Lactalbumin on the Denaturation and Aggregation of Highly Concentrated Whey Protein Systems. In *Foods* 9 (9), p. 1196. DOI: 10.3390/foods9091196.

R Core Team (2021): R: A language and environment for statistical computing. R Foundation for Statistical Computing. Vienna, Austria. Available online at https://www.R-project.org/.

Rahma, Helmy; Dudek, Steffi; Mothes, Ralf; Görnitz, Eckhard; Schwenke, Dieter (2000): Physicochemical characterisation of mung bean (*Phaseolus aureus*) protein isolates. In *Journal of Agricultural and Food Chemistry* 80 (4), pp. 477–483. DOI: 10.1002/(SICI)1097-0010(200003)80:4<477::AID-JSFA553>3.0.CO;2-0.

Reinkensmeier, Annika; Bußler, Sara; Schlüter, Oliver; Rohn, Sascha; Rawel, Hashadrai M. (2015): Characterization of individual proteins in pea protein isolates and air classified samples. In *Food Research International* 76, pp. 160–167. DOI: 10.1016/j.foodres.2015.05.009.

Ricci, Lucia; Umiltà, Eleonora; Righetti, Maria C; Messina, Tiziana; Zurlini, Chiara; Montanari, Angela et al. (2018): On the thermal behavior of protein isolated from different legumes investigated by DSC and TGA. In *Journal of the science of food and agriculture* 98 (14), pp. 5368–5377. DOI: 10.1002/jsfa.9078.

Roefs, S. P.; Kruif, K. G. de (1994): A model for the denaturation and aggregation of beta-lactoglobulin. In *European Journal of Biochemistry* 226 (3), pp. 883–889. DOI: 10.1111/j.1432-1033.1994.00883.x.

Rombouts, Ine; Lagrain, Bert; Brunnbauer, Markus; Koehler, Peter; Brijs, Kristof; Delcour, Jan A. (2011): Identification of isopeptide bonds in heat-treated wheat gluten peptides. In *Journal of Agricultural and Food Chemistry* 59 (4), pp. 1236–1243. DOI: 10.1021/jf103579u.

Rubio, Luis A.; Pérez, Alicia; Ruiz, Raquel; Guzmán, M. Ángeles; Aranda-Olmedo, Isabel; Clemente, Alfonso (2014): Characterization of pea (Pisum sativum) seed protein fractions. In *Journal of the science of food and agriculture* 94 (2), pp. 280–287. DOI: 10.1002/jsfa.6250.

Sánchez-Obando, Juan-David; Cabrera-Trujillo, María Alejandra; Olivares-Tenorio, Mary-Luz; Klotz, Bernadette (2020): Use of optimized microparticulated whey protein in the process of reduced-fat spread and petit-suisse cheeses. In *LWT - Food Science and Technology* 120, p. 108933. DOI: 10.1016/j.lwt.2019.108933.

Sandoval-Castilla, O.; Lobato-Calleros, C.; Aguirre-Mandujano, E.; Vernon-Carter, E. J. (2004): Microstructure and texture of yogurt as influenced by fat replacers. In *IDF Symposium on Science and Technology of Fermented MilkIDF Symposium on Microstructure of Dairy Products* 14 (2), pp. 151–159. DOI: 10.1016/S0958-6946(03)00166-3.

Sava, N.; van der Plancken, I.; Claeys, W.; Hendrickx, M. (2005): The Kinetics of Heat-Induced Structural Changes of β-Lactoglobulin. In *Journal of Dairy Science* 88 (5), pp. 1646–1653. DOI: 10.3168/jds.S0022-0302(05)72836-8.

Schädle, Christopher N.; Eisner, Peter; Bader-Mittermaier, Stephanie (2020): The combined effects of different fat replacers and rennet casein on the properties of reduced-fat processed cheese. In *Journal of Dairy Science* 103 (5), pp. 3980–3993. DOI: 10.3168/jds.2019-17694.

Scharbert, Susanne; Hofmann, Thomas (2005): Molecular definition of black tea taste by means of quantitative studies, taste reconstitution, and omission experiments. In *Journal of Agricultural and Food Chemistry* 53 (13), pp. 5377–5384. DOI: 10.1021/jf050294d.

Schindler, Sabrina; Zelena, Kateryna; Krings, Ulrich; Bez, Jürgen; Eisner, Peter; Berger, Ralf Günter (2012): Improvement of the Aroma of Pea (Pisum sativum) Protein Extracts by Lactic Acid Fermentation. In *Food Biotechnology* 26 (1), pp. 58–74. DOI: 10.1080/08905436.2011.645939.

Schlutt, Birgit; Moran, Noelia; Schieberle, Peter; Hofmann, Thomas (2007): Sensory-directed identification of creaminess-enhancing volatiles and semivolatiles in full-fat cream. In *Journal of Agricultural and Food Chemistry* 55 (23), pp. 9634–9645. DOI: 10.1021/jf0721545.

Schmidt, Jesper Malling; Damgaard, Henriette; Greve-Poulsen, Mathias; Sunds, Anne Vuholm; Larsen, Lotte Bach; Hammershøj, Marianne (2019): Gel properties of potato protein and the isolated fractions of patatins and protease inhibitors – Impact of drying method, protein concentration, pH and ionic strength. In *Food Hydrocolloids* 96, pp. 246–258. DOI: 10.1016/j.foodhyd.2019.05.022.

Schmidt, Jesper Malling; Larsen, Lotte Bach; Hammershøj, Marianne (2017): Appearance and Textural Properties of Sheared Low Concentration Potato Protein Gels-Impact of Drying Method, pH, and Ionic Strength. In *Journal of Food Science* 82 (9), pp. 2056–2061. DOI: 10.1111/1750-3841.13818.

Schmitt, Christophe; Bovetto, Lionel; Buczkowski, Johann; Oliveira Reis, Guilherme de; Pibarot, Patrick; Amagliani, Luca; Dombrowski, Jannika (2021): Plant proteins and their colloidal state. In *Current Opinion in Colloid & Interface Science* 56, p. 101510. DOI: 10.1016/j.cocis.2021.101510.

Shand, P. J.; Ya, H.; Pietrasik, Z.; Wanasundara, P.K.J.P.D. (2007): Physicochemical and textural properties of heat-induced pea protein isolate gels. In *Food Chemistry* 102 (4), pp. 1119–1130. DOI: 10.1016/j.foodchem.2006.06.060.

Shimada, Kazuko; Cheftel, Jean Claude (1988): Texture characteristics, protein solubility, and sulfhydryl group/disulfide bond contents of heat-induced gels of whey protein isolate. In *Journal of Agricultural and Food Chemistry* 36 (5), pp. 1018–1025. DOI: 10.1021/jf00083a029.

Simpson, Stephen J.; Raubenheimer, David (2005): Obesity: the protein leverage hypothesis. In *Obesity reviews : an official journal of the International Association for the Study of Obesity* 6 (2), pp. 133–142. DOI: 10.1111/j.1467-789X.2005.00178.x.

Simpson, Stephen J.; Raubenheimer, David (2014): Perspective: Tricks of the trade. In *Nature* 508 (7496), S66. DOI: 10.1038/508S66a.

Singer, Norman S; Dunn, J. M. (1990): Protein microparticulation: the principle and the process. In *Journal of the American College of Nutrition* 9 (4), pp. 388–397. DOI: 10.1080/07315724.1990.10720397.

Singer, Norman S; Yamamoto, Shoji; Latella, Joseph (1988): Protein product base on 3/29/1988. Patent no. US4734287A.

Singh, Jaspreet; Kaur, Lovedeep (2016): Advances in Potato Chemistry and Technology: Elsevier.

Sondermann, C. (1991): Sensorische Prüfung. In Wolfgang Frede (Ed.): Taschenbuch für Lebensmittelchemiker und -technologen. Band 1. Berlin, Heidelberg, s.l.: Springer Berlin Heidelberg, pp. 97–105.

Sonne, Alina; Busch-Stockfisch, Mechthild; Weiss, Jochen; Hinrichs, Jörg (2014): Improved mapping of in-mouth creaminess of semi-solid dairy products by combining rheology, particle size, and tribology data. In *LWT - Food Science and Technology* 59 (1), pp. 342–347. DOI: 10.1016/j.lwt.2014.05.047.

Sosulski, F. W.; Hoover, Ratnajothi; Tyler, Robert T.; Murray, E. Donald; Arntfield, Susan D. (1985): Differential Scanning Calorimetry of Air-Classified Starch and Protein Fractions from Eight Legume Species. In *Starch - Stärke* 37 (8), pp. 257–262. DOI: 10.1002/star.19850370803.

Spelbrink, Robin E. J.; Lensing, Hellen; Egmond, Maarten R.; Giuseppin, Marco L. F. (2015): Potato Patatin Generates Short-Chain Fatty Acids from Milk Fat that Contribute to Flavour Development in Cheese Ripening. In *Applied Biochemistry and Biotechnology* 176 (1), pp. 231–243. DOI: 10.1007/s12010-015-1569-3.

Spiegel, Thomas (1999a): Thermische Denaturierung und Aggregation von Molkenproteinen in Ultrafiltrationsmolkenkonzentraten. Dissertation. Technische Universität München, Freising.

Spiegel, Thomas (1999b): Whey protein aggregation under shear conditions - effects of lactose and heating temperature on aggregate size and structure. In *International Journal of Food Science & Technology* 34 (5-6), pp. 523–531. DOI: 10.1046/j.1365-2621.1999.00309.x.

Spiegel, Thomas; Huss, M. (2002): Whey protein aggregation under shear conditions - effects of pH-value and removal of calcium. In *International Journal of Food Science & Technology* 37 (5), pp. 559–568. DOI: 10.1046/j.1365-2621.2002.00612.x.

Stark, Timo; Bareuther, Sabine; Hofmann, Thomas (2006): Molecular definition of the taste of roasted cocoa nibs (Theobroma cacao) by means of quantitative studies and sensory experiments. In *Journal of Agricultural and Food Chemistry* 54 (15), pp. 5530–5539. DOI: 10.1021/jf0608726.

Steffl, Annemarie; Schreiber, Regina; Hafenmair, Michael; Kessler, Heinz-Gerhard (1999): Effect of denatured whey proteins on the rennet-induced aggregation of casein micelles. In *IDF Symposium on Science and Technology of Fermented MilkIDF Symposium on Microstructure of Dairy Products* 9 (3-6), pp. 401–402. DOI: 10.1016/S0958-6946(99)00106-5.

Stone, Andrea K.; Karalash, Anna; Tyler, Robert T.; Warkentin, Thomas D.; Nickerson, Michael T. (2015): Functional attributes of pea protein isolates prepared using different extraction methods and cultivars. In *Food Research International* 76 (1), pp. 31–38. DOI: 10.1016/j.foodres.2014.11.017.

Stone, Herbert; Sidel, Joel L. (2012): Sensory evaluation practices. 4th ed. Amsterdam: Elsevier/AP.

Sturaro, Alba; Marchi, Massimo de; Zorzi, Elisa; Cassandro, Martino (2015): Effect of microparticulated whey protein concentration and protein-to-fat ratio on Caciotta cheese yield and composition. In *IDF Symposium on Science and Technology of Fermented MilkIDF Symposium on Microstructure of Dairy Products* 48, pp. 46–52. DOI: 10.1016/j.idairyj.2015.02.003.

Sun, Xiang Dong; Arntfield, Susan D. (2010): Gelation properties of salt-extracted pea protein induced by heat treatment. In *Food Research International* 43 (2), pp. 509–515. DOI: 10.1016/j.foodres.2009.09.039.

Sun, Xiang Dong; Arntfield, Susan D. (2011): Dynamic oscillatory rheological measurement and thermal properties of pea protein extracted by salt method: Effect of pH and NaCl. In *Journal of Food Engineering* 105 (3), pp. 577–582. DOI: 10.1016/j.jfoodeng.2011.03.008.

Sun, Xiang Dong; Arntfield, Susan D. (2012): Molecular forces involved in heat-induced pea protein gelation: Effects of various reagents on the rheological properties of salt-extracted pea protein gels. In *Food Hydrocolloids* 28 (2), pp. 325–332. DOI: 10.1016/j.foodhyd.2011.12.014.

Sussmann, Daniela; Halter, T.; Pickardt, C.; Schweiggert-Weisz, Ute; Eisner, Peter (2013a): An Optimization Approach for the Production of Fatlike Protein Isolates from Different Leguminous Seeds Using Response Surface Methodology. In *Journal of Food Process Engineering* 36 (6), pp. 715–730. DOI: 10.1111/jfpe.12013.

Sussmann, Daniela; Pickardt, C.; Schweiggert-Weisz, Ute; Eisner, Peter (2013b): Influence of different processing parameters on the isolation of lupin (Lupinus Angustifolius L.) protein isolates: A preliminary study. In *Journal of Food Process Engineering* 36 (1), pp. 18–28. DOI: 10.1111/j.1745-4530.2011.00647.x.

Swanson, Barry G (1990): Pea and lentil protein extraction and functionality. In *Journal of the American Oil Chemists' Society* 5 (67), pp. 276–280. DOI: 10.1007/BF02539676.

Taherian, Ali R.; Mondor, Martin; Labranche, Joey; Drolet, Hélène; Ippersiel, Denis; Lamarche, François (2011): Comparative study of functional properties of commercial and membrane processed yellow pea protein isolates. In *Food Research International* 44 (8), pp. 2505–2514. DOI: 10.1016/j.foodres.2011.01.030.

Tanford, Charles; Taggart, Valerie G.: Ionization-linked Changes in Protein Conformation. II. The N ? R Transition in ß-Lactoglobulin.

Tang, Chuan-he; Choi, Siu-Mei; Ma, Ching-Yung (2007): Study of thermal properties and heat-induced denaturation and aggregation of soy proteins by modulated differential scanning calorimetry. In *International journal of biological macromolecules* 40 (2), pp. 96–104. DOI: 10.1016/j.ijbiomac.2006.06.013.

Tanger, Caren; Andlinger, David Julian; Brümmer-Rolf, Annette; Engel, Julia; Kulozik, Ulrich (2021a): Quantification of protein-protein interactions in highly denatured whey and potato protein gels. In *MethodsX*, p. 101243. DOI: 10.1016/j.mex.2021.101243.

Tanger, Caren; Engel, Julia; Kulozik, Ulrich (2020): Influence of extraction conditions on the conformational alteration of pea protein extracted from pea flour. In *Food Hydrocolloids* 107, p. 105949. DOI: 10.1016/j.foodhyd.2020.105949.

Tanger, Caren; Müller, Michaela; Andlinger, David Julian; Kulozik, Ulrich (2022): Influence of pH and ionic strength on the thermal gelation behaviour of pea protein. In *Food Hydrocolloids*, 106903The p. DOI: 10.1016/j.foodhyd.2021.106903.

Tanger, Caren; Quintana Ramos, Paola; Kulozik, Ulrich (2021b): Comparative Assessment of Thermal Aggregation of Whey, Potato, and Pea Protein under Shear Stress for Microparticulation. In *ACS Food Science & Technology* 1 (5), pp. 975–985. DOI: 10.1021/acsfoodscitech.1c00104.

Tanger, Caren; Schmidt, Florian; Utz, Florian; Kreissl, Johanna Karoline; Dawid, Corinna; Kulozik, Ulrich (2021c): Pea protein microparticulation using extrusion cooking: Influence of extrusion parameters and drying on microparticle characteristics and sensory by application in a model milk dessert. In *Innovative Food Science & Emerging Technologies*, p. 102851. DOI: 10.1016/j.ifset.2021.102851.

Taylor, S. M.; Fryer, P. J. (1994): The effect of temperature/shear history on the thermal gelation of whey protein concentrates. In *Food Hydrocolloids* 8 (1), pp. 45–61. DOI: 10.1016/S0268-005X(09)80144-6.

Temiz, Hasan; Kezer, Gizem (2015): Effects of Fat Replacers on Physicochemical, Microbial and Sensorial Properties of Kefir Made Using Mixture of Cow and Goat's

Milk. In *Journal of Food Processing and Preservation* 39 (6), pp. 1421–1430. DOI: 10.1111/jfpp.12361.

Thomas, C. R.; Geer, D. (2011): Effects of shear on proteins in solution. In *Biotechnology letters* 33 (3), pp. 443–456. DOI: 10.1007/s10529-010-0469-4.

Tian, Shaojun; Kyle, William; Small, Darryl (1999): Pilot scale isolation of proteins from field peas (Pisum sativum L.) for use as food ingredients. In *International Journal of Food Science & Technology* (34), pp. 33–39.

Tolkach, Alexander; Kulozik, Ulrich (2005): Effect of pH and temperature on the reaction kinetic parameters of the thermal denaturation of β-lactoglobulin. In *undefined*. Available online at https://www.semanticscholar.org/paper/Effect-of-pH-and-temperature-on-the-reaction-of-the-Tolkach-Kulozik/c695ad936053cc8b642508ca2ed7d1d138791dea.

Tolkach, Alexander; Kulozik, Ulrich (2007): Reaction kinetic pathway of reversible and irreversible thermal denaturation of β-lactoglobulin. In *Le Lait* 87 (4-5), pp. 301–315. DOI: 10.1051/lait:2007012.

Toro-Sierra, José (2016): On the separation, thermal and shear induced modification, and study of the functional properties of the major whey protein fractions. Dissertation. Technische Universität München, Freising.

Toro-Sierra, José; Schumann, Jens; Kulozik, Ulrich (2013): Impact of spray-drying conditions on the particle size of microparticulated whey protein fractions. In *Dairy Science & Technology* 93 (4-5), pp. 487–503. DOI: 10.1007/s13594-013-0124-7.

Torres, I. C.; Janhøj, Thomas; Mikkelsen, B.Ø.; Ipsen, Richard (2011): Effect of microparticulated whey protein with varying content of denatured protein on the rheological and sensory characteristics of low-fat yoghurt. In *IDF Symposium on Science and Technology of Fermented MilkIDF Symposium on Microstructure of Dairy Products* 21 (9), pp. 645–655. DOI: 10.1016/j.idairyj.2010.12.013.

Tournier, Carole; Martin, Christophe; Guichard, Elisabeth; Issanchou, Sylvie; Sulmont-Rossé, Claire (2007): Contribution to the understanding of consumers' creaminess concept: A sensory and a verbal approach. In *IDF Symposium on Science and Technology of Fermented MilkIDF Symposium on Microstructure of Dairy Products* 17 (5), pp. 555–564. DOI: 10.1016/j.idairyj.2006.07.003.

Udabage, P.; McKinnon, I. R.; Augustin, M. A. (2000): Mineral and casein equilibria in milk: effects of added salts and calcium-chelating agents. In *The Journal of dairy research* 67 (3). DOI: 10.1017/s0022029900004271.

Urgu, Müge; Türk, Aylin; Ünlütürk, Sevcan; Kaymak-Ertekin, Figen; Koca, Nurcan (2019): Milk Fat Substitution by Microparticulated Protein in Reduced-fat Cheese Emulsion: The Effects on Stability, Microstructure, Rheological and Sensory Properties. In *Food Science of Animal Resources* 39 (1), pp. 23–34. DOI: 10.5851/kosfa.2018.e60.

Utz, Florian; Kreissl, Johanna Karoline; Stark, Timo D.; Schmid, Christian; Tanger, Caren; Kulozik, Ulrich et al. (2021): Sensomics-Assisted Flavor Decoding of Dairy Model Systems and Flavor Reconstitution Experiments. In *Journal of Agricultural and Food Chemistry* 69 (23), pp. 6588–6600. DOI: 10.1021/acs.jafc.1c02165.

van Dijk, Erik; Hoogeveen, Arlo; Abeln, Sanne (2015): The hydrophobic temperature dependence of amino acids directly calculated from protein structures. In *PLOS Computational Biology* 11 (5), e1004277. DOI: 10.1371/journal.pcbi.1004277.

Vilotte, Alice; Bodiguel, Hugues; Ako, Komla; Gunes, Deniz Z.; Schmitt, Christophe; Loubens, Clément de (2021): Kinetic and structural characterization of whey protein aggregation in a millifluidic continuous process. In *Food Hydrocolloids* 110, p. 106137. DOI: 10.1016/j.foodhyd.2020.106137.

Wang, Kun; Arntfield, Susan D. (2014): Binding of carbonyl flavours to canola, pea and wheat proteins using GC/MS approach. In *Food Chemistry* 157, pp. 364–372. DOI: 10.1016/j.foodchem.2014.02.042.

Wang, Ning; Hatcher, David W.; Warkentin, Thomas D.; Toews, Ruth (2010): Effect of cultivar and environment on physicochemical and cooking characteristics of field pea (Pisum sativum). In *Food Chemistry* 118 (1), pp. 109–115. DOI: 10.1016/j.foodchem.2009.04.082.

Wang, Ren; Zhou, Xing; Chen, Zhengxing (2008): High pressure inactivation of lipoxygenase in soy milk and crude soybean extract. In *Food Chemistry* 106 (2), pp. 603–611. DOI: 10.1016/j.foodchem.2007.06.056.

Wang, Wei; Chen, Guohua (2005): Heat and mass transfer model of dielectric-material-assisted microwave freeze-drying of skim milk with hygroscopic effect. In *Chemical Engineering Science* 60 (23), pp. 6542–6550. DOI: 10.1016/j.ces.2005.05.036.

Weigle, David S.; Breen, Patricia A.; Matthys, Colleen C.; Callahan, Holly S.; Meeuws, Kaatje E.; Burden, Verna R.; Purnell, Jonathan Q. (2005): A high-protein diet induces sustained reductions in appetite, ad libitum caloric intake, and body weight despite compensatory changes in diurnal plasma leptin and ghrelin concentrations. In *The American Journal of Clinical Nutrition* 82 (1), pp. 41–48. DOI: 10.1093/ajcn.82.1.41.

Welinder, Karen G.; Jørgensen, Malene (2009): Covalent structures of potato tuber lipases (patatins) and implications for vacuolar import. In *Journal of Biological Chemistry* 284 (15), pp. 9764–9769. DOI: 10.1074/jbc.M809674200.

Welke, Juliane Elisa; Zanus, Mauro; Lazzarotto, Marcelo; Alcaraz Zini, Cláudia (2014): Quantitative analysis of headspace volatile compounds using comprehensive two-dimensional gas chromatography and their contribution to the aroma of Chardonnay wine. In *Food Research International* 59, pp. 85–99. DOI: 10.1016/j.foodres.2014.02.002.

Wijayanti, Heni B.; Bansal, Nidhi; Deeth, Hilton C. (2014): Stability of Whey Proteins during Thermal Processing: A Review. In *Comprehensive Reviews in Food Science and Food Safety* 13 (6), pp. 1235–1251. DOI: 10.1111/1541-4337.12105.

Wit, J. N. de; Swinkels, G.A.M. (1980): A differential scanning calorimetric study of the thermal denaturation of bovine β-lactoglobulin Thermal behaviour at temperatures up to 100°C. In *Biochimica et Biophysica Acta (BBA) - Protein Structure* 624 (1), pp. 40–50. DOI: 10.1016/0005-2795(80)90223-8.

Wolz, Magdalena (2018): Thermal aggregation of whey proteins under shear stress and the effects on microparticulation in a high moisture extrusion process. Dissertation. Technical University Munich, Freising, Germany. Lehrstuhl für Lebensmittel- und Bio-Prozesstechnik.

Wolz, Magdalena; Kastenhuber, Simon; Kulozik, Ulrich (2016a): High moisture extrusion for microparticulation of whey proteins –Influence of process parameters. In *Journal of Food Engineering* 185, pp. 56–61. DOI: 10.1016/j.jfoodeng.2016.04.002.

Wolz, Magdalena; Kulozik, Ulrich (2015): Thermal denaturation kinetics of whey proteins at high protein concentrations. In *International Dairy Journal* 49, pp. 95–101. DOI: 10.1016/j.idairyj.2015.05.008.

Wolz, Magdalena; Kulozik, Ulrich (2017): System parameters in a high moisture extrusion process for microparticulation of whey proteins. In *Journal of Food Engineering* 209, pp. 12–17. DOI: 10.1016/j.jfoodeng.2017.04.010.

Wolz, Magdalena; Mersch, Eugenia; Kulozik, Ulrich (2016b): Thermal aggregation of whey proteins under shear stress. In *Food Hydrocolloids* 56, pp. 396–404. DOI: 10.1016/j.foodhyd.2015.12.036.

Xiong, Youling L.; Dawson, Karl A.; Wan, Liping (1993): Thermal Aggregation of β-Lactoglobulin: Effect of pH, Ionic Environment, and Thiol Reagent1. In *Journal of Dairy Science* 76 (1), pp. 70–77. DOI: 10.3168/jds.S0022-0302(93)77324-5.

Yan, Lei; Yu, Dongjin; Liu, Rui; Jia, Yuanyuan; Zhang, Min; Wu, Tao; Sui, Wenjie (2021): Microstructure and meltdown properties of low-fat ice cream: Effects of microparticulated soy protein hydrolysate/xanthan gum (MSPH/XG) ratio and freezing time. In *Journal of Food Engineering* 291, p. 110291. DOI: 10.1016/j.jfoodeng.2020.110291.

Yang, Jingqi; Zamani, Sara; Liang, Li; Chen, Lingyun (2021): Extraction methods significantly impact pea protein composition, structure and gelling properties. In *Food Hydrocolloids* 117, p. 106678. DOI: 10.1016/j.foodhyd.2021.106678.

Yeh, An-I; Hwang, Shiuan-Jer; Guo, Jing-Jiuan (1992): Effects of screw speed and feed rate on residence time distribution and axial mixing of wheat flour in a twin-screw extruder. In *Journal of Food Engineering* 17 (1), pp. 1–13. DOI: 10.1016/0260-8774(92)90061-A.

Zhan, Fuchao; Shi, Minqi; Wang, Yuntao; Li, Bin; Chen, Yijie (2019): Effect of freeze-drying on interaction and functional properties of pea protein isolate/soy soluble polysaccharides complexes. In *Journal of Molecular Liquids* 285, pp. 658–667. DOI: 10.1016/j.molliq.2019.04.126.

Zhang, Shuning; Holmes, Melvin; Ettelaie, Rammile; Sarkar, Anwesha (2020a): Pea protein microgel particles as Pickering stabilisers of oil-in-water emulsions: Responsiveness to pH and ionic strength. In *Food Hydrocolloids* 102, p. 105583. DOI: 10.1016/j.foodhyd.2019.105583.

Zhang, Tao; Guo, Jian; Chen, Jia-Feng; Wang, Jin-Mei; Wan, Zhi-Li; Yang, Xiao-Quan (2020b): Heat stability and rheological properties of concentrated soy protein/egg white protein composite microparticle dispersions. In *Food Hydrocolloids* 100, p. 105449. DOI: 10.1016/j.foodhyd.2019.105449.

Zhao, Qiang; Xiong, Hua; Selomulya, Cordelia; Chen, Xiao Dong; Huang, Shengfang; Ruan, Xia et al. (2013): Effects of Spray Drying and Freeze Drying on the Properties of Protein Isolate from Rice Dreg Protein. In *Food and Bioprocess Technology* 6 (7), pp. 1759–1769. DOI: 10.1007/s11947-012-0844-3.

Zhou, Qi; Jia, Xiao; Yao, Ying-Zheng; Wang, Bei; Wei, Chang-Qing; Zhang, Min; Huang, Fenghong (2019): Characterization of the Aroma-Active Compounds in Commercial Fragrant Rapeseed Oils via Monolithic Material Sorptive Extraction. In *Journal of Agricultural and Food Chemistry* 67 (41), pp. 11454–11463. DOI: 10.1021/acs.jafc.9b05691.

Zúñiga, R. N.; Tolkach, Alexander; Kulozik, Ulrich; Aguilera, J. M. (2010): Kinetics of formation and physicochemical characterization of thermally-induced beta-lactoglobulin aggregates. In *Journal of Food Science* 75 (5), E261-8. DOI: 10.1111/j.1750-3841.2010.01617.x.

8 APPENDIX

The following publications and presentations have emerged from this work . They are listed in chronological order.

8.1 Peer reviewed publications (included in this thesis)

1. Tanger, C., Engel, J., Kulozik, U. (2020). Influence of extraction conditions on the conformational alteration of pea protein extracted from pea flour. Food Hydrocolloids, 107, 105949
2. Tanger, C., Andlinger, D., Brümmer-Rolf, A., Engel, J., Kulozik, U. (2021). Quantification of protein-protein interactions in highly denatured whey and potato protein gels. MethodsX, 8, 101243
3. Tanger, C., Müller, M., Andlinger, D., Kulozik, U. (2022). Influence of pH and ionic strength on the thermal gelation behaviour of pea protein. Food Hydrocolloids, 123, 106903
4. Tanger, C., Quintana-Ramos, P., Kulozik, U. (2021). Comparative Assessment of Thermal Aggregation of Whey, Potato, and Pea Protein under Shear Stress for Microparticulation. ACS Food Science and Technology, 1, 5, 975-985
5. Tanger, C., Mertens, J., Kulozik, U. (2022). Influence of extraction method on the aggregation of pea protein during thermo-mechanical treatment. Food Hydrocolloids, 127, 107514
6. Tanger, C., Schmidt, F., Utz, F., Kreissl, J., Dawid, C., Kulozik, U. (2022). Pea protein microparticulation using extrusion cooking: Influence of extrusion parameters and drying on microparticle characteristics and sensory by application in a model milk dessert. Innovative Food Science & Emerging Technologies, 74, 102851
7. Tanger, C., Utz, F., Spaccasassi, A., Kreissl, J., Dawid, C., Dombrowski, J., Kulozik, U. (2021). Influence of pea and potato protein microparticles on texture and sensory properties in a fat-reduced model milk dessert. ACS Food Science and Technology, 2,1, 169-179

8.2 Peer reviewed publications (not included in this thesis)

1. Utz, F., Kreissl, J., Stark, T., Schmid, C., Tanger, C., Kulozik, U., Hofmann, T., Dawid, C. (2021). Sensomics-assisted flavor decoding of dairy model systems and flavor reconstitution experiments. Journal of Agricultural and Food Chemistry, 69, 23, 6588–6600
2. Andlinger, D., Rampp, L., Tanger, C., Kulozik, U. (2021). Viscoelasticity and protein interactions of hybrid gels produced from potato and whey protein isolates. ACS Food Science and Technology, 1, 7, 1304–1315
3. Utz, F., Spaccasassi, A., Kreissl, J., Stark, T., Tanger, C., Kulozik, U., Hofmann, T., Dawid, C. (2022) . Sensomics-assisted Aroma Decoding of Pea Protein Isolates (Pisum sativum L.). Foods, 11, 3, 412

8.3 Non reviewed publications

1. Tanger, C. (2021). Functionalisation of pea protein for fat reduction. Milchwissenschaftliche Forschung Weihenstephan 2020, 63, 56-58 ISBN: 978-3-947492-20-6

8.4 Oral presentations

1. Tanger, C., Kulozik, U.: Struktur und Sensorik fettreduzierte Lebensmittel. 1. Projekttreffen zum AiF/FEI-Forschungsvorhaben 20197 N, 04.12.2018
2. Tanger, C., Kulozik, U.: Struktur und Sensorik fettreudzieter Lebensmittel. 2. Projekttreffen zum AiF/FEI-Forschungsvorhaben 20197 N, 17.10.2019
3. Tanger, C., Kulozik, U.: Extraction of pea protein – a comparison of methods. 34th EFFoST International Conference, Online Konferenz, 11.11.2020
4. Tanger, C., Kulozik, U.: Struktur und Sensorik fettreduzierte Lebensmittel. 3. Projekttreffen zum AiF/FEI-Forschungsvorhaben 20197 N, 19.11.2020
5. Tanger, C., Kulozik, U.: Struktur und Sensorik fettreduzierte Lebensmittel. 4. Projekttreffen zum AiF/FEI-Forschungsvorhaben 20197 N, 29.04.2021
6. Tanger, C., Kulozik, U.: Projektvorstellung. Sitzung des Begleitgremiums der Nationalen Reduktions- und Innovationsstrategie für Zucker, Fette und Salz in Fertigprodukten, Online Seminar, 04.05.2021
7. Tanger, C., Kulozik, U.: Entwicklung neuer Konzepte zur Optimierung von Struktur und Sensorik fettreduzierter Lebensmittel durch Proteinfunktionalisierung und molekular-sensorische Methoden am Beispiel der Erbse. UFOP Ernährungsfachtagung, Online Tagung, 02.11.2021